University of Plymouth

PEARL **https://pearl.plymouth.ac.uk**

04 University of Plymouth Research Theses 01 Research Theses Main Collection

2008

In situ measurements of building materials using a thermal probe

Pilkington, Brian

http://hdl.handle.net/10026.1/612

http://dx.doi.org/10.24382/4771
University of Plymouth

All content in PEARL is protected by copyright law. Author manuscripts are made available in accordance with publisher policies. Please cite only the published version using the details provided on the item record or document. In the absence of an open licence (e.g. Creative Commons), permissions for further reuse of content should be sought from the publisher or author.

IN SITU MEASUREMENTS OF BUILDING MATERIALS USING A THERMAL PROBE

by

BRIAN PILKINGTON

A thesis submitted to the University of Plymouth
in partial fulfilment for the degree of

DOCTOR OF PHILOSOPHY

School of Engineering

Faculty of Technology

July 2008

University of Plymouth
Library
Item No. 9007937982
Shelfmark
THESIS 620.11296 PIL

Brian Pilkington

In situ measurements of building materials using a thermal probe

Abstract

This work concerns the in situ measurement of thermal conductivity and thermal diffusivity of building materials, so as to provide improved data for the estimation and prediction of energy efficiency in buildings. Thermal data sources and measurement methods currently used by industry to inform building design were found to give flawed values for the thermal properties of materials as found in situ. A transient measurement technique, carried out by means of a thermal probe, and used in various other industries, was investigated as an alternative, relatively non-destructive, rapid and economic means of obtaining representative results.

An analysis of the literature associated with the technique's history, theory and practice was carried out. Four strands of scientific research were undertaken: traditional thermal probe solutions were assessed; computer simulations were used to model probe behaviour while avoiding practical, experimental error; laboratory based measurements were carried out with materials of known and unknown thermal properties using varied parameters, including moisture content; an apparatus was developed for fieldwork, and in situ measurements were carried out on real buildings, using novel analysis routines.

Results for thermal diffusivity values achieved by the thermal probe method were found to be unreliable. Representative thermal conductivity values were achieved for structural materials with varied moisture content, both in controlled laboratory environments and in situ under diverse environmental conditions, which had not previously been achieved. Heat losses from the probe open end and the material adjacent to it were shown to currently prevent reliable values being obtained for building insulation materials.

The thermal probe technique was successfully transferred from laboratory to in situ measurements. It was shown that various calibration factors reported in the literature could not be relied upon to transfer successfully between material types. A significant cause of error in the measurement of insulation materials was identified and a guarded probe was proposed to overcome this. The technique was shown to provide much improved thermal conductivity data for structural building materials, whether as samples or in situ, with the potential to expand this success to insulation materials in the future.

CONTENTS

List of tables

List of charts

List of figures

List of equations

Acknowledgements

This study was suggested by Dr SM Goodhew, to whom the author is grateful for the excellent levels of guidance and support provided.

The main part of the work was interwoven with a research project managed by the author at the University of Plymouth for, and with funding from, the Carbon Trust.

Many other colleagues are deserving of thanks, especially:

Dr. Pieter deWilde for building the Voltra model, inputting the data and returning the results, as well as ongoing lively, stimulating and explorative conversations.

Dr. Richard Griffiths for helping me get to grips with the physics and for providing frequent challenges to my work, which ensured careful checking and revisions along the way.

Keith Stott for his technical help, especially in building the field apparatus.

Dr. Paul Hewson for introducing me to a variety of mathematical software and helping assess issues with data scatter and regression analyses.

Dr. Hazel Shute for advising on complex equations containing many exponential and logarithmic values.

Graham Titley and all the team at the Interlibrary Loans department at the University of Plymouth for their unceasing efforts, help and support in finding many obscure articles.

Thanks go to Brian Anderson at BRE, Colin Pearson at BSRIA, Neil Lockmuller at NPL and many others who have shown an interest in the work.

Thanks also go to the various building owners and Architects who allowed the use of their buildings, including the Eden Project, Mike McCrae, Chris Morgan, Tom Morton, Ralph Carpenter.

http://www.gordonengland.co.uk/conversion/xindex.htm provided quick and convenient online conversion calculators which proved invaluable in unravelling historic units from early articles.

Finally, my heartfelt thanks go to Noreen, to whom this work is dedicated. She has never wavered in her support, despite my many periods of distraction and occasional patches of despair!

"Heat, like gravity, penetrates every substance of the universe, its rays occupy all parts of space. The object of our work is to set forth the mathematical laws which this element obeys. The theory of heat will hereafter form one of the most important branches of general physics".
Jean Baptiste Joseph Fourier,1768 – 1830, Analytical Theory of Heat

Author's declaration

At no time during the registration for the degree of Doctor of Philosophy has the author been registered for any other University award.

The work presented here is exclusively that of the author, albeit with support as indicated within the acknowledgements and text.

The author attended various University of Plymouth Postgraduate Skills Development sessions and received individual tuition from staff in the Schools of: Engineering; Architecture; and Mathematics and Statistics. External consultations were held at: the Building Research Establishment, East Kilbride; the Building Services Research & Information Association, Bracknell; and the National Physics Laboratory, Teddington.

Related publications:

De Wilde, P., R. Griffiths, B. Pilkington, S. Goodhew, 2007. *Simulation of heat flow from a line source in support of development of a thermal probe.* In: Jiang, Zhu, Yang and Li, eds. Building Simulation '07, 10th International IBPSA Conference, Beijing, China, September 3-6 2007, 1858-1865

Pilkington, B., P. de Wilde, P., S. Goodhew, R. Griffiths, 2006. *Development of a Probe for Measuring In-situ the Thermal Properties of Building Materials.* In: Compagnon, Haefeli and Weber, ed. PLEA'06, 23rd International Conference, Geneva, Switzerland, September 6-8 2006, 665-670

Pilkington, B., R. Griffiths, S. Goodhew, P. de Wilde, 2007. *Thermal probe technology for buildings: the transition from laboratory to field measurements.* ASCE Journal of Architectural Engineering – in press

Related conferences and presentations:

University of Plymouth Environmental Building Group 10th Anniversary Conference (organiser) November 2006, presented: *In-situ thermal conductivity measurements of building materials*

Constructing Excellence South West conference, University of Plymouth, March 2007, presented: *Thermal Probe Measurements of Building Materials related to Passive Energy Strategies*

Schumacher College, Dartington, New Economics group, June 2007, presented: *Environmental building, material spirituality, passive energy strategies, climate change and well-being*

Word count

The main body of the thesis contains approximately 57,500 words

Signed.....

Date.....20/11/08.....

Nomenclature

Units within the thesis are those of the current International System of Units (SI) plus those below, with others as indicated in the text.

λ	=	Thermal conductivity, $Wm^{-1}K^{-1}$
α	=	Thermal diffusivity, m^2s^{-1}
H	=	Probe conductance, $Wm^{-2}K^{-1}$ (unless stated otherwise)
Q'	=	Power supplied to the probe per unit length, Wm^{-1}
Q^*	=	Rate of energy generation per unit volume, Wm^{-3}
t	=	Elapsed time, s
T	=	Temperature, K
ΔT	=	Change in temperature, K
θ	=	The slope of $\Delta T/\ln t$
ρ	=	Density, $kg.m^{-3}$
C	=	Specific heat capacity, $Jkg^{-1}K^{-1}$
ρC	=	Volumetric heat capacity, $Jm^{-3}K^{-1}$
r	=	Radius of the probe, m
l	=	Length of the probe, m
d	=	Shortest radial distance from the probe to the sample boundary, m
$_p$	=	A subscript indicating a property relating to the probe
γ	=	Euler's constant, 0.5772156649.....
TK	=	A K type thermocouple

Chapter 1: Introduction

This thesis is an assessment of the thermal probe technique as an in situ method to simultaneously measure the thermal conductivity, thermal diffusivity and hence volumetric heat capacity of building materials. The technique relies on the particular features of temperature rise over time of a line source heated at a constant power within the material of interest. The basis of the measurement is that the rate of temperature rise measured at or near the line source is dependent on the thermal conductivity of the material being measured, while the extent of the change in temperature at any given power input is dependent on the material's heat capacity.

The introductory chapter sets out the context, such as the imperative of energy efficiency in buildings, and leads into the background of the work.

The Context of the research

Human induced climate change was referred to as the 'world's greatest environmental challenge' by the former British Prime Minister (Blair, 2004), a view supported by the works of various scientific bodies, economists and individual scientists, including the Intergovernmental Panel on Climate Change (Alley et al, 2007; Nicholas Stern, 2007; UNEP, 2007; and James Lovelock, 2006).

Whilst not the most powerful greenhouse gas, the quantities of carbon dioxide currently emitted from fossil fuel burning cause it to make the greatest contribution to human induced climate change (Hockstad et al, 2005). A

significant contributor to the sum of CO_2 emissions is the generation of energy required to heat and cool buildings, whether homes, offices, or factories, etc. The Building Research Establishment calculate that around 40% of all greenhouse gas emissions in developed countries arise from energy use in buildings (Hitchin, 2007). The UK Greenhouse Gas Inventory apportions 85% of UK emissions to energy production (Baggott et al, 2005). The Department for Trade and Industry (DTI, 2005) estimate 30% of this energy is consumed in domestic property, and various studies, including the recent Stepping Forward (Chambers N et al, 2005), have shown around 60% of this is used for space heating.

Carbon dioxide emissions rise and fall with the particular energy mix being used at any one time. At the time of writing, the mix has recently been subject to a rise in coal input to electricity generation of almost 25% in the UK (DTI, 2006a) as North Sea gas production and nuclear output are reduced. From these figures it can be deduced that space heating UK domestic property alone accounts for a significant proportion of UK greenhouse gas emissions.

Parts of the developed and developing world are becoming more demanding of energy as greater comfort conditions are sought. As world population rises from the current 6.5 billion to the predicted 10 billion over the next half century (DESA, 2004; Lutz et al, 2004), the imperative of ensuring greater energy efficiency in buildings becomes vital. This may be achieved through greater levels of insulation and through increased capture, storage and use of passive gains, such as arise from solar irradiation or internal activities. Recent developments in the UK, such as the BedZED project in south London (Twinn, 2003 & Lazarus, 2003) and the Jubilee Wharf project in Penryn, Cornwall, have

shown the potential, in the UK climate, to obviate the need for dedicated heating systems altogether by making dynamic use of the thermal properties of structural building materials to capture and release passive gains.

The rise in global temperatures (Alexander et al, 2006) creates the risk of more buildings overheating beyond acceptable comfort conditions (Hacker et al, 2005), which is leading to increased electricity consumption through greater use of air conditioning (Parkpoom et al, 2004). Organisations such as the American Society of Heating (2003) and the Concrete Centre (de Saulles, 2005) show how, in combination with the benefits of thermal storage, the thermal mass of building structures can, in absorbing excess heat, reduce the demand for additional cooling.

In order to design for passive energy systems in this way, knowledge of the thermal properties of the building materials employed is a prerequisite.

Reduction in fossil fuel consumption through better insulation, and the reduced need for heating and cooling systems, would lead to financial benefits for building owners, as well as environmental benefits. The average UK domestic energy bill has recently risen to over £1,000 per annum for the first time, with some 2.5 million homes living with fuel poverty, where more than 10% of household income is spent on heating the home (dti, 2006b). Domestic energy prices have risen by 35% over two years between 2004 and 2006 (FPAG, 2007). It may be borne in mind that the initial costs of improved insulation, or passive heating and cooling, may be offset against savings which accrue through the lifetime of a building.

Best practice for energy use in new building, at the time of writing and as outlined in EcoHomes 2006 (BREEAM Office, 2006) and the Standard Assessment Procedure for Energy Rating of Dwellings (DEFRA, 2005), does not fully recognise the potential benefits of passive gains. The received wisdom is that considered orientation of normal window sizes, with due care to airtightness and insulation levels, can lead to energy savings in the region of 20% compared to developments built only to current building regulation standards and with random orientation (Spanos, 2005). The Energy Saving Trust (1997) are more conservative and predict just 8% – 10% potential savings using passive solar designed houses with passive solar estate layouts. It is the author's conviction that projects such as BedZED are leading the way to much higher fossil fuel energy savings but that take up is limited, in part, by a lack of reliable information on the thermal properties of building materials and a lack of understanding on how to design for, or model, such passive gains using these thermal properties.

Traditionally, there has been no tool readily and economically available to construction professionals that can reliably measure the thermal properties of building materials. This work assesses the suitability of thermal probe technology, which has often been used in other industries, to quickly and economically measure the thermal conductivity, thermal diffusivity and, hence, the volumetric heat capacity of building materials, simultaneously, either in situ or as characteristic samples.

Motivation for the work comes from the potential to reduce harmful greenhouse gas emissions as well as from a natural curiosity to see whether the theoretical

and practical obstacles to the successful application of the thermal probe method can be overcome.

Approaches to the research

The two thermal properties of materials that are of most interest to this project are thermal conductivity (λ) and volumetric heat capacity (ρC). The thermal conductivity of a material determines the rate of heat flow through it, hence the level of thermal resistance or insulation that can be achieved by incorporating that material into a building envelope. Volumetric heat capacity determines the quantity of heat energy that a material is able to absorb in relation to its temperature change, hence its contribution towards both storing and reducing heat gains, to reduce heating and cooling loads respectively. This section starts with an introduction to these thermal properties and then provides a background to the thermal probe technique, before presenting the structure of the thesis.

Thermal conductivity

Fourier in the early 19th century, following experiment and observation, developed his theories regarding steady-state heat conduction. Where this was in one direction through a homogeneous and isotropic solid, it would give rise to equation (1), where the heat flux (Q') was dependent on the thermal conductivity of the material, the cross sectional area of the material (A), and the temperature difference over distance (x) (Fourier J et al, 1888).

$$Q' = \frac{-\lambda . A(T_1 - T_2)}{x}$$

Equation (1)

The symbol λ denotes thermal conductivity, which is a fundamental property of a material and, in the case above, determines the heat flux through that

material. The units used to describe thermal conductivity are $Wm^{-1}K^{-1}$ and, as watts are comprised of joules (a basic unit of energy) per second, the units describe the quantity of energy over time transferred through one metre of material with a temperature difference of 1K (or 1°C). Thermal conductivity values of building envelope components are used to calculate potential levels of heat loss from buildings using 'U' Values, with units of $Wm^{-2}K^{-1}$, denoting the quantity of energy that would be lost through an area of building envelope at a steady state, where the external temperature was lower then the internal temperature.

In transient conduction, equation (1) is combined with the principle of conservation of energy. In three dimensions, this results in the heat conduction equation (2), which forms the basis for most of the heat conduction analyses relevant to the thermal probe transient line source methodologies, as described in chapter 2, the literature review.

$$\frac{\partial}{\partial x}\left(\lambda\frac{\partial T}{\partial x}\right)+\frac{\partial}{\partial y}\left(\lambda\frac{\partial T}{\partial y}\right)+\frac{\partial}{\partial z}\left(\lambda\frac{\partial T}{\partial z}\right)+Q^{*}=\rho C\frac{\partial T}{\partial t}$$

Equation (2)

Heat transfer occurs when a temperature gradient exists in or between materials. The transfer can occur by three distinct means:

- Conduction
- Convection
- Radiation

Often a combination of these can take place simultaneously, such as: in a porous or granular opaque material, heat transfer through the solid component may occur by conduction, and through pores containing air by convection and radiation; or, in a translucent solid, both conduction and radiation may occur

through the solid. Convection, as a generic term, may include mass transfer, where, in gases and liquids, the density of material is reduced by heat induced expansion and thus the warmed material rises through the effects of buoyancy.

This project concerns the effective thermal conductivity of construction materials, that is the overall potential for heat loss through the body of these materials. No distinction has therefore been made between thermal conductivity, which relates to a property of a homogenous isotropic material, and effective thermal conductivity as defined in BS EN ISO 7345:1996 (BSI, 1996), which is used for regularly inhomogeneous materials, including granular or fibrous materials with voids.

Heat transfer from, and into, buildings may occur by convection (including mass transfer), for example in passive ventilation systems, or by radiation, for example through glazed elements. These two forms of heat transfer do not form part of the current work.

Volumetric heat capacity

The heat capacity of materials is a fundamental property and describes their ability to store heat. The specific heat capacity, C ($Jkg^{-1}K^{-1}$), describes the energy in joules required to raise the temperature of one kilogram of material by one degree Kelvin. The volumetric heat capacity, ρC ($Jm^{-3}K^{-1}$), describes the energy in joules required to raise the temperature of one cubic metre of material by one degree Kelvin, which energy may then be considered to be stored within that material.

Materials with high specific heat capacity may, where they have low density, be of limited use as energy storage mediums. For example, the specific heats of air

and concrete at room temperature are in the region of 1,007 $Jkg^{-1}K^{-1}$ and 880 $Jkg^{-1}K^{-1}$ respectively, whereas their volumetric heat capacities are in the region of 1,170 $Jm^{-3}K^{-1}$ and 2,024,000 $Jm^{-3}K^{-1}$ respectively.

In considering the heat storage capacity of building materials in situ, it is the volumetric heat capacity of materials which is of interest, that is the heat storage capacity of any particular building element at its particular density. It should be noted that if the volumetric heat capacity of the material can be found directly, there is no need to establish the density of the material to understand its heat storage capability. This means that samples may not need to be taken, weighed and measured, thus avoiding potentially destructive testing.

Thermal diffusivity

Thermal diffusivity, α (m^2s^{-1}), describes the ratio of thermal conductivity to volumetric heat capacity:

$$\alpha = \frac{\lambda}{\rho C}$$

Equation (3)

Materials with a large thermal diffusivity respond quickly to changes in their thermal environment, while materials with small thermal diffusivity values will take longer to reach equilibrium with their surroundings (Incropera & DeWitt,1996). It is of note that where α and λ are known, volumetric heat capacity, ρC, can be established immediately. The literature review, chapter 2, will show that this feature has frequently been relied upon in thermal probe analyses.

Introduction to the thermal probe technique

Thermal probe technology approximates transient line source theory. From Fourier's early 19th century work, researchers, such as: van der Held (1932); Carslaw and Jaeger (1947); and Blackwell (1953 and 1954), showed that, where an infinitely long and infinitely thin line source is heated at a constant power within an infinitely large homogenous, isotropic and thermally stable material, the chart of temperature rise over the natural logarithm of time would, after a short time, be linear with a slope dependent on the thermal conductivity of the material, and intercept dependent on its thermal diffusivity. Thermal diffusivity is the relationship between thermal conductivity and volumetric heat capacity, hence the latter can be found directly from the first two.

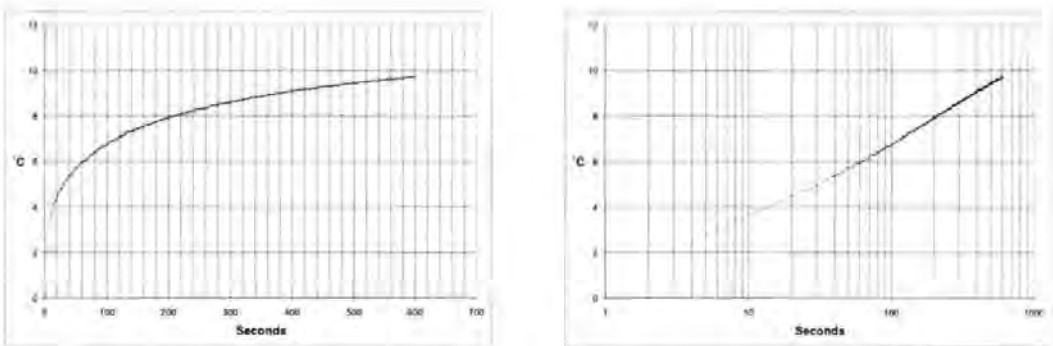

Figure 1: Example charts of temperature rise over time for aerated concrete

Figure 1 shows an example of data achieved from a thermal probe (Figure 2), which approximates an infinitely long and infinitely thin line source, heated within aerated concrete. The presence of a physical probe, finite dimensions and experimental conditions have given rise to various corrections and approximations to the fundamental transient line source theory. Such approximations have been employed to measure the thermal properties of

various building materials at the University of Plymouth, in thermally controlled, laboratory conditions (Goodhew and Griffiths, 2004, 2005).

Figure 2: A Hukseflux TP08 thermal probe

Three unknowns exist in the established equation (4) that represents the heating curve of the probe during a measurement cycle: thermal conductivity (λ); thermal diffusivity (α); and a property with notation *H*, which has not been defined absolutely but is usually taken to denote the reciprocal of contact resistance between the probe and sample material, sometimes termed probe conductance. Further explanation of equation (4) is given in chapter 2, the literature review, indexed there in two forms as equations (7) and (14), and in a further form in chapter 4, indexed there as equation (33).

$$\Delta T \cong \frac{Q'}{4\pi\lambda}\left\{\ln\left(\frac{4\alpha.t}{r^2}\right)-\gamma+\frac{2\lambda}{r\,H}+\frac{r^2}{2\alpha.t}\left[\ln\left(\frac{4\alpha.t}{r^2}\right)-\gamma+1-\frac{\alpha.M_p C_p}{\pi.r^2\lambda}\left(\ln\left(\frac{4\alpha.t}{r^2}\right)-\gamma+\frac{2\lambda}{r\,H}\right)\right]+O\left(\frac{r^2}{\alpha.t}\right)^2\right\}$$

Equation (4)

Apart from these three unknowns in equation (4), many other unknowns were foreseen in taking forward the previous laboratory work, regarding the practical application of the thermal probe approach. These included: the effect of reduced contact between the probe and sample with the varying hole diameters envisaged when drilling coarse materials; the effects of different fillers used to improve contact; lack of or incomplete fillers; and whether heat from the hole drilling process or heating cycles would cause sufficient moisture migration,

where moisture was present in the material of interest, to significantly affect results.

The effects of external environmental conditions expected with in situ measurements were unknown, such as temperature fluctuations, temperature levels, direct solar irradiation and wind effects on the probe and on the sample material. Levels of error arising from heat losses at the probe ends and axially along the probe to the ends were unclear. The effects of different circumstances at each probe end were unknown, as one would be inserted into the sample material and the other attached to the probe base and cables. These and the sample adjacent to the probe entry location would be exposed to the surrounding air. Levels of error from heat losses at, or reflections from, the boundary of the sample were unclear, as were the effects of sample material non-homogeneity, anisotropy, or possible radiant and convective heat transfer mechanisms within the sample material. Also to be assessed were the length of time required for a probe to sufficiently stabilise its temperature with that of the sample before a measurement, either following insertion or between successive measurement heating cycles.

Further unknowns in the practical application concerned the equipment, measuring and logging devices to be used, whether current and temperature rise could be measured with sufficient accuracy over time, whether current could be sufficiently controlled and whether data storage and handling could be sufficiently robust.

In considering the resolution of these numerous interrelated unknowns, and bearing in mind the dearth of available relevant control or reference materials

with known thermal properties (Touloukian and Buyco, 1970; Zarr and Filliben, 2002; Tye, Kubičár and Lockmuller, 2005), a loosely structured and flexible set of experiments, combined with a literature review, was developed, initially using pre-existing laboratory based equipment before constructing a robust field apparatus.

The structure of the thesis, which outlines this overall methodology, is given in Figure 3. The introduction now considers the regulatory framework surrounding the energy efficiency of buildings, before examining alternative sources and measurement methodologies used to establish the thermal properties of building materials.

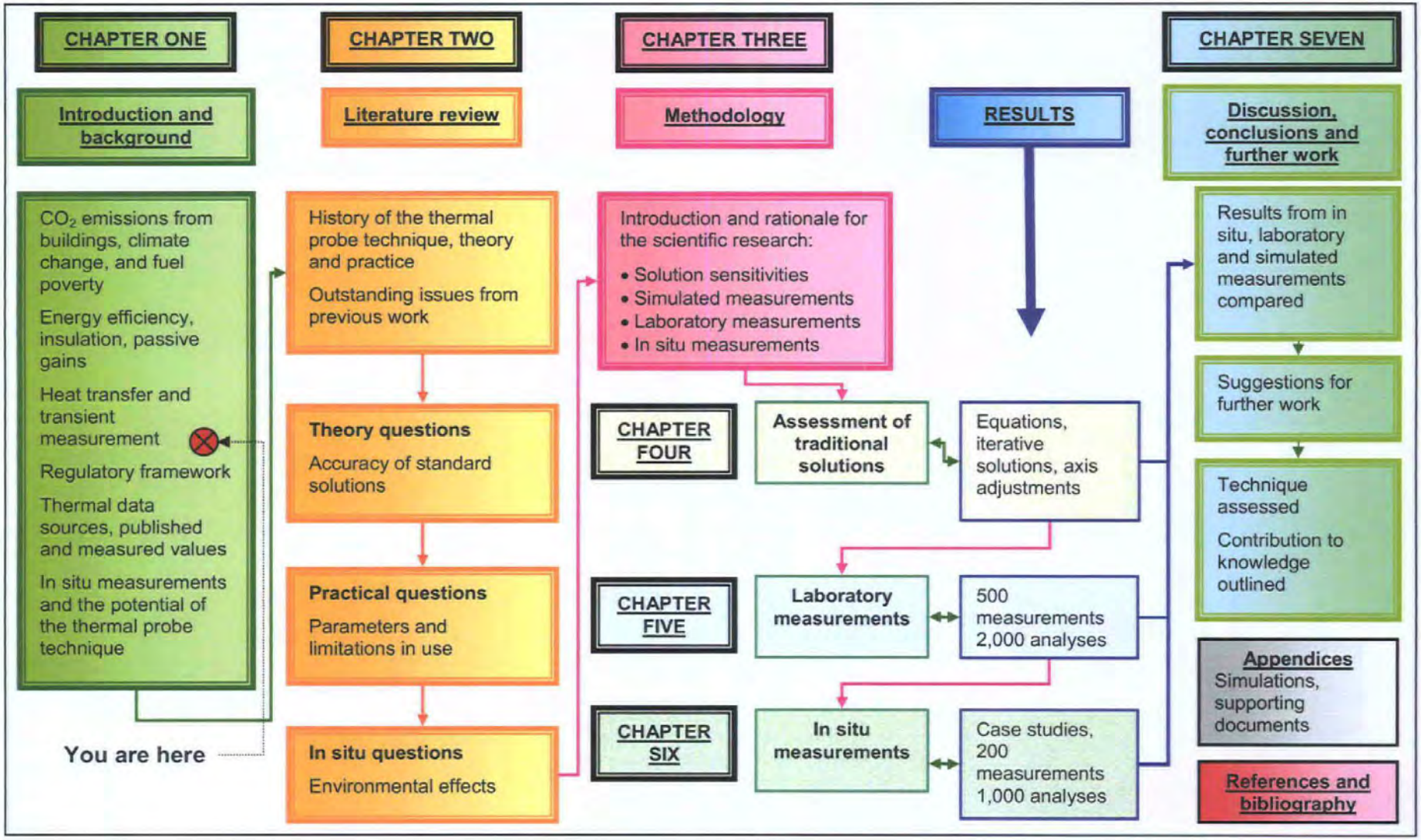

Figure 3: Structure of the thesis

Regulatory framework

The construction of new and proposed UK buildings has principally been controlled through a system of building regulations since the great fire of London in 1666. Poor health conditions of an increasing population during the industrial revolution led to the Public Health Act 1875, which was significantly revised in 1936 and 1961. The first set of national building standards appeared as The Building Regulations 1965 (these have now been superseded by The Building Regulations 2000 (as amended) under The Building Act 1984). The regulations were developed historically to legislate for safer and healthier buildings. The specific provisions for the conservation of fuel and power did not appear until 1979 (Powell-Smith and Billington, 1995), as the environmental impacts of energy use became more apparent.

Global carbon emissions from energy generation by fossil fuel burning are rising (Figure 4) and the resultant climate change is believed to be near, or past, a tipping point, where effects, such as sea level rise and dangerously increased global average temperatures, are irreversible (Lindsay and Zhang, 2005; Hansen, 2005; and Lovelock, 2006), as atmospheric carbon dioxide levels rise (Figure 5). This is driving and accelerating the regulatory control of building energy use at local, national, European and global levels.

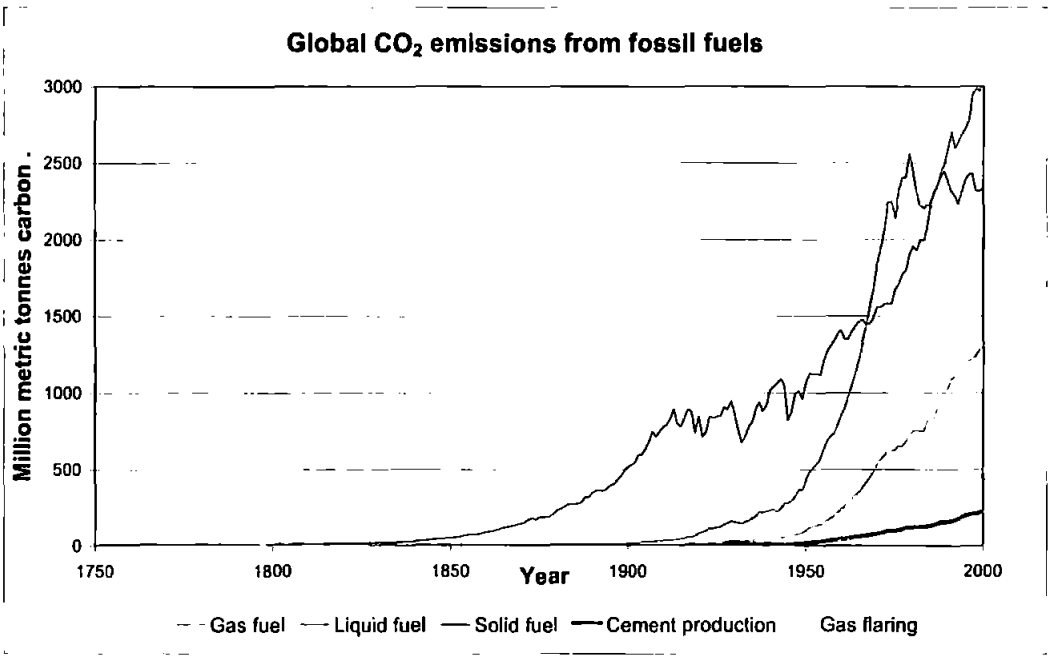

Figure 4: Global carbon emissions from fossil fuel burning (Marland et al, 2003)

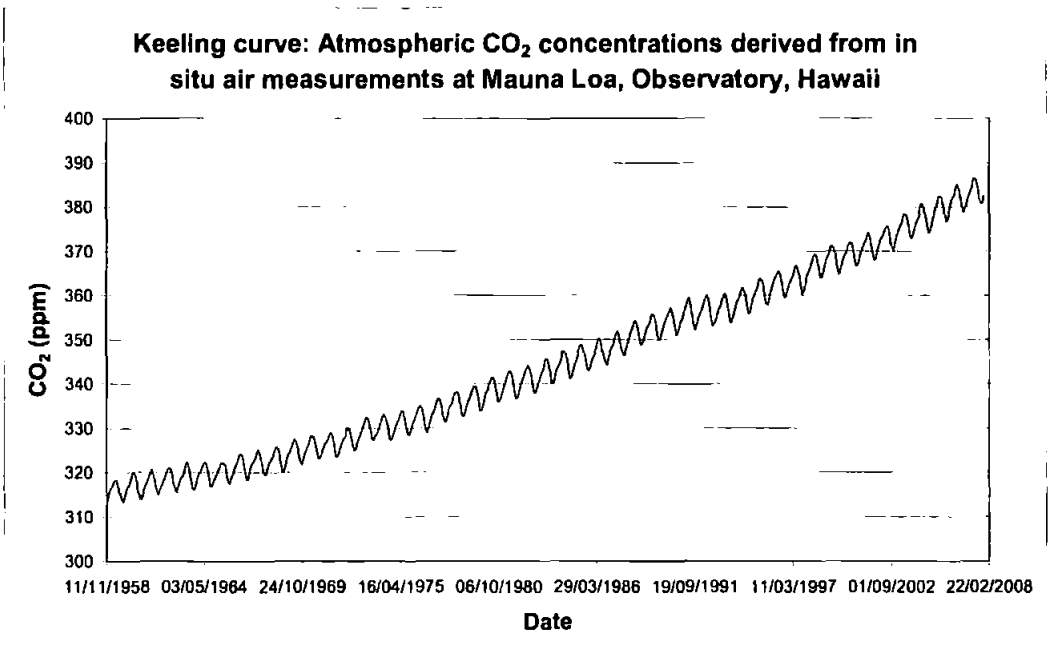

Figure 5: Keeling Curve of atmospheric carbon dioxide (Scripps, 2007)

The Building Regulations are supported by Approved Documents that provide a range of solutions to meet the requirements of the regulations. The European

Energy Performance of Buildings Directive, which came into being in 2002, has a stated purpose to:

"promote the improvement of energy performance of buildings within the Community taking into account outdoor climatic and local conditions, as well as indoor climate requirements and cost-effectiveness".

This has led, at the national level, to revisions of Approved Document Part L to the Building Regulations. Compliance had previously been possible through an elemental method whereby a whole building was considered sufficiently energy efficient if each element, such as floor, wall, roof, etc. met minimum standards of insulation. This has been abandoned in favour of a Standard Assessment Procedure (SAP) to calculate a building's overall environmental impact in terms of energy use and carbon emissions. Dedicated software programmes have been developed to carry out the calculations, such as the Simplified Building Energy Model from the BRE for non-dwellings, or numerous private sector software packages recommended by the BRE for dwellings.

SAP 2006 recognises that volumetric heat capacity of materials, commonly referred to as their thermal mass, can play a part in reducing overheating in buildings, and hence saving on cooling energy. However, it does not yet provide a calculation methodology or suggestions for dedicated passive solar designs whereby solar or other passive gains are stored in thermal mass for later release (Todd S, 2006).

A reliable and economical method of measuring volumetric heat capacity, and thermal diffusivity, could further the attainability of passive solar, low or zero carbon design and allow hard data to be used in modelling building designs. Once such savings can be accurately and reliably quantified and measured,

they can contribute not only to revised SAP calculations but to the higher requirements of the Code for Sustainable Homes (DCLG, 2006).

Passive technology can also help in meeting the Government's stated 2016 target, supported by the WWF, for new homes to create zero additional carbon emissions (Kelly, 2006). The current technical guidance for the Code for Sustainable Homes, as part of the strategy towards this target, recognises the importance of the building fabric in reducing energy demand but only in regard to insulation levels and airtightness (DCLG, 2007). This appears to be a lost opportunity regarding capture of zero carbon passive gains, and a risk regarding potential overheating of well insulated, airtight homes with little ability to absorb excess heat gains.

The construction industry has traditionally resisted radical change, as planning for developments is a long term process, material lead in times are long, and material manufacturing bases are firmly established. The industry may not see increased profit from changes, such as increased levels of insulation. An example of such resistance was illustrated by industry lobbying against more onerous requirements proposed for Part L of the Approved Documents to the Building Regulations in 2001. This resulted in the draft requirements being eased, notably with allowable heat loss through walls increasing from an initial target of 0.25 $Wm^{-2}K^{-1}$ through 0.3 $Wm^{-2}K^{-1}$ in the published draft to a final figure of 0.35 $Wm^{-2}K^{-1}$ (Ross, 2001).

The industry is changing, though, and many of the UK's leading construction companies have joined together, with the support of Government, the WWF and others, to form a UK Green Building Council with the mission statement:

"To dramatically improve the sustainability of the built environment by radically transforming the way it is planned, designed, constructed, maintained and operated" (UK-GBC, 2007).

The UK-GBC, along with organisations such as the Energy Saving Trust and the Carbon Trust, offer hope that environmental impacts of buildings will be reduced with regard to energy efficiency, although the current regulatory framework does not recognise the extent that passive heating and cooling can contribute towards lowering emissions from buildings. This is despite solar irradiation falling on a typical $80m^2$ UK building footprint being in the region of 88 MWh per year (Energie-Atlas GmbH, 2007), over four times the average, measured energy usage of existing buildings in south west England, at 21.5 MWh per year (Chambers et al, 2005). An obstacle to the take up of low energy, passive solar design is the lack of reliable thermal data on building materials.

The upgrading of existing buildings and the thermal modelling of all new buildings, under current regulations, requires heat loss calculations for the building envelope. These are based on the thermal conductivity of the materials used, as in standard 'U' value calculations. The following two sections consider the thermal data sources and measurement methods currently relied upon in building design. The chapter concludes with a rationale for adopting the thermal probe technique.

Data sources for the thermal properties of building materials

There are three distinct areas from which building designers can currently obtain thermal data for building materials. These are:

- Published values
- Commissioned measurements

- Empirical knowledge and experience

There follows an overview of current published sources and measurement techniques. The assessment of empirical knowledge available to the industry does not form part of this work.

Published values

A standard work for material thermal properties is Touloukian's Thermophysical Properties of Matter, published by Plenum in 14 volumes between 1970 and 1979. Only small parts of this work deal with compounds and minerals relevant to the study of building materials, and the composition of similar building materials is variable. As an example, Touloukian (1970a) gave 338 separate and distinct values for the thermal conductivity of concrete, dependent on exact mix and density. None of these measurements related to concretes containing moisture. No values were given for the thermal diffusivity or volumetric heat capacity of concrete. As concrete mixtures vary by location, dependent on local sources of aggregate, mix proportions by manufacturer, and variations by the same manufacturer on different days, by cement and pulverised fuel ash content, etc. and by moisture content in use, these values can not be relied upon for accurate thermal modelling and prediction.

Another standard work is the Handbook of Chemistry and Physics (Lide et al, 2004), which listed few building materials. It gave thermal conductivity values for various rocks, although these values in situ would vary dependent on the particular make up of the rock, its density and grain. No guidance on the thermal diffusivity or volumetric heat capacity of rocks was given.

The National Institute of Standards and Technology in the USA (NIST) provides an online, searchable database entitled Heat Transmission Properties of Insulating and Building Materials (Zarr, 2000). Many of the values given for thermal conductivity (no data was given for thermal diffusivity or volumetric heat capacity) are historic. 80 values were given for concrete, based not only on density but also on the manufacturers' names. As many of the measurements given were carried out in the 1940s and 1950s, and many companies have ceased to trade or changed their names, this is of limited use to contemporary building design. NIST decommissioned most of their thermal testing equipment in the early 1960s and retired their guarded hot plate in 1983 (Svincek, 1999).

The CIBSE Guide (Oughton et al, 1986) has more comprehensive tables of thermal conductivity values for building materials. These were mostly based on historical data which have been extrapolated using empirical relationships to give values for varying density and moisture content. The guide recognised that actual values can vary radically from those given. Only a few, rounded and approximate, values were given for specific heat capacity, from which, as density was also given, volumetric heat capacity values could be estimated. However, this would increase the level of approximation and, as with the thermal conductivity values, the results could be unreliable and likely to be unsuitable for accurate thermal behaviour prediction.

The ASHRAE Handbook (Parsons, 2005) gave historical values for thermal conductivity and a few values for specific heat capacity, sometimes given with density, of various building materials. However, these values were usually given as ranges with the caveat that they may differ in situ and with manufacturing variability.

Guide thermal property values are often to be found in building science books, such as McMullan (1992), Szokolay (2004), etc. Generally just one value per material or material type is given, whereas we see from Touloukian and others that values can vary significantly in particular circumstances.

The limited ranges of values in the standard works are usually given for the more manufactured materials commonly found in industrialised societies, such as concrete, gypsum plaster, expanded foam, etc. Values for more innovative or localised materials, such as earth, lime or hemp based, are harder to find in the literature, and may be more variable. As an example, Norton (1997) gave a range of thermal conductivity values from 0.45 $Wm^{-1}K^{-1}$ to 0.65 $Wm^{-1}K^{-1}$ for earth based materials, while Middleton (1987) gave 1.3 $Wm^{-1}K^{-1}$ to 1.4 $Wm^{-1}K^{-1}$. Neither of these publications gave values for the thermal diffusivity or volumetric heat capacity of earth based materials.

This short review has shown that the standard reference works for obtaining thermal property values for building materials can not be relied upon to give reliable and accurate data for materials used in the field and incorporated into real buildings. Without reliable data for materials generally, it follows that thermal property value estimates for materials subject to changes caused by environmental conditions, such as changes to moisture content, would be equally or more unreliable.

Where values are required for building design, it is usually recommended that the particular materials envisaged should be subjected to actual measurements. For instance, the ASHRAE Handbook (Parsons, 2005) qualified its table of thermal values by stating that they are not for specification use and that, for any

particular product, the manufacturer's value or one achieved through unbiased testing should be used. Manufacturers frequently give thermal conductivity, and less frequently heat capacity values, for their materials, based on measurements by standard means. Current measurement methods are considered in the next section.

Approaches to measuring the thermal properties of building materials

The previous section reviewed the efficacy of relying on published values for the thermal properties of building materials and concluded that accurate and reliable data was more likely to be achieved through measurement of the particular materials, or representative material samples, to be used. This section reviews contemporary issues regarding the measurement of thermal conductivity and volumetric heat capacity of prospective or in situ building materials.

Thermal conductivity tests of building materials are generally carried out by guarded hot plate measurement to: BS EN 12667 (BSI, 2001a) for low or medium thermal conductivity; BS EN 12664 (BSI, 2001b) for dry and moist materials with medium and high thermal conductivity, generally taken to be above 2.0 $Wm^{-1}K^{-1}$; or BS EN 12939 (BSI, 2001c) for thicker materials, generally above 150mm, with low or medium thermal conductivity.

Measurements in the UK are carried out in laboratories accredited by the United Kingdom Accreditation Service (UKAS), such as exist at the National Physics Laboratory (NPL). A search of the UKAS website (19/04/2007) showed eight laboratories in the UK accredited to carry out guarded hot plate measurements, and none listed to measure heat capacity. Laboratories undertaking guarded

hot plate measurements of construction materials also have to meet the requirements of BS EN 1946-2 (BSI, 1999a). With few accredited laboratories, the time consuming preparation of samples, the expense of meeting the criteria and becoming accredited, such measurements are expensive. Measurement costs for just a few samples can run into many thousands of pounds.

The guarded hot plate essentially works by, in an insulated system, measuring the heat energy required to keep one face of a material at a constant temperature while the further face is kept at a lower temperature. This is a steady state measurement. The measurement is taken when the heat energy input remains constant, hence the material must not be undergoing any physical changes.

A significant physical change that can occur during such testing is the migration of moisture, hence the majority of tests are carried out on dry materials, as a steady state will not be reached while the change is occurring. BS EN 12667, for materials with thermal conductivity below 2.0 $Wm^{-1}K^{-1}$, which includes the majority of insulating materials of interest in buildings, does not have a procedure for measuring moist materials. Jespersen (1953), who used a form of guarded hot plate to measure moist materials using low temperature difference and sealed samples, showed the likely percentage increase in thermal conductivity of various building materials by moisture content, with lightweight materials such as rock wool increasing by 100% with 2% moisture content by volume.

BS EN 12664 gives guidance on measuring moist materials over 2.0 $Wm^{-1}K^{-1}$, within their normal hygroscopic range, although this gives rise to greater error

and involves very long times in sample conditioning. BS EN ISO 10456 (BSI, 1999b) provides guidance on conversion factors for a limited range of materials where the dry thermal conductivity value is known and the current moisture content is known.

Dryness, according to BS EN 12664, is when the mass of the material heated in an oven at 105°C, vented to air at 23°C with 50% relative humidity, does not change by more than 0.1 $kg.m^{-3}$ over a 24 hour period. Once dried, the sample normally needs to be contained in a vapour tight envelope to prevent hygroscopic moisture take up. In both BS EN 12667 and BS EN 12664, consideration has to be given to the contact resistance between the equipment's plates and the sample, and the effects of the vapour tight envelope on this resistance.

The thermal properties of samples dried or conditioned in this way, even where accurate values are obtained, are unlikely to be representative of the materials as they would be in real buildings, exposed to variable external and internal environmental conditions. However, in a market economy, manufacturers may have a preference for measured values that show their products' performance is as proficient as possible, and dry materials invariably have lower thermal conductivities than materials containing moisture. Dry values, obtained through established and accredited means, are then used in design specifications and, as Doran (2000) observed when reporting Building Research Establishment work for the Department for Environment, Transport and the Regions (DETR), this leads to buildings not performing as expected.

With a supposed accuracy of better than ± 2% for results by BS EN 12667, work for the European Union by Salmon et al (2002) showed that steady state measurements may not always be so reliable. A dry hollow brick type supplied from a single manufacturer was tested at 6 separate laboratories. The results for thermal conductivity values ranged from 0.256 $Wm^{-1}K^{-1}$ to 0.416 $Wm^{-1}K^{-1}$.

Volumetric heat capacity values of building materials are harder to reliably achieve than values for thermal conductivity. There is no British Standard method and the ASTM method (ASTM Committee E37.01, 2005) relies on differential scanning calorimetry (DSC) and is not generally suitable for building materials. DSC relies on minute samples, measured in micrograms, and the nature of building materials, often composite and less than homogenous, results in non-representative sampling.

An alternative to the DSC is the method of mixtures using a drop calorimeter, as illustrated by Touloukian and Buyco (1970). A sample is prepared, heated and dropped into a liquid of known thermal properties at a known temperature within an insulated container. From the change in temperature of the liquid, the heat capacity of the material can be calculated. While this provides a reasonably accurate result, it may not be representative of the material in situ, depending on whether moisture content or other physical properties are changed during heating or sample preparation, and whether the sample is representative of the average value for the bulk material.

The previous two sections have suggested that neither published values or current measurement methods can be relied upon to give accurate, representative values for the thermophysical properties: conductivity; diffusivity;

and volumetric heat capacity, of building materials as found in, or proposed for, real buildings. The lack of available and reliable data for in situ thermal properties, and the imperative of improving energy efficiency in buildings, show the benefits that would be gained from a simple, fast, economic tool that could simultaneously measure these properties. The thermal probe technique, as previously used to measure materials in a laboratory environment at the University of Plymouth, potentially offers such a solution.

Chapter 2 investigates the thermal probe technique through a broad literature review. The investigation includes the theoretical and practical development of transient line source measurements, with a particular focus on their relevance to materials of the type used in construction. This is followed in chapter 3 by an introduction to the methodologies used in the subsequent investigation of outstanding issues.

Chapter 2: Literature review, the thermal probe

Introduction to the primary literature review

The previous sections have shown the current lack of suitable methods to obtain reliable values for the thermal properties of building materials, whether as representative samples or in situ. This literature review aims to establish the existing and potential value of the thermal probe approach towards measuring the thermal conductivity (λ), thermal diffusivity (α) and volumetric heat capacity (ρC) of building materials in situ and to determine the likely steps needed to take the technique forward.

The historical developments of the probe and theory are outlined in approximately chronological order. This starts with a section on the early history of the method, before a comprehensive theory was developed. This is followed by a description of work that took place around the middle of the 20th century, when the theoretical bases used today, of thermal conductivity and thermal diffusivity measurements by hot wires and thermal probes, were established. A critique of later researchers' applications of the theoretical work is then given. Current standards relating to the thermal probe are described. Issues arising from the literature review are then discussed and areas for further study identified.

The review includes work in diverse industries and research areas, such as geotechnical studies of soils and rocks, using the thermal probe and other similar methods, as well as prior uses of the technique to measure the thermal properties of building materials.

The early history of the thermal probe

Schleiermacher (1888) was a pioneer of measurements by a line source in the late nineteenth century. The thermal conductivities of gases were measured using a hot wire technique. A cylinder held the gas to be measured and a heating wire was placed along its axis. The current, and temperature of the wire, gas and cylinder, were measured and the thermal conductivity calculated. By 1903 this technique had become known as the Schleiermacher Method (Schwarze, 1903).

Niven (1905) carried out experiments with a platinum wire acting as a line source of heat along the central axis of solid cylindrical samples, including various timbers and sands (Figure 6). Platinum wires or thermocouples were used to take temperature readings at a choice of radii across the sample, which had sufficient dimensions that were considered adequate to avoid the effects of heat losses at the boundary during measurements. Thermal conductivity was calculated from the temperature difference between the radii once a steady state had been reached in the sample, which occurred after a number of hours. Thermal diffusivity values were not reported but said to be available from the calculations, based on the elapsed time taken to reach the steady state.

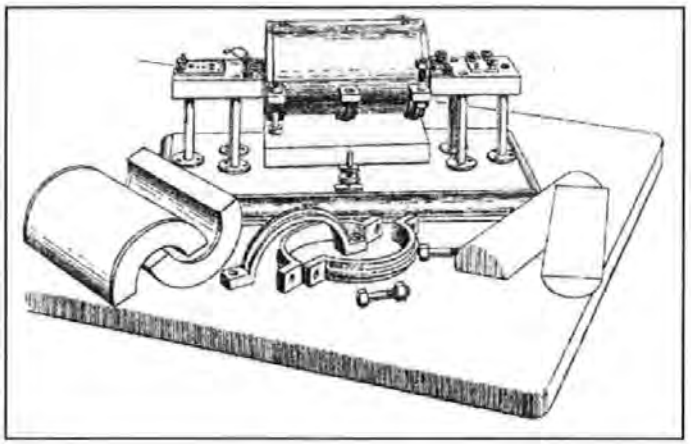

Figure 6: Niven (1905), hot wire apparatus showing a timber sample prepared

Stalhane and Pyk (1931) developed the technique, cased the hot wire within a tube and attached a mercury thermometer, forming a similar arrangement to that used today, albeit with older technology (Figure 7). They are commonly accredited, along with Albrecht (1932) also working in Scandinavia, with the initial creation and implementation of the time-dependent methodology employed by later researchers and practitioners.

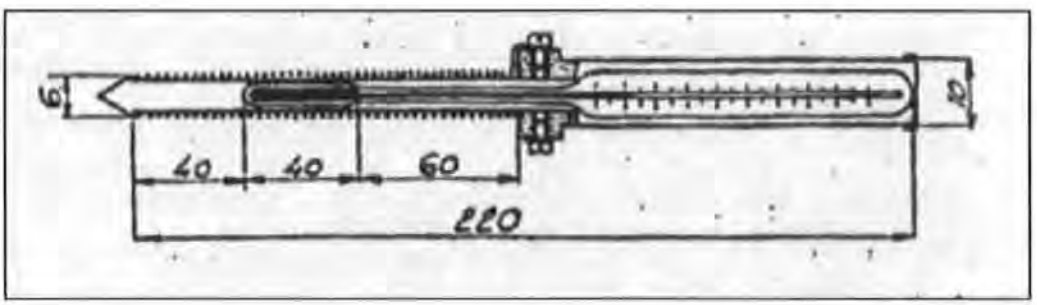

Figure 7: Stalhane and Pyk (1931) thermal probe

Carslaw (1921), Carslaw and Jaeger (1940, 1947, 1948) and Jaeger (1944) were significant early contributors to, and compilers of, mathematical and theoretical solutions to heat conduction problems, including those of radial heat flow from a heated cylinder within a solid medium. Jaeger cited Whitehead and

Hutchings (1938) as having developed the approximate solution for this particular problem. Whitehead (1944) was chiefly concerned with heat conduction effects to and from underground pipes and cables.

Carslaw and Jaeger (1948 pp.280-286) noted that their solution for radial heat transport in a composite cylinder, e.g. a thermal probe within a cylindrical or infinite sample, "corresponds roughly to the transient heating of a buried cable carrying electric current" although "a still closer approximation" would include contact resistance between the cable and the surrounding medium. This contact resistance was also described as outer or exterior conductivity, termed H, with units $Wm^{-2}K^{-1}$ (Carslaw and Jaeger, 1948 pp.13-14). H was considered a constant, with the heat flux between two touching faces of material given as $H(T_1-T_2)$, showing that its effect was dependent on the temperature difference between the two faces. No calculations were given to allow the determination of H theoretically, although some example values were given. These showed that, at similar temperatures and pressures, H could vary greatly between one material, e.g. a thermal probe, and various other materials, such as water and air.

It was maintained that, where a heat flux existed across two materials, temperature at their touching surfaces could only be assumed equal where there was intimate contact, such as in a soldered joint. A contact resistance would still exist even where two optically flat surfaces were pressed together (Carslaw and Jaeger, 1948 pp.17-18).

This was carried forward to a description of thermal resistivity in a composite wall where the total thermal resistance was described as being made up of the

thermal resistance inherent to each material plus the product of contact resistances and temperature differences between each pair of materials (Carslaw and Jaeger, 1948 pp.75-76).

An analogy is thus provided for a thermal probe containing various components, such as a heater wire, a temperature measurement device, a filler and an outer sheath, with separate thermal properties and contact resistances between them. (As an aside, this may also be of interest to the study of composite or layered insulation materials).

Another matter of interest arises from the table of thermal properties given by Carslaw and Jaeger (1948, A.VI). Values are given for timber, namely spruce, of similar density. Thermal conductivity along the grain is given as 83% higher than the value across the grain, yet the specific and, consequently, volumetric heat capacities are shown as equal. As thermal diffusivity α is defined as $\lambda / \rho C$, this results in a 88% higher value for thermal diffusivity along the grain.

Van der Held (1932) was interested in measuring the thermal conductivity of liquids by a transient line source, using a hot-wire. Stalhane and Pyk (1931) had empirically deduced mathematical constants *A* and *B* to establish a value for thermal conductivity in the solution of:

$$\theta = A\frac{Q'}{\lambda}\ln\left(\frac{r_{wire}^2}{t} + B\right)$$

Equation (5)

As the change in temperature after an elapsed time, power input and dimensions could all be measured, a thermal conductivity value, as the only unknown remaining, could then be calculated. Van der Held mathematically

deduced values for *A* and *B*, introducing material dependent thermal diffusivity and Euler's constant (γ) to the calculation.

Van der Held and Van Drunen (1949) outlined the basis for non-stationary, or transient, thermal conductivity measurement as the recording of the temperature at the mid point of the heating wire and the plotting of the temperature rise over the natural logarithm of time, thermal conductivity being deduced from the slope of this straight line by the term:

$$\theta = \frac{Q'}{4\pi.\lambda}$$

Equation (6)

It was maintained, from calculations, that the diameter of the line source, which had been increased by encasement within a glass capillary tube, displaced rather than altered the slope of $\Delta T/\ln t$ after the first few seconds.

Calculations based on measurements of carbon tetra chlorine suggested that axial and end heat losses could be ignored for the duration of the measurement period, as the error would be less than 5% after 4,800 seconds for axial losses, dispersion of heat along the probe, and less than 0.5% for the duration of the measurement for end losses, loss of heat from the probe ends. It was assumed that after a few seconds the temperature at the surface of the capillary tube maintained a constant difference to the temperature of the thermocouple on the heater wire placed within it.

This assumption is open to question as Carslaw and Jaeger (1948 pp.13-14) deduced that, while contact resistance may have a constant value, its effect was a product of contact resistance and temperature difference. As the heater

temperature rises more slowly after an initially steep rise, it would seem that the temperature difference between the heater wire and material may reduce at later times.

Hooper and Lepper (1950) recognised the limitations of the guarded hot plate method of measuring thermal conductivity in their investigation concerning the thermal properties of moist soils. Not only did moisture migration present difficulties but the physical structure of the soils had to be disturbed to prepare samples, problems previously recognised by Patten (1909). This is a similar problem to that which may be found when attempting to establish in situ values for construction materials. Removing samples from a construction could disturb their physical structure (e.g. powdered samples of solid materials) or moisture levels could change while transporting, shaping and preparing samples. Samples may in any case have to be dried before measurements by guarded hot plates to comply with British Standards (BS EN 12667, BSI, 2001a; BS EN 12939, BSI, 2001c).

Hooper and Lepper visited van der Held, after which they adapted the transient line methodology, now named the thermal conductivity probe, for use with solid and granular materials, including building insulations. An aluminium probe with a steel tip, approximately 475mm long by 5mm diameter, was built containing a heater wire and several thermocouples.

Following van der Held and van Drunen (1949), a time was subtracted from the elapsed times of each measurement to compensate for the delay in the instrument heating up. It was believed that this time would be reasonably constant for a particular probe in most materials, 5 seconds with the aluminium

instrument used, hence the process of calculating the delay for each measurement was eventually discarded.

The appropriate start time for the analysis was also considered constant for a particular instrument in most materials, which, in their case, was after four minutes of heating. Believing that the heating curve over the natural logarithm of time, $\Delta T/\ln t$, would then always be straight after this time, it was assumed that only two temperature – time observations were needed to create a straight line asymptote for analysis, that is at four and ten minutes. It was not reported whether periodic checks were then made to ensure linearity of the $\Delta T/\ln t$ curve.

Hooper and Lepper listed the advantages of the thermal conductivity probe as:

- Ability to measure moist or dry materials
- Ability to measure in situ undisturbed materials
- Inexpensive, compact and portable equipment
- Fast achievement of results
- Adequate degree of precision for engineering use

Unresolved problems with measuring fibre insulating materials were reported but it was stated that no contact effects were otherwise found. A probe length to diameter ratio of at least 100:1 was recommended. It was maintained that thermal diffusivity, and hence volumetric heat capacity, were readily measurable by the instrument although no claims for the accuracy of these values were made.

D'Eustachio and Schreiner (1952), at the Pittsburg Corning Corporation, were attracted by the line heat source method, used by van der Held and van Drunen, as a more convenient and economic alternative to the guarded hot

plate method for thermal conductivity measurements of insulation materials. It was recognised as advantageous that thermal conductivity could be found independently of thermal diffusivity by this method, which allowed relatively simple equipment to be used to give adequate precision for their purposes. Recognising van der Held and van Drunen's time correction to compensate for the probe's finite radius and length, such a correction was thought to be unnecessary for any but the most exacting work.

A stainless steel probe was used, 100mm x 0.75mm outside diameter, with a wound heater inside and thermocouples within the winding. Measurements were taken within an insulated cabinet. To cancel out potential thermal drifts that may still have existed, the reference junctions for the thermocouples were placed in a double Dewar flask arrangement elsewhere within the controlled environment and all left for at least 6 hours to reach thermal equilibrium.

It was noted that a small air space between the probe and insulation being measured did not affect results at low power inputs. In studying potential end losses, temperature measurements were made along the length of the probe. It was calculated that the heat flow along the tube, in the central portion, was less than 0.1% of the heat input, which was more than the axial heat flow during the measurement interval. From this it was concluded that, in this particular situation, end losses were negligible. It was not thought that this could always be the case and even smaller probes with less heat capacity were proposed, potentially sheathed in glass fibre and plastic, which, it was then thought, could make it possible to measure changes in the thermal conductivity of insulation materials caused by moisture content.

Hooper and Chang (1953), reporting that the thermal conductivity probe was now in common use for many field applications and laboratory situations, revised the Hooper and Lepper time delay, previously used in the chart of $\Delta T/\ln t$, in favour of a shift in the temperature axis. They stated that this gave more reliable results, while the dimensions of the previous probe, 475mm x 5mm, were maintained as still appropriate, if the sample was of sufficient size.

End losses from the probe were considered, especially in insulation materials. These were reduced by ensuring connecting wires were of minimal dimensions. It was reported, following tests on wet clay and rock wool insulation, that no lower thermal conductivity limit was found for the probe.

Two other sets of probe dimensions were used. A 100mm x 1.5mm probe was used to accomplish measurements in dairy products. No particular problems were found with the smaller size, this said to be only being limited by workmanship, as long as the length to radius ratio was maintained. 1.5m and 2.5m probes were also constructed to measure the thermal conductivity of the ground for heat pump sites. These long probes had thermocouples placed at 300mm centres, which was considered a sufficiently accurate methodology for the particular application, to assess varied thermal properties at diverse depths.

It was reasoned that, while the inhomogeneity of the sample could be assessed as above, the available theoretical solutions were not capable of accommodating the inhomogeneity of the probe itself, being made up of various materials: the hot-wire; the thermocouple wires; the tubing; and the material between the wires and tubing. It was not possible to identify a precise dimension for r, the radius at which temperature increase was measured, partly

because there was a temperature difference between the probe and sample. Nevertheless, it was determined that the traditional solution, equation (7), was still valid if the radius of the measurement position divided by the square root of the sample's calculated thermal diffusivity produced a constant result over the time of the measurement.

The methodology then relied on using thermal diffusivity values from the literature and a series of iterations to establish a theoretical value for *r*, which did not need to bear resemblance to the physical situation. A chart was developed that could be used with the probe to read off appropriate values of *r* for various power input, temperature rise, time and thermal diffusivity combinations, which value was then used to obtain thermal conductivity results. With *r* linked to thermal diffusivity α in the solution of equation (7) it seems unlikely that a real value for α could be reliably found by this method, however, the article concluded that:

"the device is no longer of experimental interest only, but is a practical tool available for direct engineering application".

Difficulties with thermal probe applications from the mid 20th century

Blackwell completed his PhD thesis entitled "Transient Heat Flow Problems in Cylindrical Symmetry" at Western Ontario in 1952 (NASA, 2007). In a letter to the Physics Society, Blackwell and Misener (1951) argued that the methodology developed by Hooper and Lepper used simplifying assumptions that were too extreme for their present use of a 40mm diameter probe in a medium where contact resistance was likely to be high. Referring to earlier work by Carslaw and Jaeger (1947), they stated that the contact resistance between the probe

and sample was significant. This property was termed 'contact conductance', again with the symbol *H*. It was suggested that *H* increased towards infinity at large times and, as *H* appears in Carslaw and Jaeger's solution as a denominator, it could then be ignored. Carslaw and Jaeger's solution for large times, in similar form to that presented by Blackwell and Misener, is given here and assumes the probe wall is a perfect conductor:

$$\theta \cong \frac{r_{int}Q'}{2\lambda}\left[\ln 4t - \gamma + \frac{2\lambda}{b_{ext}H} + \frac{1}{2t}\left\{\ln 4t - \gamma + 1 - \frac{x\alpha}{r_{ext}\lambda}\left(\ln 4t - \gamma + \frac{2\lambda}{r_{ext}H}\right)\right\} + O\left(\frac{1}{t^2}\right)\right]$$

Equation (7)

Where:

r_{int}	=	internal probe radius
r_{ext}	=	external probe radius
x	=	$(r_{ext}^2 - r_{int}^2)\,\rho C_p / r_{ext}$

Large times were defined as:

$$\frac{\alpha t}{r^2} \geq 1$$

Equation (8)

Equation (8) shows that, for a thermal diffusivity value of 1.4 $x10^{-7}$ m^2s^{-1}, the value for water, large times would be approximately 3,000 seconds for Blackwell's 40mm diameter probe, small times being those below this. For smaller probes, this time would be reduced, e.g. just 2.57s for a 1.2mm diameter probe.

It was suggested that by taking measurements at large and small times, *H* values could be roughly calculated from the difference in results, as other properties would be constant. Values for *H*, and therefore thermal diffusivity, could then be more accurately determined by a series of iterations. As the

temperature rise at very early times is predominantly related to the thermal properties of the probe itself, this indicates that, to establish values for *H*, larger diameter probes would be needed to provide sufficiently extended small times for measurement.

A probe length to diameter ratio of 20:1 was suggested as being sufficient to reduce error levels from axial and end losses below other experimental errors. In Blackwell and Misener's case, this would be a minimum probe length of 0.8m. Blackwell carried out further calculations in 1952 regarding the relationship between radial and axial heat flow (Blackwell, 1953), and published further theoretical solutions in 1954 (Blackwell, 1954), following a revision of the theory prompted by an approach by geophysicists wishing to use the thermal conductivity probe technique to measure the thermal properties of rock.

In this later paper, a number of approximations and doubts became apparent, related to Blackwell's and others' work. Blackwell stated that the solution in equation (7): was not rigorously justified; that disregarding probe end losses was the least satisfactory part of the work, but was seen as a necessary assumption; that contact resistance need not be considered in calculating the relationship of axial to radial heat flow; and that some of the calculations for a cylindrical probe were based on a theoretical rectangular model.

The new solutions introduced a radial temperature gradient in the probe wall, where previously the probe had usually been considered as a perfect conductor. A method to calculate a value for the level of thermal contact between the probe and medium was described. It was necessary to obtain this value, *H*, in order to obtain a thermal diffusivity value for a measured sample,

unless the *H* value was known or could be considered large. It was considered that *H* would be large in the case of "very good thermal contact", also that only rough values for *H* were needed where it was "not very small" as its influence in finding values for thermal conductivity and thermal diffusivity of the sample decreased as it increased.

The solution to finding *H* was given as the *Y* intercept of a linear asymptote occurring at an early part of the heating cycle, found by:

$$Y = \frac{M_p c_p / \pi . r_{p(ext)}}{t^2}\left[t - \left\{ \frac{1}{\alpha_p}\left(0.125 r_{p(ext)}^2 + 0.125 r_{p(int)}^2 - 0.5 \ln\left\langle \frac{r_{p(int)}}{r_{p(ext)}} \right\rangle \left\langle \frac{r_{p(int)} r_{p(ext)}}{r_{p(ext)} - r_{p(int)}} \right\rangle \right) \right\} - \frac{\left(M_p c_p / \pi . r_{p(ext)}\right) T_p}{2\left(Q'/2\pi . r_{p(ext)}\right)} \right]$$

Equation (9)

Through the relationship of:

$$Y \approx H - \left(\frac{16 H^2 h_2}{15\left(\sqrt{\pi}\right)\lambda} \right) t^{0.5}$$

Equation (10)

where:

M = mass per unit length

int and *ext* = internal and external surfaces of the probe walls

the term h_2 remained undefined in the article

and where thermal conductivity had already been found through:

$$\Delta T = \ln t \left(\frac{r_{p(ext)}\left(Q'/2\pi . r_{p(ext)}\right)}{2\lambda} \right)$$

Equation (11)

The solution did not include potentially variable temperature gradients in the hot wire itself, or that between the wire and the walls of the probe, or in any contact material or air gap between the probe and sample material. It is open to question whether a mathematical solution containing a range of small values,

such as the probe wall thickness, could have allowed for what must have been a gap of unknown and variable dimension between the probe and sample. Probes had been proposed for use in predrilled holes in hard and rough materials such as rock, where levels of contact would have been unknown.

Of note in the 1954 paper was the use of a least squares method to fit experimental data to equation (7), which removed unspecified objections to line fitting by eye. No mention of the time or temperature adjustment used by previous researchers was made. The article was the first of two to be published, the second was to deal with experimental results. No trace of this second paper has been found in the literature and it is assumed that no such paper was published.

In a final paper by Blackwell (1956) concerning the thermal conductivity probe, based in part on earlier calculations by Jaeger (1955) regarding heat losses through thermocouple wires affecting temperature measurements, theoretical error levels were mathematically deduced for various probe length to diameter ratios. For hollow probes, which were used by Blackwell with a heater wire wound around them, a ratio of 25:1 gave an error of 0.7% while at 30:1 the error was considered negligible at 0.051%. For solid probes, a ratio of 25:1 gave a theoretical error of 1.7% and at 30:1, 0.12%. A worked example of the calculations was given for a 32mm diameter hollow brass probe with a wall thickness of 3.175mm.

These values were based on the existence of an axial symmetry and an assumption that $\alpha.t/r^2$ would be unlikely to exceed 25 in the practical use of thermal probes. This assumption was based on relatively large probes. With

Blackwell's 32mm diameter probe and a sample material with thermal diffusivity value of 1.4 $x10^{-7}$ m^2s^{-1}, 25 would not be exceeded until 46,000s. The condition would be reached much sooner with smaller probes and higher thermal diffusivity values. For example, with a 1.2mm diameter probe, such as the 150mm long Hukseflux TP02 previously used at Plymouth, $\alpha.t/r^2$ would be exceeded after 64s, or just 10s where the thermal diffusivity value was 9.0 $x10^{-7}$ m^2s^{-1}.

Jaeger (1956) expanded on the contact resistance between the probe and medium. He noted that earlier researchers, such as van der Held et al (1953), had not included contact resistance in their calculations whereas Blackwell had. Jaeger considered the case of large probes, such as those described at the time by himself and Blackwell, having diameters between 30mm and 40mm. In dry rock, the contact resistance was described as equal to the thermal resistance of 1mm air, whereas, if there was good contact or a contact medium was used, contact resistance could reasonably be neglected.

Jaeger (1958) suggested an iterative methodology to obtain the correct value for thermal diffusivity of a sample where the probe was a perfect conductor and where there was perfect thermal contact between the probe and sample. This was suggested for large probes only, as it was stated that:

"there is no possibility of measuring K *(thermal diffusivity) accurately with a single probe of small diameter".*

This was in response to an article by Buettner (1955) who concluded that diffusivity was impossible to obtain by cylindrical probe whatever the diameter, partly because moist soils of varied thermal conductivity and heat capacity

could have identical thermal diffusivity values. Buettner also stated that where the ratio between the volumetric heat capacity of the probe to that of the sample medium was between 1 and 30, the temperature rise of the medium was independent of its volumetric heat capacity.

Another matter of interest in Buettner's article was the use of a probe constant in the calculation of the sample materials' thermal properties. It was suggested that this could be found or calibrated by taking a measurement in a material of known thermal conductivity and that this material should have a similar heat capacity to that of the unmeasured medium. Calibrations in materials with low ρC had been found to be of little practical use. This suggested that the probe constant was actually a variable, and dependent on the thermal properties being measured.

Jaeger (1959) suggested a "relatively simple" reduction method to determine thermal conductivity and thermal diffusivity, and therefore ρC, from data produced by a thermal probe in the early part of the heating curve, before the linear asymptote was reached, although thermal diffusivity values were used as a method of checking calculations rather than an end in their own right.

An experimental result for vesicular basalt was given where a contact medium of water was used and contact resistance presumed to be zero. The thermal conductivity result was reported as 1.757 $Wm^{-1}K^{-1}$ and volumetric heat capacity reported as 2,789 $kJm^{-3}K^{-1}$. This was stated as being rather high, which was suspected to be a result of water filling the vesicles in the rock. This reduction methodology relied on an estimation of the contact resistance and an estimation of the materials' ρC. In a further example given, Jaeger stated that the

methodology could not be carried out because, without further explanation, the "peculiar nature of the material" meant the ρC was not available for use. This indicated that the volumetric heat capacity, or thermal diffusivity, could not be measured unless it was reasonably well known already.

Jaeger and Sass (1964) later did not mention a thermal probe in their article on line source measurements to give thermal conductivity and diffusivity of rock, rather describing a rock core sample, between 20mm and 40mm diameter, with a shallow longitudinal groove cut into either side of it into which were placed a line source on one side and a thermocouple on the other side. A mathematical constant was required in their calculations, which constant was dependent on the thermal diffusivity of the sample, hence either thermal diffusivity or volumetric heat capacity needed to be known before either could be measured.

Joy (1957), in a programme sponsored by the American Society for Testing and Materials (ASTM), carried out assessments of thermal conductivity probe measurements in moist insulation materials. Two types of steel tube probe were used, both 0.5mm diameter by 203mm long ($L/r \approx 400{:}1$). One, developed by D'Eustachio and Schreiner, contained a heater and a thermocouple, and the other, developed for the programme at the Pennsylvania State University, contained the heater and resistance thermometer in one nickel wire. Results of each were found to be comparable in most cases. Reproducibility was found to be in the region of 1% in dry materials, 2% in evenly moist materials and 6% in materials with irregularly dispersed moisture. However, it was found that, where moisture was not uniformly distributed in the sample, linearity of $\Delta T/\ln t$ was not always achievable, sometimes resulting in "a peculiar S-shaped curve".

A small cylinder of acrylic material, 6.35mm diameter by 6.35mm length, was placed within a dry insulation sample to test inhomogeneity effects, with the probe passed through a hole made in it. Measurements were taken with the probe at various positions relative to the cylinder and the results were described by Joy as absurd, especially when the thermocouple was within the cylinder.

Further work on inhomogeneity was carried out, using a uniform grid of similar glass beads set into cork boards. This was measured by guarded hot plate and then by the probe in various positions relative to the rows of glass beads. It was reported that the probe gave values around 5% higher than the GHP when randomly placed, ± 5% dependent on its proximity to the beads. The nature of the heating curve was not described.

It was concluded that the thermal probe methodology was suitable for thermal conductivity measurements of insulation materials containing uniformly distributed moisture, but:

"that it (the method of measurement) is a laboratory based method, not one for use in the field where water in insulation is almost sure to be non-uniformly distributed".

Picot and Fredrickson (1968) used Carslaw and Jaeger's solution (equation 7) for a wire heated and in perfect contact with an homogenous medium where end losses were not considered, the hot wire method. They showed that, while the solution held for isotropic and homogenous materials, it failed when applied to anisotropic liquid crystals, as the solution had been based on an assumption of spatially homogenous thermal properties.

Contemporary with Jaeger, de Vries (1952a, 1952b), at Wageningen, was interested in the thermal properties of moist soils and used, among other

methods, single needle thermal probes and transient line source theory to measure thermal conductivity and thermal diffusivity. It was suggested that the method was suitable because the moisture transport through the soil was minimal, as was the disturbance to the sample by the needle insertion.

Thermal conductivity was calculated from the straight line of temperature rise over the natural logarithm of time. This line would apparently only be straight in the perfect model and, in the experimental situation, a time correction was introduced, partly to correct for the finite radius of the probe, although this correction was not needed after about 60 seconds. Based on the work of van der Held and van Drunen, accuracy was expected to be better than 3% for laboratory measurements and 5% for field studies. However, de Vries reported accuracy only better than 10% for his experiments in moist soils and variations of up to 30% for soils with low moisture content.

De Vries (now based in the Commonwealth Scientific and Industrial Research Organisation, Australia) and Peck (1958) further developed the work of van der Held, Jaeger and Blackwell regarding the approximation of the perfect model of a transient line source to incorporate the finite conductivity of the probe itself. An assumption was made that a dimensionless contact resistance, termed η and comprising λ/RH (where R = radius of probe and H = a heat transfer coefficient), would exist due to an air gap between the heating wire and the sample medium. This suggested that total thermal resistance between the probe and sample was a result of, jointly and variably, the level of physical contact and the thermal properties of both probe and sample. According to de Vries, large positive and even negative values of η were observed, although

negative values were thought to be caused by a "leakage current" to the galvanometer measurement device.

It was concluded that thermal conductivity values for soils and materials with similar thermal properties could be measured to within 5%, as long as the probe itself had a high volumetric heat capacity and thermal conductivity in comparison to the sample medium. Thermal diffusivity measurements required both a knowledge of the contact resistance η and an estimate of the materials' volumetric heat capacity and, unless η was accurately known, no high degree of accuracy could be expected. It was stated that an error of 3% in thermal conductivity could result in a further error of 20% in thermal diffusivity. As thermal diffusivity could be calculated directly from thermal conductivity and volumetric heat capacity values, it is debateable whether an improved result could have been obtained by introducing an estimate of the latter into a further calculation containing the unknown η.

Vos (1955), working at TNO (Netherlands Organisation for Applied Scientific Research), Delft, following van der Held, to whom he was an assistant in the early part of his career, and Carslaw and Jaeger, discussed preferences between steady state and transient methods to measure the thermal conductivity of insulating materials. It was stated that transient methods had been used successfully to do this for many years. Experiments were carried out with cork, foam-plastic, lightweight concrete, insulating wool and unspecified inhomogeneous materials, sometimes with varied moisture contents and at varied temperatures.

An attempt to use the resistance of the heater wire rather than thermocouples to measure the temperature rise was mentioned as having "all sorts of difficulties" and thus abandoned. The error levels of this method were said to be dependent on the kind of material being tested.

Applied transient line source theory depends on a linear asymptote being achieved when temperature rise is plotted over the natural logarithm of elapsed time. Vos identified three causes for deviation from the linear:

1) The effect of the probe's thermal capacity, which was calculated to not produce effects after 50 seconds, where, in most circumstances:

$$\frac{4\alpha.t}{r^2} > 50$$

Equation (12)

This illustrated an advantage with smaller probe radii, but relied on a knowledge of the sample thermal diffusivity. For a 1.2mm diameter probe and a sample thermal diffusivity of 1.4 $x10^{-7}$ m^2s^{-1}, the term is greater than 50 up to 32s, but for a 32mm diameter probe this increases to 23,000s.

2) Reflection of heat from the boundary of the sample medium for which time and distance were said to be noticeable when:

$$\frac{4\alpha.t}{d^2} > 0.6$$

Equation (13)

where d = the smallest distance between the heater wire and the boundary of the sample medium. With a 50mm radius sample at thermal diffusivity 1.4 $x10^{-7}$ m^2s^{-1}, boundary effects would therefore be noticeable after 2,700s and, with a 10mm distance, at 107s. It was not shown

whether the outcome was dependent on the level of heat flow from the probe.

The calculation again relied on a knowledge of the sample thermal diffusivity.

3) The effect of inhomogeneity where the thermal conductivity of the sample medium changes in parts away from the probe. The article described $\Delta T/\ln t$ becoming less steep as time elapsed indicating that, if the inhomogeneity argument held true, the thermal conductivity of samples would be higher at greater distances from the probe. This is unlikely as there is no practical reason why thermal conductivities should not be randomly spread in inhomogeneous materials.

Vos suggested the method could be used in buildings to measure the moisture content of walls, as higher moisture contents created higher thermal conductivities. The connotations of increased heat losses through building envelopes were not discussed.

Lightweight concrete was measured at temperatures up to about 350°C and its thermal conductivity found to be almost double at this temperature than at room temperature. This phenomenon did not occur when measurements were taken with a guarded hot plate and Vos deduced that, unlike the transient line source method, the GHP suppressed radiation effects. No rationale for this was given and, as no corroborating measurements were undertaken, it must remain open to question whether the higher values achieved with the probe at higher temperatures were truly representative of thermal conductivity values or

Figure 8: The author visiting San Sebastiano, Venice, in 2007

whether they were as result of unknown problems with the probe measurements.

It was concluded that the thermal conductivity of the studied materials could be measured to ± 3% by the transient line method, although it was said that interpretation of the charted line of temperature rise over elapsed time could only be carried out by highly skilled persons and hence the method could not be made routinely accessible.

Vos later went on to use the thermal probe in conservation work, using thermal conductivity measurements to map moisture content through the structures of various historic buildings, such as: the St. Bavo Cathedral, Haarlem, Netherlands; the San Sebastiano church in Venice (Figure 8); and a fifteenth century church at Weesp in the Netherlands (Boekwijt and Vos, 1970).

Probes were formed with the heater wire and thermocouples encased in polythene tubes around 120mm long, which were then pushed into glass tubes set in 4mm diameter holes in the sample material. Thermocouples were placed at 20mm centres along their length so that thermal conductivity could be

measured at various depths through the structure, e.g. in sandstone at St. Bavo's.

Electronic recording equipment was set up to automatically record results and to calculate moisture contents. Using up to 28 probes simultaneously, and measuring thermal conductivity internally and externally at various heights, helped identify the type of moisture penetration occurring, such as whether moisture was rising from the ground or was penetrating rainwater. Probes were left in situ for a number of months and measurements repeated over that time. The results then formed the basis of critical conservation decisions.

Problems with incidental environmental effects on the surfaces of the walls being measured, such as solar gain or wind chill, unduly affecting the heating curve during measurements, were avoided by using a second probe. The cold junctions of the thermocouples in the heating probe were placed in this second probe, presumably of matching dimensions and beyond the area heated by the first probe, to separate the temperature rise by probe heating from the temperature fluctuations of incidental environmental effects.

Woodside (1958), working in the Building Services Section of the National Research Council in Canada, followed up the methodologies of Stalhane and Pyk, van der Held and van Drunen, Hooper and Lepper, and de Vries. Woodside was interested in the way that probe heating affected moisture migration. He carried out experiments on dry silica aerogel with a thermal conductivity in the region of 0.024 $Wm^{-1}K^{-1}$ and achieved results within 1% of expected values. Transferring the methodology to moist sawdust and moist clay, he found that thermal conductivity values decreased over time during 10

minute measurements and concluded that this was caused by the material drying out adjacent to the probe. He proposed that the solution was a larger diameter probe with a lower power input, with corrections used to compensate for the errors caused by the larger diameter, as described by Blackwell (1956).

The measurement of thermal conductivity in anisotropic materials, especially wood, fibre board and rock wool insulation, was discussed and a method described whereby measurements were taken both along and perpendicular to the grain or plane in which most of the fibres were orientated. Heat flow perpendicular to the plane was then given by: measurement parallel to the plane, squared, divided by the measurement perpendicular to the plane. Woodside used the term 'effective thermal conductivity' to encompass such factors as well as the effects of radiant heat transfer within the sample material. Notably, the term reproducibility was used rather than accuracy for many of the results.

A methodology to achieve values for thermal diffusivity was described. The linear section of the chart of temperature rise over the natural logarithm of elapsed time was extrapolated back to the ordinate, where the time used was the sum of elapsed time plus a probe time correction. It appears to have been assumed that the probe was a perfect conductor at a steady state, as the radius of the probe was used as the distance of the temperature measurement from the heating wire, to accord with transient line source theory, whereas the thermocouple was encased within the probe. Using an undefined term *C'*, equal to summed negative values of Euler's constant and the natural logarithm of the above radius squared and divided by four times the thermal diffusivity, the value

for thermal diffusivity was achieved. It was reported that the value achieved for silica aerogel accorded well with its published value.

The assumption of the probe as a perfect conductor, with equal temperature at its centre and external radius, seemingly compensated for by a time delay, seems an approximation that is open to question. The equations used to deduce the results were to be published as an appendix in a later version of the paper, which has not been found in the literature.

Woodside and Messner (1961a, 1961b), working for the Gulf Research and Development Company, Pittsburgh, Pennsylvania, were interested in the thermal conductivity, and thermal diffusivity, of oil-bearing sands and rocks, as well as heat dissipation from underground nuclear tests, heat loss from the earth's core, sizing of underground electricity cables, and the thermal properties of insulating and refractory materials. Experiments were carried out with a thermal probe on unconsolidated sands, glass beads, lead shot and consolidated porous sandstones, all at various levels of saturation by various liquids and gases at various pressures. Steady state measurements were considered inappropriate as results were then dependent on sample size and temperature applied, as the measurement method created non-uniform liquid saturation distribution. It was stated that the thermal probe was in common use at that time.

Potential errors in the thermal probe method were recognised as being:

- Neglect of higher order terms in Carslaw and Jaeger's solution, which could be minimised by placing the thermocouple near to the heating wire and discounting the early part of the $\Delta T/\ln t$ curve;

- The finite length of the probe, which could be minimised by exceeding Blackwell's recommendation of probe length to radius ratio, which was taken to be 30:1. They used probes around 150mm long in the range of 64:1 to 100:1;

- Boundary conditions, which they negated by ensuring that their measurement time was taken before any temperature increase occurred at the boundary, limiting their measurements to around 180 seconds;

- Contact resistance between the probe and the sample medium;

- Variable resistance of the heater wire, the effects of which were made negligible by using a wire with a low temperature coefficient of resistance.

The check on whether these errors had been sufficiently avoided was to rely on the existence of a linear asymptote of $\Delta T/\ln t$ as a guarantee that suitable conditions had been met.

Temperature rise over time was recorded on a Speedomax Recorder. Only two points of a linear asymptote were considered necessary to calculate thermal conductivity, so discarding the early time section was not considered to be a problem.

Tests were first carried out on foamed plastic insulations with reported thermal values and then dry sand and rock. In all cases reproducibility was reported as being better than 2.5% while using different probes, circuitry, power sources and using either no contact medium or mercury. In their following measurements of consolidated rocks, Woods Metal, a fusible alloy with a density close to that of lead and a melting point of 70°C, was used as the contact medium.

It is of note that quartzitic sandstones were reported to be anisotropic, dependent on the axis of the quartz crystals. Ratcliffe (1959) at the National Physical Laboratory observed that thermal conductivity of quartz in the crystal axis direction was twice that in the perpendicular direction. Similar and varied anisotropic differences are reported in the more obvious case of wood species (Steinhagen,1977). Woodside and Messner took a value of 8.4 $Wm^{-1}K^{-1}$ as the average thermal conductivity for quartz in their sands, where it was assumed that the distribution of crystal axis orientations was random.

It was concluded, in both articles, that the line heat source method was satisfactory for measuring effective thermal conductivity of unconsolidated sands and consolidated rocks. A range of values were given for sandstones, from 0.5 $Wm^{-1}K^{-1}$ to 7.4 $Wm^{-1}K^{-1}$ dependent on porosity and saturation. For example, teapot sandstone with 29% porosity was measured dry in air at normal pressure and temperature to give 1.54 $Wm^{-1}K^{-1}$ whereas, when saturated with water, in the region of 0.6 $Wm^{-1}K^{-1}$, a value of 4.05 $Wm^{-1}K^{-1}$ was achieved. Apart from the foamed plastic, measurements were not corroborated by another method of measurement. The use of a calibration material not

matching the thermal properties of the test samples and also of low ρC ran against the advice of Buettner (1955).

Underwood and McTaggart (1960), working for Monsanto in Springfield, Massachusetts, were interested in the thermal conductivity of plastics, including polystyrene and polyethylene. They carried out measurements over a wide range of temperatures appropriate to plastics' engineering, using disposable equipment. They reported their results as being in agreement with values published by ASTM. As the radius of their probes was slight (they used an uncased heater wire with a thermocouple wire loosely wrapped around it), terms in their line source equation referring to probe radius could be ignored, which also meant that terms for thermal diffusivity were removed.

The heater and thermocouple were placed within the plastic samples by either: slicing the sample in half, cutting a groove, laying in the wires and clamping the sample back together; or pouring a hot melt of plastic around the wires; or lowering the wires into a melted sample. The advantages or disadvantages of each method were not described. Thermal equilibrium was then checked by comparing the thermocouple temperature to that of the surrounding ambient temperature and checking whether any thermal drift occurred to the thermocouple over 4 – 5 minutes duration.

Following van der Held and van Drunen, a time correction was employed to account for possible resistance between the heater and sample and the finite radius of the heater and thermocouple arrangement. This they managed to do by horizontally offsetting each data point on their chart of temperature rise over the natural logarithm of time by a set number of seconds until a straight line was

achieved, believing that small compromises had to be made because of slight inaccuracies in observation, thus their time corrected chart could transform a curved line into a linear asymptote. They noted that this time correction could be positive or negative. They then used the temperature difference between 10s and 100s on this line for their analyses. Their illustrated example showed temperature readings taken at approximately 5.5, 9, 20, 32, 56, 83, 100, 110 and 120 seconds. Values were given for polystyrene at various densities and cell sizes ranging from 0.028 to 0.042 $Wm^{-1}K^{-1}$.

In the article conclusion, the method was recommended as being easy and economical to carry out, with samples able to be held at various temperatures and positions, such as in ovens or refrigerators. It was suggested that a sample could be placed in a bomb to assess the effects of high pressure on the thermal conductivity.

Veziroglu (1967) reviewed and contributed to the literature concerning contact conductance between surfaces, the whole or part of *H* in equation (7). Experiments were carried out with various metals and metal alloys at various temperatures and pressures using different interstitial mediums, such as air and paraffin. Roughness of the contact surfaces varied from 0.07 μm to 84 μm and resultant contact resistances varied from 340 $Wm^{-2}K^{-1}$ to 230,000 $Wm^{-2}K^{-1}$. Prediction of contact conductance was said to only be possible within ± 35%, even with carefully measured and milled surfaces. The greatest sources of error were described as (a) the estimation of the gap width between surfaces and (b) the number of and area of actual contact points, both (a) and (b) being based on the roughness and unevenness of the surfaces assessed. This confirmed the Carslaw and Jaeger (1948 pp.13-14) view that *H*, required in the

calculations of Blackwell (1954) to measure thermal diffusivity, was difficult to estimate with confidence, especially in rough or hard materials where the level of contact was likely to be random and could not be seen or directly measured.

Nix et al (1967) at Aubern University, Alabama, were contracted by the U.S. Army Missile Command to develop thermal conductivity and thermal diffusivity measurements of rubber based propellants. Following Underwood and McTaggart's time correction methodology, and citing a solution given by Ingersoll et al (1954) to solve the thermal probe problem, they simultaneously measured the thermal conductivity and thermal diffusivity of silicon rubber at normal room temperatures.

A heater wire and two thermocouples were set in the molten rubber, which was left to solidify. The first thermocouple was placed adjacent to the heater and used to establish values for thermal conductivity, as later terms in Ingersoll's solution could be ignored where the radius of the measurement position from the heater was negligible. The second thermocouple was placed at a known distance from the heater, around 3.175mm. Thermal diffusivity was then established by incorporating estimated values for thermal diffusivity into Ingersoll's equation, including the later terms, and the resultant calculated temperature compared with the measured temperature. This process was repeated until the calculated and measured temperatures were coincident.

Relying on van der Held and van Drunen's work with liquids, contact resistance was considered negligible at low power inputs. It was maintained that, in the particular experiments carried out, the time correction for the second thermocouple's data was so negligible as not to be needed. It would appear that

the whole temperature rise over their 300s measurement may have been used in their analyses, as no time window was mentioned and no curves were illustrated.

Three sets of results were given for the thermal conductivity of room temperature vulcanising silicon rubber. The first runs appeared to be carried out without the second thermocouple and gave an average thermal conductivity of 0.363 $Wm^{-1}K^{-1}$. A table of published values by the National Bureau of Standards was given, with an average value of 0.379 $Wm^{-1}K^{-1}$. A third table was given where thermal conductivity and thermal diffusivity were measured simultaneously. The average value for these runs was 0.302 $Wm^{-1}K^{-1}$. The average thermal diffusivity value for this set was 1.62 $x10^{-7}$ m^2s^{-1}, compared with the 40% higher value published by Mastin (1964) of 2.29 $x10^{-7}$ m^2s^{-1}. Despite this, it was stated that an analysis of experimental errors indicated an accuracy of ± 5% for both thermal conductivity and thermal diffusivity.

The article concluded by pointing out the substantial benefits that the methodology offered, namely:

- No special dimensions were needed for the sample
- The test time was short, compared to steady-state devices
- Only a small temperature change was required
- The method was portable and suitable for field tests
- The apparatus was relatively inexpensive
- Could be used at extreme temperatures
- Thermal diffusivity was measured simultaneously

Agrawal and Bhandari (1970), in the Department of Physics, University of Rajasthan, carried out simultaneous measurement of thermal conductivity and thermal diffusivity in dry porous materials: asbestos cement; desert sand;

sawdust; and fireclay using a thermal probe. The finite length of the probe, the finite size of the medium, contact resistance between the probe and the medium, and the different thermal properties of the probe and the medium were all examined.

The issues of axial and end losses caused by the finite length of the probe were resolved by exceeding what was viewed as Blackwell's recommended length to radius ratio of 30:1, achieving 68:1 in an 80mm probe. The boundary issues caused by the finite size of the medium were resolved by using low power inputs, around 0.6 Wm^{-1}, and monitoring the temperature at a distance from the probe. It was found that no temperature increase was discernable at 35mm distance in dry sand until 3 hours had passed, hence a 90mm diameter container for the samples was deemed to represent an infinite sample in practice. Contact resistance, which was recognised as causing a higher observed temperature, was assessed based on the work of de Vries and Peck (1958). The effects were considered negligible for their well packed samples.

It was deduced from errors in fireclay results, where experimental results averaged at 0.273 $Wm^{-1}K^{-1}$ compared to the expected value from the literature of 0.896 $Wm^{-1}K^{-1}$, that the thermal probe method was not suitable where the thermal conductivity of the sample was higher than that of the probe. However, it was concluded that the thermal probe was suitable for simultaneous measurement of thermal conductivity and thermal diffusivity.

Haarman (1971), in the physics department at Delft, wished to develop existing theory, following its use by Stalhane and Pyk (1931) to measure granular materials, de Vries (1952) to measure soils, and van der Held and van Drunen

(1949) to measure liquids, to more accurately measure the thermal conductivity of gases. Various subject matters were studied, including radial convection, pressure changes, and finite line source length. Also studied was an effect referred to as a temperature jump between the hot wire and the gas being studied. Reference was made to previous work by Smoluchowski (1910, 1911a, 1911b, 1953) where it was shown that the difference in temperature between a flat wall and an adjacent gas was proportional to the temperature gradient in the gas, and dependent on the mean free path of molecules. It was concluded that the temperature jump, out of the various factors studied, was the only one that could not be calculated in advance or eliminated experimentally, although its influence could be determined experimentally.

The temperature jump appears to be similar to contact resistance H in transient line solutions. It appears the effect may still be significant in the case of very good contact, which is assumed where a gas meets a solid. The effect, as described by Haarman, was dependent on the temperature gradient in adjacent materials, which would be complex in the case of a composite thermal probe, a filler and a sample material. It was suggested the temperature jump required further investigation, both theoretically and experimentally.

Novichenok and Pikus (1975) used an uncased hot wire to measure the thermal properties, both conductivity and diffusivity, of various oils, including the petroleum jelly Vaseline. It was recognised that errors were caused by the limiting factors in the use of Blackwell's solution, such as ignoring terms for the thermal capacity of the wire and contact resistance between the wire and the medium. A relative method was used to solve this problem, where both the

sample of interest and a sample of a material with known properties were measured.

Four types of oil were tested and thermal conductivity values given for each at three different temperatures, 20°, 50°, and 80°. The value for petroleum jelly at 20°C was 0.127 $Wm^{-1}K^{-1}$ against their expected value of 0.125 $Wm^{-1}K^{-1}$. Experimental results for thermal diffusivity were only given for transformer oil across the three temperatures and for industrial type 20 oil at 20°C. The entries for the petroleum jelly thermal diffusivity results were left blank in table 1 of their article, although a value of 0.79 $x10^{-7}$ m^2s^{-1} from the literature was given. This would give a volumetric heat capacity in the region of 1 $MJm^{-3}K^{-1}$, using the experimental conductivity result with the expected diffusivity value.

Healy (based in the Department of Industrial Chemistry at Queens University, Belfast), de Groot and Kestin (1976) were interested in measuring the thermal conductivity of fluids by the methodologies suggested by Stalhane and Pyk, and van der Held and van Drunen. It was considered that the theory was in need of revision, requiring more systematic and rigorous corrections. In the study, it was attempted to identify and provide corrections for the more significant potential errors. A common sense rule was used whereby corrections need not be applied where their magnitude was of one order or more smaller than the required accuracy of the result.

It was observed that experimental results differed widely from the mathematical model and the finite length of the heating wire was considered the most significant cause of the error. The problem was considered insoluble by analysis

and instead two wires of different lengths were used. By comparing results from each, the error caused by their finite length was estimated.

Concern was expressed that sample heating by the probe caused a variation in sample density, and therefore an inhomogeneity, which was considered to create practically insurmountable difficulties in analysis. In the case of measuring gases, the error was considered sufficiently small to leave aside under the common sense rule above.

Deductions were made, using Carslaw and Jaeger's (1959) solutions, that the temperature history at a given radius was independent of the radius of the line source, so accurate cylindricality of the hot wire was not vital. Furthermore, based on Carslaw and Jaeger, and Fourier, it was deduced that the thermal conductivity and volumetric heat capacity of the hot wire or probe merely shifted the curve of temperature rise over the natural logarithm of time while retaining the slope, hence results for thermal conductivity were not affected.

Sandberg et al (1977) discussed a method of obtaining values for thermal conductivity and thermal diffusivity from a hot wire measurement. Developing Carslaw and Jaeger's solution, where higher order terms are generally expected to become insignificant at later times, a "polynomial in the inverse powers" was used to prevent this. An iterative methodology was then used to establish thermal diffusivity and volumetric heat capacity. Long times were defined as when $\alpha.t/r^2 \geq 1$.

Measurements for distilled water, and glycerol at various temperatures and pressures, including both glass and crystalline forms, closely matched expected

values for thermal conductivity and thermal diffusivity. It was stated that contact resistance between the wire and medium could be taken into consideration as long as it was axially symmetric, but the method was not shown. It was said that subjecting the samples to pressure increased thermal contact and it was recommended that this be done to remove voids even where the measurement then takes place at atmospheric pressure. Finding less than 3% difference in volumetric heat capacity values achieved for liquid and crystalline glycerol at a range of pressures, increased from atmospheric pressure to 0.8 MPa and back again, convinced the authors that contact resistance did not then seriously influence their results.

Cull (1978), working for the Bureau of Mineral Resources in Australia, following a period of research including transient line source measurements at Oxford University for the Natural Environment Research Council (NERC), made a study of contact resistance between transient line sources (hot wires and probes) and sample mediums. Using thin wires to measure fine grained granite and silica glass, with their thermal conductivity previously measured by a divided bar apparatus, it was calculated that contact resistance, termed *H*, was 300 $Wm^{-2}K^{-1}$, which was said to be equivalent to 0.08mm of air between the wire and sample. For a best case scenario with a thermal probe, *H* was estimated to be 500 $Wm^{-2}K^{-1}$, and equivalent to 0.05mm of air.

The contact resistance was explained as having more cause than just poor physical contact. Within the heater wire, conduction was primarily by free electrons whereas transfer to the sample was assumed to be solely by phonons, a quantized mode of vibration occurring in the atomic lattice. As free electron energy could only excite phonon motion indirectly, this introduced what

was described as equivalent to a grain boundary. In Cull's methodology to establish thermal diffusivity and then thermal conductivity by using the maximum rate of temperature rise over time, contact resistance was held responsible for up to 40% error in thermal conductivity values.

Cull suggested that Blackwell's large time solution to overcome contact resistance was largely subjective, being dependent on probe construction, probe radius, sample diffusivity and contact resistance. The practical solution was to wait for a linear asymptote in $\Delta T/\ln t$, although a linear asymptote was not always obvious in measurements, often leading to undetected errors. Cull emphasised the reflection of heat from the boundary of small samples as a significant cause of non-linearity.

Modeling the data achieved with the hot wire in fine grained granite and silica glass, and using Carslaw and Jaeger's solution of a cylindrical region bounded internally by a wire, it was concluded that, for a probe with radius of 0.5mm under ideal contact conditions, errors in thermal conductivity results greater than 2% would occur before 270s.

Gustafsson et al (1979) considered the hot wire, and by inference the thermal probe, as fundamentally inadequate for the measurement of thermal conductivity and thermal diffusivity in solid materials. It was regarded as too difficult or even impossible to achieve sufficient thermal contact between the heater and the medium. Using similar theory and basing work on that of Carslaw and Jaeger, a hot strip was developed, in the region of 4mm wide and 0.008mm thick. This was used (a) sandwiched between two smooth planes of the sample medium (fused quartz), (b) suspended in liquid (glycerol), and (c)

cast into Araldite. With quartz, a low viscosity oil of known thermal properties was used to improve thermal contact. It was shown that the slight lack of full contact at the strip edges was negligible.

An improved version of the hot strip was also discussed whereby the metal was evaporated onto a ground surface of the sample medium, where an accuracy of better than 0.3% was indicated for specific heat results.

The methodologies involved either sandwiching a flexible strip or carrying out an evaporation process in a vacuum, and so neither would be suitable for in situ measurements.

Davis and Downs (1980) of the British Ceramic Research Association, working with the National Physical Laboratory (NPL), carried out a critical review of the hot wire, transient line source method, as applied to the measurement of thermal conductivity in insulating refractory bricks with thermal conductivities in the region of 0.12 to 0.6 $Wm^{-1}K^{-1}$. There was concern that hot wire measurements were generally 10% higher than those achieved by steady state methods, and that there was a spread of mean results by the hot wire method between separate laboratories of ± 12%, with a total spread in the region of ± 25%.

Their method was to sandwich and tightly clamp a hot wire between softer refractory bricks or, with harder samples, to cut a fine groove slightly larger than the wire to accommodate it. In the latter case, a setting paste or a dry dust was used, either containing dust from the bricks themselves, as a contact filler and it was found that both methods gave similar results for the same sample. A

thermocouple was attached to the hot wire at the mid point and led out at 60° from the wire to avoid electrical interference that had been encountered at different angles. A calculation termed the 'variance coefficient' was employed to assess the repeatability of results. This consisted of the standard deviation of results divided by their mean average value. The variance coefficient was expressed as a percentage within which repeatability could be assumed, e.g. ± 10%. Where no filler was used or poor contact could be assumed for other reasons, the variance coefficient for results was significantly higher. The wire length to radius ratio was 900:1, hence it was assumed that end losses could be safely ignored.

The spread of results increased considerably with samples of higher thermal conductivity, above 1.5 $Wm^{-1}K^{-1}$, which was thought to be a result of lower temperature rises causing proportionally larger errors, combined with boundary effects being reached sooner. It was also stated that the equipment used did not have sufficient heat output to bring the chart of temperature rise over the natural logarithm of elapsed time to a linear section. Citing Eschner et al (1974), 2.0 $Wm^{-2}K^{-1}$ was recommended as the higher limit for the hot wire method. It was also noted that higher temperature rises from increased power inputs gave rise to higher thermal conductivity measurement values.

In heating the wire and charting the temperature rise over the natural logarithm of elapsed time, it was said that the initial curve was a consequence of the sample thermal diffusivity, the heat capacity of the wire, and the relative heat transfer coefficient ($Wm^{-2}K^{-1}$) between the wire and the sample. This was then followed by a linear asymptote from which the thermal conductivity was calculated, followed by a further curve caused by boundary losses from the

sample's edge and end losses from the probe. The tests in refractory bricks used, as the linear portion, times from either 60s or 120s to 600s with, initially, around 36 recorded points, although repeat tests only used two points, at the start and end times of the then assumed linear section. The authors were careful to control ambient temperatures and used the criterion that this should not fluctuate by more than 0.05°C over 300s. A check on linearity was carried out by noting the temperature change over a series of time intervals with the same ratio, e.g. 60s – 240s, 80s – 320s, etc. where the ratio was 1:4. For linearity, it was said that the temperature rises over these intervals should be roughly constant.

The article was inconclusive regarding the resolution of interlaboratory differences. Up to 50% of the variation was estimated as possible in worst case scenarios from such as sample differences, although great care was taken in ensuring continuous manufacture, matching densities, and equipment accuracy. The use of only two data points from $\Delta T/\ln t$ where these may have strayed from the linear asymptote was also considered a potential source of error.

Anisotropy was mentioned as a potentially significant consideration. It was thought to be caused by the raw material for insulating refractory bricks containing sawdust, pitch or other combustible materials, which were then burnt out during the firing process. It was suggested that this could result in aligned lenticular pores. Previous work using steady state methods was cited (Barrett et al, 1946) that showed perpendicularly opposed measurements in a sample of refractory bricks had given thermal conductivity results of 0.83 $Wm^{-1}K^{-1}$ and a 36% higher value of 1.13 $Wm^{-1}K^{-1}$. It was thought that the radial flow from the hot-wire test would tend to give an average result for both directions and hence

this could have explained discrepancy between the methodologies. Of note, it was suggested that the direction of measurement may only be assumed in manufacturers' values achieved by steady state methods, such as the guarded hot plate, hence errors could be introduced to practical engineering applications.

Riseborough et al (1983), in studying permafrost, carried out a sensitivity analysis on Jaeger's solution, equation (7), and it was found that markedly different combinations of thermal conductivity, thermal diffusivity, and therefore heat capacity, could produce indistinguishable probe heating curves. It was then construed that attempts to establish all values simultaneously were prone to error. The solution was to establish the heat capacity of the soils independently by using time domain reflectometry, measuring electrical conductivity to establish the water content, and so subsequently calculate heat capacity theoretically from known values of dry soil. Jaeger's solution to the probe heating curve was then constrained by the value achieved for the heat capacity to give values for thermal conductivity.

A critique of late 20th century and contemporary research

Batty et al (1984a) carried out an extensive review of thermal probe theory and performed numerous trial measurements in pursuance of a method to provide a thermal conductivity and thermal diffusivity measuring methodology for construction materials. The interest was in moving thermal probe technology from controlled laboratory situations to use in real engineering situations, e.g. in situ measurements. The effects of moving away from the perfect model of an

infinite homogenous sample heated by a minutely thin, infinitely long, perfectly conducting line source in perfect contact with the sample were studied.

Matters of concern included: probe length to radius ratio with regard to axial loss errors; the effect of the probe's own thermal capacity on measurements; contact resistance between the probe and sample material; probe diameter related to the conductivity of its sheathing; sample size and boundary effects; radiation effects; inhomogeneity and anisotropy of the sample material.

An illustration of the solution for the temperature change over time at the thermal probe's surface when inserted into a sample was given, from Blackwell, as below:

$$\Delta T \cong \frac{Q'}{4\pi\lambda}\left\{\ln\left(\frac{4\alpha t}{r^2}\right)-\gamma+\frac{2\lambda}{r\,H}+\frac{r^2}{2\alpha t}\left[\ln\left(\frac{4\alpha t}{r^2}\right)-\gamma+1-\frac{\alpha . M_p C_p}{\pi . r^2 \lambda}\left(\ln\left(\frac{4\alpha t}{r^2}\right)-\gamma+\frac{2\lambda}{r\,H}\right)\right]+O\left(\frac{r^2}{\alpha t}\right)^2\right\}$$

Equation (14)

where M_p denotes the mass of the probe per unit length and *O* denotes further, relatively small terms in the order of $\frac{r^2}{\alpha t}$.

Equation (14) was reduced to:

$$\Delta T \cong A\left[\ln t + B + \left(\frac{1}{t}\right)(C\ln t + D)\right]$$

Equation (15)

where:

$$A = \frac{Q'}{4\pi\lambda}$$

Equation (16)

$$B = \left[\ln\left(\frac{4\alpha}{r^2}\right) - \gamma + \frac{2\lambda}{rH}\right]$$

Equation (17)

$$C = \frac{r^2}{2\alpha}\left[1 - \frac{\alpha.M_p C_p}{\pi.r^2\lambda}\right]$$

Equation (18)

$$D = \frac{r^2}{2\alpha}\left[\ln\left(\frac{4\alpha}{r^2}\right) - \gamma + 1 - \frac{M_p C_p \alpha.B}{\pi.r^2\lambda}\right] + O\left(\frac{1}{t^2}\right)$$

Equation (19)

where *O* denotes further, relatively small terms in the order of $\frac{1}{t^2}$.

It was identified that in Blackwell's, and Vos', solutions the thermal diffusivity value of the sample being measured was required to calculate appropriate probe length to radius ratios, so that axial losses did not compromise thermal conductivity measurements. Thermal diffusivity values were also needed to identify after which time the *C* and *D* terms of equation (15) could be neglected, i.e. when $\alpha.t/r_o^2 \geq 1$, after which time thermal conductivity values could be determined directly from term *A*.

Term *B* showed that measurement of thermal diffusivity by the thermal probe would require knowledge of the contact resistance between the probe and sample, the reciprocal of which is, or is part of, *H*, unless this resistance could

be considered negligible, i.e. towards perfect contact. Conversely, values for contact resistance could only be established where the sample thermal diffusivity was known. It was noted that Blackwell had deemed it desirable to determine contact resistance independently.

Potential values for thermal conductance *H* were cited from the literature (Ozisik and Hughes, 1966; Holman, 1981). Three values were given:

- 1,900 $Wm^{-2}K^{-1}$, stainless steel surfaces of 0.2 and 1 μm root mean square (r.m.s.) roughness at 167°C and 0.71 MPa.

- 1,890 $Wm^{-2}K^{-1}$, stainless steel surfaces of 1.14 μm r.m.s. roughness at 20°C and 5.57 MPa

- 3,790 $Wm^{-2}K^{-1}$, stainless steel surfaces of 2.54 μm r.m.s. roughness at 145°C and 1.42 MPa

It was put forward, based on these values, that an *H* value of 100 $Wm^{-2}K^{-1}$ for metal sheathed probes would be a reasonable assumption for measurements in tight holes within masonry materials. No calculations were given to show how this figure was arrived at, and the pressure at which measurements were taken was not discussed, hence the validity of the assumption can not be assessed.

Consideration of the comparative thermal conductivities and thermal diffusivities of the probe and samples was also needed to further assess errors from axial losses. Blackwell was cited as providing the following expression to obtain the minimum probe length to radius ratio:

$$\frac{L}{r} \geq \left(\frac{\alpha.t}{0.0632r^2} \right)^{1/2}$$

Equation (20)

and cited again as giving the following expression for the relative error that would be caused by axial losses:

$$\Delta R = \pi^{-1/2} \left\{ \exp\left[-\left(\frac{L}{r} \right)^2 \div \left(\frac{4\alpha.t}{r^2} \right) \right] \right\} \times \left\{ \left[\left(\frac{4\alpha.t}{r^2} \right)^{1/2} \div \frac{L}{r} \right] + 2\sigma \frac{LS}{r} (\varepsilon - \eta) \left(\frac{4\alpha.t}{r^2} \right)^{-3/2} \right\}$$

Equation (21)

where:

ΔR = Relative error due to the presence of an axial heat flow

$\varepsilon = \frac{\lambda_p}{\lambda}$

$\eta = \frac{\lambda_p \alpha}{\lambda \alpha_p}$

$\sigma \approx \frac{2\delta}{r}$

$S = \ln\left(\frac{4\alpha.t}{r^2} \right) - \gamma + \frac{2\lambda}{r\,H}$

Equation (22)

and

δ = thickness of the probe wall

Various uncertainties remain in this part the methodology employed by Batty et al. The choice of 100 $Wm^{-2}K^{-1}$ for H in masonry materials was not substantiated, as no derivation or interpolation was shown. Cull (1978) had discussed H as being dependent on material properties distinct from, as well as combined with, contact levels, raising the possibility of it never being negligible. Both Carslaw and Jaeger (1948 pp.13-14) and Veziroglu (1967) had shown the difficulty with

measuring H independently. It is therefore possible that the thermal diffusivity value, calculated from equation (17) and used to establish probe dimensions, could be in error. The expression to calculate axial losses, equation (20), also depended upon knowledge of both the probe and sample's thermal diffusivity, where the latter would usually be unknown at the time of measurement.

Batty et al cited Vos as having concluded that a linear asymptote of the $\Delta T/\ln t$ slope could only be relied upon within experimental error where the effect of the probe's finite radius was reduced to the point where $4\alpha.t/r^2 > 50$. From this, as the sample thermal diffusivity and the probe radius were presumed constant, a time window was chosen in analyses, before which a linear asymptote could not be assumed. This elapsed time before the analysis window decreased for materials with higher thermal diffusivity, and increased with an increase in probe radius.

Vos was also cited in consideration of sample size and boundary effects, with corroboration from Andersson and Backstrom (1976), based on previous work by Carlsaw and Jaeger. Boundary effects were considered significant where $4\alpha.t/b^2 > 0.6$ (or, according to Andersson and Backstrom, the error was less than 0.1% when $4\alpha.t/b^2 < 1$) where b was the shortest distance between the heater wire and the nearest boundary of the medium. With thermal diffusivity and time both positive in the numerator, this shows that an increase in either required larger radius samples to avoid boundary effects. It was considered that, where boundary effects occurred, these were dependent on the thermal properties of the medium beyond the boundary, and that the disturbance would take twice the time taken for heat to travel to the boundary before creating effects.

The boundary condition raises further difficulty. As the probe was presumably inserted through the open face of a material, the boundary condition here would have been different to that elsewhere, i.e. at a radial distance from the probe, or at the other, inserted end. This factor was not discussed.

Andersson and Backstrom (1976) had noted that end effects would reveal themselves as non-linearity in curves of $\Delta T/\ln t$. They also considered contact resistance as a boundary condition between the insulating material being measured and the 0.1mm nickel wire, used in their work as a heater and temperature measurement device. It was stated that the temperature of the wire would be higher by a constant term than the temperature of the insulator's internal boundary. However, it was estimated that, in the case of their 0.1mm wire, the effect would be negligible.

The inhomogeneity of construction materials was considered by Batty et al (1984a), especially in regard to air content in mineral wool insulation. An S curve was shown of $\Delta T/\ln t$ for mineral wool insulation at 19.7 $kg.m^{-3}$ where the decreasing gradient of the curve towards linearity at later times, after about 100s, was attributed partly to inhomogeneity. It was considered that the 300mm long hot-wire being used, of 0.28mm radius ($l/r \approx 1{,}000:1$), had pushed together the fibres of the mineral wool, which had lowered its thermal conductivity nearer to the probe. Some consideration was also given to relative contact resistance, with that between the probe and the fibres being regarded as better than that between the fibres. The curve gave approximate values of thermal conductivity of 0.038 $Wm^{-1}K^{-1}$ between 50s and 500s, which was the expected value, and only 0.015 $Wm^{-1}K^{-1}$ between 20s and 50s.

Batty et al gave guarded hot plate values from the literature (Anon, 1981) that showed thermal conductivity values of glass fibre should fall from around 0.04 $Wm^{-1}K^{-1}$ at 10 $kg.m^{-3}$ to around 0.033 $Wm^{-1}K^{-1}$ at 50 $kg.m^{-3}$ to 180 $kg.m^{-3}$, which values have been corroborated by Anderson (2005). However, lower thermal conductivity values were achieved at early times, despite the hot wire length to radius ratio condition having been exceeded and where the condition $\alpha.t/r^2 > 50$ existed after 14s.

Radiation effects were considered in the mineral wool measurements. It was considered, from Woodside (1958), following van der Held, that radiation effects in an open pored material would lead to higher apparent thermal conductivities than those of pure conduction and that higher probe powers would increase this effect. This was shown in a charted comparison between the hot-wire measurements and published guarded hot plate values (Anon, 1981) where the hot-wire values were between 13% and 15% higher.

Mineral wool was also used in an assessment of anisotropic thermal effects. It was found that, using a hot-wire, denser samples of mineral wool, where radiation effects should be significantly reduced, also gave higher apparent thermal conductivities than those found by the guarded hot plate method. To investigate this phenomenon, a series of thermocouples were placed in mineral wool radially equidistant at 30mm from an unspecified thermal probe. Various wool densities and probe powers were used. It was shown that the thermal anisotropic effects of uncompressed mineral wool were slight but increased significantly when the material was compressed. It was concluded that the greater heat flow in the fibre layer plane, perpendicular to the heat flow direction in guarded hot plate measurements, gave rise to the higher values achieved by

the probe. Hence thermal conductivity results were found to exceed guarded hot plate results in uncompressed fibre insulation through radiation effects and in compressed material through anisotropic effects.

A section of the article addressed the assessment of accuracy. It was put forward that accuracy was a function of repeatability and systematic uncertainty. In a series of experimental measurements to assess systematic uncertainty, repeatability was easily assessed by a number a measurements being taken with the same probe in the same sample under carefully controlled conditions. Systematic uncertainty was found by calibration, which it was said should be against equipment with four times the accuracy of the calibrated item. Various probes of various radii and composition were used to measure a sample of paraffin wax, which was also measured by a plain (unguarded) hot plate method. It may be noted that the plain hot plate standard, BS 874 (BSI, 1973), was replaced by later editions from 1987 onwards. These made no mention of the method, which had been replaced by the guarded hot plate. Probes that gave unacceptable levels of difference to the plain hot plate results were abandoned. Uncertainty in the remaining probes was established by the difference between probe results and those of the plain hot plate. Accuracy as low as 4.6% was reported for individual probes although overall accuracy was reported as 10.6%.

Batty et al (1984b) assessed the thermal probe methodology in measurements with moist materials, wet clay and aerated concrete blocks. The stated aim was to assess whether the thermal probe could be used to provide reliable measurements of building materials in situ, including their moisture content.

This was to provide accurate data for predictions, mathematical models and heat loss assessments for the behaviour of buildings.

Probe diameter was studied to see whether it was essential for this to be as small as practically possible. Blackwell was cited as showing this was not essential and Woodside was cited as showing that larger probes reduced errors from moisture migration. Probes with various radii and length to radius ratios were calibrated in paraffin wax against plain hot plate measurements and assessed against a 95% confidence limit based on repeatability and systematic uncertainty. A range of reported accuracies was given, from 7.8% to 17.4%, which values were higher than those previously reported (Batty et al, 1984a). A simple calibration factor was then applied to the results of each probe, which assumed that probes would exhibit similar behaviour in diverse materials.

It was concluded that results for thermal conductivity measurements in clay with a 42% by volume water content showed no significant difference with different probe diameters. These ranged from 2.4mm to 4.85mm, while length to radius ratios ranged from 48:1 to 25:1. Tables of mean values showed that thermal conductivity results rose from 1.72 $Wm^{-1}K^{-1}$ at 2.4mm diameter to 2.01 $Wm^{-1}K^{-1}$ at 4.85mm diameter, a rise of 17%. Despite a noticeable trend of higher thermal conductivity results at increased probe diameters, the significance was discounted on the basis of the confidence level used. Lower thermal conductivity results had been expected at higher diameters, contrary to the achieved results.

Probe calibration was carried out by applying a simple probe factor to the measured results. This was calculated for each probe as a multiple based on

the difference in results for paraffin wax compared to those achieved by the plain hot plate method. It is of note that two of the probes used, numbers (3) and (4), were similar in construction, both copper sheathed, 3.3mm diameter with lengths of 58mm and 64.5mm. When used in paraffin wax, probe (3) gave an 11% higher value than probe (4), before the calibration factors had been applied. Following the application of the calibration factors, probe (4) gave an 11% higher value than probe (3) in wet clay, and an almost identical value beforehand. This strongly suggests that, using the methodology of Batty et al, this simple calibration factor, based on measurements in one material with known thermal properties, could not be relied upon for use with other materials.

Charted results for thermal conductivity in aerated concrete block showed an expected increase with moisture content. It was concluded that the probe was an:

"accurate and rapid technique for the measurement of thermal conductivities of moist masonry materials".

The conclusion is open to question as the calibration factor may not have been appropriate. No reference values were given to substantiate the values for wet clay or aerated concrete. Thermal diffusivity measurements, dependent on the intercept of $\Delta T/\ln t$, are more difficult to achieve than those of thermal conductivity. A 17% difference in thermal conductivity results, as was reported for moist clay, based on the slope of $\Delta T/\ln t$, would suggest a wider variance in the intercept of $\Delta T/\ln t$, and hence valid thermal diffusivity results were probably not achievable by this method. As a footnote to the review of Batty et al, it is of interest that neither of the articles mention the time delay methodology suggested by earlier researchers.

Davis (1984), in a book reviewed by Blackwell and members of America's National Oak Ridge Laboratory, repeated the view that thermal diffusivity values became negligible in the traditional solution, equation (14), relating to $\Delta T/\ln t$ at later times. It was stated that the equation could only be applied to the linear asymptote, that the first part of the curve was a function of the probe heating up, and the last part of the curve was a boundary effect. It was concluded that a probe should be matched to its test material to avoid difficulties in obtaining a linear section on the $\Delta T/\ln t$ graph. This implied that, as with Batty et al (1984a), the thermal properties of the sample needed to be estimated before valid measurements could be taken. This would pose a difficulty for the current work where blind testing may be required, and where the published thermal properties for many materials are not given as hard and fast values. For instance, Hukseflux (2007) gave a range of thermal conductivity values from 0.15 $Wm^{-1}K^{-1}$ to 4.0 $Wm^{-1}K^{-1}$ for soils and, as was seen in chapter 1, published values for thermal diffusivity are often unavailable.

Greg at al (1985) developed a hot wire apparatus that was reported to measure thermal conductivity and thermal diffusivity of unconsolidated materials to an accuracy of 1% and 6% respectively. Equipment comprised a platinum heater wire, also acting as a resistance thermometer, mounted in a pressure container. The wire radius was kept as small as practically possible, without breaking, at 25.4 μm, to represent a perfect line source. Measurements were taken at 100Hz over 2s – 3s periods. Differentiating Carslaw and Jaeger's equation for later times, when $r^2/4\alpha t \leq 1$, led to the recognised solution for thermal conductivity:

$$\lambda = Q'/4\pi.A$$

Equation (23)

and the following equation for thermal diffusivity:

$$\alpha = Cr^2 / 4\exp(B/A)$$

Equation (24)

where: C = the exponential of Euler's constant

B = the ordinate-intercept of the linear asymptote

A = the slope of the linear asymptote

An automated schedule was set up for measurements whereby a computer assessed thermal drift prior to a measurement, during which time power was directed to a dummy heater. Power was then switched to the hot wire and data recorded on a 10Mb hard drive. Data was reduced and analysed using a least squares fit to the asymptote.

The equipment was first calibrated in glycerin at two temperatures and then used to measure uniform 50μm glass beads at various temperatures and pressures, and then spent oil shale. Values achieved for thermal conductivity and thermal diffusivity of glycerin at room temperature, 21.8°C, were accurate to expectations by 1% and 6% respectively, based on values from Venart and Krishnamurthy (1968), and Sandberg et al (1977). An asymptote of $\Delta T/\ln t$ was given for these measurements showing slight deviations from linearity. Asymptotes were not given for the glass bead measurements so it is not known whether they were linear and, as no comparative results by another means were given, it is not possible to gauge the accuracy of results. Results were not given for the spent oil shale measurements.

Singh et al (1985) were interested in simultaneously measuring the thermal conductivity and thermal diffusivity of building materials. Their chosen method was the transient hot strip developed by Gustafsson. The method used an enclosed cell where the hot strip was suspended and surrounded by dry

powders of such as brick dust, sand, mud, etc. A constant current device was used to ensure that the power output and resistance temperature measurements could be made from the same element. Charts showed that, using derivations from Carslaw and Jaeger's solutions, linearity was achieved in curves of voltage, representing change in temperature, over a function of elapsed time for measurements in the region of 16s.

The reported error in thermal conductivity measurements was 2%-3% and, for thermal diffusivity, 9%-10%, when compared to previous thermal probe measurements for thermal conductivity (Pande et al, 1984) and hot wire measurements for thermal diffusivity (Sharma et al, 1984a). Tabled results showed up to 15% variation for thermal conductivity and non corresponding variations of up to 26% for thermal diffusivity in these comparisons. Pande et al had used a thermal probe to make their measurements but did not describe any corrections for contact resistance, end or axial losses. It was not shown whether controls were in place to ensure samples, such as brick and mud dusts, measured by each researcher were comparable.

Contemporary measurements of thermal properties in liquids were being carried out by the transient hot wire methodology to a reported accuracy of 0.4% for thermal conductivity and 1% for thermal diffusivity by Knibbe (1987) using 80ms measurements with around 1.6°C temperature rises.

Drury (1988), at the Geological Survey of Canada, was interested in heat flow through seabed and lake floor sediments. It was upheld that thermal probes had been used successfully in these saturated materials to measure thermal conductivity but had not produced reliable results for thermal diffusivity. It was

put forward that the measurement radii of probes in common use were indeterminately small, as the temperature measurement devices were within them. This was not significant for thermal conductivity measurements, as, once $t \geq r^2/4\alpha$, terms for r disappeared from the simplified solution derived from Carslaw and Jaeger. However, at these later times, terms for α also disappeared. A larger probe radius was not considered a solution as it would have compromised simple line source theory and required the more complex solution as previously attempted by Riseborough et al (1983).

The solution offered by Drury was to introduce a second probe to measure the temperature change at a known distance from the standard thermal probe, thus increasing values for r. Axial and end loss effects were not discussed in this regard or whether these may have increased with larger radii.

In the experimental work described, the probes were placed 13mm apart. Thermal drift caused by ambient environmental effects was assessed by comparing temperatures before the heating cycle with temperatures after ten times the heating period, at which time it was assumed that thermal equilibrium should have been regained. Data were then adjusted for this drift prior to analysis. Analysis was carried out by an iterative line fitting method, comparing observed data with data calculated by the Carslaw and Jaeger solution, using root mean square minimisation. It was suspected that, as thermal diffusivity results were inaccurate, compensation for thermal drift had been excessive.

A loss of resolution in the data at later times was reported and line fitting was less close during the middle of the heating cycle. This was attributed to a suspected but unspecified systematic error. The greatest cause of uncertainty

was said to be connected to probe separation, where a 0.5mm difference could lead to a 5% uncertainty in thermal diffusivity results. It was suggested that the most appropriate probe spacing for saturated sediments, with expected thermal diffusivities in the range of 4.0 $x10^{-7}$ m^2s^{-1} to 1.0 $x10^{-6}$ m^2s^{-1}, was between 20mm and 25mm. No comparative data were given although it was said that results were in the expected range for such materials.

Another experiment was briefly reported, where Patterson et al (1987) had used a similar methodology in frozen silty soil. Here the material required pre-drilling and a highly conductive filler was used to minimize contact resistance. It was thought, based on inferior line fitting and resolution, that normal line source theory may not have been appropriate for this measurement, where the filler introduced a material with substantially different thermal properties than those of the sample.

Håkansson et al (1988) used a hot-wire technique to measure glycerol and two powdered solids, sodium chloride and caesium chloride. Nickel wires, of both 0.1mm or 0.3mm diameter, were used as simultaneous heaters and resistance thermometers. These were placed as a horseshoe shape within an enclosed Teflon cell of 39mm diameter and 18mm height. Powders were thoroughly tamped into two plates with the hot wires pressed between these. The length to radius ratios of the wires were 800:1 and 270:1 respectively. Part of the stated work aim was to assess the appropriate wire diameter for the thermal properties of the sample being measured.

As with previous researchers, an iterative, least squares, line fitting process was used to analyse data from $\Delta T/\ln t$. Measurements were taken over a 1s period

where the early times, identified from their previous work as being between 400μs and 1,000μs, were used to measure thermal diffusivity and later times used to measure thermal conductivity. In order to avoid small fluctuations in temperature measurements, average temperatures were used over 20ms periods, i.e. from t-10ms to t+10ms. It was put forward that line fitting would not be affected.

100 values for glycerol produced a standard deviation of 0.18% from the mean for thermal conductivity and 0.9% for thermal diffusivity, with both reported as within 1% of published values. However, it was found that an increase from 0.1mm to 0.3mm in the potential leads to the hot wire caused an increase in the thermal conductivity result and a decrease in the thermal diffusivity result, both of 3%.

Calculations, based on previous work by Knibbe (1986), were carried out to assess the possible effect of end losses, and it was found that the potential leads could theoretically lead to errors of 5% and 10% for thermal conductivity and thermal diffusivity respectively. It was recommended that unwanted cooling of the hot wire be minimised by making potential leads as thin as possible. Knibbe had shown that not only would end effects decrease with an increase in length over radius ratios, they would increase where the ratio of probe thermal conductivity to that of the sample increased.

Results for caesium chloride were reported as being within 1% of published values, although the table given shows a 3% difference in volumetric heat capacity values when using the thinner potential leads. Problems were reported with measurements of NaCl as systematic deviation in the residuals of the least

squares method was found. This was thought to be as a result of boundary effects, as the shortest distance between the hot wire and the Teflon vessel was just 5mm. Calculations were made using a Carslaw and Jaeger solution for temperature perturbation at the centre of a 5mm diameter cylinder. When the derived corrections were applied to the line fitting technique, this showed errors in thermal conductivity and thermal diffusivity of 3% too low and 16% too high, respectively, using the 0.3mm wire, and 3.3% and 60% in the 0.1mm wire. Based on the thinner wire reaching 41% of its final temperature at the first point of measurement compared with 20% for the 0.3mm wire, it was put forward that the 0.1mm wire was more sensitive to the boundary effect, although no other corroborating evidence or theoretical justification was given.

According to the Vos term, for the thermal properties given, boundary conditions should not have occurred during the time of the measurement at 5mm. While the shortest boundary distance was 5mm, the maximum distance, in the circular container, was 34mm, hence boundary distance was variable, which would create further complexity. Contact resistance was not mentioned, which may have affected results and $\Delta T/\ln t$ curves for the different materials.

Hust and Smith (1989), in a project sponsored by the American Society for Testing and Materials (ASTM), coordinated an interlaboratory comparison of thermal conductivity measurements by the hot-wire and thermal probe techniques. Six laboratories measured five materials, including fibre glass insulation, extruded and expanded polystyrene foams, paraffin wax, and Ottawa sand at varied moisture content.

Results achieved with the thermal probe lay 14% - 35% lower than those achieved with the hot-wire. As values for these materials were not corroborated by alternative established means, it could not be said which method might be more accurate. Scatter in the results gave differences of over 100%, e.g. for Ottawa sand with 3.5% by weight moisture content, values ranged from 0.25 $Wm^{-1}K^{-1}$ to 1.8 $Wm^{-1}K^{-1}$. Paraffin wax values measured by a 150mm x 3mm thermal probe ranged from 0.195 $Wm^{-1}K^{-1}$ to 0.335 $Wm^{-1}K^{-1}$.

It was stated that the accuracies of both methods were in doubt. The quotes below are taken from their conclusions:

"Thus it is debateable whether either apparatus (hot wire or thermal probe) is suitable even for use in comparative measurements"

and

"Further work needs to be done to establish and / or improve the reliability of each of these methods for use in a laboratory environment such as quality control or research".

Van Haneghem (1981) produced his thesis at Wageningen University based on improvements to the thermal probe method to measure thermal conductivity, heat capacity, and contact resistance between the probe and the sample. An approach was developed called the Modified Jaeger Method (MJM). Probes were first calibrated in agar immobilised water, where it was assumed there would be no contact resistance. This correction for the residual resistance, termed the 'internal resistance', of the probe was subsequently applied to measurements in other materials. A temperature time correction, as applied by Hooper and Lepper (1950) and Hooper and Chang (1953) was used. The standard Carslaw and Jaeger solutions were used with a calculated rather than

a measured radius, the radius values being adjusted to give the known thermal property values for water. The calculated radius was termed the 'effective radius'. It was stated that a rough estimate of volumetric heat capacity, described as obtainable to within 20%, was sufficient to calculate an accurate value for thermal conductivity. Measurements of saturated glass beads of a similar diameter to the probe's radius, and measurements of dry glass beads, showed that the method was not satisfactory for highly inhomogeneous materials.

In considering the Modified Jaeger Method, it may be borne in mind that Carslaw and Jaeger (1948 pp.13-14) had shown that the effects of the *H* term, which was then referred to as exterior conductivity, were dependent on the temperature difference between the materials under consideration. Thus the temperature difference between each probe component would, in part, be dependent on the thermal properties of the sample medium. It thus remains unclear whether the internal resistance of a probe would remain constant or whether it would change, dependent on the particular thermal properties of the sample medium. Cull (1978) had shown that contact resistance, in terms of heat transfer, was affected by the atomic nature of materials as well as their level of physical contact. With the Modified Jaeger Method, heat transfer resistance was considered to be dependent only on physical contact, thus it is uncertain whether the correction value found in agar would transfer successfully to materials with diverse thermophysical properties and physical states.

In Bruijn, van Haneghem and Schenk (1983), the perfect line source model was discounted as inadequate for measuring the thermal conductivity, and entirely unsuitable for measuring the thermal diffusivity, of granular materials

without consideration of contact resistance. It was recognised that the Modified Jaeger Model had two sources of inaccuracy: the use of an effective radius for the temperature measurement position away from the heating element; and the inhomogeneity of the probe composition.

Van Haneghem et al (1983), reporting the results from Bruijn et al (1983), discussed the internal resistance and the effective radius of the probe. These were found by adjusting their values to ensure calculated results, based on measurements taken in agar immobilised water, fitted the well known thermal properties of water. Probe accuracy for thermal conductivity was then stated as available within 1%, and results were reported for glass beads and silver sand. Probe accuracy for volumetric heat capacity was stated as available within 20%, although no results were given.

The calibration involved adjustments to internal resistance values and the introduction of an effective radius for the temperature measurement position in one material and then reliance on these corrections for measurements in other materials. Comparative reference values for the granular materials measured were not given, hence the success of this method could not be substantiated by the evidence of the results.

Van Haneghem later collaborated on a new thermal probe model (van Loon et al, 1989). The introduction to this article stated that thermal probe technology was, by this time, widely used in such applications as measuring the thermal conductivity and volumetric heat capacity of building materials at various moisture contents.

The new work was based on the Modified Jaeger Method and introduced further time corrections to increase accuracy, especially for volumetric heat capacity results. Stainless steel probes of 200mm x 1mm to 2mm diameter were used, enclosing a heater wire and a thermocouple. The cold junction of the thermocouple was placed in the base of the probe and assumed to retain its original temperature. Reliance on the calculation of probe internal resistance through measurements in agar gel was maintained, as was the use of an effective radius for the temperature measurement location. A non-linear solution was employed to analyse temperature rise at earlier times by a least squares method of iterations that produced simultaneous values for thermal conductivity, volumetric heat capacity and contact resistance. It was stated that a disadvantage of the method was that initial guessed values for the iterations needed to be near the value to be calculated, otherwise wrong values would result.

Accuracy for thermal conductivity was claimed to be achievable within 3% and volumetric heat capacity within 25%, with values given only for agar immobilised water. The level of error that could be introduced by inappropriate input guesses to the iterative analysis methodology was not discussed. This gives rise to uncertainty should the method be considered for in situ measurements of building materials. Building materials of similar appearance may have a wide range of reported thermal conductivity values (e.g. aerated concrete and earth based materials), and often no published thermal diffusivity values. This would create difficulty in accurately estimating initial values for the iterations with confidence.

Van Haneghem et al (1998) had more or less abandoned the pursuit of volumetric heat capacity values when they developed a portable thermal probe device, although the device was designed so that data could be stored and subsequently reanalysed by the Modified Jaeger Method.

This equipment had been developed to be transportable, robust, stand alone, and to be accurate to within 5% for thermal conductivity values measured in situ. The device was suggested as being useful to measure building materials, with heat storage again being mentioned. It was also intended to be useful to agriculture and food storage industries. Probe dimensions had not changed from 200mm x 1mm to 2mm diameter. A resolution of 10nV was available for the thermocouple and it was found that noise, over a 60s period was around 15nV.

This equipment was again calibrated in agar gel. Results were achieved within 5% of published values, which was considered to be more than adequate for practical use. The results were based on the perfect line source model with terms only for thermal conductivity, at long times, and volumetric heat capacity, although it was recognised that no reliable value for this last property could be obtained by this method. The article does not discuss time windows for analyses, contact resistance or correction for thermal drift, shown as about 0.1°C over a 60s period.

Jones (1988), following van der Held and van Drunen, and Batty, worked on obtaining thermal conductivity results from $\Delta T/\ln t$ at early times, before linearity had necessarily been reached, by finite element analysis. Estimation of contact resistance between the probe and samples was considered as having an effect

on the curve. The short time solution of Blackwell (1954) was considered inappropriate as it was based on an idealised probe, i.e. with no internal contact resistances between the heater, thermocouple and probe walls.

Jones' solution was to digitally generate simulated curves using known inputs, such as probe dimensions and power supplied per unit length, and then adjust other inputs, the thermal conductivity and volumetric heat capacity of the sample, and contact resistances within and without the probe, until curves fitted those found experimentally. An aerated concrete block and a cellular plastic were used as reference materials before measuring the thermal conductivity of a mixture of flint and sandstone pebbles. Manufacturer's data were used for the aerated concrete and data from NPL were used for the cellular plastic. It was found that changes in volumetric heat capacity input could be offset by changes in outer contact resistance, to give indistinguishable curves, hence the reference input ρC values were relied upon to provide values for contact resistance H with a qualification that, if H were known, then ρC could be found. Values of H were reported as around 66 $Wm^{-2}K^{-1}$ for aerated concrete, > 100 $Wm^{-2}K^{-1}$ for cellular plastic and 33 $Wm^{-2}K^{-1}$ for the pebbles.

This work raised a similar issue to that raised by Riseborough et al (1983), where a sensitivity analysis was reported as showing that a change in thermal diffusivity input values to Carslaw and Jaeger's solution could be offset by a change in contact resistance values.

The early 21st century saw a collaborative study (Spiess, 2001) of thermal probe measurements between various researchers, including: van Haneghem at Wageningen; David Salmon at the National Physical Laboratory; Mike Morley

at the University of Bristol; and others at: the Catholic University of Leuven, Belgium; University College, Cork; and the Institution of Refrigeration in Madrid. This work was chiefly concerned with the measurement of thermal conductivity in food stuffs so as to develop national standards, which would, among other outcomes, help prevent loss of vitamins through overheating during processing.

Food stuffs from the same source were circulated to each researcher, as were consistently sampled and sized nylon beads and glass beads. It was reported that the difference in results for thermal conductivity for similar samples amounted to 30%, including those for the inert samples. The difference was thought to be partly caused by variations in experimental methods, especially regarding contact resistance where the drying method of washed beads was, for an unspecified reason, considered significant. Variation in the time window of $\Delta T/\ln t$ chosen for analysis was also considered to be a factor in the differences.

No mention was made of thermal diffusivity or volumetric heat capacity measurements and it is presumed that these were not envisaged or coordinated. De Vries and Peck (1958) had calculated that a 3% error in thermal conductivity could create a 20% error in thermal diffusivity. Applying the same ratio to these interlaboratory results shows that, had thermal diffusivity measurements been attempted, they could have been in error by 200%.

Two more recent articles featured work on thermal conductivity measurements by van Haneghem (van Ginkel et al, 2002; Witte et al, 2002). In the first, the thermal conductivity of compost was measured at varied moisture and temperature levels. In the second, the thermal conductivity of soil samples were

measured for heat pump installations. Neither of these articles reported on thermal diffusivity measurements, beyond commenting that their accuracy would be low. Values for thermal conductivity reported in the second article varied by up to 15% for an individual sample, although the accuracy of the method was stated to be within 5%.

Campbell, of the Department of Agronomy and Soils at Washington State University and the founder of Decagon Devices in 1983, et al (1991) used two parallel probes to measure thermal diffusivity in various soils, in a similar method to that used by Drury (1988) and Morabito (1989). Thermocouples were placed in one hypodermic needle and a heater wire in another. Both needles were attached to a base plate to enable a constant distance to be kept between them. It was put forward that, in the ideal case of an infinite sample, where a heat pulse was created by a line source, the temperature rise at a certain distance from the line source was inversely related to the volumetric heat capacity of the medium, hence volumetric heat capacity could be determined from the maximum temperature rise at a known distance from a known power input.

Measurements were carried out as short heat pulses over 1s to 8s periods. The device was calibrated in agar immobilised water and the effective radius corrected by about 2% to bring results to match the known values. It was shown that, for this particular measurement, a sample radius over 29mm was sufficient to replicate an infinite sample, which was less than the sample size used. Measurements were then taken in various soils at various known moisture contents and results were said to compare well with published values for dry soils and calculated values for moist soils. However the reference materials

cited were quite different form the measured materials, as they included concrete, marble and quartz, and the soil values varied from those found by de Vries. The use of a calibration factor, based on measurements in agar immobilised water, for measurements in diverse materials was not therefore substantiated by the evidence of results.

Kluitenberg et al (1993) carried out an error analysis of the work by Campbell et al (1991). It was shown through mathematical modelling that:

- error caused by the finite dimensions of the heating probe was negligible
- error caused by assuming an instant rather than a short duration heat pulse was in the region of 0.8%
- error caused by a 1% too high temperature measurement would cause a 1% underestimate of volumetric heat capacity
- error caused by a 0.3mm difference in a needle spacing of 6mm would produce a 10% underestimation of volumetric heat capacity

The analyses assumed no contact resistances and homogenous, isotropic soils. It was concluded that the accuracy of results was predominantly related to the measurement of temperature, radius and power input. A 0.1°C resolution in temperature measurement was said to be a prerequisite of accuracy within 10%. A balance had to be sought between increasing the heat input, which potentially would increase moisture migration, and increasing the needle distance, which would make relative errors smaller. It was suggested improved rigidity in manufacture and improved temperature measurement would go some way towards reducing the errors identified.

Davies et al (2004), in using dual thermal probes to measure relative and fluctuating moisture content of building envelopes, relied on Kluitenberg et al

(1993) to assume volumetric heat capacity of soil could be measured within 1% by typical probe geometry and heating times. Moisture content could then be calculated either by comparing results with those of a dry sample or with values from the literature. It was recognised that contact resistance remained a source of potential error, as were assumptions about the sample material's homogeneity. While Kluitenberg's mathematical error analysis may have been robust regarding the data and calculations presented by Campbell et al (1991), other systematic or random errors may well have arisen from practical measurements, such as: the levels of thermal contact between a probe and sample in granular materials; the relative thermal properties of a probe and a sample in regard to axial and end losses, where the thermal properties of the sample were unknown; the effects of asymmetrical heat losses; etc. Hence, without corroborating measurements, the error analysis remains of limited use and does not substantiate the 1% accuracy assumption of Davis et al.

Campbell et al (2004) were interested in the effects of contact mediums, to avoid contact resistance, where thermal conductivity probes were used in dry granular materials. They experimented with measuring the thermal conductivity of quartz sand and glass beads of various diameters by a steady state method and then compared results to those achieved by the thermal probe with and without two types of grease: Thermal Cote with a reported thermal conductivity of 0.4 $Wm^{-1}K^{-1}$; and Arctic Silver with a reported value of 8 $Wm^{-1}K^{-1}$.

Probes were initially used in immobilised water, glycerin, mineral oil and expanded polystyrene, it is assumed without contact material, following the ASTM standard: D-5334 (ASTM Committee D18, 2000). Two probes were used, 60mm x 1.27mm and 100mm x 2.41mm, length to radius ratios of 47:1

and 42:1 respectively, containing a heater wire and a thermistor. Temperature over time data were fitted to:

$$\Delta T = \frac{Q'}{4\pi\lambda} Ei\left(\frac{-r^2}{4\alpha.t}\right)$$

Equation (25)

where *Ei* was an exponential integral, and also, ignoring the later terms, to:

$$\Delta T = \frac{Q'}{4\pi.\lambda}\left[-\gamma - \ln\left(\frac{r^2}{4\alpha.t}\right)\right] = \frac{Q'}{4\pi.\lambda}\left[\ln t - \ln\left(\frac{r^2}{4\alpha.\exp\gamma}\right)\right]$$

Equation (26)

Data was shown and reported as fitting these terms extremely well. However, thermal conductivity values for the liquid samples found with the larger probe were up to 47% above the known values, whereas results for the insulation were reported as "very close". Conversely, values achieved with the smaller probe were within 10% for the liquids but 52% low for the insulation. Probes were then calibrated to be within 10% for insulation and 1% for water, although the method of calibration was not explained, apart from stating in the conclusion that:

"thermal conductivity errors as large as 30 to 50% are possible unless corrections are made using standards"

The article also suggested that the extrapolated ordinal intercept of equation (26) "apparently can be used to find thermal diffusivity" using:

$$\alpha = \frac{r^2}{4(\exp\gamma)x_o}$$

Equation (27)

where x_o is the ordinal intercept.

Steady state measurements were carried out using a 10mm diameter heater placed along the axis of a 30mm copper tube, with the sample medium packed

in between. Measurements were taken over three hour periods and steady state assumed when temperatures at the heater and copper wall were stable. This method was recognised to be relatively unreliable as end and axial losses from the heater were not calculated. However, the results were used as a qualified reference for the thermal probe results in the granular materials.

Results for the smaller probe, using both types of contact grease, were mostly lower, by up to 20%, than the steady state results, which were reported as too high by an unknown amount. No significant difference was found between results for each grease, although the more conducting grease gave slightly higher values. Results without grease were significantly lower, giving between 34% and 66% of the steady state thermal conductivity values. The data was considered robust enough to conclude that contact resistance errors with no grease increased as particle size increased, whereas, with grease, beads much larger in diameter than the probe could be measured with reasonable accuracy.

Thermal drift in the sample was reported as a major cause of error. A simulation was carried out whereby a $0.001°Cs^{-1}$ drift was described as creating a 50% error in thermal conductivity results for water. This was said to be cancelled out to a great extent by using the cooling curve as well as the heating curve for analysis. It is of note that terms for contact resistance, or probe conductance *H*, did not appear in the solutions used, equations (25) and (26).

Cheng et al (1994) described a method of calibration. In measuring the thermal conductivity of foods, a probe constant was calculated when they calibrated a small hypodermic needle probe, incorporating a 25 ply copper wire as a heater and resistance thermometer. This constant was based on the sample thermal

diffusivity value and the length of the probe. As the length of the probe was fixed, the value of thermal diffusivity was adjusted to ensure calculations gave the reference thermal conductivity value of the sample, in this case glycerin. This constant was then used in other measurements of similar materials, resulting in a reported accuracy of 3%. This appears to have been derived mathematically as no substantiated reference materials were cited. Values achieved for powdered graphite and sodium chloride were 0.095 $Wm^{-1}K^{-1}$ and 0.331 $Wm^{-1}K^{-1}$ respectively, whereas values for these materials from the literature, including those given by NIST, are 25 $Wm^{-1}K^{-1}$ to 470 $Wm^{-1}K^{-1}$, and 6.0 $Wm^{-1}K^{-1}$ respectively. Information on the densities and forms of the samples was not given so the difference in results could not be assessed.

Seiferlin et al (1996) wished to ensure that thermal conductivity probe technology was robust enough and appropriate to place on board a future Mars explorer mission. Their methodology relied on the past work of Blackwell (1954, 1956), Buettner (1955), de Vries and Peck (1958), and Healy et al (1976). Metal cylinders up to 200mm x 2mm were used with multi stranded copper heating elements, also acting as resistance thermometers. This was said to be an improvement over a heater and thermocouple placed at the mid point as a more average temperature over the length of the probes would be measured. It was upheld that the metal cylinder, being of a high thermal diffusivity material, would quickly find equilibrium with the hot wire and hence any effects caused by the presence of a physical probe would be insignificant over the run times of the measurements used, between 120s and 3,600s. It was said that these effects would not in any case alter the slope of $\Delta T/\ln t$.

The probe was calibrated in PTFE, after some deliberation due to the lack of suitable reference materials available. A 1mm diameter probe was used in a 1.5mm hole backfilled with oil to create better thermal contact. Two values for PTFE were given from the literature, 0.23 $Wm^{-1}K^{-1}$ and 0.25 $Wm^{-1}K^{-1}$. Values achieved by the probe varied by ± 5% from 0.243 $Wm^{-1}K^{-1}$. Further measurements were taken in a vacuum chamber after cleaning away the oil. Values achieved for these measurements varied by ± 20% from 0.250 $Wm^{-1}K^{-1}$.

Charts of thermal conductivity values taken from a local slope of $\Delta T/\ln t$ over time were given. These showed that a reasonable value for thermal conductivity with the oil filler was reached after about 120s, within 5% of the reference value of 0.25 $Wm^{-1}K^{-1}$, whereas, with the evacuated hole measurement, results rose from around 0.14 $Wm^{-1}K^{-1}$ to expected values after around 900s – 1,200s. It was not stated over what periods of the $\Delta T/\ln t$ slopes these thermal conductivity values were taken.

Following calibration in PTFE, the probes were then used to measure dunite powder, fine grained water ice and carbon dioxide ice at various pressures. Greater errors were found with these measurements, especially with carbon dioxide ice, and linearity in $\Delta T/\ln t$ was not always achieved. This was said to be caused by changes in thermal conductivity and vapour flows of the ices with the temperature rise introduced by the probe, to which the carbon dioxide ice was more sensitive.

It was maintained that the sources of errors were easily identifiable by their particular effect on the chart of $\Delta T/\ln t$, including: bad thermal contact, where the effect would disappear after time; poor adjustment of heating power, where the

symptoms in $\Delta T/\ln t$ were not given; too short a cooling time between measurements, said to be very difficult to detect because the influence of ΔT in $\Delta T/\ln t$ was quite small; thermal drift, where the effect on $\Delta T/\ln t$ was not shown but said to be obvious when it happened, bearing in mind that measurements were being attempted at temperatures below 100K.

Overall, accuracy was reported as being mostly within 15%, after careful sample preparation and the discarding of data sets incorporating obvious errors in $\Delta T/\ln t$. This was an improvement on previously reported work by some of the authors where errors had been in the region of 40% (Spohn et al, 1989; and Seiferlin, 1990).

The results presented by Seiferlin et al (1996) were an example of calibration in one material being transferred to other materials, where greater errors were found.

Banaszkiewicz et al (1997), following Seiferlin et al (1996) and citing prior successes by de Groot et al (1974) in gases, Sandberg et al (1977) in liquids, Buettner (1955) and Seiferlin et al (1996) in solids, followed traditional line source solutions. Rather than the short time heat pulse, models for infinite and finite probes emitting heat over time were used. Algorithms were developed whereby, rather than using just two points as a linear asymptote of $\Delta T/\ln t$, a least squares optimisation process was carried out. This covered each data point of various chosen time windows from $\Delta T/\ln t$ at 1Hz, whereby values for thermal conductivity and thermal diffusivity were said to be available from the residuals. It was suggested in the concluding section that these values could be obtained from any part of the heating curve, as long as the temperature data

was highly accurate, even at very short times where $\Delta T/\ln t$ was non-linear. This was quantified as:

"A 0.01K accuracy of temperature data should guarantee the thermal diffusivity determination with an error of about 5%".

The experimental conditions used by Seiferlin et al (1996) were reemployed. The probe was considered as a perfect conductor and contact resistance was considered to be zero by using a filler of pump oil. Measurements were carried out on Teflon as a reference material and then dunite, compact ice and porous ice. It was noted that there was a dearth of reliable and suitable reference materials and hence the work concentrated more on internal consistency rather than substantiating results by comparison with samples of known thermal properties. Despite the suggested potential accuracy, a table of results for the measured thermal properties of Teflon for similar time periods ranged from 0.215 $Wm^{-1}K^{-1}$ to 0.265 $Wm^{-1}K^{-1}$ for thermal conductivity and 0.69 $x10^{-7}$ m^2s^{-1} to 2.45 $x10^{-7}$ m^2s^{-1} for thermal diffusivity, a difference of 255% from the lowest to highest value.

Inaccuracy was suggested to be a result of not considering contact resistance and it was said that the effect was greater in the middle of a measurement period, although the method of determining the measurement period was not given.

Banaszkiewicz et al (2007) used a number of short thermal probes stacked in series with independent platinum wire resistance thermometers and isotan wire heating elements for greater accuracy of power input and temperature measurement. Results for the thermal conductivity of Teflon matched NIST

published values well. Thermal diffusivity measurements were not discussed. The article concluded that the ideal assumptions of measurements are very often violated and, as thus, systematic errors arise. An example was given of contact resistance where this was dependent on the contact pressure between probes and sample, which could vary between measurements. A suggested solution to this problem was the use of expanding elastic rings fitted to the exterior of the probes.

Spohn et al (2007) referred back to Banaszkiewicz et al (1997) for the method of obtaining values of both thermal conductivity and thermal diffusivity in the anticipated compact ice on the surface of comet Churyumov-Gerasimenko with equipment on board the Rosetta space mission, launched in 2004 and due to arrive in 2014. A thermal probe measuring 320mm x 10mm with the walls formed of a 1mm thick fibrous compound was to be hammered into the comet's surface. The fibrous compound was chosen as a compromise between structural strength and low thermal conductivity to reduce axial losses. The probe contained individual cells of heater / resistance thermometers as described in Banaszkiewicz et al (2007).

Kubicar (1999) chaired a workshop on transient methods for measuring thermophysical properties at the 15th European Conference on Thermophysical Properties. The workshop highlighted the dearth of reference materials for thermal conductivity and thermal diffusivity measurements. It was considered necessary to have a wide range of reference materials to match the many and various uses to which transient methods were becoming increasingly attractive. It was noted that there was an escalating introduction of new and innovative

materials. It seems only one reference material was being developed, namely a specific batch of Pyroceram 9606.

Part of the rationale for this range of reference materials being needed was the inconsistency between values reported by individual laboratories. Accuracies were usually reported as less than 5%, compared with differences between laboratories, which were often in excess of 20%. The need for improved mathematical models to fit transient line source data was emphasised, as it was put forward that models may not have been representative of the precise physics occurring during the measurements. Models could include systematic errors, such as the thermal resistance and capacitance of the heater wire, unaccounted heat losses, non-uniform heating and many more potential issues that researchers may not be aware of. The use of standard reference materials across a range would help identify such outstanding issues.

These systematic errors were said to generally appear in the chart of $\Delta T/\ln t$ as S or U curves and it was suggested that, when reporting on thermophysical properties, these curves should be shown, alongside the residual values of least squares optimisation, to give an indication of the error level in the values. This could be used to indicate but not accurately quantify the error. The importance of identifying correct time windows for analyses was also discussed.

Ren et al (1999), in developing a dual purpose, dual probe to measure the moisture content of soils by time domain reflectometry while at the same time measuring thermal properties by the heat pulse method, relied on the work of Kluitenberg et al (1993), discussed earlier in this chapter, and Welch et al (1996), who had also studied soil thermal properties. This had shown that errors

from assuming an infinitely long line source were less than 2% and errors from assuming a line source rather than a probe with a physical radius were less than 0.6%. Accuracy depended on precise measurements of time, power, radius and temperature rise. Probes were made with length to radius ratios exceeding 25:1, which was considered to meet Blackwell's recommendations for preventing axial losses.

Probes were calibrated in agar immobilised water by adjusting the value of the measured radius *r*. Two types of soil were then measured at various moisture contents. In silica sand at about 5% water content by volume, charted results showed thermal conductivity to be 1.8 $Wm^{-1}K^{-1}$, and thermal diffusivity to be 3.7 $x10^{-7}$ m^2s^{-1}. A value for ρC was shown as 1.5 $MJm^{-3}K^{-1}$. As thermal diffusivity is defined as thermal conductivity divided by volumetric heat capacity, the two values given for these properties should have resulted in a thermal diffusivity value of 1.2 $x10^{-6}$ m^2s^{-1}, some 225% larger. The values for the same sand at 30% water content were, however, born out by the mathematical relationship.

It is not clear why such a large error existed in the thermal diffusivity or volumetric heat capacity value. A possible cause is that the probe apparatus was calibrated in one material, agar immobilised water, by changing certain parameters in the calculations, which changes were retained when measuring different materials. Another cause may have involved the length to radius ratio. It may be remembered that Blackwell's probes had radii in the region of 15mm to 20mm and that, rather than a rule of thumb length to radius ratio, Blackwell (1956) provided a calculation based on the thermal diffusivity of the sample material. As shown earlier in this chapter, the ratios used by Blackwell are not always appropriate for thin probes.

Goodhew and Griffiths, at the University of Plymouth, were interested in the development of the thermal probe technique to measure building materials for a number of years, following work by Batty, in the then Department of Applied Energy at Cranfield University. Various probes were manufactured using copper tubing of assorted diameters with a variety of fillers, such as epoxy, containing a heater wire and thermocouples, before procuring commercially available Hukseflux TP02 150mm probes, and then the shorter 70mm TP08 probes.

Goodhew (2000), in his thesis, recognised that the probe's outer conductance, or contact resistance between the probe and sample, termed *H*, was generating a greater influence on results for thermal diffusivity than many previous researchers had accounted for. Three methods of calculating *H* were explored: short time analysis; rate analysis; and an iterative solution.

The short time analysis employed Blackwell's solution for a for a *Y* parameter, equations (9) and (10). Trials with this methodology led to an initial *H* value of 327 $Wm^{-2}K^{-1}$ in cob, using a silicone based contact medium that had a stated thermal conductivity of 2.9 $Wm^{-1}K^{-1}$.

The rate analysis compared the rate of temperature change during heating with the temperature difference between the probe and the sample. This methodology produced an initial *H* value of 136 $Wm^{-2}K^{-1}$ in paraffin wax.

The third method used the iterative, line fitting, least squares optimisation, MS Excel add-in programme Solver, from Frontline Systems, Inc. (2007). Spreadsheets were developed that fitted Batty's arrangement of Blackwell's equation for the three unknowns in $\Delta T/\ln t$ (λ, α and *H*). The spreadsheets also

assessed after what time the heat capacity of the probe itself ceased to have undue influence on the temperature rise, and another spreadsheet calculated before which time the axial heat flow from the probe unduly compromised data for the radial heat flow.

The Solver solution required initial estimates for λ, α and H, from which the least squares, non linear regression, iterative optimisation was carried out. A thermal conductivity estimate could first be worked out by a separate regression analysis, using a visually recognised linear asymptote of $\Delta T/\ln t$. Value estimates for contact resistance, or rather probe conductance, were taken from the range of values achieved by the short time and rate analyses or estimated from previous experience. Value estimates for thermal diffusivity relied on values from either the literature or from previous measurements.

Laboratory measurements of paraffin, glycerine, phenolic foam and aerated concrete showed close correlation with published values for thermal conductivity. Achieved values for thermal diffusivity and volumetric heat capacity varied in correlation. Results for paraffin were within 12%, results for phenolic foam and aerated concrete were smaller by factors of six and eight respectively, while values for glycerine were 22 times larger than the published value, with the thermal probes in various states of development.

Goodhew and Griffiths (2003), in a handbook for thermal probe studies, discussed the appropriate time section of $\Delta T/\ln t$ for analysis using the Solver routines. Thermal conductivity was found via a regression analysis of the earliest available part of a linear asymptote, and before the effects of an undefined thermal drift became significant.

Results were reported for agar immobilised water and PTFE. The spread of agar results gave a range of ± 4% for thermal conductivity and ± 11% for volumetric heat capacity. For PTFE, the range of thermal conductivity values was ± 4.5% and specific heat capacity ± 24%. Both sets of results encompassed the known values for these materials.

An example of a Solver spreadsheet was given showing the estimated input values for the agar analysis of: thermal conductivity, 0.6 $Wm^{-1}K^{-1}$; thermal diffusivity, 1.5E-07 m^2s^{-1}; and probe conductance *H*, 400 $Wm^{-2}K^{-1}$. The Solver outcome values were shown as very close to these values at: thermal conductivity, 0.620 $Wm^{-1}K^{-1}$; thermal diffusivity, 1.5E-07 m^2s^{-1}; and probe conductance *H*, 505 $Wm^{-2}K^{-1}$.

Goodhew and Griffiths (2004) reported thermal conductivity, thermal diffusivity and volumetric heat capacity values for mineral oil, magna, paraffin wax and PTFE, measured by thermal probes and using the Solver analysis routines. These were within 20% for thermal conductivity and 36% for volumetric heat capacity, when compared to values given from the literature. Also given were values for lightweight clay straw pads, with a density of 110 kgm^{-3}. The mean reported values for these were: thermal conductivity 0.073 $Wm^{-1}K^{-1}$; volumetric heat capacity 47 $kJm^{-3}K^{-1}$; and specific heat capacity 424 $Jkg^{-1}K^{-1}$. No corroborative values were given from other forms of measurement and no other published values have been found for this material. The volumetric and specific heat capacities appear low when compared to those of straw, i.e. 150 $kJm^{-3}K^{-1}$ at 112 kgm^{-3}, and 1,339 $Jkg^{-1}K^{-1}$ respectively (California Energy Commission, 2005, p.3-52). A methodology to establish the initial estimated values for the Solver input data was not described.

Goodhew and Griffiths (2005) reported thermal conductivity, thermal diffusivity and volumetric heat capacity of three further earth and straw based materials measured with commercially available Hukseflux TP02 thermal probes. These were straw bales, unfired earth bricks with straw and wood shaving content, and another clay straw mix. The results were not corroborated by alternative measurements or published values. The values for thermal conductivity and volumetric heat capacity were then used to model the transient behaviour of buildings so as to establish their potential compliance with thermal efficiency requirements.

This work highlighted the limitations of depending on 'U' value calculations to calculate the thermal efficiency of buildings. 'U' values were based on the thermal conductivity and dimensions of materials only, while assuming a steady state of internal and external temperature conditions, whereas it was shown that energy efficiency may be increased by intelligent use of materials' thermal diffusivity and heat capacity in transient situations, e.g. to dynamically store and release incidental heat gains.

Manohar et al (2000) sought to measure the thermal conductivity of sands and soil following the thermal probe methodology suggested by ASTM D-5334 (ASTM Committee D18, 2000). A 100mm x 3mm diameter stainless steel tube was used with a heater and thermocouple set in epoxy resin. Two reasons were given for $\Delta T/\ln t$ deviating from the linear asymptote. At early times, it was considered an effect of the probes physical presence acting as a time delay, as van der Held and van Drunen had described. At later times, the levelling of the S curve was deemed to denote the reaching of a steady state.

Identification of the linear asymptote in $\Delta T/\ln t$ was carried out by multiple regression analyses. These were calculated over 0s-1000s, then 50s-950s, 100s-900s, etc. until the slope achieved differed by less than 2.5% over three consecutive steps. No substantiation was offered for this assumption, that the central part of the appropriate time window would always occur at 500s.

Probes were calibrated in fine cryogenic perlite by measuring this at various temperatures between 9°C and 46°C using a heat flow meter. This was described as compliant with ASTM C518 and designed to give an accuracy of ± 1% with a reproducibility of ± 0.5%. The calibration measurements of three samples gave one thermal conductivity value of 0.0420 $Wm^{-1}K^{-1}$ and two of 0.0424 $Wm^{-1}K^{-1}$. A simple multiple was used to convert probe results to match those of the heat flow meter. This then placed reliance on the multiple being appropriate for diverse materials.

Mean thermal conductivity results from a number of practical experiments on two sands used were 0.52 $Wm^{-1}K^{-1}$ and 0.44 $Wm^{-1}K^{-1}$, whereas the result for soil, of "a brown, sandy-clay nature", with a 20.3% moisture content by weight, was given as 2.11 $Wm^{-1}K^{-1}$. This is quite different from de Vries' (1952) value, where the result for Healy clay at approximately 20% moisture content by weight was 1.25 $Wm^{-1}K^{-1}$. Without alternative reference measurements, it is not possible to gauge the accuracy of these values. It was noted in the conclusion that the probes were calibrated in a material of significantly lower thermal conductivity, which brought the accuracy into doubt.

Xie and Cheng (2001) used a fine needle probe to measure the thermal conductivity of fruit and animal flesh. 20s measurements were made using a

25mm x 0.6mm stainless steel needle probe with a multi-stranded copper heating element, which also acted as a resistance thermometer. It was shown that, after about three seconds, the physical presence of the probe could be reasonably ignored in their calculations.

Following calibration in glycerol, with thermal conductivity given by Touloukian et al (1970b) as 0.286 $Wm^{-1}K^{-1}$, measurements carried out in ethylene glycol were found to be within 1% of the published value of 0.258 $Wm^{-1}K^{-1}$. Charts showing the deviation from linear fitting of $\Delta T/\ln t$ before about 3.5s and the linear asymptote from about 3.5s to its end at 20s were given.

Values were then given for distilled water, apples and muscle. These were all within 4.9% of reference values shown from the literature. The article concluded with an accuracy estimate of ± 3%. Contact resistance was not factored into calculations, and it was stated that good thermal contact was achieved. This raises an interesting comparison with previous researchers, such as van Haneghem, who had calculated that probe conductance existed through internal resistance even where perfect contact was achieved. While good values were found for ethylene glycol with similar thermal properties to the calibration material, it is not possible to assess the validity of the results in fruit and animal flesh, as factors such as their moisture content and density were not given in comparison to those of the reference materials.

The effects of contact resistance were graphically portrayed by Assael et al (2002). Pyroceram 9606, a hard ceramic material with stable and known thermal properties, was measured by the hot wire technique, in a method similar to BS EN 993-15 (BSI, 2005). The resultant curves were compared to

those found through computer simulation using the known thermal properties in a finite element method (FEM). The FEM used a two dimensional grid system. Line fitting was carried out on a trial and error basis, by repeatedly adjusting input values.

A hot wire was placed between two smooth slabs of the material, which were pressed together leaving a reported air gap of 30μm, although it seems reasonable to assume, from Veziroglu (1967), that a certain amount of complete, probably random, contact must have existed. Experimental results for temperature measurement were initially found to be a factor of two higher than the FEM predictions. A slight improvement was found by filling the air gap with a ceramic powder. A heat transfer compound in the form of a paste (Electrolube HTC) was then used as a filler, following which, experimental and predicted curves appeared coincident. This was the case when using the values of the paste for the FEM input at short times, up to 0.12s, and the values of the Pyroceram 9606 later in the 20s measurements, which were carried out at up to 1000Hz.

Assael et al were seeking improvement to the hot wire technique as they reported that, although frequently used, significant problems reoccurred and solutions were based on approximations, with no absolute theory existing. The identification of the correct linear section of $\Delta T/\ln t$ for analysis caused difficulties whereas the FEM described reportedly overcame this by matching the whole curve rather than a linear section. Heating curves were portrayed in the article as over time rather than logarithm of time, hence it is not known whether any linear sections did exist in the measurements.

The problem of contact resistance was reported as having been sometimes overcome by using more power and larger temperature rises. It was concluded that the use of a semi-solid contact paste was a better solution. Good values were found by the hot wire technique for toluene and Pyroceram 9606 with the uncertainty in ceramics reported as ± 1% for thermal conductivity and ± 3% for volumetric heat capacity.

It was described as possible to independently measure the thermal properties of each layer, i.e. the heater wire, the contact paste and the sample material. It was not shown why the air gap or ceramic dust filler could not be used as well as the contact paste to produce representative temperature curves, or whether contact resistance was factored into the model.

Krishnaiah and Singh (2004) developed an apparatus to measure both the thermal conductivity and thermal diffusivity of soils. This consisted of a cylindrical chamber with a thin copper walled thermal probe, containing a heater element and central thermocouple, at its axis. Soils were compacted around the probe within the chamber, which was considered to ensure good thermal contact. Thermal conductivity measurements were carried out following the method of Hooper and Lepper. Thermal diffusivity was not attempted by the thermal probe alone. Rather, the whole chamber was heated and then cooled. Thermal diffusivity was calculated by the cooling rate of the known volume of the sample, using the thermocouple in the probe to measure the temperature drop.

Krishnaiah et al (2004) attempted measurements of solid rock by a thermal probe, again following Hooper and Lepper. It was considered inappropriate to

grind rocks to dust for use with the cylindrical chamber method as the sample would be non-representative of the particular formation of the rocks in situ. The probe used was 95mm x 6mm and entailed pre-drilling of the material. It was considered that this would compromise the thermal contact between the probe and sample. To assess the degree of this effect, a number of bricks were formed, some with holes tightly fitting the probes and some with 7mm holes. Probes were then fitted to the larger holes with a filler of heat sink fluid. The thermal conductivity results for the tight fitting holes were around 17% higher than those with the filler hence a factor of 1.17 was then used to correct future measurements in solid rock with pre-drilled holes.

Thermal diffusivity was estimated by:

$$\alpha = \frac{r^2}{2.246 \times x_{int}}$$

Equation (28)

where x_{int} was the intercept on the time axis from the linear section of $\Delta T/\ln t$.

An explanation for using the factor 2.246 was not given, neither was any derivation or source for equation (28). The use of a numerical constant derived from measurements in one material to calibrate thermal probes was not substantiated by a comparison of results from measurements in other materials with known thermal properties, such as recognised reference materials or those measured by an alternative method.

Garcia-Gutierrez and Espinosa-Paredes (2004), in researching thermal conductivity values for cement systems used in the walls of geothermal wells, compared results achieved between single and dual thermal probes. The experimental arrangement had two probes within a sample. One probe acted as

both a stand-alone probe with a heater and thermocouple and as the heater for the other, which was used as a temperature measurement device at a known radius from the heater probe. Measurements were taken by both techniques at temperatures varying from 30°C to over 200°C. Error levels for the single probe were reported as within 4% and, for the dual probe, within 12%, and within 2% and 3% respectively for a calibration measurement in fused quartz. However, the difference in results by the two methods was reported as having a maximum of 36%. A comparison of the charted values showed this to be 53% for one sample, with results at 30°C being 0.53 $Wm^{-1}K^{-1}$ with the dual probe and 0.81 $Wm^{-1}K^{-1}$ with the single probe. The difference in results between the methods shows that the error levels for each method were underestimated, which would indicate that not all parameters had been included in the analyses.

Dedrick et al (2005), following Blackwell and using the standard ASTM thermal probe method D-5334 (ASTM Committee D18, 2000), measured the thermal conductivity of sodium alanates, proposed as a high density storage medium for a potential hydrogen based energy infrastructure. Blackwell's short time solution for contact resistance between probe and sample was discounted, as in Jones (1988), as practical probe construction was considered a non-ideal representation of Blackwell's proposition, hence published rather than measured values for volumetric heat capacity were used in calculations for the samples measured.

The probe comprised a nichrome heating element and thermocouple set in epoxy, surrounded by a thermal paste within a stainless steel tube. This was held in a pressure vessel. Checks were first undertaken with measurements of Teflon, polyurethane foam and Ottawa sand, although it was recognised that

none of these materials were of certified and traceable calibration quality. Values achieved were within 10% of expectations. Values of *H* for the probe to sample were given for the sodium alanates at varied pressures and gas content as being in the range of 300 $Wm^{-2}K^{-1}$ to 560 $Wm^{-2}K^{-1}$.

Tye et al (2005) reported on working towards a recognised standard for contact transient measurements (CTM) of thermophysical properties (National Physical Laboratory, 2007a), including the thermal probe. This was following three CTM workshops at the 14th and 16th European Conference on Thermophysical Properties 1999 and 2002, and the 26th International Thermal Conductivity Conference in 2001. Concerns were expressed that, as these methods became more common through their convenience and economic advantages, measurements were becoming automated and subsequently carried out by inexperienced personnel. Examination of available data showed that the claimed precision of these methods, often better than 3%, was not borne out by results, hence reliance on automated results could compromise engineering applications. It was noted that:

"such differences and uncertainties create serious problems for the scientist and engineer requiring reliable data".

Internal inconsistency and significant deviation from accepted values were common, even where no such differences should occur, due to the homogenous, isotropic and stable, etc. nature of the materials. An example was given whereby the measurement of Pyroceram 9606 carried out by the standard hot wire method gave a thermal conductivity result of 5 $Wm^{-1}K^{-1}$ whereas the equivalent certified guarded hot plate value was 4 $Wm^{-1}K^{-1}$. The uncertainty in

thermal diffusivity results could be much greater. It was stated that errors in thermal probe measurements were likely to be higher than those by the hot wire, which would have smaller heat capacity and reduced contact resistance.

Uncertainty was illustrated in the example of a Gustafsson probe used in ice. Two techniques were used: firstly, the probe was sandwiched tightly between two slabs of ice, with a contact grease; secondly, ice was frozen around the probe. The thermal conductivity results for the two measurements were 1.79 $Wm^{-1}K^{-1}$ and 2.33 $Wm^{-1}K^{-1}$ respectively, a difference of 30%. The accepted value was given as 2.38 $Wm^{-1}K^{-1}$.

Issues that required resolution for a standard included:

- Sample size and boundary effects
- Power levels used
- Time windows used for analysis
- Effects of internal and external contact resistance
- The difficulty in recognising combined heat transfer mechanisms without direct relationships
- The need for additional reference materials for thermal conductivity, thermal diffusivity and specific heat capacity

An interlaboratory study was reported as in progress to assess measurements by various of the contact transient means, with an emphasis on the Gustafsson method, although this study has not, at the time of writing, been pursued beyond the measurement of plastics (Lockmuller, 2007).

Two recommendations included in the draft generic standard were:

- the use of a heat sink filler to overcome contact resistance;

- the use of the longest period over which results remained constant to identify the time window for analysis

The National Physical Laboratory (2007b) have published a draft standard, under the umbrella of the generic standard above, specifically for the thermal probe. In this standard, the technique was considered suitable for thermal conductivity measurements between 0.05 $Wm^{-1}K^{-1}$ and 20 $Wm^{-1}K^{-1}$, and particularly useful for molten materials, particulates, powders and moist materials.

The thermal probe was not considered useful in measuring thermal diffusivity as, in practice, it was found to give inaccurate values. It was suggested that the probe was particularly useful, especially in molten materials, to compare the thermal conductivity of similar samples, as opposed to an absolute measurement device.

Contact resistance was recognised as a particular cause of measurement errors, especially in dry granular materials. This problem could be overcome in part by using the Modified Jaeger Method, as described by van Haneghem (1981).

It was recommended that the probe be calibrated in two or more materials of known thermal properties. Examples included agar gel, Ottawa sand and polydimethylsiloxane, with values only for the latter given in the draft generic standard. Accuracy for in situ thermal conductivity measurements was not thought to then be better than ± 10% and worse for dry, coarse, granular materials.

Contemporary standards relating to thermal probe measurements

The literature review now closes with an overview of three current standards relevant to this study. These comprise two British / European standards and one ASTM International standard.

BS EN 993-14 (BSI, 1998), which follows closely the methods described by Davis and Downs (1980), describes a method to measure the thermal conductivity of dielectric refractory materials, whether in solid, powdered or granular form, including measurements at elevated temperatures, where sample thermal conductivity is less than 1.5 $Wm^{-1}K^{-1}$.

A hot wire of recommended dimensions 200mm x < 0.5mm is placed between two samples of sufficient dimensions, recommended as standard brick sizes of 230mm x 114mm x 64mm, and smoothness and flatness, less than 0.2mm deviation over 100mm. A thermocouple is attached to the middle of the hot wire and its leads then led out perpendicularly to the wire. In harder materials, wires can be let into formed grooves and then backfilled with a weak mortar using the powdered material as aggregate with 2% dextrin as the binder.

Temperatures are monitored for 10 minutes prior to a measurement cycle and should not vary over this time by more than 0.05°C. Circuitry is brought into balance before heating by use of a dummy heater of matching resistance to that of the hot wire. The wire is then heated at a steady, known current, which should not vary by more than 2% over the recommended 15 minutes of each measurement. Measurements should be repeated three times, allowing thermal equilibrium to be re-established between each cycle.

Thermal conductivity is then calculated by:

$$\lambda = \frac{Q'}{4\pi} \times \frac{\ln(t_2/t_1)}{\Delta T_2 - \Delta T_1}$$

Equation (29)

No indication of accuracy is given for results although the repeatability is given as in the order of 8%. It is advised that issues concerning moisture content and anisotropic materials were outside the scope of the standard and should be agreed between the parties involved.

The standard advises that a plot of $\Delta T/\ln t$ should be linear and where not, either the material does not fulfill the conditions necessary for the test and therefore results have no significance, or an operating error has been made and the test should be repeated. Where $\Delta T/\ln t$ is found to be non-linear at the beginning, it is said that this may be caused by the material surrounding the wire, presumably the filler, and it is advised that:

"a valid result can possibly be obtained by choosing another value for t_1 (the analysis start time)".

Where $\Delta T/\ln t$ is found to be non-linear at the end of the heating cycle, this is ascribed to the sample perhaps having an over-high thermal diffusivity, in which case it is stated that a shorter measurement time could possibly give a valid result.

It is advised that non-linear curve measurements should be discounted. It is also advised that S or U curves containing a linear section could possibly give valid results, without further advice as to how these results could be verified. No

directions are given to accommodate the potential for two or more distinct linear sections that could be encountered within an S curve.

It is interesting to note that the boundary condition is said to be dependent on sample thermal diffusivity, that is on the relation of heat transfer to volumetric heat capacity, rather than on the rate of heat transfer alone. The boundary effects occur at a time dependent on the rate of heat transfer but the level of the effect depends on the volumetric heat capacity, which was recognised by Ingersoll et al (1954).

BS EN 993-15 (BSI, 2005) fulfills a similar function, with similar sample preparation, controls and caveats to BS EN 993-14 above, for materials with thermal conductivities up to 25 $Wm^{-1}K^{-1}$, albeit by a slightly different method. This upper limit can be raised by increasing the sample dimensions, e.g. at 230mm x 180mm x 95mm materials up to 40 $Wm^{-1}K^{-1}$ can be measured.

In this method, the thermocouple and its leads are set parallel to the hot wire at a known distance from it, recommended as 15mm. A table of suggested measurement times and power levels is given for various thermal conductivity values, e.g. for 0.1 $Wm^{-1}K^{-1}$, test duration is 1,200s at 3 Wm^{-1}; at 25 $Wm^{-1}K^{-1}$ test duration is 65s at 375 Wm^{-1}. Initial values can be estimated from preliminary tests or gauged from experience.

Thermal conductivity is then calculated by:

$$\lambda = \frac{Q'}{4\pi} \times \frac{-Ei\left(\frac{-r^2}{4\alpha.t}\right)}{\Delta T(t)}$$

Equation (30)

where:

$\Delta T(t)$ = the temperature change at time t from the start of heating

r = the distance between the hot wire and thermocouple

and $-Ei\left(\frac{-r^2}{4\alpha.t}\right)$

is an exponential integral function of $\Delta T(t_2)/\Delta T(t_1)$ for which values are given from the literature (Carslaw and Jaeger, 1959; Abramowitz and Stegun, 1972; Grosskopf and Kilian, 1980) and presented in a tabular format.

The analysis of the heating curve relies on repeated calculations of equation (30) using tabulated values of the exponential integral at successive time periods e.g: $t_1 \rightarrow t_2$ = 4s → 8s ; 8s → 16s; 12s → 24s; 16s → 32s; etc. Measurements are said to be valid where the ratio $\Delta T(t_2)/\Delta T(t_1)$ lies between 1.5 and 2.4. The mean value of results complying with this condition is then given as the thermal conductivity result.

The standard does not mention the linearity of $\Delta T/\ln t$ or contact resistance. It is also interesting to note that sample size is considered dependent on thermal conductivity, whereas boundary effects in BS EN 993-14 had been considered dependent on thermal diffusivity.

The ASTM "standard test method for determination of thermal conductivity of soil and soft rock by thermal needle probe procedure" (ASTM Committee D18, 2000) is said to be applicable for undisturbed and remoulded soil, and in situ and laboratory soft rock specimens, all of an isotropic nature. Dry or moist samples may be measured. This would indicate that the method was also readily available for the laboratory sample or in situ measurement of many construction materials. The standard recognises that the carrying out of

measurements requires prior technical knowledge of heat transfer mechanisms and that the further development of improved methods was to be welcomed.

A probe construction is described as 115mm x either 1.8mm (64:1) or 1.4mm (82:1) stainless steel hypodermic tubing containing a hairpin heater and thermocouple set in epoxy. Samples should have a minimum diameter of 51mm and length of 200mm (± 30mm) with the probe pushed into the central axis, with or without a predrilled hole as appropriate to ensure a tight fit. Thermal grease may be used as a contact medium.

The probe should be calibrated in one or more materials of known thermal properties with thermal conductivities between 0.2 $Wm^{-1}K^{-1}$ and 5.0 $Wm^{-1}K^{-1}$ before use. Suggested reference materials are Ottawa sand, Pyrex 7740, fused silica and Pyroceram 9606, although the first two are not approved reference materials.

Thermal conductivity values are then found by physically plotting temperature rise against the natural logarithm of elapsed time, visually recognising a linear section and drawing a straight line through this. The temperature rises at two distinct times on this straight line are then used in the familiar calculation:

$$\lambda = \frac{Q'}{4\pi(T_2 - T_1)} \ln(t_2/t_1)$$

Equation (31)

The standard states that, based on the work of Hust and Smith (1989), a precision of between ± 10% and ± 15% is indicated, with a tendency for results to be higher than known values. It is interesting to note that Hust and Smith's conclusions included the following paragraph:

"With the exception of the results for paraffin wax, thermal conductivity test results measured in this ILC (interlaboratory comparison) with the needle probe lie 14 to 35 percent lower than the results with the hot wire. This large difference in results from the two apparatus casts doubt on the accuracy of measurements performed on either apparatus"

Thermal diffusivity values are not mentioned in the standard.

Discussion arising from the literature review

The literature review has described the theory and practice of the thermal probe and hot wire techniques as they have been applied to various materials, either as samples or in situ. It has shown that the temperature rise of a line heat source within a material has been used to measure both thermal conductivity and thermal diffusivity with varying degrees of success. Most commonly, researchers have used derivations from the work of Carslaw and Jaeger (1947) to analyse the chart of temperature rise over the natural logarithm of elapsed time.

The slope of part of this curve, under certain conditions, has been assumed by researchers from the early 20th century onwards to be dependent on the thermal conductivity of the sample medium. The ordinate intercept has likewise been assumed, under certain conditions, to be dependent on the thermal diffusivity of the sample medium and, sometimes, contact resistance between the line source and the medium.

Various researchers, especially from the 1950s onwards, concluded that the methodology had transcended its experimental stage and had become a practical engineering tool, available to measure either construction or similar materials. Hot wire and thermal probe techniques are reportedly being used today in various industries, including food, plastics, refractories and even space exploration.

The review has shown that the experimental results have not always matched the high accuracy claims made. Interlaboratory comparisons have found

marked differences between results for similar materials. Claims of accuracy have not always been backed up by comparison to available reference materials or to measurements made by alternative, standard methods. Usually, measurement and analysis methodologies, including calibrations, have been developed for one, and at most two, materials of known thermal properties before the methodology has been transferred to materials with unknown thermal properties. Such calibration in only one, or two, materials has been shown to be unreliable as the difference from directly calculated values to calibrated values has varied from material to material.

Measurements of liquids by thin wire line sources under well controlled conditions have produced consistent thermal conductivity results within 1% of known values. In contrast, claimed levels of accuracy for thermal conductivity and thermal diffusivity measurements by a thermal probe in solid or granular materials have been progressively downgraded in recent years. For example, Van Haneghem et al (1983) claimed accuracies of 1% and 20% for thermal conductivity and thermal diffusivity, respectively, in granular materials with a thermal probe, whereas the National Physical Laboratory (2007b) report that inaccuracy for thermal conductivity measurements in granular materials is likely to be greater than ± 10% and that thermal probes may not be suitable for obtaining reliable thermal diffusivity values at all.

Attempts to establish thermal diffusivity of solid or granular materials by this method, which was said by some in the middle of the last century to be easily achievable, have been less frequent over recent decades, presumably because of the difficulties encountered, with errors or inaccuracies reported being significantly greater than those in thermal conductivity measurements.

In measurement analyses derived from Carslaw and Jaeger (1947), the quantification of error and correction levels has been frequently based on thermal diffusivity values. These have either been taken from the literature or, in materials with unknown thermal properties, taken from the measurements being assessed. In the first case, this implied that thermal diffusivity values would need to be known before they could be measured. In the second case, corrections were applied based on a value derived from their outcome so that, without an alternative method of measurement, neither the correction nor the outcome value could be reliable.

Blackwell's solution for linear sections of $\Delta T/\ln t$ derived from Carslaw and Jaeger and relied upon by many later researchers, equation (14), was found by Riseborough et al (1983) and Jones (1988) to be incapable of distinguishing between varied combinations of the two unknowns, thermal diffusivity and, according to Veziroglu (1967), practically unmeasurable, contact resistance.

Jones and other researchers used either previous estimates of contact resistance or known values of volumetric heat capacity from which thermal diffusivity could be calculated. Goodhew (2000) had attempted Blackwell's short term solution to establish H but found this impractical and later relied upon an iterative, optimised line fitting procedure. Waite et al (2006, 2007) used a derivation of this short term solution in the initial half second of heating cycles but this approach to finding values of H remained inconclusive. Tye et al (2005) identified the complex relationship between heat transfer mechanisms, such as thermal conductivity and thermal diffusivity, as one of the issues requiring resolution before a standard methodology could be developed.

Recognition of the correct time window for analysis remains unclear. At early times measurements were reported to be affected by the thermal properties of the probe, including internal and external contact resistances. This would explain why hot wires have been more successful than thermal probes, being thinner and of only one material, and thus more representative of a perfect line source. It was not found to be clear when, or whether, the thermal properties of the probe itself ceased to influence results, or whether this period would be different for thermal conductivity and thermal diffusivity measurements.

Much of the thermal probe research has been based on probes with a length to radius ratio near to or exceeding the relative levels calculated by Blackwell. These were based on probes with diameters in the region of 30mm to 50mm. Later researchers have often used Blackwell's results of around 25:1 and 30:1 as generic values rather than recalculating these for smaller radii, where the elapsed time available to comply with Blackwell's calculations would be greatly reduced.

Effects at later times have been attributed to many factors: boundary distance; length to radius ratio of the probe (axial and end losses); convection; radiation; anisotropy; and inhomogeneity. The theoretical times for the first three of these effects have often been calculated from thermal diffusivity values, either taken from the literature or taken from the measurements being assessed, which values may be unreliable. These reported difficulties could make it unlikely in many cases that the separate influences of these various effects could be readily distinguished.

Many researchers, because of the difficulties at early and later times, have relied upon visual or mathematical identification of appropriate sections of $\Delta T/\ln t$ for analyses. Visual identification has relied upon the recognition of linear sections. In some cases, unsubstantiated mathematical recognition processes have been used, with individual researchers developing dissimilar processes.

Other difficulties were found during the review, such as: whether internal and external contact resistance effects were equally constant; whether power inputs effected output values; and whether shifting values on the temperature or time (subsequently logarithmic) axes could be relied upon to counter the effects of the probe's thermal properties on $\Delta T/\ln t$.

The literature review and previous work at the University of Plymouth have raised questions concerning the forms of analyses and practical experimental arrangements for thermal probe measurements of building materials, whether as samples or in situ. These include:

- Whether the influence of thermal diffusivity can be separated from that of contact resistance on the curve of $\Delta T/\ln t$ using traditional or contemporary solutions
- Whether the appropriate section of the curve $\Delta T/\ln t$ for analyses can be predicted, or deduced from measurements
- Whether calibrations, such as: a simple multiplying factor; using a theoretical dimension for the measurement radius position; or using a time or temperature offset in $\Delta T/\ln t$, are appropriate and can transfer successfully from a measurement in one material to a measurement in a material with different thermal properties
- The effects of contact mediums between the probe and sample

- The effects of hole size for pre-drilled holes in sample materials, with or without contact mediums or fillers
- The time needed for the probe to achieve sufficient thermal equilibrium with a sample before a reliable measurement can be taken
- After what time the retained heat from previous measurements ceases to influence following measurements in the same position
- The effects of carrying out measurements in unstable thermal environments
- Whether moisture migration compromises the measurement of moist materials
- How probe power levels affect results
- What the effects of anisotropy in sample materials are, on thermal conductivity and thermal diffusivity measurements
- Whether the thermal properties of inhomogeneous materials can be usefully assessed

The attempted resolution of these unresolved issues forms the basis for the experimental work described in following chapters.

Chapter 3: Introduction to the methodologies

This work is based on the hypothesis that the thermal probe technique for measuring thermal conductivity and thermal diffusivity could be successfully transferred from laboratory-based measurements to the measurement of building materials in situ. The rationale for the work was described in the introductory chapter, where the need for improved thermal data was shown. The thermal probe technique was chosen for its potential to carry out measurements quickly and economically in a relatively non-destructive manner, with minimum disturbance to the physical properties of subject materials, including their moisture content.

The literature review brought into question the high claims of accuracy for laboratory-based measurements by the thermal probe technique, often found expressed in the literature. This has led to four strands of work, which are:

1) Assessment of traditional solutions
2) Computer simulations
3) Laboratory measurements
4) In situ measurements

These diverse threads have meant the traditional approach of presenting an overall "methodology – experiment – results" format in this work was regarded as inappropriate. Rather, a similar arrangement was used for each of the four threads. This chapter introduces their individual rationales and methodologies, three of which are then developed under individual chapter headings. The results and interim conclusions from each of these chapters then inform the

overall discussion and conclusions of the work. This structure has been illustrated in Figure 3.

Over 700 measurements have been made, 500 simulations carried out and over 3,500 analyses undertaken. These, along with experiment descriptions, digital photographs, etc. have created a great deal of electronic data. As each data set required revisiting and analysing a number of times, and as the data is potentially valuable to following researchers, a stand alone storage system was developed using an accessible filing system, with incorporated hyperlinks to data sets from a central, searchable database. A more complete description of the filing system is presented in the introduction to chapter 5.

The central rationale and methodology for each of the four strands of scientific research is now introduced.

Assessment of traditional solutions

Three areas were identified in the literature review where traditional solutions had been brought into question, with issues left unresolved. These were:

- The ability of equation (14) to differentiate between causes of temperature rise
- The reliance of iterative solutions upon estimated input values
- Shifts in the time or temperature axes of $\Delta T/\ln t$

It was deemed necessary to resolve these three outstanding issues to avoid errors in the analyses of experimental data.

The literature review had shown it unlikely that contact resistance could be independently measured or accurately estimated. The ability of equation (14) to

differentiate between the temperature rise dependent on sample thermal diffusivity and that caused by contact resistance therefore required consideration in pursuance of reliable thermal diffusivity measurements. The methodology adopted was to assess the sensitivity of the equation over time using the MS Excel Goalseek facility with varied input values.

The iterative solution, based on the MS Excel Solver add-in programme, was examined, as this would provide a convenient alternative to repeated individual calculations and checks, where many hundreds of data points potentially derive from one measurement. The literature review had shown that a lack of clarity existed regarding the input values of λ, α and H, in iterative solutions. These are necessary to run the programme, and have been referred to by van Loon et al (1989) as needing to be near the actual values. As the Solver solution is based, in part, on equation (14), questions remain as to how near the input value estimates have to be and whether the Solver analysis routines developed at the University of Plymouth could differentiate between the effects of thermal diffusivity and contact resistance. The methodology involved running the Solver routine with data generated from thermal probe heating cycles in materials of known and unknown thermal properties. Varied input value estimates were then used in the Solver routine to assess their effects and the sensitivities of the programme.

The technique of shifting the time axis to compensate for the presence of a physical probe was explored. This method was used throughout the 20th century by some researchers yet discounted or not mentioned in the methodologies of many later researchers. It was therefore deemed advisable to make a focussed study of the method. The axis adjustment section of chapter 4 also introduces a

new and simple method of assessing linearity in $\Delta T/\ln t$ which is then used later in the work to assess the practical measurements.

Computer simulations

The rationale for computer simulations arose from two strands of research. Firstly, the literature review showed that line fitting over the whole measurement period created the potential to differentiate between the separate and interacting probe temperature rise effects caused by the thermal properties of the probe, any filler used, and the material, through fitting experimental curves to curves from simulated measurements. Secondly, simulations of probe heating cycles would produce measurement data without the presence of a physical probe, thus avoiding many potential sources of error. This would allow these errors to be differentiated from those that may have been remaining in the traditional solutions. The methodology entailed inputting thermal values to a dedicated software programme to create specific materials, heating these with an infinitely thin line source at a known power, and recording the temperature rise at various radii to produce curves of $\Delta T/\ln t$. The resultant data could be analysed using the recognised solutions and the curves could be compared to those created by practical measurements. A description of this work, where thermal diffusivity results were not eventually achieved, may be of interest to following researchers and is given in Appendix A. Further details are given in de Wilde et al (2007), which has been bound in at the end of this thesis.

Laboratory work

Three strands of work were carried out under controlled laboratory conditions. These were:

- An assessment of measurements using commercially available thermal properties' meters
- Measurements with apparatus based on Hukseflux TP08 thermal probes
- A thermographic assessment of probe heating cycles

The rationale and methodology of each is given below:

Thermal properties meters

The rationale for assessing the thermal properties meters was that they came to the market during the time that the work reported here was being undertaken and, had they been found to give reliable and accurate results for thermal conductivity, thermal diffusivity and volumetric heat capacity, this work may have proved largely redundant. The method of assessment was to carry out measurements with the meters and compare the results to known values for various materials, and with those achieved using the apparatus built for the project. The meters also supplied an opportunity to assess the effectiveness of calibrations in one material when measuring diverse materials.

Laboratory based measurements

Practical laboratory measurements were carried out in a controlled thermal environment, using apparatus built for and during the project. This was deemed necessary to resolve various issues in experimental work that had arisen from the literature review and from previous work at Plymouth, including: the effects of varied hole sizes; the influences of contact fillers; contact resistance; temperature stabilisation periods; the effects of inhomogeneity and anisotropy; input power levels; and moisture migration within sample materials. These aspects of the work required resolution for in situ measurements. It was deemed necessary to carry out this work under controlled conditions, to avoid

potential difficulties in differentiating the effects of these factors from those of fluctuating environmental conditions, which were expected to be encountered with in situ measurements. Measurements were used to assess the parameters above, such as by carrying out sequences of measurements with stepped changes to parameters. Through comparisons between the results of consecutive measurements, and to known values, the effects of each change could be assessed. The results were achieved by using analysis routines developed during the assessments of traditional solutions.

The laboratory measurements gave rise to new results for various materials, including aerated concrete at varied moisture content, which results are also reported in chapter 5.

Thermography

Infrared thermography was used to carry out a study of radial heat transfer during measurements. Thermal probe technology approximates a perfect line source, where the radial heat profile in an infinite homogenous material will be parallel to the line source. The study was designed to record and assess heating profiles during practical measurements, where axial and end losses would exist, for comparison with the perfect model.

In situ measurements

The rationale for in situ measurements is the basis of the project and has been described in chapter 1. The broad methodology was: to carry out a literature review and assessment of historic and contemporary work; to carry out simulated and laboratory measurements to resolve outstanding issues before building a field apparatus; to carry out and make an assessment of in situ

measurements using various case study buildings. The case study buildings were chosen in part on the basis of materials and climate so that in situ measurements could be compared to laboratory measurements, and so the effects of diverse climatic conditions could be evaluated.

Chapter 6, which describes the in situ measurements, details the construction of the field apparatus. This includes a description of the probe temperature measurement methodology, and an assessment of the extent and implications of scatter in the probe heating data. The rationale for the choice of case study buildings is given in more detail and the in situ measurements described.

The next chapter describes the assessment of traditional solutions, the first of the four strands of scientific research introduced above.

Chapter 4: Assessment of traditional solutions

This chapter examines three methods, found in contemporary practice, for measuring thermal conductivity and thermal diffusivity using the curve of $\Delta T/\ln t$ obtained from heating a thermal probe placed within the material of interest. These examinations were undertaken to inform the analyses of practical measurements. Interim conclusions are given at the end of the chapter. The three methods are: the Blackwell equation; the Solver routine; and axis adjustments.

The literature review had identified potential difficulties with these methods. Various authors from the middle of the 20th century, such as Hooper and Lepper (1950), had stated that thermal diffusivity values were readily available from thermal probe data. Buettner (1955), studying moist soils, pointed out that various combinations of thermal conductivity and volumetric heat capacity could have the same thermal diffusivity value. Riseborough et al (1983) found that, with similar thermal conductivity, varied combinations of thermal diffusivity and contact resistance could generate indistinguishable curves, which was also recognised by Jones (1988). This then raised the question as to whether the contemporary solutions could differentiate between the effects of thermal conductivity, thermal diffusivity and contact resistance on the heating curve $\Delta T/\ln t$. The three methods are now examined in more detail.

The Blackwell equation

Three examinations were made of this solution, used by Goodhew (2000), Batty (1984) and derived from Carslaw and Jaeger (1947) by Blackwell and Misener

(1951). The sensitivity of the equation was tested by altering combinations of the α and *H* terms on one side of the equation while constraining the product of the whole term containing them. Secondly, the equation was rearranged to assess the extent of difference in thermal diffusivity results that could be generated by differences in *H* input estimates. The equation was then used to examine the predictability of *H* under conditions of excellent physical contact with sample mediums.

The Blackwell equation for linear asymptotes of $\Delta T/\ln t$, describing their slope and intercept, is:

$$\Delta T = \frac{Q'}{4\pi\lambda}\left[\ln t + \left\{\ln\left(\frac{4\alpha}{r^2}\right) - \gamma + \frac{2\lambda}{rH}\right\}\right]$$

Equation (32)

where the later terms of equations (18) and (19) have been shown to be negligible after the initial probe heating period.

The sensitivity of this equation was tested by modelling values for thermal probes in agar immobilised water using MS Excel. These represented linear asymptotes matching those found in agar measurements between 10s and 160s. The thermal conductivity value for water was fixed. Sequential estimates for *H* were entered and, using the MS Excel Goalseek facility, values for α were found for each estimate of *H*, while constraining the equation to give the predetermined values for ΔT for the linear asymptote at times *t*.

Charts 1 and 2, displaying α results for small and large *H*, show an S curve for thermal diffusivity values dependent on input *H* values. Without prior knowledge of either α or *H* and relying on equation (32), thermal diffusivity could, in this

instance, be anywhere between zero and 1.6 $x10^{-7}$ m^2s^{-1}, leading to volumetric heat capacity values ranging from 3.75 $MJm^{-3}K^{-1}$ towards infinity.

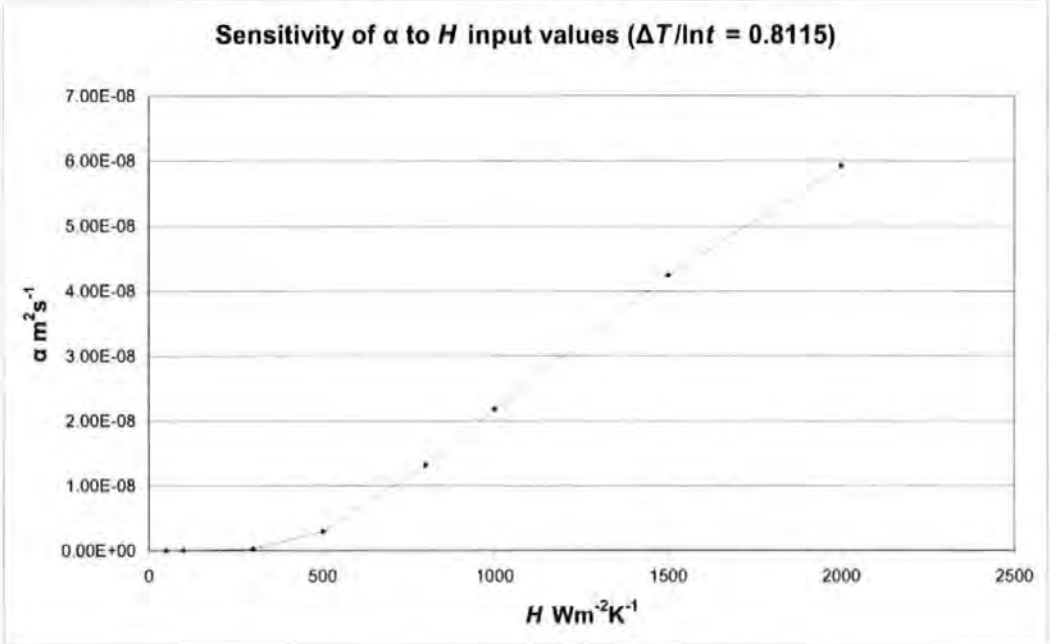

Chart 1: Thermal diffusivity by contact resistance estimates, smaller *H*

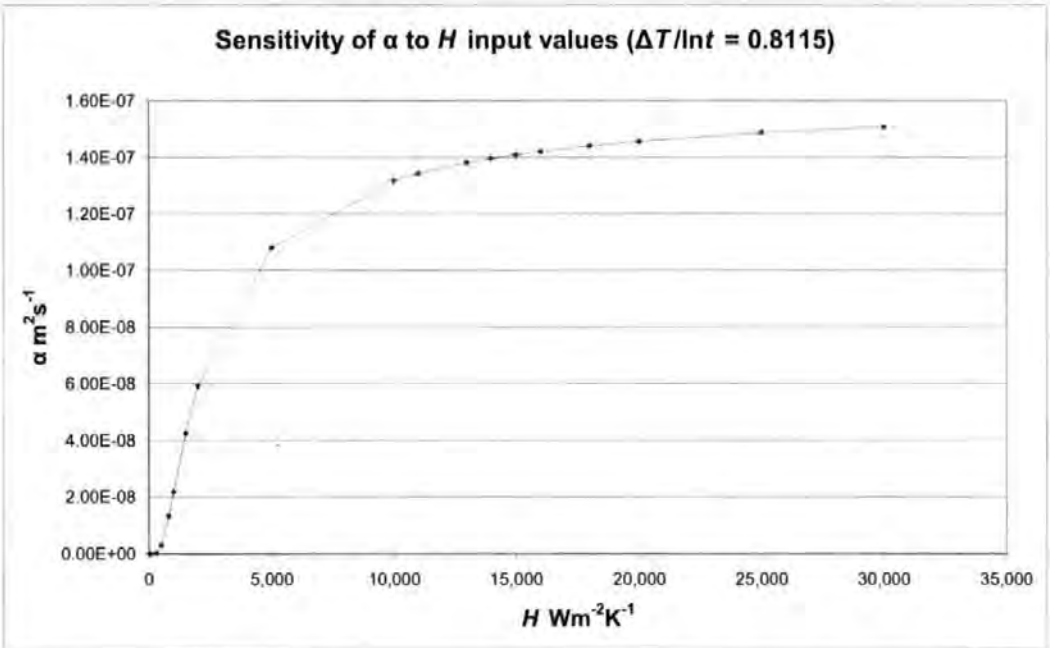

Chart 2: Thermal diffusivity by contact resistance estimates, larger *H*

The Blackwell equation including later terms is:

$$\Delta T = \frac{Q'}{4\pi\lambda}\left[\ln t + \left(\ln\left(\frac{4\alpha}{r^2}\right) - \gamma + \frac{2\lambda}{rH}\right) + \left(\frac{1}{t}\right)\left(\left(\frac{r^2}{2\alpha}\right)\left[1 - {mc_p\alpha}/{\pi r^2 L\lambda}\right]\ln t + \left(\frac{r^2}{2\alpha}\right)\left[\ln\left(\frac{4\alpha}{r^2}\right) - \gamma + 1 - \frac{\left[\ln\left(\frac{4\alpha}{r^2}\right) - \gamma + \frac{2\lambda}{rH}\right]mc_p\alpha}{\pi r^2 L\lambda}\right]\right)\right]$$

Equation (33)

where m, c_p, L are: mass; specific heat capacity; and length of the probe, respectively.

Blackwell suggested further terms may be needed, although the effect of such later terms would be of increasing insignificance (Lavelle M, 2006).

Rearranging equation (32) gives the following:

$$\ln\alpha = 2\ln r - \ln(4t) + \frac{4\pi\lambda.\Delta T}{Q'} + \gamma - \left(\frac{2\lambda}{rH}\right)$$

Equation (34)

Equation (34) was used to assess the influence of the H parameter on thermal diffusivity outcomes for measurements in a number of materials. Firstly a value for thermal conductivity was found through traditional regression analysis of the earliest available time window to give a linear asymptote of $\Delta T/\ln t$ using equation (6). Equation (34) was then used at each data point at 1Hz within the same time window using the calculated value for thermal conductivity and a range of estimates for H. The MS Excel Goalseek facility was then used to provide values for the natural logarithm of α for each estimate. The results were used to calculate values for volumetric heat capacity through the relationship $\alpha = \lambda / \rho C$. Volumetric heat capacity values for the data points used, those within

the time window, were then averaged and results given with their variable coefficient.

Chart 3 shows the result for a sample of oak measured across the grain. Thermal conductivity and volumetric heat capacity were calculated over the period 60s – 160s. The variable coefficient for thermal conductivity values at 95% confidence was 1.01% and for volumetric heat capacity values, 1.41%. The volumetric heat capacity of the oak was not measured by other means therefore an accurate value remained known. From the literature, a value in the region of 800 $kJm^{-3}K^{-1}$ may be expected. This shows that, within a relatively small range of estimated *H* values, Blackwell's α solution used with a thermal probe could produce results varying by orders of magnitude. Similar sensitivities were found with other materials. This shows that Blackwell's equation, in the materials studied, could not differentiate between temperature rise caused by contact resistance and that caused by the heat capacity of the sample material.

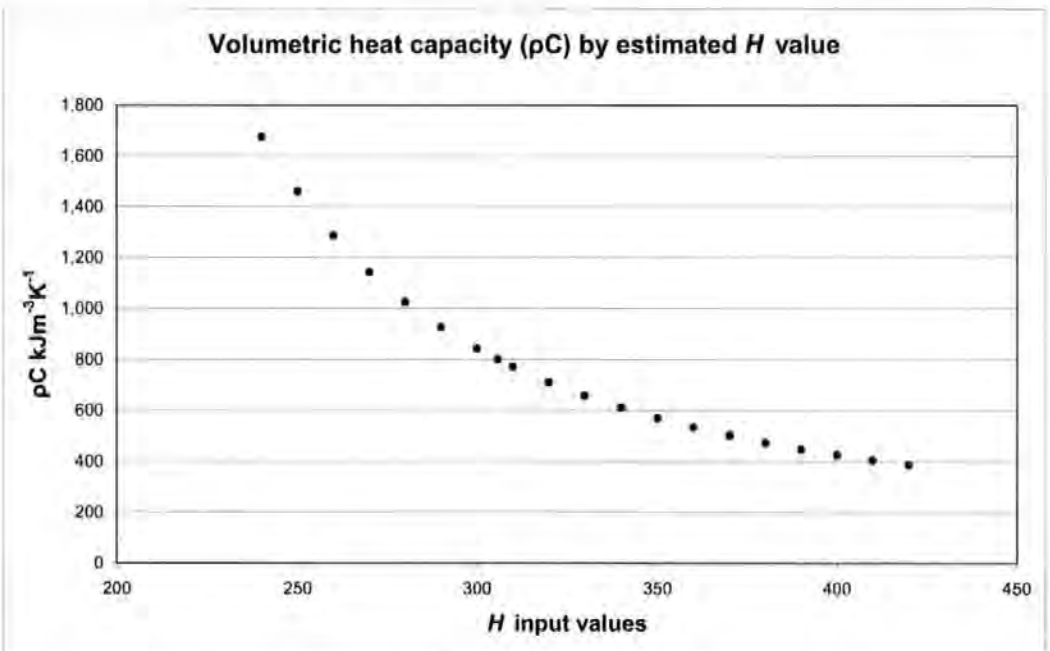

Chart 3: Oak volumetric heat capacity by *H* estimate

A further study was carried out to assess the *H* parameter. Four Hukseflux TP08 probes were used to measure two materials with reasonably well known thermal properties, agar immobilised water and PTFE. Four measurements were carried out with each probe in each material. The agar immobilised water was contained in a thermally stable insulated container with internal dimensions of 330mm x 210mm x 110mm and probes were placed at 70mm from the boundary. The PTFE was in cylindrical form, 100mm diameter x 150mm long, with a 1.5mm hole drilled along the central axis to a depth of 72mm.

Equation (34) was used, after establishing thermal conductivity from the linear asymptotes of $\Delta T/\ln t$ by equation (6), to establish the value of *H* that would give the known value of α, thermal diffusivity, for each material. Chart 4 shows the *H* value was consistent for each probe in agar but differed by up to a factor of almost two between probes. The first measurement for each probe in the PTFE was carried out without any contact filler whereas the twelve other measurements were carried out using the high thermal conductivity paste, ArcticSilver5. Again these measurements were consistent for each probe and differed between probes. However, the pattern of differences between probes varied between the materials.

This brings into question van Haneghem's (1981) Modified Jaeger Method, whereby it was assumed that perfect contact was made in agar measurements and that the corresponding *H* value would therefore be a property of the probe alone. The disproportionate changes in the pattern of *H* results between the two materials show that values may be dependent on more complex relationships between the thermal properties of the various probe components and the sample materials than have previously been considered.

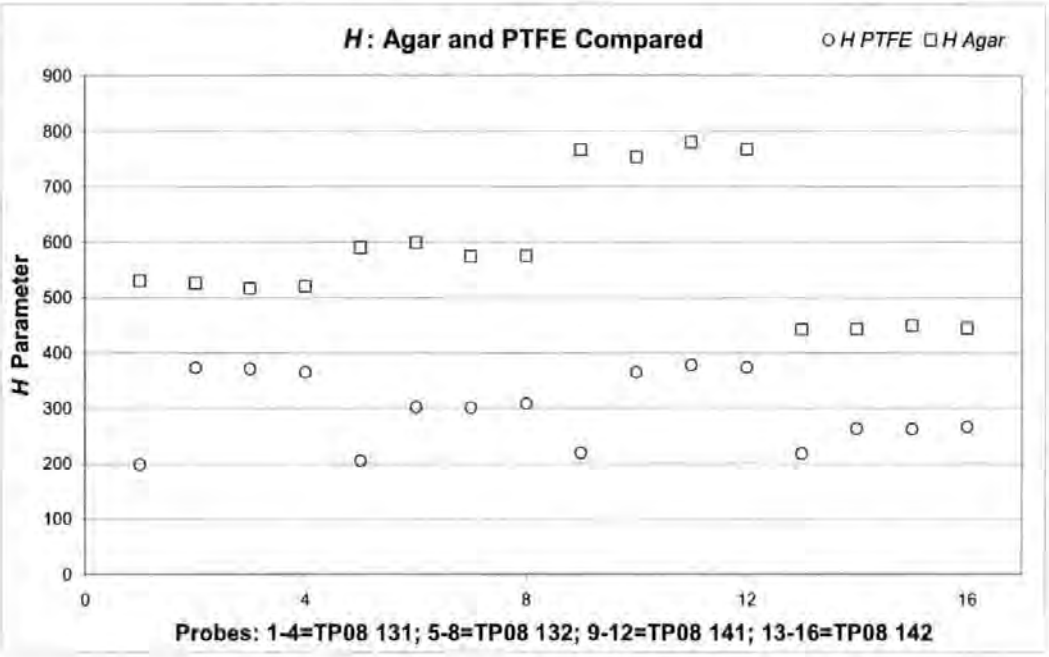

Chart 4: *H* values for TP08 probes in agar and PTFE

Solver

Goodhew and Griffiths (2004), following Banaszkiewicz et al (1997), developed an iterative software method to establish the three unknowns, α, λ and *H* in equation (4). The Solver add-in programme to MS Excel 1997 was used to create workbook templates with the iterative calculation method embedded. These templates were developed further in the current project and the Solver solutions were evaluated.

Macros were introduced so that experimental data values, the electrical signals recorded from the probe apparatus, could be automatically converted into temperatures and power in a worksheet, named 'data'. The probe power output was calculated through a link to another worksheet, named 'Constant G', where probe resistance values could be updated according to their marked values. A graphical representation of the temperature stability for 200s prior to the

measurement was introduced to the data worksheet, so that measurement stabilities could be assessed and analyses broken off where temperature drifts were excessive. The initial temperature, before a heating cycle, was calculated based on the average temperature for the prior 50 seconds. This reduced the error that could be caused by data scatter where a single data point might be used. The 50s average temperature was subtracted from the recorded temperatures to give the temperature rise. An early example of the data worksheet is given below (Figure 9). This was later updated, with separate sheets introduced to depict the temperature stability, the temperature rise over time, and over the natural logarithm of elapsed time.

The data worksheet was linked to other worksheets containing the Solver solutions and end time calculations.

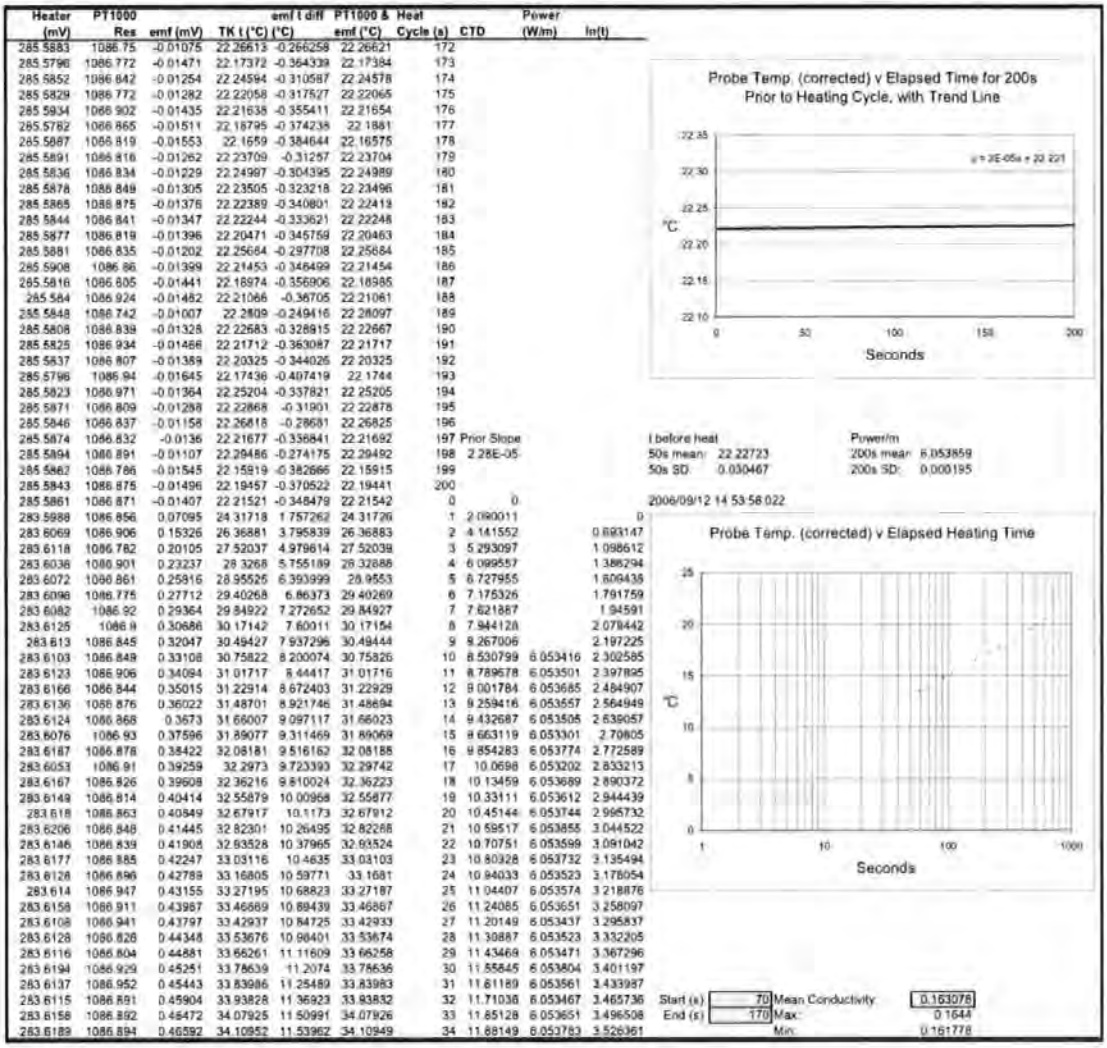

Heater (mV)	PT1000 Res	emf (mV)	TK t (°C)	emf t diff (°C)	PT1000 & emf (°C)	Heat Cycle (s)	CTD	Power (W/m)	ln(t)
285.5883	1086.75	-0.01075	22.26613	-0.266258	22.26621	172			
285.5796	1086.772	-0.01471	22.17372	-0.364339	22.17384	173			
285.5852	1086.842	-0.01254	22.24594	-0.310587	22.24578	174			
285.5829	1086.772	-0.01282	22.22058	-0.317527	22.22065	175			
285.5934	1086.902	-0.01435	22.21638	-0.355411	22.21654	176			
285.5782	1086.865	-0.01511	22.18795	-0.374238	22.1881	177			
285.5887	1086.819	-0.01553	22.1659	-0.384644	22.16575	178			
285.5891	1086.816	-0.01262	22.23709	-0.31257	22.23704	179			
285.5836	1086.834	-0.01229	22.24987	-0.304395	22.24989	180			
285.5878	1086.849	-0.01305	22.23505	-0.323218	22.23496	181			
285.5865	1086.875	-0.01376	22.22389	-0.340801	22.22413	182			
285.5844	1086.841	-0.01347	22.22244	-0.333621	22.22248	183			
285.5877	1086.819	-0.01396	22.20471	-0.345759	22.20463	184			
285.5881	1086.835	-0.01202	22.25684	-0.297708	22.25684	185			
285.5908	1086.86	-0.01399	22.21453	-0.346499	22.21454	186			
285.5816	1086.805	-0.01441	22.18974	-0.356906	22.18985	187			
285.584	1086.924	-0.01482	22.21066	-0.36705	22.21061	188			
285.5848	1086.742	-0.01007	22.2809	-0.249416	22.28097	189			
285.5808	1086.839	-0.01328	22.22583	-0.328915	22.22667	190			
285.5825	1086.934	-0.01486	22.21712	-0.363087	22.21717	191			
285.5837	1086.807	-0.01389	22.20325	-0.344026	22.20325	192			
285.5796	1086.94	-0.01645	22.17436	-0.407419	22.1744	193			
285.5823	1086.971	-0.01364	22.25204	-0.337821	22.25205	194			
285.5871	1086.809	-0.01288	22.22868	-0.31901	22.22878	195			
285.5846	1086.837	-0.01158	22.26818	-0.28681	22.26825	196			
285.5874	1086.832	-0.0136	22.21677	-0.336841	22.21692	197	Prior Slope		
285.5894	1086.891	-0.01107	22.29486	-0.274175	22.29492	198	2.28E-05		
285.5862	1086.786	-0.01545	22.15819	-0.382666	22.15915	199			
285.5843	1086.875	-0.01496	22.19457	-0.370522	22.19441	200			
285.5861	1086.871	-0.01407	22.21521	-0.348479	22.21542	0	0		
283.5988	1086.856	0.07095	24.31718	1.757262	24.31726	1	2.080011		0
283.6069	1086.906	0.15326	26.36881	3.795839	26.36883	2	4.141552		0.693147
283.6118	1086.782	0.20105	27.52037	4.979614	27.52039	3	5.293097		1.098612
283.6036	1086.901	0.23237	28.3268	5.755189	28.32688	4	6.099557		1.386294
283.6072	1086.861	0.25916	28.95525	6.393999	28.9553	5	6.727955		1.609438
283.6096	1086.775	0.27712	29.40268	6.86373	29.40269	6	7.175326		1.791759
283.6082	1086.92	0.29364	29.84922	7.272652	29.84927	7	7.621887		1.94591
283.6125	1086.9	0.30686	30.17142	7.60011	30.17154	8	7.944128		2.079442
283.613	1086.845	0.32047	30.49427	7.937296	30.49444	9	8.267006		2.197225
283.6103	1086.849	0.33108	30.75822	8.200074	30.75826	10	8.530799	6.053416	2.302585
283.6123	1086.906	0.34094	31.01717	8.44417	31.01716	11	8.789678	6.053501	2.397895
283.6166	1086.844	0.35015	31.22914	8.672403	31.22929	12	9.001784	6.053685	2.484907
283.6136	1086.876	0.36022	31.48701	8.921746	31.48694	13	9.259416	6.053557	2.564949
283.6124	1086.868	0.3673	31.66007	9.097117	31.66023	14	9.432687	6.053505	2.639057
283.6076	1086.93	0.37596	31.89077	9.311469	31.89069	15	9.663119	6.053301	2.70805
283.6187	1086.878	0.38422	32.08181	9.516162	32.08188	16	9.854283	6.053774	2.772589
283.6053	1086.91	0.39259	32.2973	9.723393	32.29742	17	10.0698	6.053202	2.833213
283.6167	1086.826	0.39608	32.36216	9.810024	32.36223	18	10.13459	6.053689	2.890372
283.6149	1086.814	0.40414	32.55879	10.00968	32.55877	19	10.33111	6.053612	2.944439
283.618	1086.863	0.40849	32.67917	10.1173	32.67912	20	10.45144	6.053744	2.995732
283.6206	1086.848	0.41445	32.82301	10.26495	32.82268	21	10.59517	6.053855	3.044522
283.6146	1086.839	0.41908	32.93528	10.37965	32.93524	22	10.70751	6.053599	3.091042
283.6177	1086.885	0.42247	33.03116	10.4635	33.03103	23	10.80328	6.053732	3.135494
283.6128	1086.896	0.42789	33.16805	10.59771	33.1681	24	10.94033	6.053523	3.178054
283.614	1086.947	0.43155	33.27195	10.68823	33.27187	25	11.04407	6.053574	3.218876
283.6158	1086.911	0.43967	33.46869	10.88439	33.46867	26	11.24085	6.053651	3.258097
283.6108	1086.941	0.43797	33.42937	10.84725	33.42933	27	11.20149	6.053437	3.295837
283.6128	1086.826	0.44348	33.53676	10.96401	33.53674	28	11.30887	6.053523	3.332205
283.6116	1086.804	0.44881	33.66261	11.11609	33.66258	29	11.43466	6.053471	3.367296
283.6194	1086.929	0.45251	33.78639	11.2074	33.78636	30	11.55845	6.053804	3.401197
283.6137	1086.952	0.45443	33.83986	11.25489	33.83983	31	11.61189	6.053561	3.433987
283.6115	1086.891	0.45904	33.93828	11.36923	33.93832	32	11.71036	6.053467	3.465736
283.6158	1086.892	0.46472	34.07925	11.50991	34.07926	33	11.85128	6.053651	3.496508
283.6189	1086.894	0.46592	34.10952	11.53962	34.10949	34	11.88149	6.053783	3.526361

t before heat
50s mean: 22.22723
50s SD: 0.030467

Power/m
200s mean: 6.053859
200s SD: 0.000195

2006/09/12 14:53:58.022

Start (s)	70	Mean Conductivity	0.163078
End (s)	170	Max:	0.1644
		Min:	0.161778

Figure 9: Example of a data sheet for a measurement in petroleum jelly

Following the guidelines of ASTM D 5334 (2000), where the temperature drifted by more than 0.1°C over 200s, the measurement was abandoned. Where the drift was less than this amount, it was presumed that the effects would carry forward through the measurement period and the curve of $\Delta T/\ln t$ was appropriately corrected. In practice, it was found that the effect of this correction on thermal conductivity outcome values did not appear within three significant figures for any of a number of trials undertaken. This is contrary to the findings of Campbell et all (2004), where a 0.001°Cs^{-1} drift, equating to 0.2°C over 200s, produced a 50% error in thermal conductivity outcomes.

The data sheet contained a facility to calculate an initial value for thermal conductivity through traditional regression analysis over a visually recognised linear asymptote of $\Delta T/\ln t$. This value was then used as one of the initial estimates for the Solver analyses.

An example of the Solver 4.3 sheet is given in figure 10. Solver attempts to find the line of best fit to the data using the terms of equation (33), by reducing the value of the residuals, through a least squares optimisation.

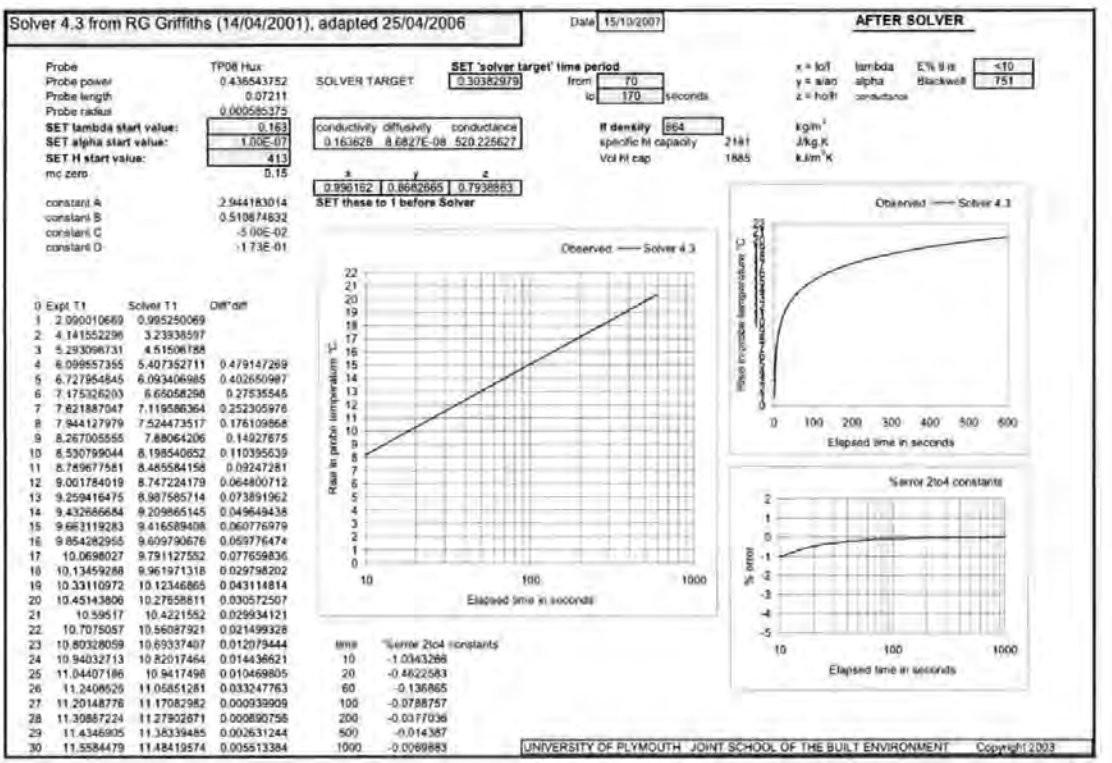

	Expt T1	Solver T1	Diff'diff
1	2.090010669	0.995250069	
2	4.141552296	3.23938597	
3	5.293096731	4.51506188	
4	6.099557355	5.407352711	0.479147269
5	6.727954845	6.093406985	0.402650987
6	7.175326203	6.65058298	0.27535545
7	7.621887047	7.119586364	0.252305976
8	7.944127979	7.524473517	0.176109868
9	8.267005555	7.88064206	0.14927675
10	8.530799044	8.198540652	0.110395539
11	8.789677581	8.485584158	0.09247281
12	9.001784019	8.747224179	0.064800712
13	9.259416475	8.987585714	0.073891962
14	9.432666684	9.209865145	0.049649438
15	9.663119283	9.416589408	0.060776979
16	9.854282955	9.609790676	0.059776474
17	10.0698027	9.791127552	0.077659836
18	10.13459288	9.961971318	0.029798202
19	10.33110972	10.12346865	0.043114814
20	10.45143806	10.27658811	0.030572507
21	10.59517	10.4221552	0.029934121
22	10.7075057	10.56087921	0.021499328
23	10.80328059	10.69337407	0.012079444
24	10.94032713	10.82017464	0.014436621
25	11.04407186	10.9417498	0.010469805
26	11.2406525	11.05851281	0.033247763
27	11.20148776	11.17082982	0.000939909
28	11.30887224	11.27902671	0.000890756
29	11.4346905	11.38339485	0.002631244
30	11.5584479	11.48419574	0.005513384

time	%error 2to4 constants
10	-1.0343288
20	-0.4622583
60	-0.136865
100	-0.0788757
200	-0.0377036
500	-0.014387
1000	-0.0069883

Figure 10: Example of Solver 4.3 sheet for a measurement in petroleum jelly

The 4.3 designation denoted four constants, as in equations (16) to (19), and the three unknowns, λ, α and *H*. With two of the constants incorporating values for the thermal probe's heat capacity, this spreadsheet was recommended, in part, for use in finding after which time the probe's thermal properties cease to have a significant effect on the curve of $\Delta T/\ln t$. This was done by observing the

"%error 2to4 constants" chart, which compared results with and without the thermal capacity of the probe. It was advised that the start of a suitable time window for analysis was 10s beyond when this difference was less than 1%. The Solver sheet was linked to a further sheet, described by Goodhew and Griffiths (2004), that used Blackwell's (1956) calculations of axial heat flow related to radial heat flow to identify a suitable end time for analysis time windows. Using manual iterations, this sheet was then used to find a suitable end time, where axial flow remained below 1% of radial flow.

Once a suitable time window had been identified in Solver 4.3, Solver 2.3 was recommended, especially where the asymptote had a clearly linear section, to find values for the three unknowns without consideration of the probe's thermal properties. The "%error 2to4 constants" chart and the Blackwell end time could be rechecked in relation to this sheet.

Initially, following Goodhew and Griffiths (2004), the Solver calculation was left unconstrained. However, this resulted in frequently encountering negative values for H. As such a phenomenon would indicate negative contact resistance, a physical impossibility, this parameter was constrained to be positive. It is interesting to note that De Vries and Peck (1958) also encountered negative results which were, at that time, tentatively ascribed to a "leakage current".

The Solver analysis required estimated inputs, the 'start values' in figure 10, for thermal conductivity λ, thermal diffusivity α, and parameter H. This may be considered similar to the work of Nix et al (1967) who used successive guesses until calculated curves of $\Delta T/\ln t$ became coincident with experimental curves. It

is similar to the work of van Loon et al (1989) who also used a non-linear, least squares iterative optimisation process reliant on initial estimates, where it was stated that estimated values needed to be near actual values.

Table 1 shows the effects of input estimates for a petroleum jelly measurement, which had a visually assessed linear asymptote. This shows the thermal conductivity results for the Solver 4.3 analyses varied from 0.156 $Wm^{-1}K^{-1}$ to 0.162 $Wm^{-1}K^{-1}$ whereas those for the Solver 2.3, at 0.159 $Wm^{-1}K^{-1}$, were consistent with those achieved by the regression analysis. It can be seen that, for the same range of input estimates, the values achieved for thermal diffusivity measurements within the analysis window of 60s – 200s were different for each version of Solver. These ranged from 6.1 $x10^{-8}$ m^2s^{-1} to 1.3 $x10^{-7}$ m^2s^{-1} for Solver 4.3 and 5.67 $x10^{-8}$ m^2s^{-1} to 1.27 $x10^{-7}$ m^2s^{-1} for Solver 2.3, differences of 113% and 124% respectively from the lowest to the highest value. The limited number of input estimates resulted in volumetric heat capacity values, within the constraints of the start and end times, of between 1,256 $kJm^{-3}K^{-1}$ and 2,249 $kJm^{-3}K^{-1}$. *H* values varied from 586 $Wm^{-2}K^{-1}$ to 1,568 $Wm^{-2}K^{-1}$.

Similar disparities were found when carrying out calculations for other materials. Within the recommended parameters of the Solver routines, the volumetric heat capacity value for agar-immobilised water, from a measurement carried out in a stable thermal environment with a linear asymptote, was found to range from 1,000 $kJm^{-3}K^{-1}$ to 7,000 $kJm^{-3}K^{-1}$. The effects for materials that produced non-linear asymptotes for measurements undertaken in stable thermal environments were found to be more pronounced.

It is of note that the estimated start values affected the values for the chart of "%error 2to4 constants" and the Blackwell end times, hence time windows identified in Solver 4.3 for analysis by Solver 2.3 also remained dependent on the initial estimated input values, where the accuracy of these values would usually be unknown prior to a measurement.

Attempts to achieve reliable and consistent results for thermal diffusivity using the Solver solution with varied estimates for α and *H* inputs were undertaken without success. For example, a blind trial was carried out using data for an unfired earth and wood shaving brick. This produced a thermal conductivity value of 0.618 $Wm^{-1}K^{-1}$ and a thermal diffusivity value of 9.6 $x10^{-7}$ m^2s^{-1}, with *H* parameter at 152 $Wm^{-2}K^{-1}$, giving a volumetric heat capacity of 644 $kJm^{-3}K^{-1}$. The sample was later measured with a drop calorimeter and found to have a volumetric heat capacity in the region of 1,829 $kJm^{-3}K^{-1}$, some 300% greater.

RUN	Reg, λ Period	Mid	Upper	Lower	SD	SD/Mid	Solver start values λ start	α start	*H* start	Sol 4.3 Period	λ	α	*H*	VHC	% err *t*	B'well *t*	Sol 2.3 Period	λ	α	*H*	VHC	% err *t*	B'well *t*
Vaseline, Higher Lank, BP-0030d																							
016	60-200s	0.159	0.161	0.158	0.002	1.16%	1.000	1.00E-07	750	60-200s	0.162	1.3E-07	1221	1,269	55	496	60-200s	0.159	1.27E-07	1568	1,256	55	493
017							1.000	9.50E-08	750	60-200s	0.160	9.7E-08	848	1,648	<10	653	60-200s	0.159	1.24E-07	1471	1,285	50	645
018							1.000	9.00E-08	750	60-200s	0.162	1.3E-07	1204	1,280	55	500	60-200s	0.159	1.20E-07	1360	1,325	47	499
019							1.000	8.50E-08	750	60-200s	0.162	1.2E-07	1055	1,391	41	546	60-200s	0.159	1.14E-07	1188	1,404	38	545
020							1.000	8.00E-08	750	60-200s	0.161	1.1E-07	977	1,469	32	578	60-200s	0.159	1.01E-07	942	1,582	<20	579
021							1.000	7.50E-08	750	60-200s	0.161	1E-07	912	1,550	20	612	60-200s	0.159	9.65E-08	876	1,653	<20	613
022							1.000	7.00E-08	750	60-200s	0.159	8.1E-08	713	1,948	18	780	60-200s	0.159	8.07E-08	681	1,976	<20	781
023							1.000	6.50E-08	750	60-200s	0.158	7.9E-08	689	2,017	24	809	60-200s	0.159	7.66E-08	639	2,082	30	811
024							1.000	6.00E-08	750	60-200s	0.159	8.2E-08	719	1,926	17	770	60-200s	0.159	7.09E-08	586	2,249	43	776
025							1.000	5.50E-08	750	60-200s	0.157	6.6E-08	605	2,360	60	957	60-200s	0.159	5.44E-08	456	2,932	90	970
026							1.000	5.00E-08	750	60-200s	0.156	6.1E-08	569	2,564	70	1046	60-200s	0.159	5.67E-08	472	2,813	80	1055
027	60-200s	0.159	0.161	0.158	0.002	1.16%	1.000	7.00E-08	1000	60-200s	0.161	1.1E-07	927	1,530	24	604	60-200s	0.159	1.01E-07	950	1,575	<20	603
028							1.000	7.00E-08	950	60-200s	0.160	9.2E-08	798	1,740	<10	692	60-200s	0.159	9.40E-08	841	1,697	<20	691
029							1.000	7.00E-08	900	60-200s	0.159	8.7E-08	755	1,834	12	732	60-200s	0.159	8.91E-08	777	1,789	<20	731
030							1.000	7.00E-08	850	60-200s	0.159	8.5E-08	737	1,879	15	751	60-200s	0.159	8.50E-08	728	1,876	<20	751
031							1.000	7.00E-08	800	60-200s	0.159	8.5E-08	739	1,876	15	749	60-200s	0.159	8.30E-08	706	1,921	<20	750
032							1.000	7.00E-08	750	60-200s	0.159	8.1E-08	713	1,948	18	780	60-200s	0.159	8.07E-08	681	1,976	<20	781
033							1.000	7.00E-08	700	60-200s	0.160	9.9E-08	867	1,616	<10	639	60-200s	0.159	9.10E-08	801	1,752	<20	641
034							1.000	7.00E-08	650	60-200s	0.160	9.7E-08	847	1,650	<10	654	60-200s	0.159	9.04E-08	793	1,764	<20	655
035							1.000	7.00E-08	600	60-200s	0.160	9.1E-08	788	1,760	<10	700	60-200s	0.159	8.88E-08	772	1,797	<20	701
036							1.000	7.00E-08	550	60-200s	0.159	8.8E-08	762	1,819	11	725	60-200s	0.159	8.39E-08	716	1,900	<20	726
037							1.000	7.00E-08	500	60-200s	Solver can't compute...						60-200s	0.159	8.25E-08	700	1,933	<20	NUM!!!
038							1.000	7.00E-08	450	60-200s	0.159	8.8E-08	765	1,810	10	721	60-200s	0.159	8.43E-08	720	1,891	<20	723
039							1.000	7.00E-08	400	60-200s	0.160	9E-08	786	1,766	<10	703	60-200s	0.159	8.52E-08	730	1,871	<20	704
040							1.000	7.00E-08	350	60-200s	0.160	9.1E-08	788	1,760	<10	700	60-200s	0.159	8.52E-08	730	1,873	<20	702
041							1.000	7.00E-08	300	60-200s	0.159	8.3E-08	728	1,905	16	761	60-200s	0.159	7.95E-08	668	2,006	20	764

Table 1: Solver sensitivity for input estimates, petroleum jelly

Axis adjustments

Various researchers have employed a temperature time adjustment to counter the effects of the initial probe heating period. During this period, the rate of temperature rise is at first influenced more by the thermal properties of the probe itself than those of the sample. Then, as the radial heat wave moves away from the probe, the thermal properties of the sample exert greater influence. This, in practice, gives rise to non linearity at early times in $\Delta T/\ln t$. Researchers who employed a temperature time adjustment included: Hooper and Lepper (1950); Hooper and Chang (1953); de Vries (1952a, 1952b); Woodside (1958); Underwood and McTaggart (1960) who stated that the appropriate time offset could be positive or negative; Nix et al (1967); Van Haneghem (1981); Morabito (1989); Manohar et al (2000); and Campbell (2004).

The potential effects of this strategy on thermal conductivity results were explored in the current work. Firstly, a line of $\Delta T/\ln t = 1$ was plotted to give a perfectly linear asymptote. The logarithmic time axis values were then converted to simple time and offset by plus and minus 10s. The time values were then converted back to logarithmic values and plotted again (see chart 5).

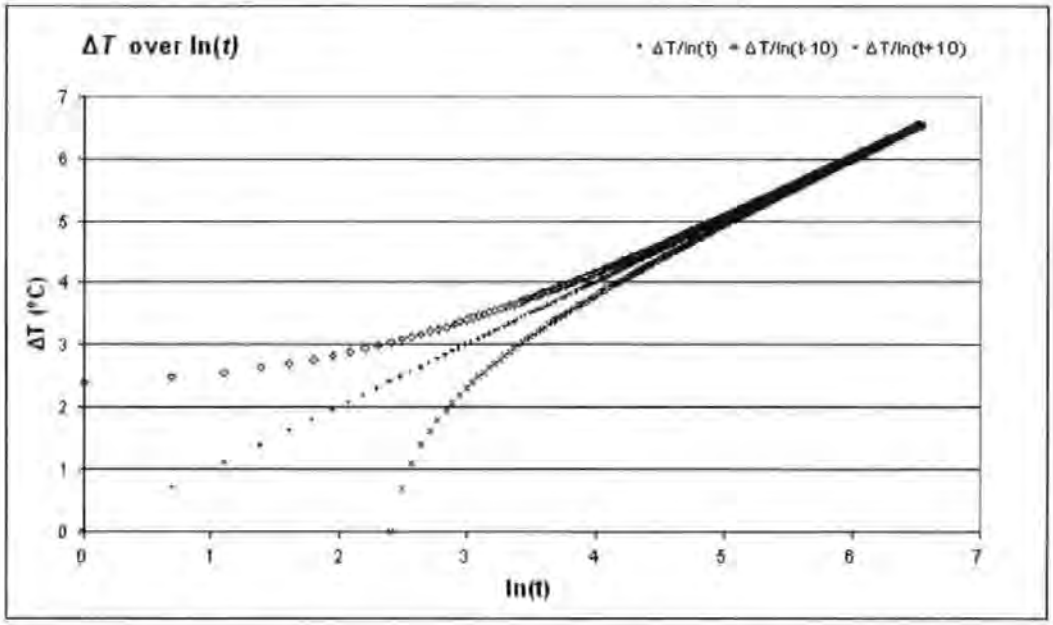

Chart 5: Charts of $\Delta T/\ln t$ for $\Delta T = \ln t$ and where t is offset by ± 10s

Chart 5 shows that, from linear data, a shift in the time axis created S and U curve effects. This raises the question as to whether the typical S and U curves found under experimental conditions could and should be adjusted towards linearity to give reliable thermal conductivity results.

A rationale for an improved assessment of linearity in $\Delta T/\ln t$ is now given, which method will be used to assess the linearity of curves subjected to the axis adjustments. Thermal conductivity values are calculated, using equation (6), from a linear sections of the slope of $\Delta T/\ln t$. Researchers such as Woodside and Messner (1961a, 1961b) and Goodhew and Griffiths (2004) have relied upon visual recognition of this linear section. Other researchers had developed different strategies, unsubstantiated by theory, to establish appropriate time windows for analyses. Davis and Downs (1980) had assessed linearity as when a series of slopes taken from the asymptote over similar multiple times, such as 40s – 160s and 60s – 240s, were roughly equal. Manohar et al (2000) had

worked back progressively from 0s – 1000s, to 10s – 990s, etc. until the slope difference became negligible. Tye et al (2005) looked for the longest time over which thermophysical values remained constant. This latter strategy removes potentially subjective decisions as to whether linearity exists, especially where data points become close at later times because of the logarithmic time scale. Hence, following Tye et al, in this work, a slope analysis has been used to asses linearity with successive slope values plotted over time, usually at 1Hz.

Contemporary computer power allows fast computation of slope linearity over various periods from each datum. Here, 30s slopes have been computed for the slopes in chart 5, giving rise to the curves in Chart 6.

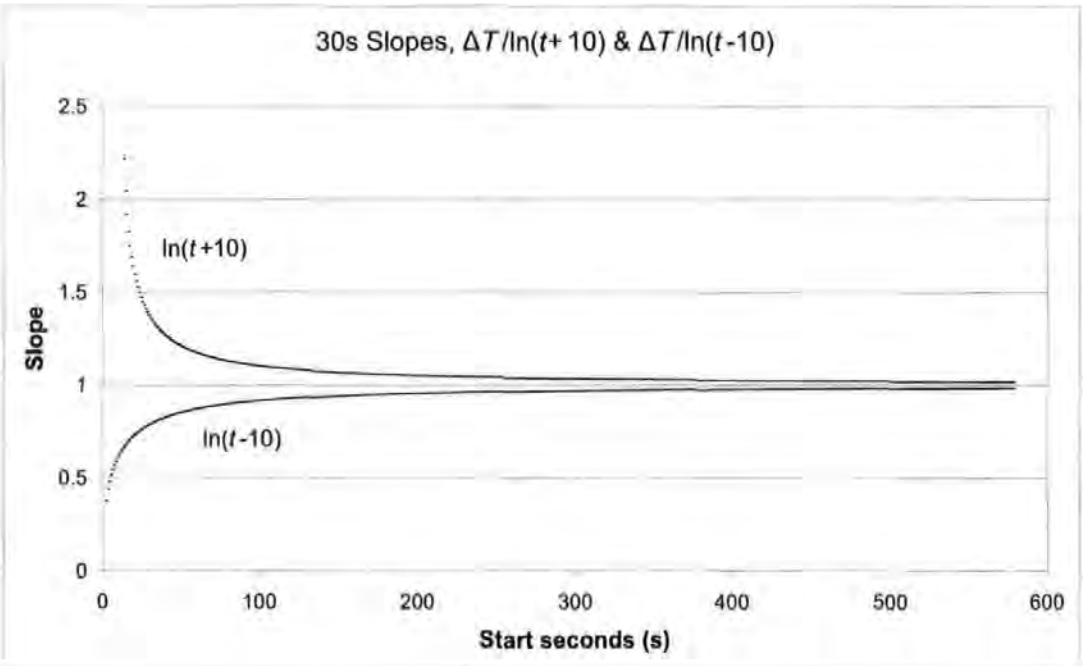

Chart 6: Slopes of $\Delta T/\ln t$ from $\Delta T = \ln t$ where t offset by ± 10s

It can be seen from chart 6, which assesses slope linearity, that a 10s shift in the time axis had a marked effect in the early part of the heating curve, here up to around 120s, and continued to exercise an effect up to 600s, and probably

beyond. These results related to a virtual measurement with a perfectly linear asymptote, whereas probe thermal properties are usually thought to cease to exert significant effects after a shorter time.

The time offset was applied to a real measurement to see if the effect could be used to move an S curve to linearity. A measurement was chosen in phenolic foam, as highly insulating materials tend to produce distinct S curves and, being a reasonably stable material with close pores allowing consistent thermal contact, phenolic foam produces relatively clean data.

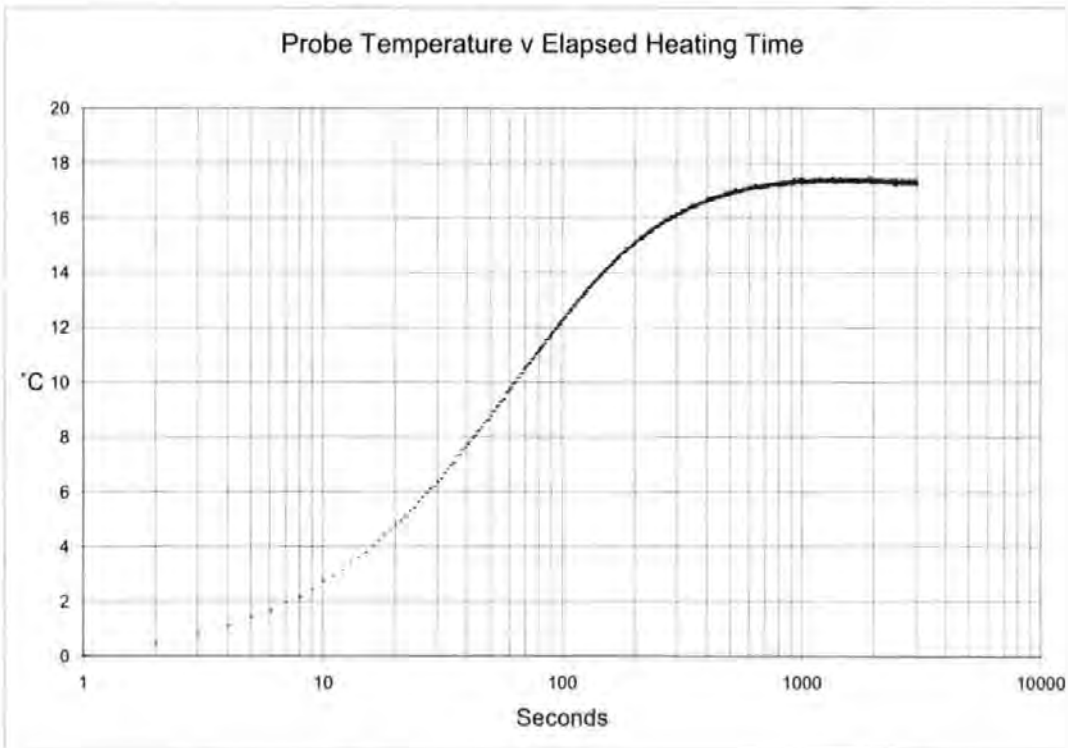

Chart 7: Typical S curve produced by a measurement in phenolic foam

Chart 7 shows a typical profile of $\Delta T/\ln t$ for phenolic foam. A visual interpretation of the curve suggests a linear section exists from about 30s – 150s. This appears as a short horizontal section in the middle plot of chart 8, where thermal conductivity values have been calculated from the slope of chart

7 using equation (6) over successive 100s periods, in a similar method to that used by Hammerschmidt (2003). It is of note that the thermal conductivity result for this linear section is approximately 0.015 $Wm^{-1}K^{-1}$ compared to the published value of around 0.023 $Wm^{-1}K^{-1}$. The chart shows that positive and negative time changes have not moved either of the plots towards consistent thermal conductivity results, rather increasing or decreasing values while retaining a similar rise in values over time.

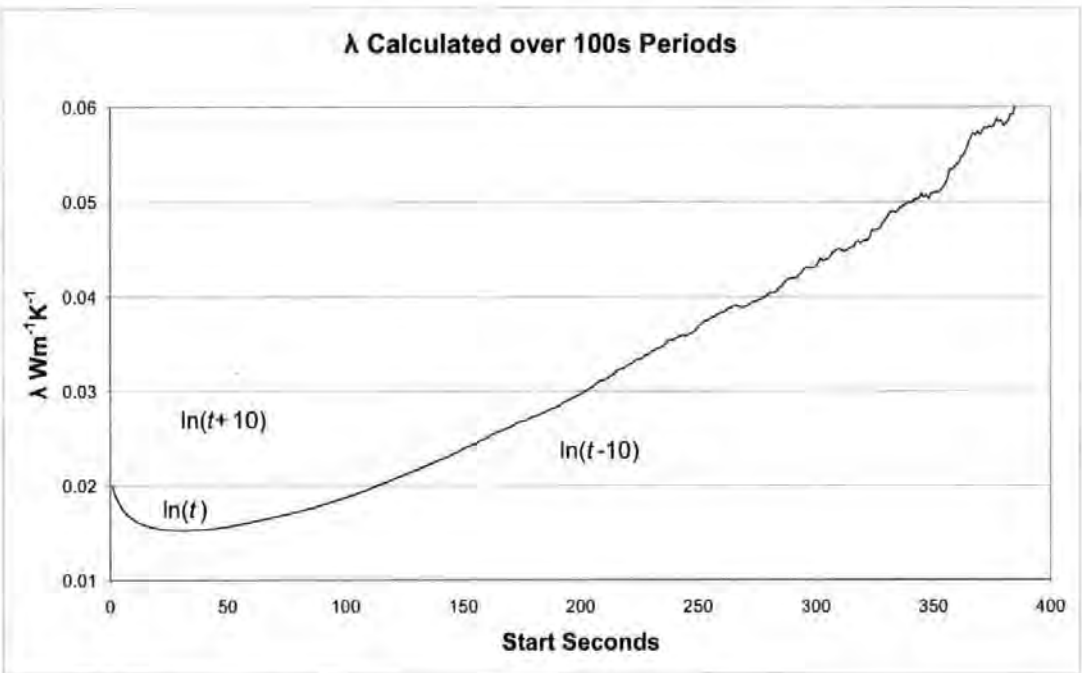

Chart 8: λ for phenolic foam over 100s intervals, *t* offset by ± 10s

The results for phenolic foam suggest that shifts in the time axis may not provide appropriate or sufficient compensation for S or U curves. It may be that some correction for the probe heating time occurs but that this only partly contributes towards the creation of S curves. The effect then remains insignificant in comparison to unknown effects.

Interim conclusion to the assessment of traditional solutions

It was found that Blackwell's equation and the Solver 2.3 solution gave thermal conductivity values consistent with those found by regression analysis and equation (6) over linear sections of $\Delta T/\ln t$.

The evidence from the sensitivity analyses of Blackwell's equation and the Solver solutions, combined with evidence from Buettner (1955), Nix et al (1967), Riseborough (1983), through van Loon et al (1989), to Goodhew (2000) showed that current thermal probe theory and application were incapable of reliably measuring the thermal diffusivity of solid granular materials in practice. It was found that these methods could not reliably distinguish between temperature rise influences from: the sample material volumetric heat capacity; contact resistance between the probe and the sample; and possibly varied thermal resistances arising from the various thermal properties and contact resistances of the probe's components.

Shifts to the time axes, which the literature review had shown to be developed empirically rather than theoretically, were not found, for the materials studied, to improve the availability of results though greater linearity in $\Delta T/\ln t$. It is doubtful whether an appropriate linearity could be achieved in this way, especially where no theoretical basis exists to establish the extent of the adjustment. The time axis adjustment was therefore not further pursued in this project.

An improved method of assessing linearity in $\Delta T/\ln t$ was described, which method was adopted as a standard means to assess the simulated and practical measurements that followed. Chapter 5 now goes on to describe

various measurements taken with thermal probes under controlled environmental conditions in a laboratory.

Chapter 5: Laboratory work

A number of laboratory tests were carried out before taking thermal conductivity and thermal diffusivity measurements of materials in real buildings in situ. The rationale for these has been outlined in chapter 3. The aim of these trials was to examine and assess the effects of various parameters, such as hole size, filler type, power levels, temperature stabilisation periods, etc. on results in practice, and to compare these results with known values, the computer simulations, and the work of previous researchers. Anisotropic effects were studied and thermographic assessments of probe heating patterns were carried out.

Four sets of apparatus were used to take measurements. The earlier work was carried out using a pre-existing device developed by Goodhew and Griffiths (Figure 11). The later work was carried out with a portable device developed by the author for fieldwork, as described in chapter 6. Two commercial instruments, being marketed as thermal conductivity and thermal diffusivity meters, with unknown forms of analysis, were taken on loan and trialled for comparison.

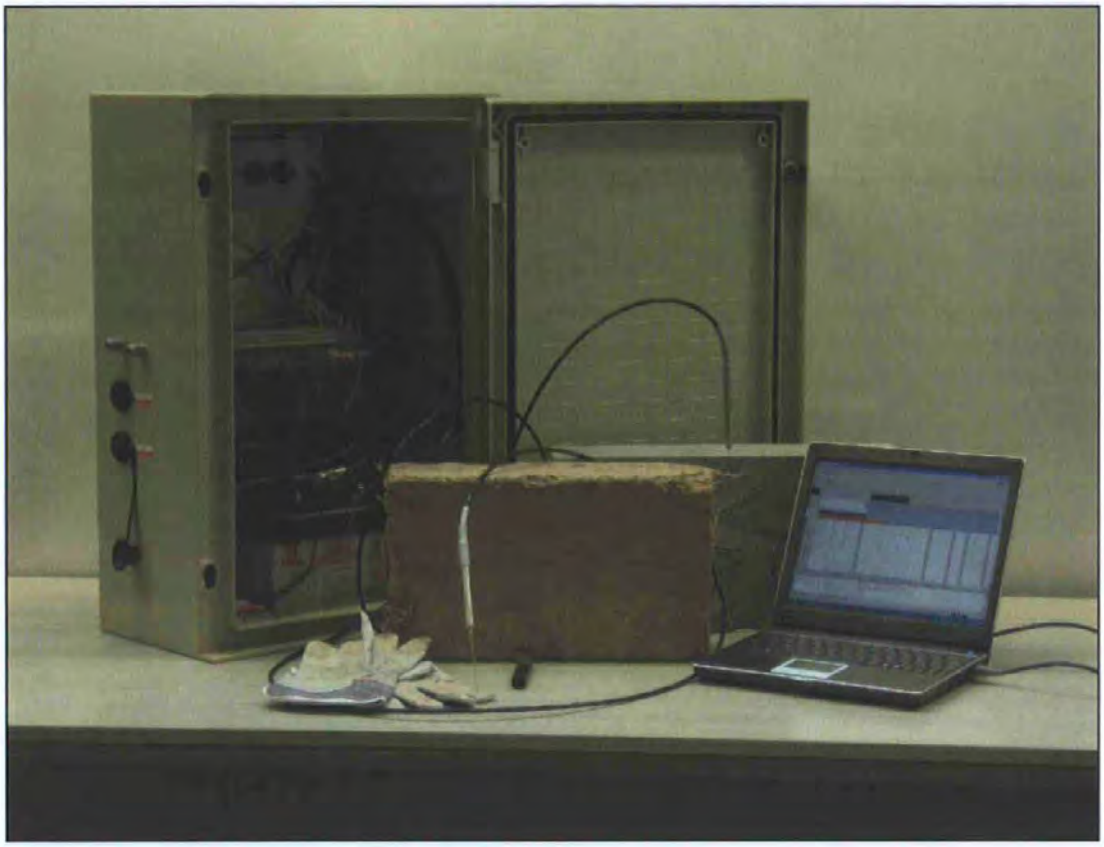

Figure 11: Laboratory based thermal probe apparatus

This chapter starts with a short note describing the method of data storage and handling. An assessment of the outcomes achieved with the commercial probe meters is then given before examining the effects of various experimental parameters, a study of anisotropic materials, and a description of the thermographical work. The penultimate section presents a study of thermal conductivity measurements in materials containing moisture and reports new values for aerated concrete. Interim conclusions from the laboratory work are then given.

A short note on data handling

It was recognised early in this work that a comprehensive data storage and retrieval system would be advantageous as the raw data of measurements

could then be revisited for further analysis at any time. This established a pool of resources against which developments could be assessed. The underlying principle was to record as much surrounding information as could be considered relevant for each measurement, such as power inputs, locations, ambient temperatures, etc.

A computer filing system was developed to hold the raw data, experiment descriptions, analysis routines, results and summaries with each file hyperlinked to a digital experiment log. Files were named with the initials of the operative carrying out the measurement followed by the number of the experimental group followed by a letter denoting the particular run within the experimental group. For example, a measurement carried out by the author would start with initials, 'BP', then the group, e.g. '0010' for the tenth group of measurements, then the run, e.g. 'a' for the first measurement in the group, giving BP-0010a. This can then be followed by further descriptive text, such as an experiment description, e.g. <BP-0010 description.doc> or an analysis template, e.g. <BP-0010a ATv10.xls>. This form of filename is suitable for computer sorting, searching and cross referencing, partly as measurements can automatically be stored in the chronological order in which they were undertaken, disregarding file creation dates. The method also allows identification of the operative should following researchers wish to raise queries concerning the data.

All data were held on a portable hard drive and regularly backed up to two laptop and two desktop machines. The use of a portable hard drive meant that data could be added from any machine, such as a site based laptop, and later analysed at whatever work station was convenient. The experiment log is presented in appendix B.

A simple gauge of repeatability was employed to aid the assessment of results, when assessing the mean values achieved over a number of similar measurements. This can be used to compare measurements in one material with those in another and to compare the current work with that of previous researchers. The method used was the variance coefficient, described by Davis and Downs (1980). Mean values are reported with their standard deviation. The standard deviation is then divided by the mean and the results given as a percentage. Results are then reported as ± x.%.

Measurements with commercial probe meters

This section reports work with two commercially available thermal probe devices and compares results to published values and other values achieved during the project, including those with the TP08.

The first apparatus, which is called for convenience 'loan 1', comprised a single needle probe 60mm long and 1.27mm diameter permanently attached via a cable to a hand held digital meter / display. It had a stated accuracy for thermal conductivity measurements between 0.02 $Wm^{-1}K^{-1}$ and 2.0 $Wm^{-1}K^{-1}$ of 5%. The apparatus was supplied with a certificate of quality assurance showing the results of a calibration measurement in glycerol. Also supplied with the device was a quantity of ArcticSilver5 thermal grease to improve contact between the probe and sample. The instrument was not designed to measure thermal diffusivity.

The method of measurement was to insert the probe into a close fitting hole in the material to be measured, using ArcticSilver5 where necessary, such as in coarse, hard or granular materials. After switching on the probe, an automated

process was instigated whereby there was a 30s delay, described as the period needed for the needle temperature to stabilise with that of the sample, then a 30s heating period followed by a 30s cooling period. The thermal resistance or thermal conductivity result was then displayed.

Material	Loan 1 mean λ $Wm^{-1}K^{-1}$	TP08 mean λ $Wm^{-1}K^{-1}$	Indicative λ - Various sources
Agar (immobilised water)	0.59	0.60	0.60
Aerated concrete, foundation block, ArcticSilver5	0.18	0.21	0.15
Aerated concrete, foundation block, dry	0.05	0.21	0.15
Aerated concrete, insulating block, ArcticSilver5	0.09	0.11	0.11
Aerated concrete, insulating block, dry	0.04	0.12	0.11
Aerated concrete, standard block, ArcticSilver5	0.11	0.20	0.15
Aerated concrete, standard block, dry	0.05	0.20	0.15
Phenolic foam, ArcticSilver5	0.03	0.02	0.02
Phenolic foam, dry	0.03	0.02	0.02
Dupre Vermiculite, dry	0.03	0.03	0.06
Unfired earth and woodshaving brick, ArcticSilver5	0.53	0.81	0.65
Unfired earth and woodshaving brick, dry	0.14	0.80	0.65
Mineral wool insulation, rolled, dry	0.03	0.02	0.04
Oak, across, ArcticSilver5	0.19	0.32	0.16
Oak, across, dry	0.11	0.32	0.16
Oak, along, ArcticSilver5	0.14	0.25	0.15
Portland Stone, ArcticSilver5	1.22	1.45	1.30
PTFE with ArcticSilver5	0.23	0.25	0.25
PTFE, dry	0.19	0.25	0.25
Sheep's wool, dry	0.04	0.03	0.04
Spruce across ArcticSilver5	0.11	0.19	0.13
Spruce, across, dry	0.07	0.19	0.13
Vaseline	0.15	0.16	Not found

Table 2: Thermal conductivity meter results, with TP08 and published values

Table 2 gives the mean thermal conductivity results of a number of measurements each in various materials by the loan 1 apparatus and by the TP08, as well as indicative published values for the same materials, albeit subject to the limitations to published values described in chapter 1.

It is interesting to note in Table 2 that the thermal grease makes a larger difference to the loan 1 results than to the TP08 results, indicating that the effect on $\Delta T/\ln t$ was greater at early times, bearing in mind that the TP08 calculations were based on visually assessed linear asymptotes, usually occurring beyond the 30s window used by the loan 1 device.

The second apparatus, called here 'loan 2', was an improved version of loan 1, now designed to also measure thermal diffusivity and volumetric heat capacity. Accuracy for thermal conductivity measurements was stated to be within 5%, and within 7% for thermal diffusivity and volumetric heat capacity. These stated accuracies were specified only for values within the ranges of:

Thermal conductivity: 0.02 $Wm^{-1}K^{-1}$ to 2.0 $Wm^{-1}K^{-1}$

Thermal diffusivity: 1.0 $x10^{-7}$ $m^{-2}s^{-1}$ to 1.0 $x10^{-6}$ $m^{-2}s^{-1}$ and

Volumetric heat capacity: 0.5 $MJm^{-3}K^{-1}$ to 4.0 $MJm^{-3}K^{-1}$

The device had a choice of probes, either 100mm x 2.4mm or 60mm x 1.27mm single probes for measuring thermal conductivity, and a dual probe, with parallel needles, both 30mm x 1.28mm and 6mm apart, for simultaneously measuring thermal conductivity and thermal diffusivity / volumetric heat capacity. All probes were interchangeable by a cable connection to a hand held digital meter / read out. The device recognised the probe attached and the operational routine of loan 1 was unchanged.

The instrument was supplied pre-calibrated, although the manual indicated that sensor performance could be checked by measurements in two sample materials provided. It was recommended that the single probes be checked in a sample of liquid glycerol and the dual probe in a solid sample of Delrin, an

acetyl resin containing around 25% PTFE (DuPont, 2007). A fixed thermal conductivity value of 0.285 $Wm^{-1}K^{-1}$ at 20 °C was given for the former, whereas the thermal properties of the Delrin were individually marked on the sample. The check was carried out for the loaned device and results were in accordance with the calibration values for thermal conductivity and volumetric heat capacity.

The equipment was first used in a sample of Hemcrete, a concrete made from hemp fibres with a hydraulic lime binder, having a measured density of 365 $kg.m^{-3}$. The 60mm probe was inserted into a 1.5mm predrilled hole using the ArcticSilver5 contact grease. This produced a thermal conductivity value of 0.065 $Wm^{-1}K^{-1}$. The sample was then measured using a TP08 thermal probe with ArcticSilver5. This gave a result in the region of 0.12 $Wm^{-1}K^{-1}$ over a 100s-250s time window, which corresponded well with guarded hot plate measurements of similar samples.

Chart 9 shows the complete TP08 heating curve for a Hemcrete measurement. Chart 10 shows thermal conductivity results to be near linearity from 100s – 350s (the x-axis values being the start times of 100s measurements), indicating a linear section in the chart of $\Delta T/\ln t$. Chart 11 shows that the TP08 measurements over a short period at early times would have given a similar result to that of the loan 2 equipment.

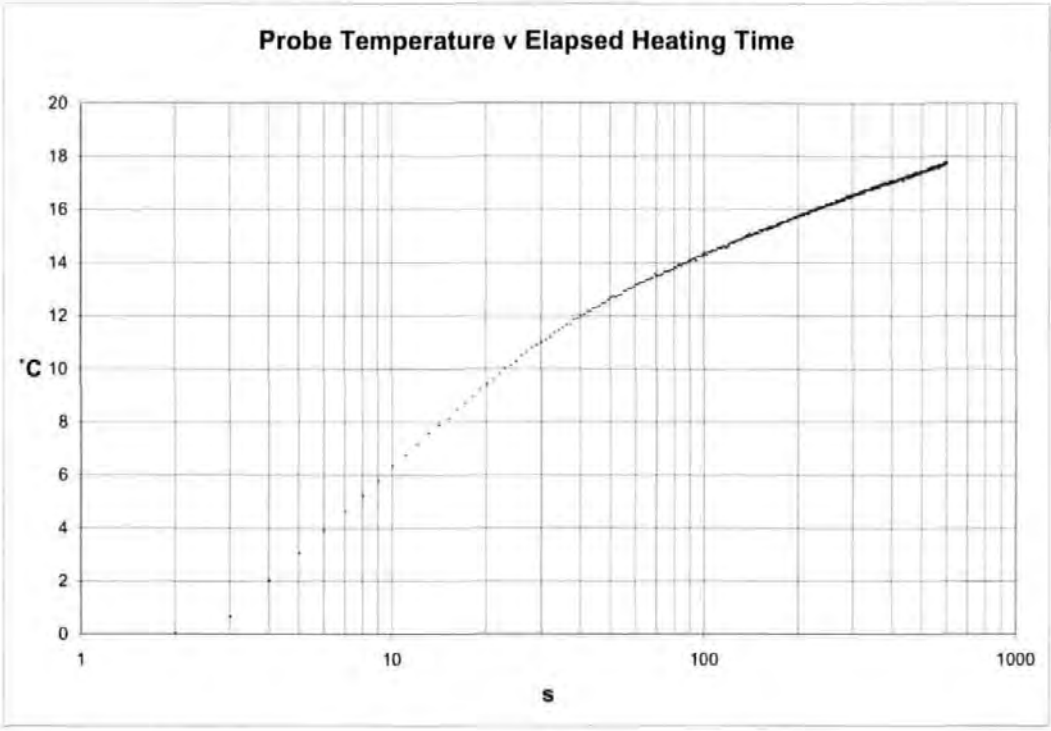

Chart 9: TP08 heating record for a sample of Hemcrete

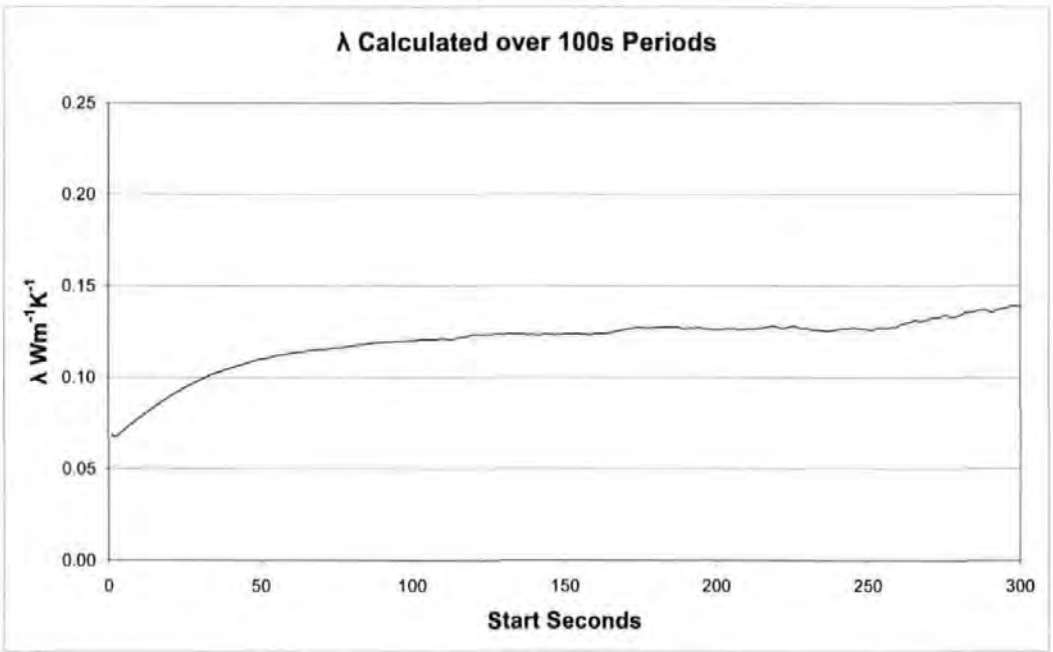

Chart 10: Hemcrete thermal conductivity, 100s time windows

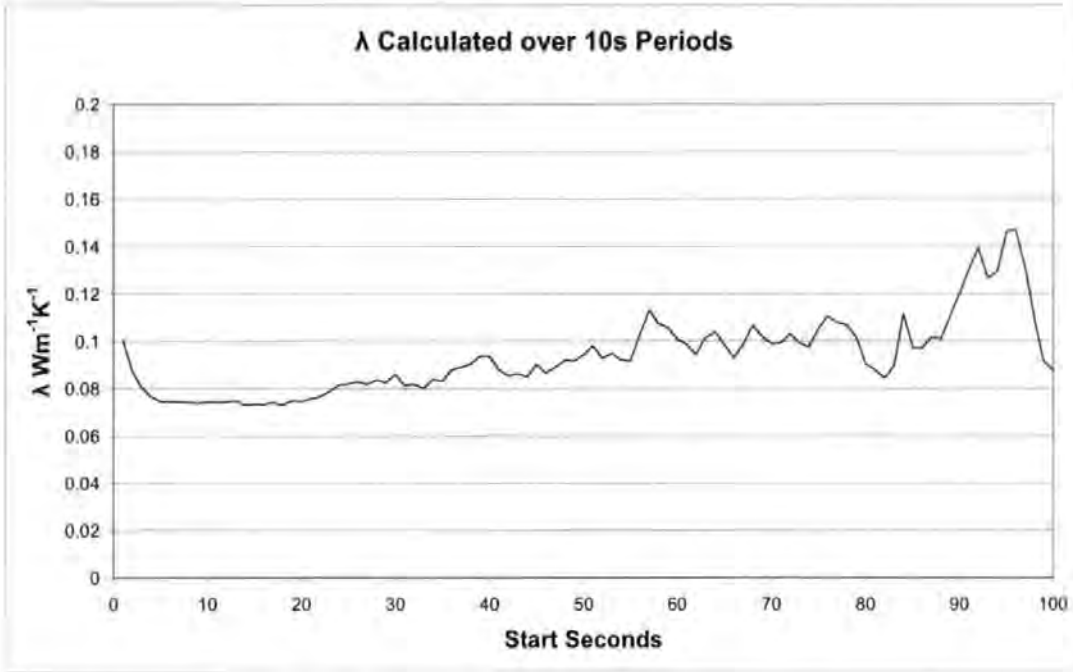

Chart 11: Hemcrete thermal conductivity, 10s time windows

A second series of measurements was carried out in an insulating aerated concrete block, for which the manufacturer's given thermal conductivity value was 0.11 $Wm^{-1}K^{-1}$. The sample was measured, after oven drying, with a TP08 to give 0.113 $Wm^{-1}K^{-1}$ whereas the loan 2, 60mm single probe gave a value 46% higher at 0.165 $Wm^{-1}K^{-1}$. Chart 12 shows the complete TP08 heating curve. Chart 13 shows the thermal conductivity values calculated over 10s periods at 1Hz peaking after 3s at around 0.165 $Wm^{-1}K^{-1}$, the loan 2 single probe value. This similar result for a similar time window indicates the likelihood that a similar analysis was carried out by the sealed unit but without a mechanism to recognise the appropriate time window for the measurement. The loan 2 dual probe gave a value nearer the published value at 0.131 $Wm^{-1}K^{-1}$.

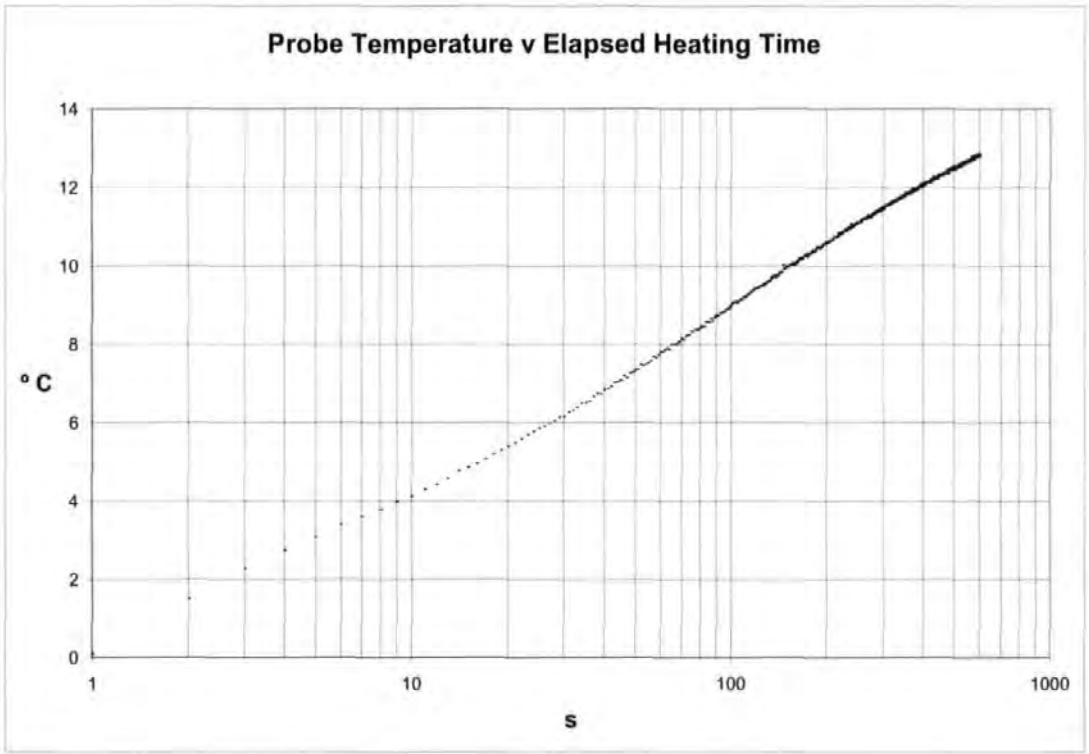

Chart 12: TP08 heating record for an insulating aerated concrete block

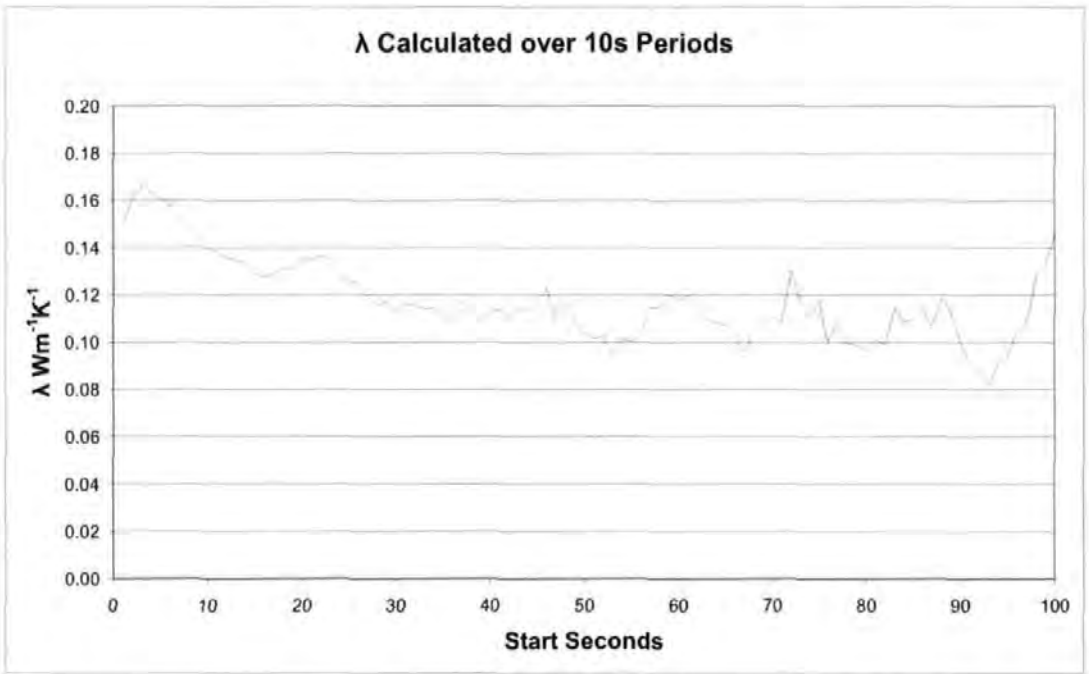

Chart 13: Aerated concrete thermal conductivity, 10s time windows

The dual probe gave a volumetric heat capacity of 0.738 $MJm^{-3}K^{-1}$ for the insulating aerated concrete. The manufacturer gave the specific heat capacity value as 1.05 $kJkg^{-1}K^{-1}$, which was not confirmed by measurement in this project, and the density at 460 kg/m^3, which was confirmed by measurement. This would give a volumetric heat capacity of 0.483 $MJm^{-3}K^{-1}$, 35% less than the dual probe result.

Similar inconsistencies were found with measurements in phenolic foam, the 60mm single probe giving a value of 0.034 $Wm^{-1}K^{-1}$ compared to published values between 0.018 $Wm^{-1}K^{-1}$ and 0.023 $Wm^{-1}K^{-1}$. The dual probe gave a value of 0.041 $Wm^{-1}K^{-1}$ and a volumetric heat capacity of 0.270 $MJm^{-3}K^{-1}$, which was outside the specified range of the instrument. Published values were found to be in the region of 0.044 $MJm^{-3}K^{-1}$ to 0.062 $MJm^{-3}K^{-1}$.

This section has shown an example of error levels and uncertainty in values that can be achieved by automated probe analysis where all parameters may not have been included. If transferred to the energy use of buildings, such errors could have significant economic and environmental connotations, illustrating the critical nature of the current work.

The evidence from the literature review that calibrations in one material may not guarantee valid results in other materials has been borne out by these results. It has been shown that the appropriate time window for analysis is likely to vary dependent on the thermal properties of the material being measured. For the unknown analysis method used by the sealed thermal properties meters and for the analysis routines based on equations (6) and (14), an appropriate time window is shown to be needed for each measurement.

Hole size and fillers

This section discusses appropriate probe and hole sizes, and difficulties encountered in forming appropriate holes. Measurement results for various hole size and filler combinations are shown and examined.

The complexity of probe to sample conductance, as previously described, suggests that better results are likely to be obtained with better contact between probe and sample. Therefore close fitting holes would work better than loose holes. It has been seen that results are affected by probe length to radius ratios, where the greater the length, the less is the chance of errors arising from axial and end losses. The modular nature of many construction materials results in a common standard thickness for walling components, such as brick and block, of 100mm. The Hukseflux TP08 probe is suited to this situation as its stainless steel tubing is robust, it has a length to radius ratio of 120:1, and at 72mm long it is unlikely to be affected by compounded end and boundary losses at the inserted end (see Figure 12). Small diameter holes are required to take advantage of these probe dimensions, which means forming small holes in often hard materials.

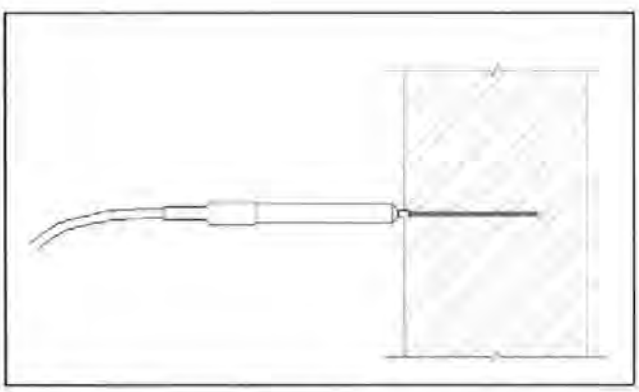

Figure 12: TP08 inserted in a 100mm sample

It was found that 1.5mm high speed steel (HSS) drill bits worked well in softer materials, such as aerated concrete, timber and most earth based materials. However, forming appropriately sized holes in harder materials, such as concrete, fired brick and various stones has proved more difficult. Masonry drill bits with tungsten tipped ends were the preferred option, as they could be used with a slow rotating "steck, dreh, sitz" (SDS) drill to avoid excessive heat generation and associated potential moisture migration. Attempts to have such drill bits made, both by small engineering works and multinational drill bit manufacturers, were not successful. 3mm was the smallest diameter procured during the project for drills of sufficient length. These were of bespoke manufacture, supplied by ADP Diamex. The bits blunted easily and it was not possible to penetrate harder materials, such as granite or Plymouth limestone. The implications of different hole diameters were assessed by carrying out measurements in aerated concrete using various hole sizes.

Four holes were formed in a lightweight insulating aerated concrete block of dimensions 250mm x 215mm x 440mm with a density of 496 $kg.m^{-3}$. The block, with a manufacturer's given thermal conductivity value of 0.15 $Wm^{-1}K^{-1}$, had been oven dried and left in a dry room for three months. The relative humidity on the day of the measurements was in the region of 59% at 17°C. Holes were formed at a minimum of 75mm from any edge or other probe. The drill bits used were: 5mm; 3mm; 2mm; and 1.5mm respectively. Six measurement runs were carried out at each hole. Three were at low, medium and then high power, with probes simply placed in the holes. Three were at low, medium and high power with probes placed in the holes surrounded by ArcticSilver5 (AS5) high thermal conductivity paste as a contact medium and hole filler. Power supplied to the

probes ranged from 0.9 Wm^{-1} to 6.5 Wm^{-1}, with corresponding temperature rises from 6°C to 60°C.

A comparison of charts 14 and 15 shows that the effects of power levels and contact paste were minimal in the 1.5mm hole compared to the 3mm hole, especially at early times. This was also the case when compared to the 2mm and 5mm holes. It is of note that both sets of data show an unexplained rise in values over time.

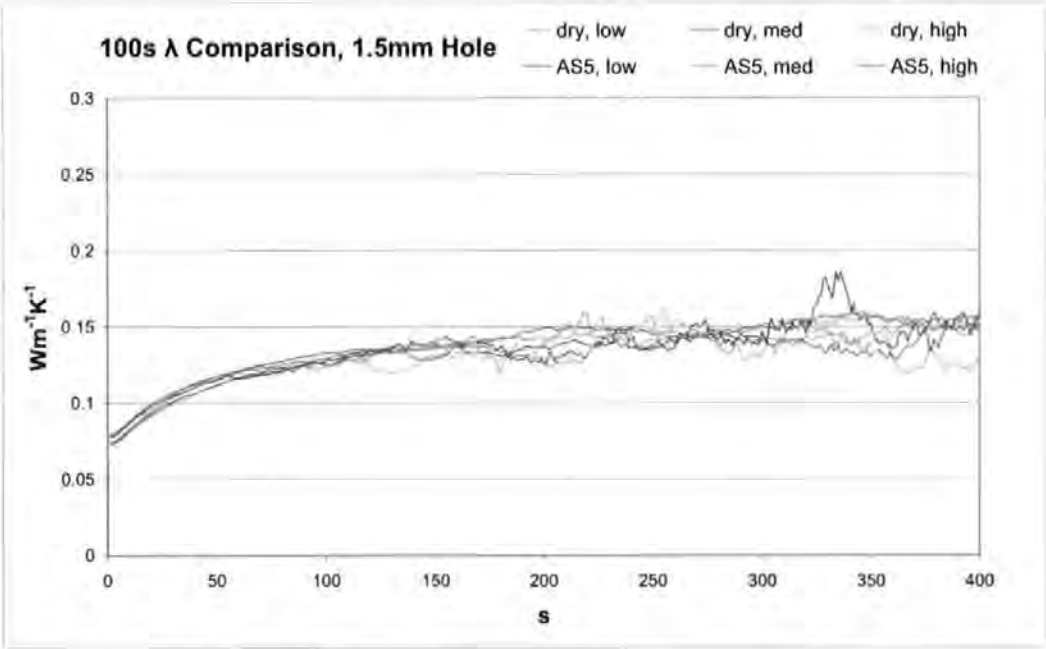

Chart 14: Thermal conductivity results from a 1.5mm hole, aerated concrete

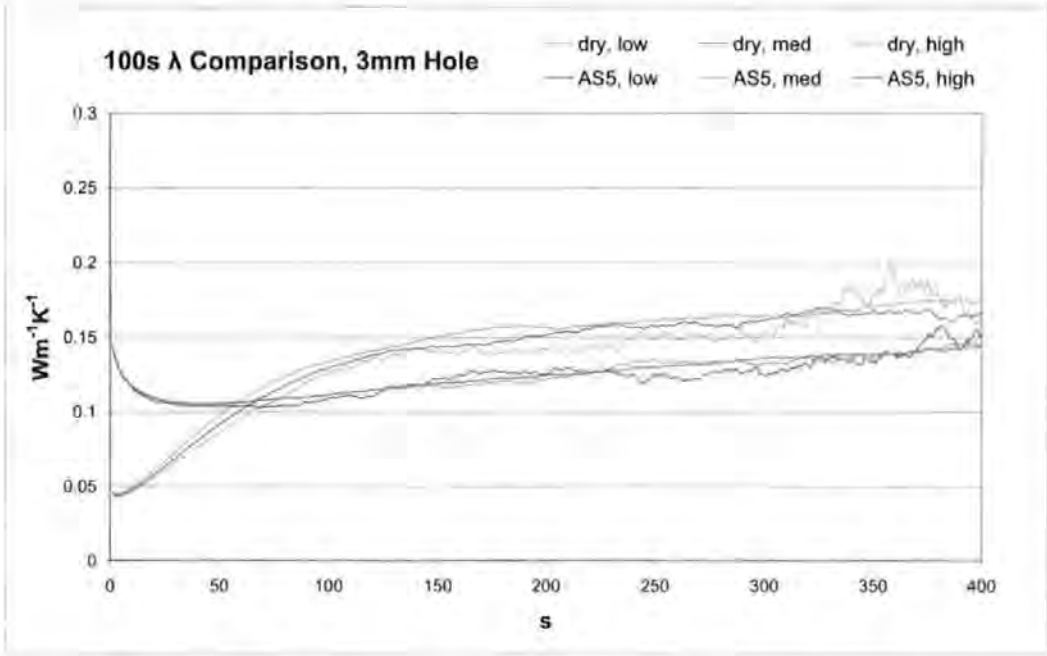

Chart 15: Thermal conductivity results from a 3mm hole, aerated concrete

Charts 16 and 17 show the temperature rises and thermal conductivity results for measurements at the same power in aerated concrete with a 1.5mm hole. It can be seen that the temperature rise (chart 16) is higher for the measurement taken without filler, as a result of poor physical and, therefore, thermal contact. However, the rate of temperature rise after the initial heating period is similar, as can be seen from the similarity of the thermal conductivity results (chart 17) obtained from these slopes using equation (6). This shows that contact resistance has, in this case of a close fitting hole, no significant effect on thermal conductivity measurements. It also illustrates the difficulty in obtaining thermal diffusivity results from the thermal probe technique, where the solution relies upon the extent that contact resistance, and possibly other factors such as internal probe resistance, affect the ordinal intercept of $\Delta T/\ln t$.

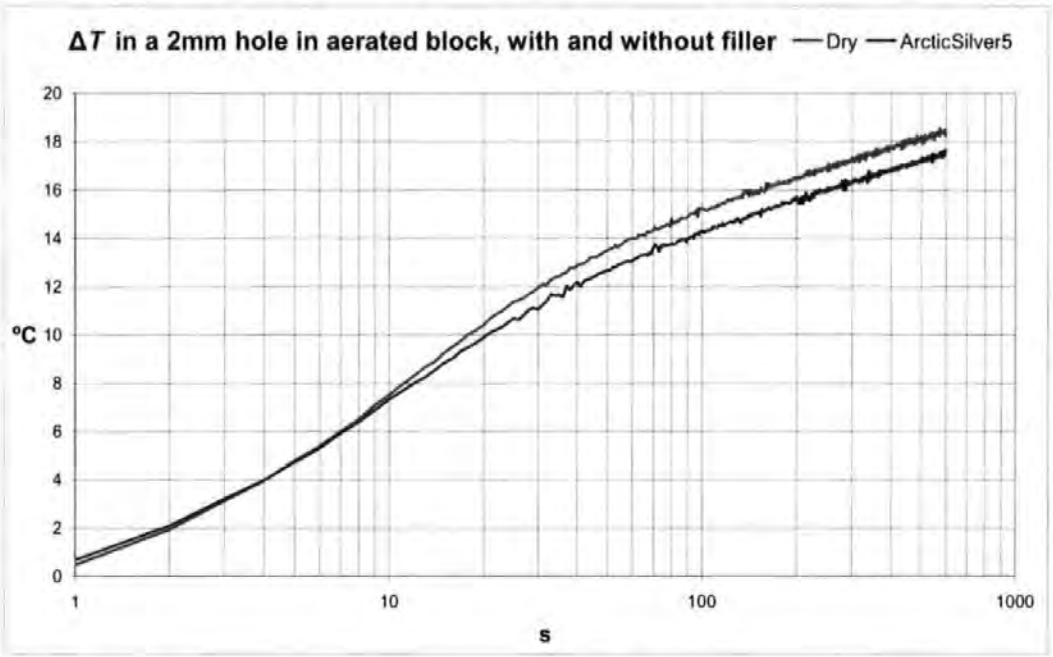

Chart 16: Δ*T*/ln*t* for a 1.5mm hole in aerated concrete, with and without filler

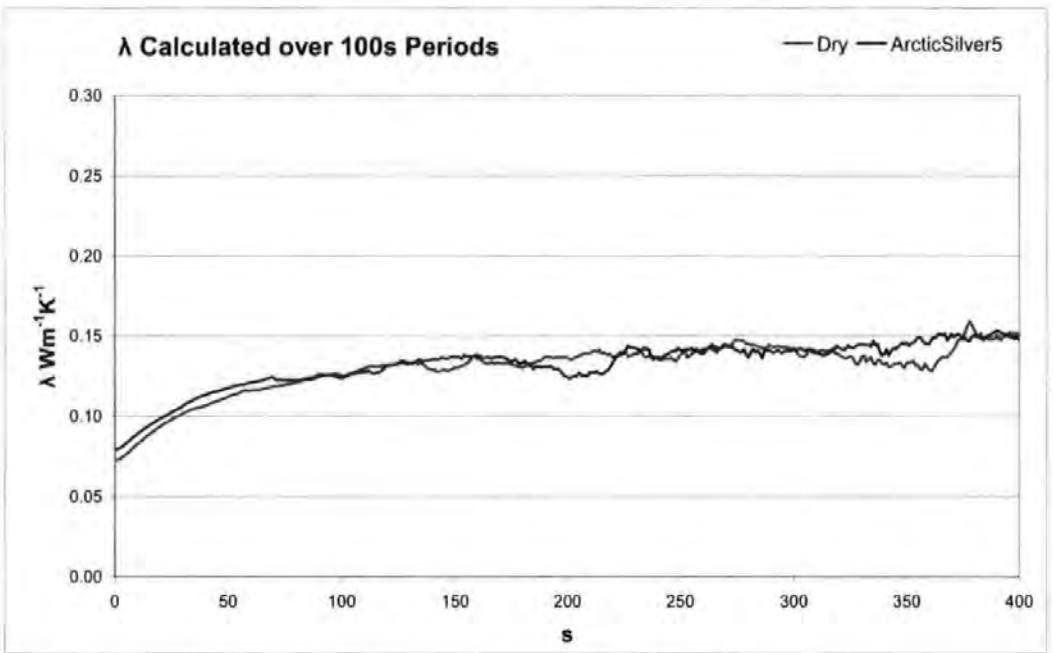

Chart 17: Thermal conductivity results for aerated concrete, with and without filler

This section has shown that smaller measurement holes allow greater confidence in results, hence, for the project, they were made as small as

practicably possible, using a 1.5mm HSS bit in softer materials that needed pre-drilling, a 2mm HSS in semi-hard materials such as lime mortar and a 3mm masonry bit in harder materials such as stone and concrete. Measurements early in the project were carried out dry or with a petroleum jelly filler. Following the good agreement found using ArcticSilver5 as a filler and contact medium, this was used for measurements later in the project.

Temperature stabilisation

Previous researchers, such as D'Eustachio and Schreiner (1952), and Goodhew and Griffiths (2004), have suggested periods from 6 up to 24 hours were required to ensure thermal equilibrium between a sample and probe following insertion, whereas instructions provided with the loan 1 and 2 devices stated that a 30 second period was used to achieve temperature equilibrium. Drury (1988) suggested that ten times the heating period was required between measurements to ensure equilibrium had been reached again, following a heating cycle. These times would be critical to a site based procedure where extended periods of thermal stability may not be available and where instrumentation could be subjected to incidental damage or disturbance if left unattended for long periods.

A number of assessments have been made of the temperature stabilisation period. Chart 18 shows the effect of removing a probe from a position of thermal equilibrium in a stable sample, a large aerated concrete block in an unheated internal room, and then heating the probe, both base and needle, and reinserting it. Thermal equilibrium is seen to be re-established after around 500 seconds. Chart 19 shows the temperature data for 500s – 700s after reinsertion

and its trend. The slope is slightly negative, whether as the probe continues to cool slightly or a as a result of a negative temperature drift in the sample. The trendline shows a temperature difference over 200s of 0.02°C, which compares well to the ASTM (ASTM Committee D20, 2005) recommended allowable deviation of ± 0.1°C over a period of 120 seconds.

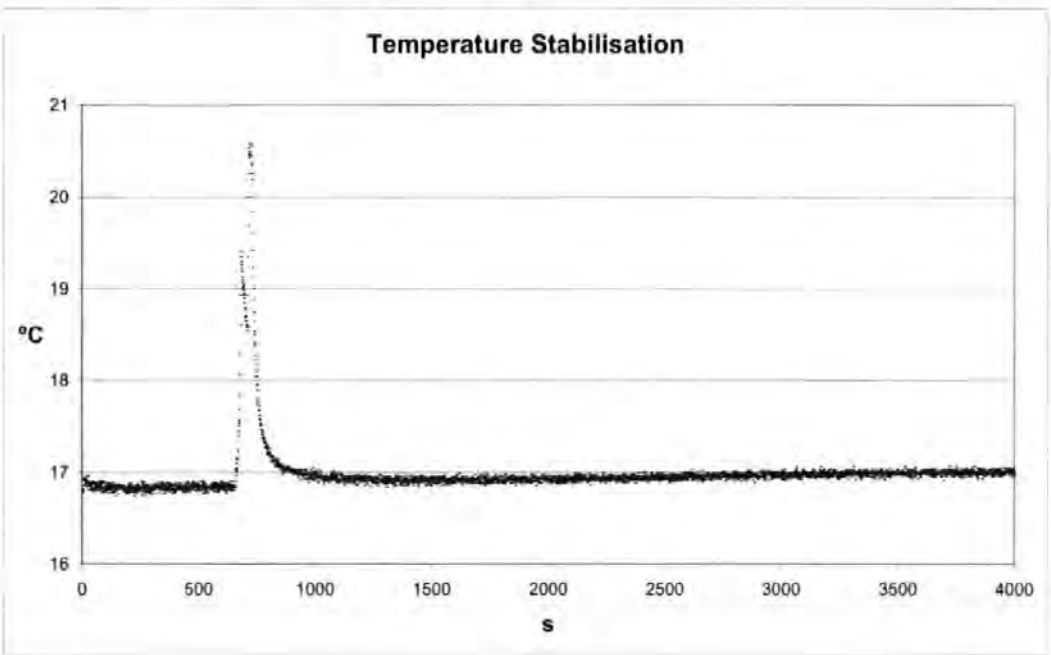

Chart 18: Temperature stabilisation following probe insertion

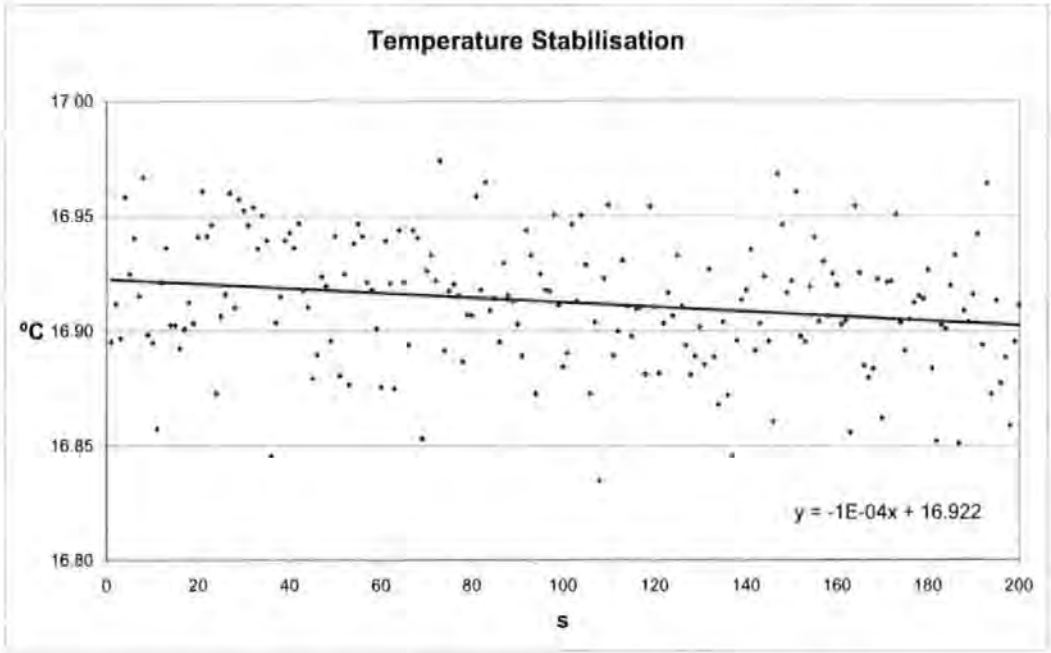

Chart 19: Temperature equilibrium from 500s after probe insertion

The surface area of the needle potentially in contact with the sample is 240 times greater than the cross sectional area, which forms the contact with the base and external temperature influences upon it. As the rate of heat conduction is a product of heat flux and area, this allowed thermal equilibrium in aerated concrete to be achieved within recommended parameters after around eight minutes. This time would be dependent on the initial temperature difference and the relative thermal properties of the sample, probe and cables. As these values for the sample are initially unknown, a live needle temperature display was set up on a computer attached to the field kit, described later, so that temperature stabilisation within acceptable parameters could be assessed by progressive visual inspection.

Temperature stabilisation following a heating period is more complex than that following probe insertion, being dependent on the heat stored within the sample rather than the temperature and heat capacity of the probe. Chart 20 shows the

temperature stabilisation before and after a heating cycle in aerated concrete, along with temperatures from two thermocouples measuring air temperature in the same location. The chart suggests that the material still retained some of the heat input an hour after the heating cycle, although chart 21 shows that, after 35 minutes, the average temperature change was less than 0.02°C over a 200s period. Multiple measurements with an hour between cycles have not shown any trend that could be linked to a build up of residual heat. The practice adopted was therefore to leave at least an hour between measurements and to assess the temperature gradient from the computer display, which assessments were then rechecked during post measurement data analyses.

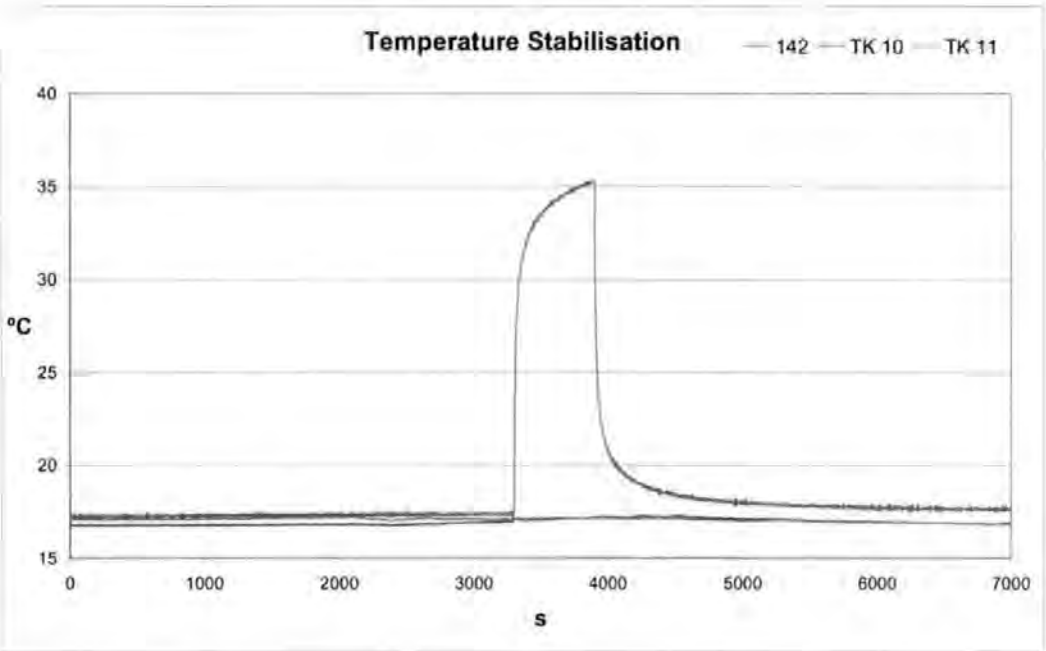

Chart 20: Temperature stabilisation following a heating cycle

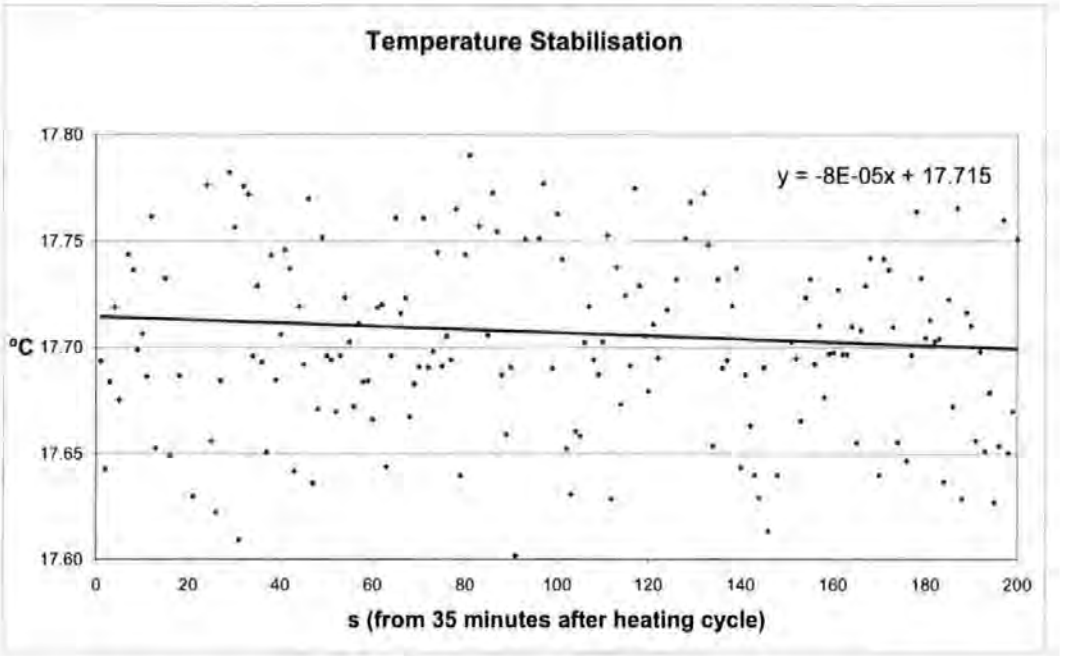

Chart 21: Temperature equilibrium in aerated concrete after a heating cycle

Measurements in anisotropic materials

Anisotropy and thermal probe measurement outcomes were studied using a range of timbers, including oak, spruce, larch, chestnut and Douglas fir. Blocks of timber typically exceeded 150mm in any one dimension, to avoid potential boundary effects. Probes were inserted at positions along and across the grain in 1.5mm or 2mm holes with petroleum jelly used as a filler. Up to 15 measurements were taken at each position.

Table 3 shows the thermal conductivity results achieved, using a regression analysis and equation (6) over visually assessed linear asymptotes of $\Delta T/\ln t$. Also shown are the variance coefficients, and the ratio of difference in thermal conductivity found between probes inserted across the grain to probes inserted along the grain. This ratio indicates that the insulation properties of timber are improved perpendicular to the grain.

Material (probe direction)	Mean Measured λ	Variance Coefficient	Difference ratio
Spruce (across)	0.194	2.17%	1.54
Spruce (along)	0.126	1.84%	
Oak (across)	0.349	1.68%	1.38
Oak (along)	0.253	2.33%	
Chestnut (across)	0.278	3.84%	1.45
Chestnut (along)	0.192	2.04%	
Larch (across)	0.201	2.71%	1.45
Larch (along)	0.139	1.85%	
Douglas Fir (across)	0.181	1.71%	1.68
Douglas Fir (along)	0.108	0.40%	

Table 3: Thermal conductivity results along and across the grain of various timbers

Chart 22 shows the distinctive difference between thermal conductivity outcomes for two measurements in a sample of oak, along and across the grain.

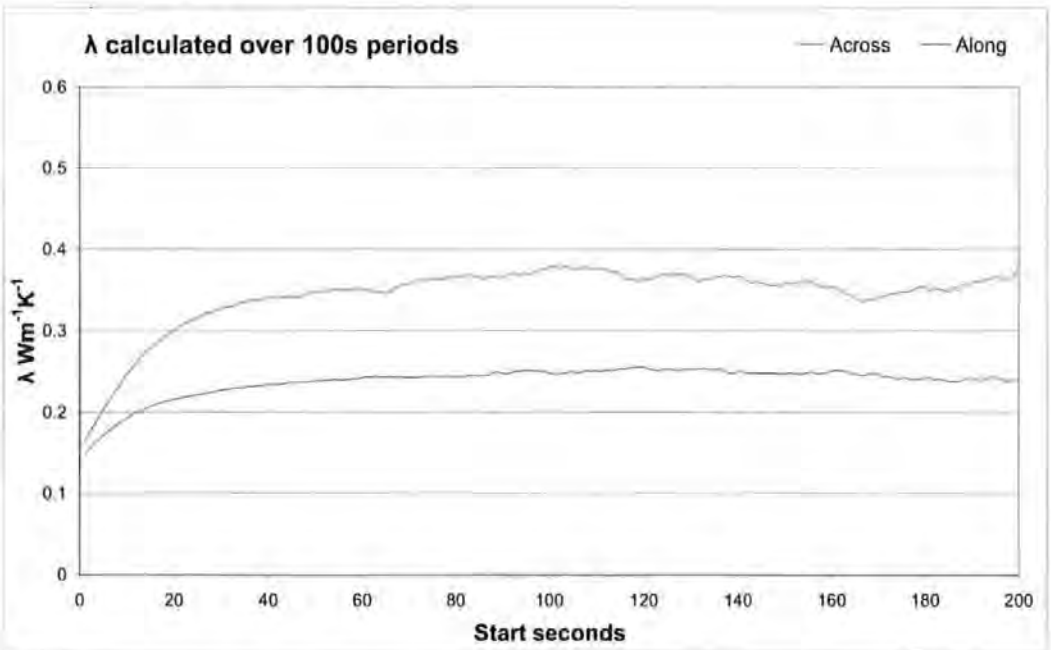

Chart 22: Thermal conductivity, oak, measured across and along the grain

Steinhagen (1977), in a literature review, had given a greater difference between tangential and longitudinal thermal conductivities in timbers, from 1.5:1 for larch with a 30% moisture content at 20°C, to 2.75:1 for red oak at 6% - 15% moisture content and at 30°C. The radial form of measurement undertaken by the thermal probe precludes it from taking purely one directional measurements. This may account for the reduced difference, although timber samples vary and, without alternative standard methods of measurement having been carried out on the current samples, it is not possible to compare the values achieved with confidence. It is of note that authors such as Szokolay (2004) and McMullan (1992) give single values, one for softwood and one for hardwood. The form of measurement most appropriate to the energy efficiency of building envelopes containing timber components has not been assessed in the current project. It would be an interesting subject for future work.

The Solver solution for thermal diffusivity was attempted with the timber samples under the hypothesis that, although thermal conductivity varied with direction, volumetric heat capacity should not. Measurements with varied thermal conductivity in the same anisotropic sample should give varied values for thermal diffusivity and similar values for volumetric heat capacity. Such an outcome was not discernable.

Through this study of anisotropic timbers, the thermal probe has shown itself to be capable of discerning variations in thermal conductivity arising from grain direction. It is also of note that, as can be seen from the relatively constant thermal conductivity results over time after the initial period, in chart 22, that the inhomogeneity of oak did not give rise to excessive S curves. This can also be seen in chart 23, the $\Delta T/\ln t$ plot for a measurement in oak along the grain.

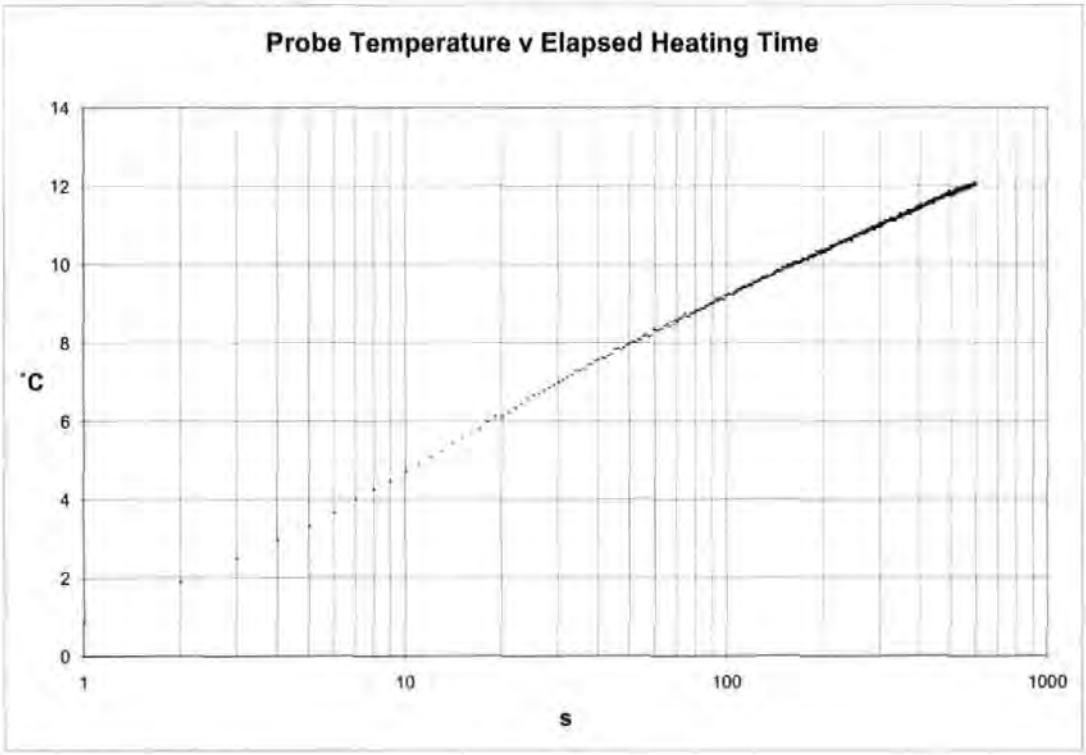

Chart 23: $\Delta T/\ln t$ plot for a measurement in oak along the grain

Power level assessment

Various factors have a bearing on choice of power levels in thermal probe measurements. It may be deduced from consideration of data scatter related to instrumentation, that where scatter is of a fixed magnitude, for instance in the region of up to ± 0.05°C for any single temperature measurement, its extent as a proportion of overall temperature rise would reduce as the rise increases. Thus, greater power levels should reduce error levels and uncertainty in regression analyses of the slope $\Delta T/\ln t$. Higher temperature rises, however, may be limited by the nature of the equipment, such as in preventing heater failure or preserving battery power. Higher temperature rises may also cause moisture migration and it is open to question as to whether they may cause increased axial and end loss errors.

Assael et al (2002) considered that higher power inputs would reduce contact resistance. Davis and Downs (1980) had found increasing power resulted in higher thermal conductivity outcome values. Tye et al (2005) suggested power levels were potentially significant to results.

Chart 14, in the earlier section entitled 'hole size and fillers', showed insignificant effects on thermal conductivity outcomes from altered power levels in a sample of aerated concrete. This was with a 1.2mm diameter Hukseflux TP08 probe in a 1.5mm hole with and without a contact filler. Further investigations were carried out by assessing measurements in samples of PTFE and phenolic foam, where the temperature rise differences in a material of lower thermal conductivity would be greater. Computer simulations at varied power inputs were also assessed.

Chart 24 shows thermal conductivity results for three power levels in a sample block of PTFE. The temperature rises over 600s and associated powers were:

low:	2.8°C	0.99 Wm^{-1};
Med:	9.7°C	3.39 Wm^{-1};
High:	18.82°C	6.61 Wm^{-1}

No significant difference in thermal conductivity outcomes was discernable between the measurements, although increased scatter can be seen in the results at the lower power.

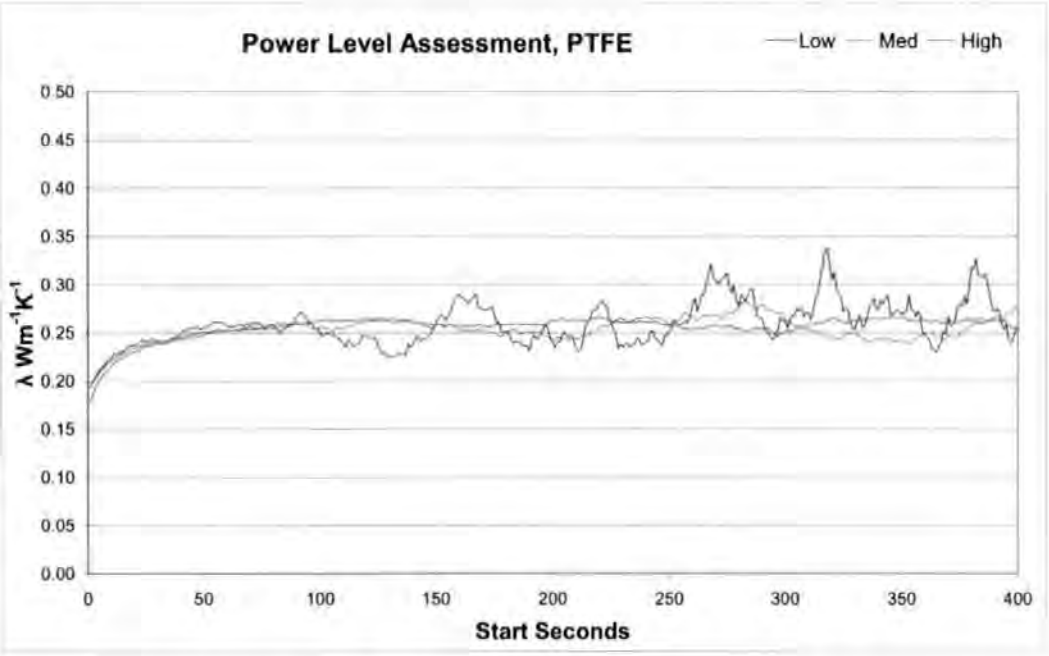

Chart 24: Thermal conductivity, PTFE at three power levels, 100s windows

Chart 25 shows thermal conductivity results for two power levels in a sample of phenolic foam. The sample was made up of three 32mm thick slabs, 150mm square with the probe pushed into the centre of the central slab. The published value for this material is in the region of 0.023 $Wm^{-1}K^{-1}$. The typical upward slope of the thermal conductivity results, which has been found in materials of lower thermal conductivity, is again illustrated, therefore the chart can not be relied upon to give representative values for thermal conductivity. However, it can be seen from the results that they are higher for the higher power input, as reported by Davis and Downs (1980).

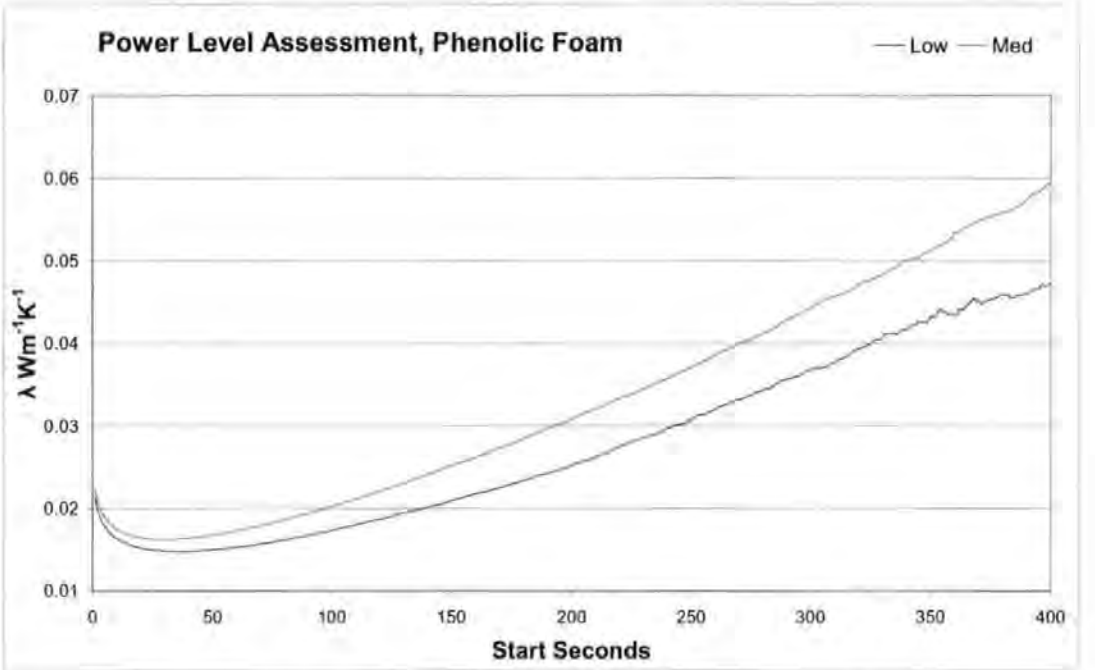

Chart 25: Thermal conductivity, phenolic foam at two power levels, 100s windows

Charts 26 and 27 show temperature rise, $\Delta T/\ln t$, and thermal conductivity results, respectively, for three TP08 measurements made in aerated concrete with 1.5mm holes and ArcticSilver5 contact filler at three power levels. These were: low, 0.90 Wm^{-1}; medium, 3.10 Wm^{-1}; and high, 6.06 Wm^{-1}. It can be seen that the different power levels did not produce significant differences in thermal conductivity results. It may be noted that all the results rose over time, albeit to a lesser extent than shown with phenolic foam. An analysis between 100s and 500s showed that the rises for thermal conductivity results at each power were: $8.03 \times 10^{-5}(x)$ at low power; $6.90 \times 10^{-5}(x)$ at medium power; and $7.87 \times 10^{-5}(x)$ at the higher power. The rises were similar at all three power levels and the analysis showed no significant difference, or trend, that could be linked to the difference in power levels.

It must be emphasised that the rises in thermal conductivity results are indicative of the measurement method rather than an actual rise in thermal conductivity during the measurement. Changes in thermal conductivity would not be expected with the small temperature rises involved. Had thermal conductivity increased with temperature rise, the increase would have been significantly greater for the higher power measurement, as the temperature rise was 6.58 times greater than that for the lower one.

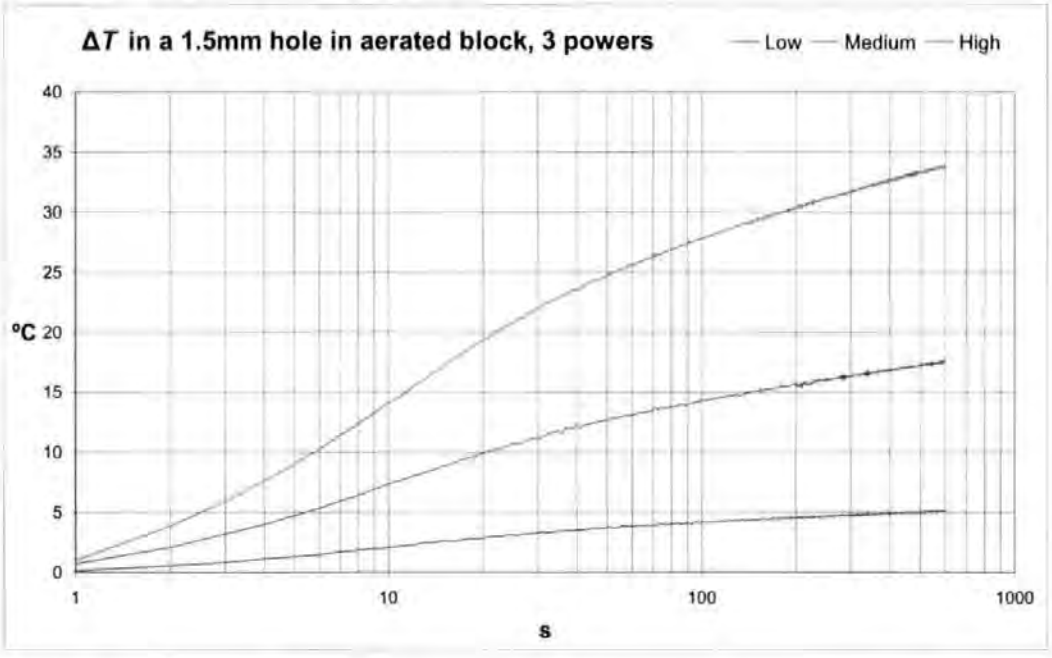

Chart 26: Δ*T*/ln*t* plots for measurements in aerated concrete at three power levels

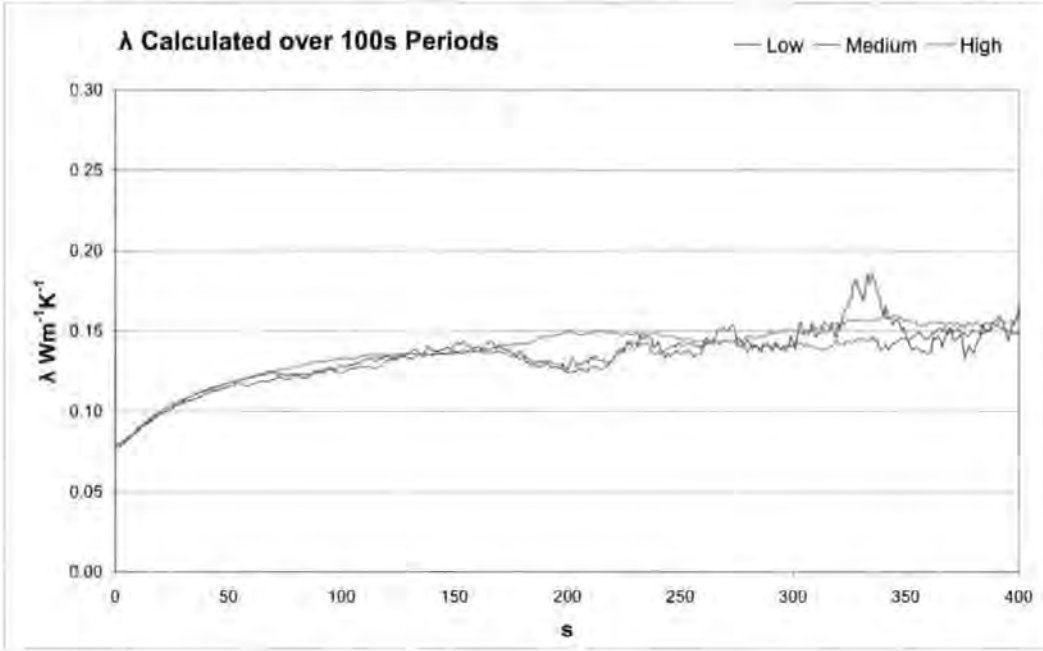

Chart 27: Thermal conductivity results for aerated concrete at three power levels

It has been shown that it is not yet possible to measure contact resistance with appropriate accuracy, although increased contact resistance to a sample has been shown to lead to higher temperature rises in $\Delta T/\ln t$. The effects of power levels on contact resistance were investigated further using the three aerated concrete measurements reported above. A spreadsheet was developed and added to the analysis workbooks containing the Solver solutions, and linked to the data sheet. The spreadsheet was based on equation (34) where Blackwell's equation had been rearranged to make thermal diffusivity the subject.

The thermal conductivity of the sample was first calculated using equation (6) over a time window assessed to give near constant values over time. This value was entered into equation (34) and MS Goalseek used to find the value of H that would produce the value of α that would give the manufacturer's value for volumetric heat capacity. The calculation was carried out at each data point, at

1 Hz, within the time window used, and a variation coefficient produced for the average of the results achieved over this period. Table 4 shows the results for the *H* values achieved, along with the time window chosen, and the variance coefficients for the thermal conductivity and volumetric heat capacity results upon which they were based.

Power level (overall temperature rise at end of time window)	Time window (s)	*H* ($Wm^{-2}K^{-1}$)	λ Variance Coefficient (%)	VHC Variance Coefficient (%)
Low (4.81°C):	100 – 300	141	2.99	6.67
Medium (16.32°C):	100 – 300	144	1.76	3.97
High (31.67°C):	100 – 300	138	0.87	1.92

Table 4: Results for *H* at varying power inputs with aerated concrete

Table 4 shows that no significant change in *H*, which is dependent to an unknown extent on contact resistance, occurred with the different power levels and temperature rises used. As neither results in PTFE, phenolic foam or aerated concrete showed a connection between power levels and contact resistance, the observation of Assael et al (2002), that contact resistance decreased with higher power inputs, could not be substantiated by this work. The findings of Davis and Downs (1980), that increased power inputs led to higher thermal conductivity values, was found with the measurement of phenolic foam but not with the samples of PTFE and aerated concrete. This phenomenon is related to the work discussed in the next section, when assessing boundary conditions. Of note in table 4 is the reduction in variance coefficients at higher power levels, as expected from data scatter reduced in proportion to the level of temperature rise.

Figure 13 shows 100s time window, thermal conductivity results from Voltra simulations, as described in Appendix A, for theoretical materials with power inputs at 3 Wm^{-1} and 30 Wm^{-1}, with thermal conductivity inputs of 2.0 $Wm^{-1}K^{-1}$, with varied volumetric heat capacity. The input ρC values were, left to right, top to bottom: 100; 1,000; 2,000; 4,000; 6,000; and 60,000 $kJm^{-3}K^{-1}$. While showing the now expected and unexplained variations in output for thermal conductivity values, it is interesting to note that power level effects were not seen with the lower and higher ρC inputs. However, higher thermal conductivity results were achieved at higher power inputs in the mid range of ρC values used.

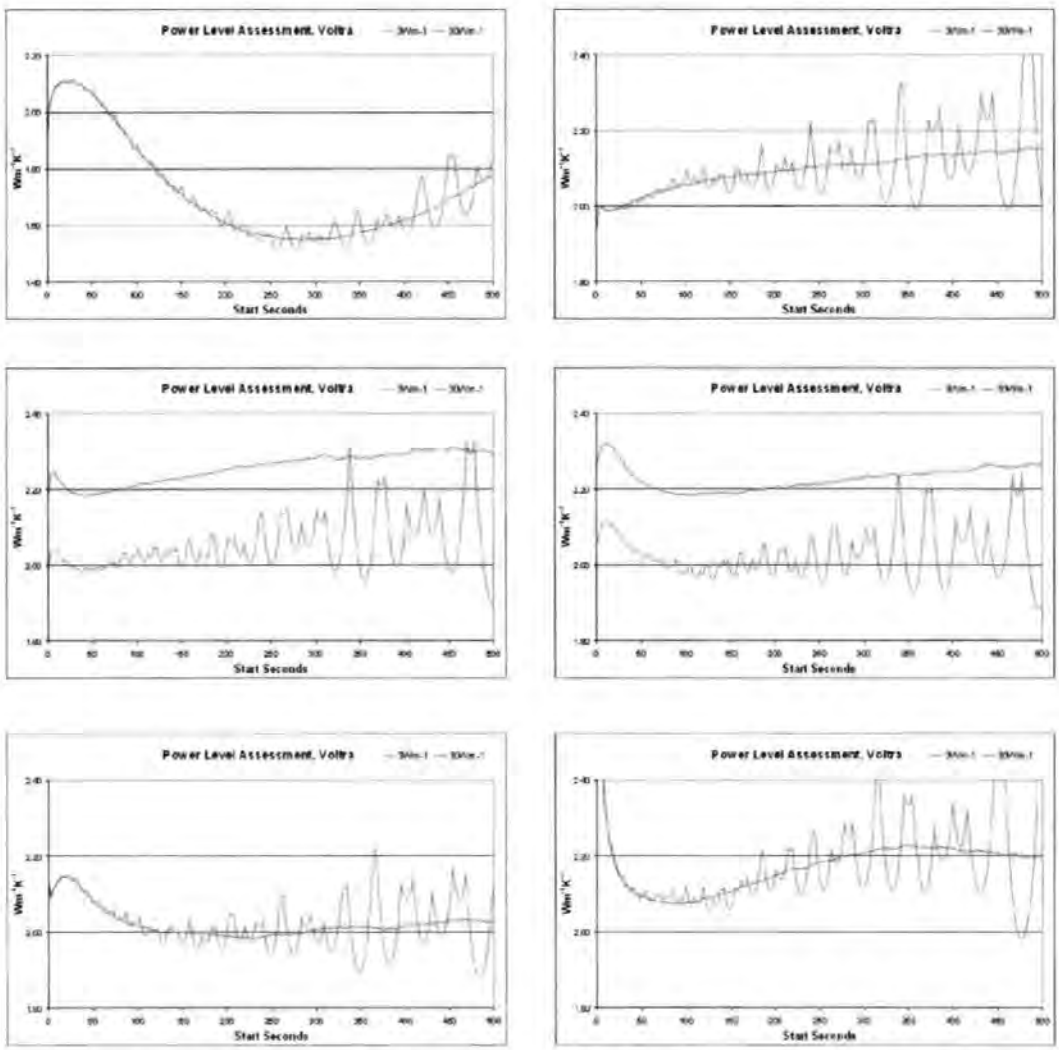

Figure 13: Voltra output λ from: 2.0 $Wm^{-1}K^{-1}$, varied ρC, at two powers

No theoretical or practical reason is apparent for the variation in the effects of the power inputs.

It is of note that the lower temperature rises with lower power inputs, typically between 0.8°C and 2.5°C for the Voltra set of measurements, produced significantly more scatter in results than the rises at the higher power, typically between 8°C and 12°C at 500s. The same effect has been seen in real materials, including the example of agar immobilised water given below.

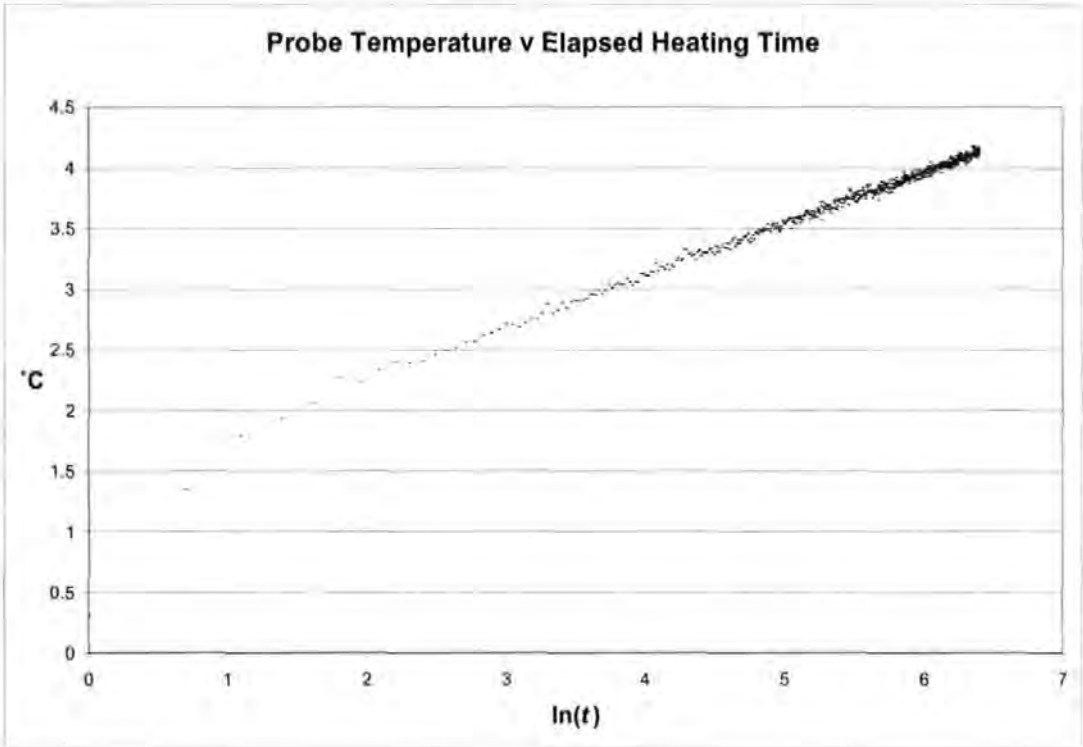

Chart 28: $\Delta T/\ln t$ for 600s measurement in agar immobilised water

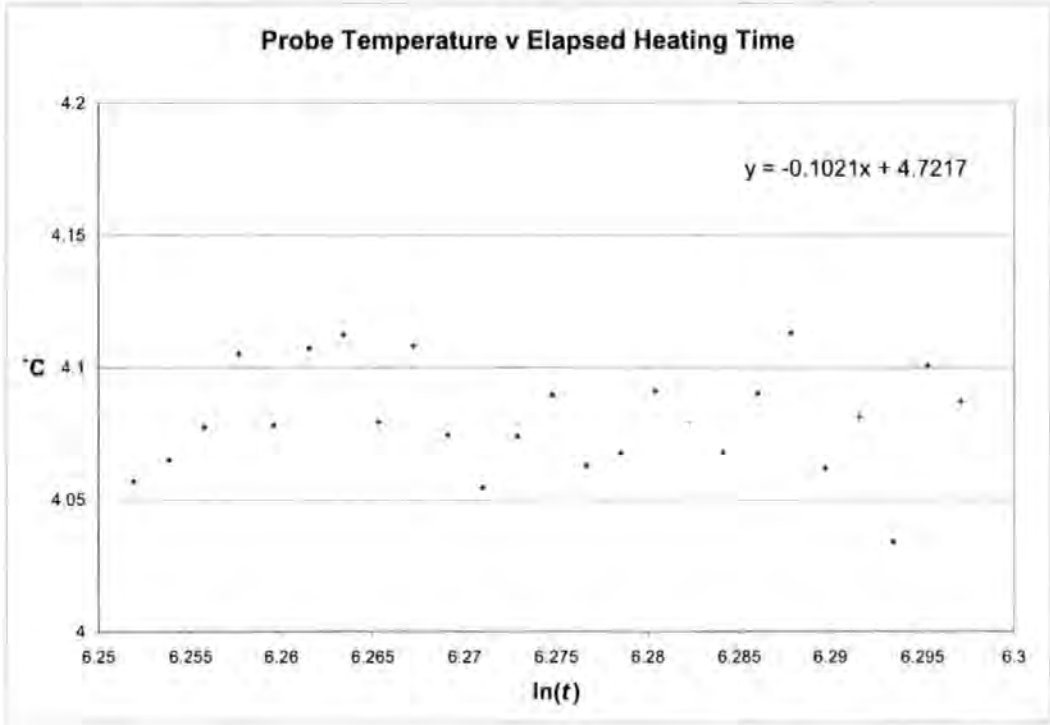

Chart 29: $\Delta T/\ln t$ for later part of a measurement in agar immobilised water

The effect of data scatter increases as time elapses where temperature rise reduces towards zero. An example is given in charts 28 and 29, which show a TP08 measurement in agar immobilised water with a 4.25°C temperature rise over 600s. Chart 29, shows a negative slope existing within the upward trend of the heating data, which would, if taken as a time window for analysis, give rise to inappropriate negative thermal conductivity results.

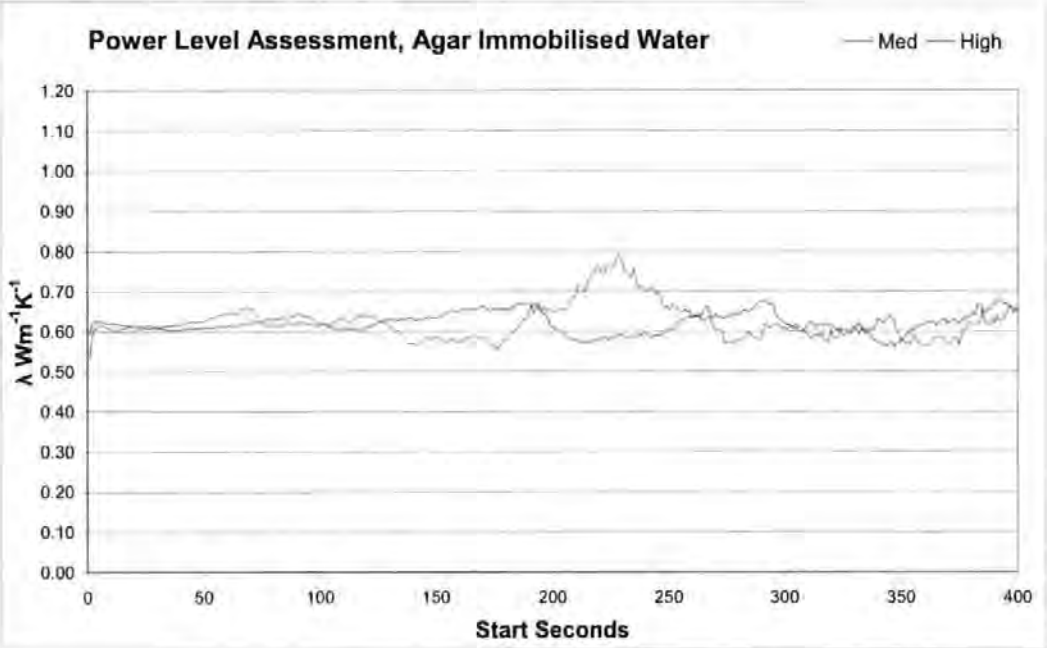

Chart 30: Thermal conductivity results for agar at two power levels

Chart 30, showing 100s thermal conductivity results for two power settings in agar immobilised water, mirrors the findings from chart 24 for PTFE in that, for real materials, not considered highly insulating, the power setting does not affect the thermal conductivity results and that higher powers reduce scatter effects. These factors were considered in the development of the field apparatus where power outputs were targeted to achieve temperature rises between around 7°C and 15°C for construction materials.

Boundary condition

The boundary condition for a sample of phenolic foam was considered, partly in the light of the increase in thermal conductivity results at later times for materials with lower thermal conductivity and partly to assess appropriate sample sizes for measurements.

Vos (1955), and later researchers such as Batty (1984) and Goodhew & Griffiths (2004), used the condition of equation (13), repeated here for convenience:

$$\frac{4\alpha t}{d^2} > 0.6 \qquad \textbf{equation (13)}$$

to assess the time before which boundary effects caused significant errors to thermal conductivity results.

Bohac et al (2003) gave a thermal diffusivity value of 7.80 $x10^{-7}$ m^2s^{-1} for phenolic foam. Using this value and equation (13), the boundary condition should be reached after 43s for a 15mm radial distance and 425s for 47mm. These values were tested by carrying out measurements in phenolic foam.

Five 32mm thick slabs of foil backed phenolic foam >150mm square were used. The first measurement used three slabs lightly clamped together with a 1.2mm TP08 probe pushed along the central axis of the central slab. The second measurement used all five slabs lightly clamped, with the probe in the same relative position. Two K type thermocouples were placed 35mm from the boundary, between the clamped slabs, at 15mm (TK10) and 47mm (TK11) perpendicularly from the centre of the 72mm probe.

Chart 31 shows the thermocouple at 15mm reacting after 39s and the one at 47mm after about 300s, albeit to a lesser extent. The first figure especially presents a good approximation of equation (13). Should these boundary states have significant effects on the probe heating, whereby thermal conductivity appeared to increase over time as more heat was lost to the surroundings,

differences should appear in results from measurements in samples of varied thickness.

Chart 32, however, shows no significant difference between measurements, with boundaries at 47mm and 79mm both showing the thermal conductivity results increasing appreciably over time, and before the condition of equation (13) is encountered. Two causes of these rises appear possible. Firstly would be the unexplained phenomenon encountered in the Voltra simulations, which appeared dependent on the relationship between the thermal conductivity and volumetric heat capacity of the sample.

The second possible cause would be a combination of interrelated influences, including axial, end and boundary losses at the open end, both to the surroundings and to the probe base and cables. The extent of the losses would be dependent on the thermal conductivity and volumetric heat capacity of the sample. These effects are considered further under the heading 'Thermographic assessment'.

The anomaly does not appear to relate to radiation issues, as suggested by Vos (1955), Powell et al (1966), and Batty (1984), as similar rises were found in measurements of multifoil insulations, designed to prevent radiant heat transfer, as well as more open insulations such as a granular vermiculite and mineral wool.

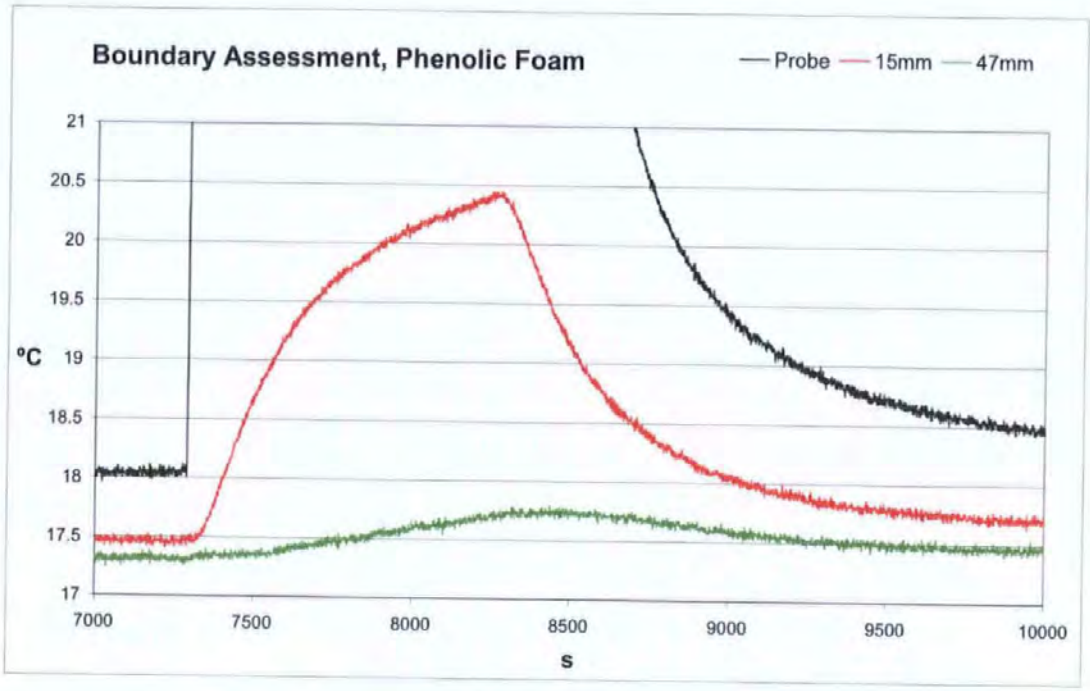

Chart 31: Temperature rise at 15mm and 47mm, phenolic foam

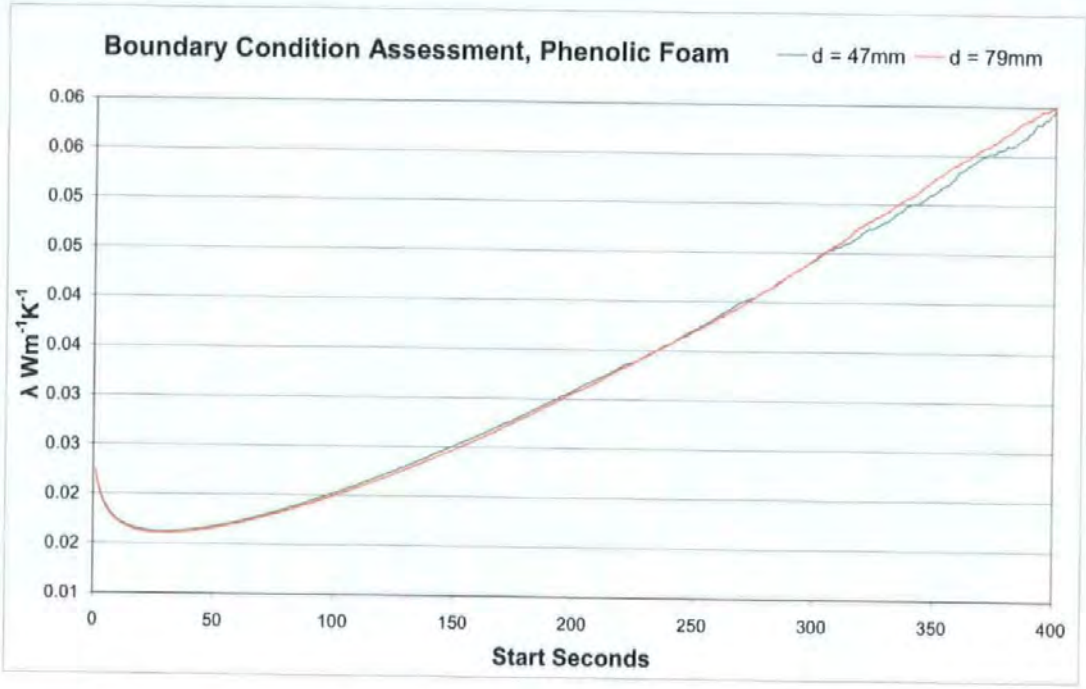

Chart 32: Thermal conductivity, phenolic foam at two thicknesses

The boundary condition was practically assessed in a less insulating sample with higher volumetric heat capacity, aerated concrete. Probes were placed at

20mm, 30mm and 50mm from, and parallel to, a heated probe. Temperature increases were observed at 20mm, less at 30mm and were not detectable at 50mm during measurements. It was therefore considered that the radial boundary condition was not likely to be a factor for in situ measurements of materials in real buildings where measurement positions were appropriately chosen away from material edges and where the material did not contain voids. Axial losses to the probe body and wires, as discussed by Hooper and Chang (1953) and Håkansson et al (1988), and heat losses to the surroundings, could be a significant cause of error in materials with lower thermal conductivity, which is assessed in the next section.

Thermographic assessment

The probe heating profile and axial loss effects were studied using an NEC Thermo Tracer 7100 thermal imaging camera connected to a laptop computer running MikroSpec RT v2.1394 software. A 72mm x 4mm hole was drilled in a dry, lightweight, aerated concrete block, 50mm from one edge and 5mm from another edge, using a pillar drill to ensure reasonable parallelity. A TP08 probe was inserted and held in position with a mild steel laboratory stand and clamp. It was recognised that atypical heat losses would occur with a 5mm boundary but, after trials at 10mm and 15mm, it was considered that a reasonable indication of the probe heating profile could be achieved. Figure 14 shows the experimental arrangement whereby the temperature rises at the surface of the block and the probe base were recorded.

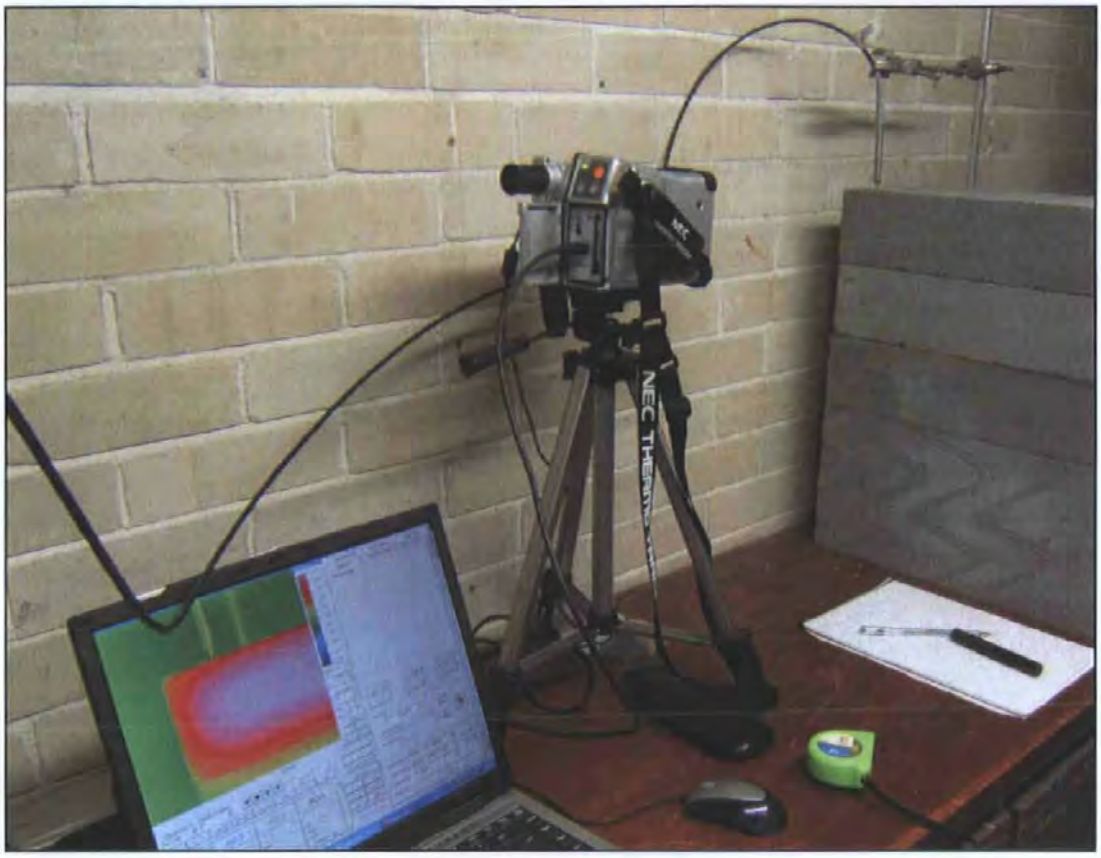

Figure 14: Thermal imaging arrangement for probe heating profile assessment

Power was supplied to the probe at approximately 4.7 Wm^{-1}, with a recorded temperature rise of 16.7°C over 600s at the probe's thermocouple. Figure 15 shows six stages of the heating cycle. These images provide evidence that heat losses to the probe base are significant. Table 5 shows a temperature rise occurring at the surface of the probe base after just 15s. The 3D image, figure 16, provides evidence that heat losses to the surrounding air would also be significant, either directly from the probe components or from the sample material adjacent to the probe entry position, although it is not possible to quantify the relative levels of significance.

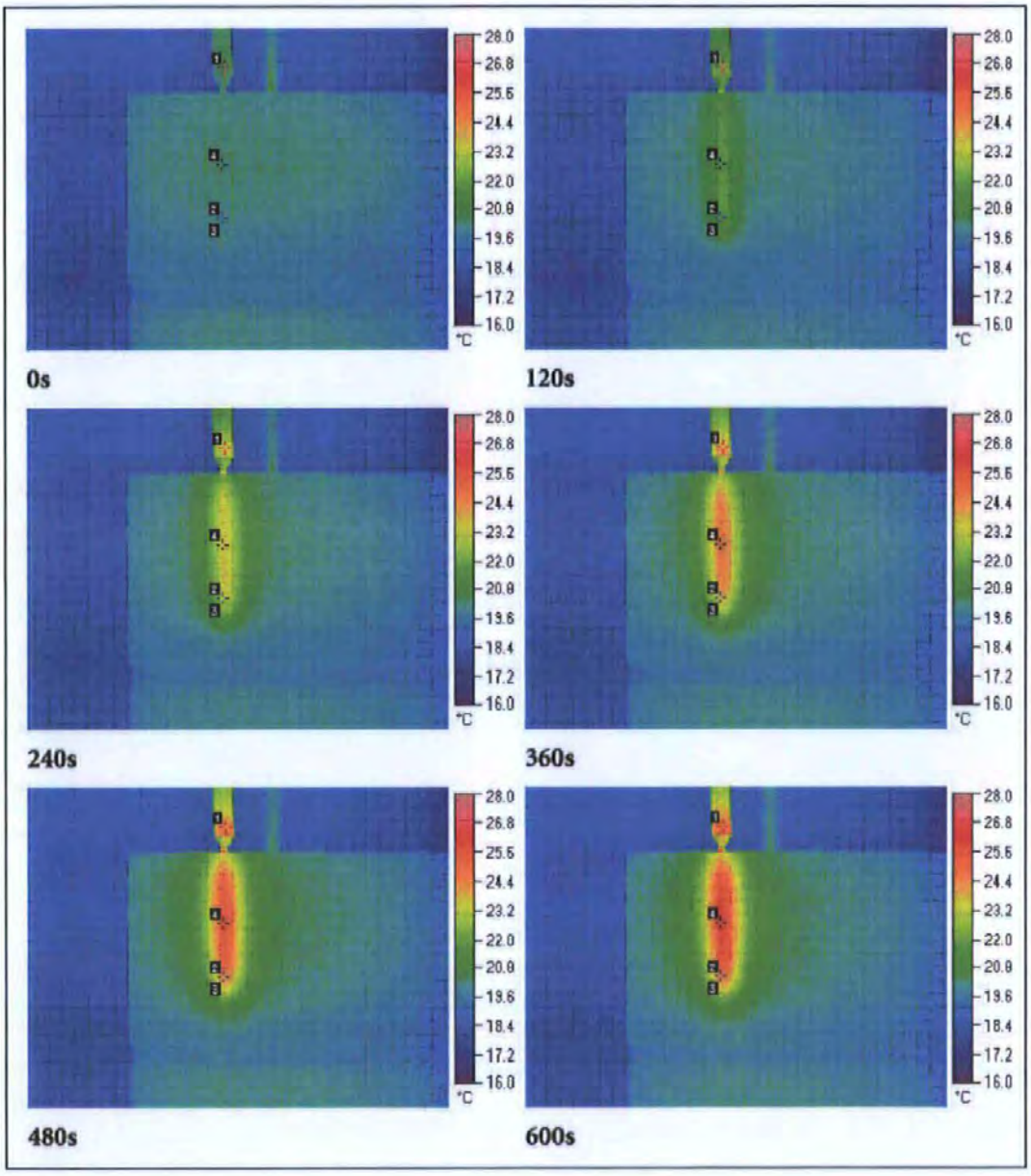

Figure 15: Thermal images of a probe heating profile in aerated concrete

Seconds:	0	15	30	45	60	75	90	105
Point 1 (Base)	20.4	20.6	20.9	21.3	21.4	21.6	21.8	21.9
Point 2 (56mm)	20.1	20.3	20.3	20.6	20.9	21.2	21.2	21.5
Point 3 (Tip)	19.7	20.1	20.0	20.1	20.3	20.3	20.4	20.5
Point 4 (Mid Point)	20.1	20.3	20.3	20.5	20.8	21.2	21.4	21.5
Seconds:	120	135	150	165	180	195	210	225
Point 1 (Base)	22.1	22.3	22.4	22.6	22.8	22.9	22.9	23.2
Point 2 (56mm)	21.7	22.1	22.1	22.3	22.4	22.7	22.7	23.0
Point 3 (Tip)	20.7	21.0	20.9	21.1	21.2	21.3	21.2	21.5
Point 4 (Mid Point)	21.9	22.2	22.4	22.4	23.1	23.2	23.3	23.6

Table 5: Temperature rises at probe base and aerated block surface

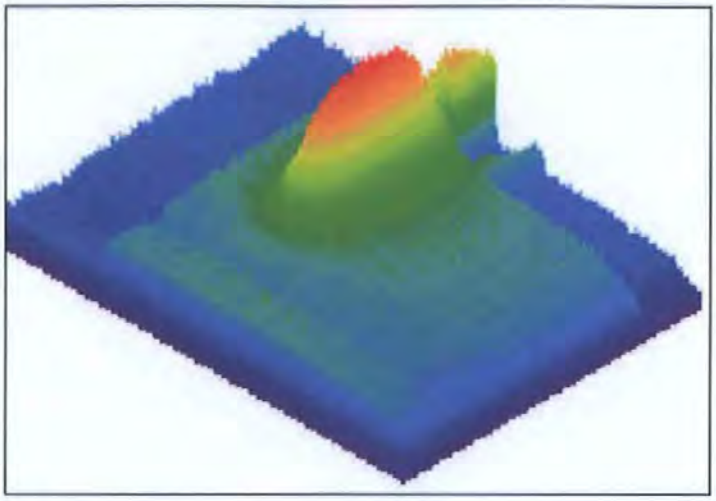

Figure 16: 3D thermal image of a probe heating profile in aerated concrete

The thermal imaging work has illustrated the probe heating profile, which, as a representation of an infinite line source with a consistent radial heat output, comes close to parallelity at the mid point, as can be seen in Figure 15. However, it has been demonstrated that losses to the base and surroundings are significant, which significance would clearly increase with greater thermal resistance in the sample material. This was seen with other insulation materials studied, including multi-layer, sheep's wool, mineral wool, polystyrene, and Dupre vermiculite, where thermal conductivity results increased over time. From this, it was considered that valid thermal conductivity results for materials below approximately 0.07 $Wm^{-1}K^{-1}$ were unobtainable by the current method.

Moisture migration and thermal conductivity

The first part of this section examines the effects of probe heating cycles on moisture content to assess whether moisture migration might produce significant errors. The second part presents some thermal conductivity measurements for materials with varied moisture content, such as would be expected when carrying out in situ measurements in real buildings.

A number of measurements were carried out in standard, aerated concrete blocks, each at a different moisture content. The example given here is for a block with 5% moisture content by weight. The block, measuring 440mm x 250mm x 215mm, was saturated and gradually dried in ambient room conditions over a period of three months, which ensured a reasonably even moisture distribution. The manufacturer's given thermal conductivity value was 1.5 $Wm^{-1}K^{-1}$, achieved by a guarded hot plate in a UKAS accredited laboratory. This value was subsequently attained to a reasonable approximation by thermal probe measurements in an oven dried block (see chart 33).

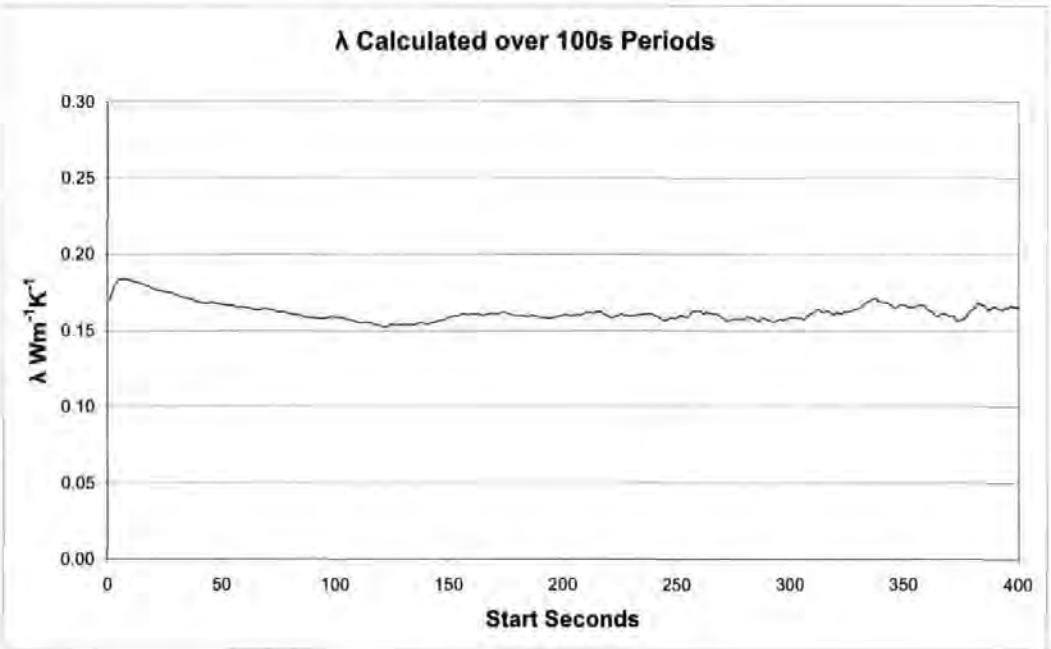

Chart 33: Thermal conductivity results for aerated concrete after oven drying

Five measurements were taken in one hole position with approximately two hours between measurements. Temperature rises were in the region of 8°C - 9°C over 600s measurements. Table 6 presents the results for each measurement with upper and lower values from the regression analysis at 95% confidence, and the variance coefficient for the set of measurements. This set

of measurements, and eleven others of between 5 and 8 measurements each, gave an average variance coefficient of 2.32%, ranging from 1.03% to 6.10%, with no overall trend towards lower thermal conductivity values for measurements carried out later in the sequences. Reasonable linearity of $\Delta T/\ln t$ was achieved in the samples containing moisture, as assessed visually (see chart 34), by the variance coefficients, and by the consistency of results over time (see chart 35).

The consistency of thermal conductivity results over time and between consecutive measurements indicated that moisture content had not changed significantly during the measurements, hence no significant moisture migration had taken place.

Aerated concrete at 5% moisture content by weight	TP08 Probe	Time Period for RegAnls	Mean λ	Upper λ	Upper %	Lower λ	Lower %
BP-0043c	141	60-300s	0.182940	0.184341	0.77%	0.181561	0.75%
BP-0043g	141	60-300s	0.183268	0.184688	0.77%	0.181870	0.76%
BP-0043k	141	60-300s	0.180832	0.182089	0.69%	0.179593	0.69%
BP-0043n	132	60-300s	0.179825	0.180885	0.59%	0.178778	0.58%
BP-0043r	132	60-300s	0.178356	0.179388	0.58%	0.177335	0.57%
Mean:			0.181044	0.182278		0.179827	
St. Deviation:			0.002080	0.002258		0.001907	
Var. Coefficient			1.15%	1.24%		1.06%	

Table 6: Thermal conductivity results in aerated concrete at 5% moisture content

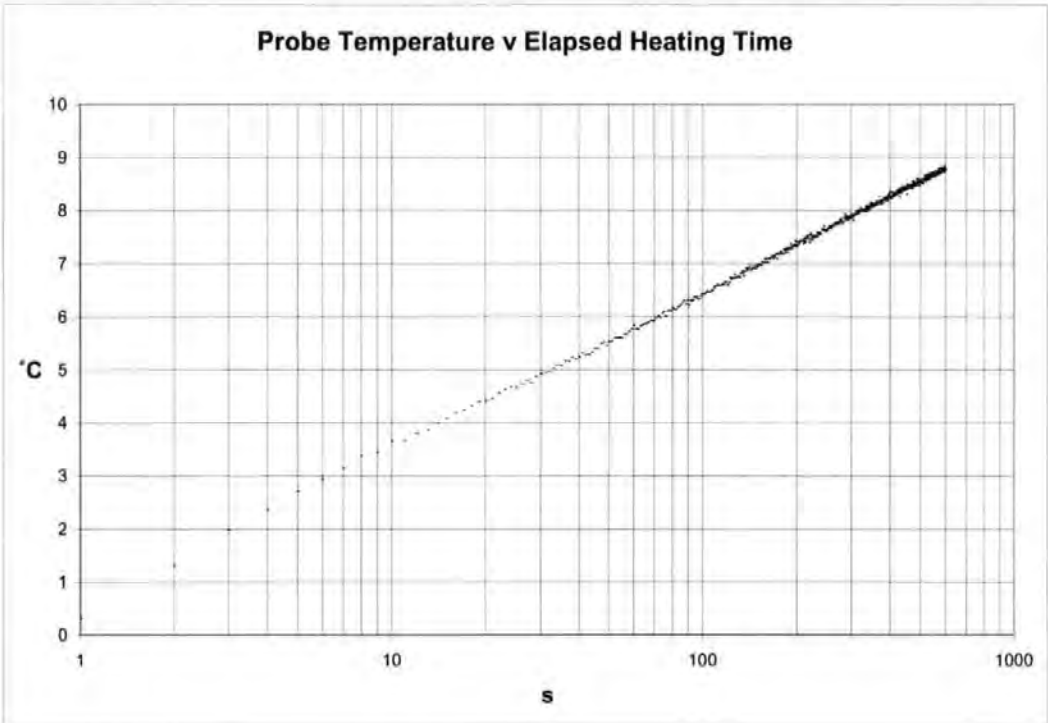

Chart 34: $\Delta T/\ln t$ for aerated concrete at 5% moisture content by weight

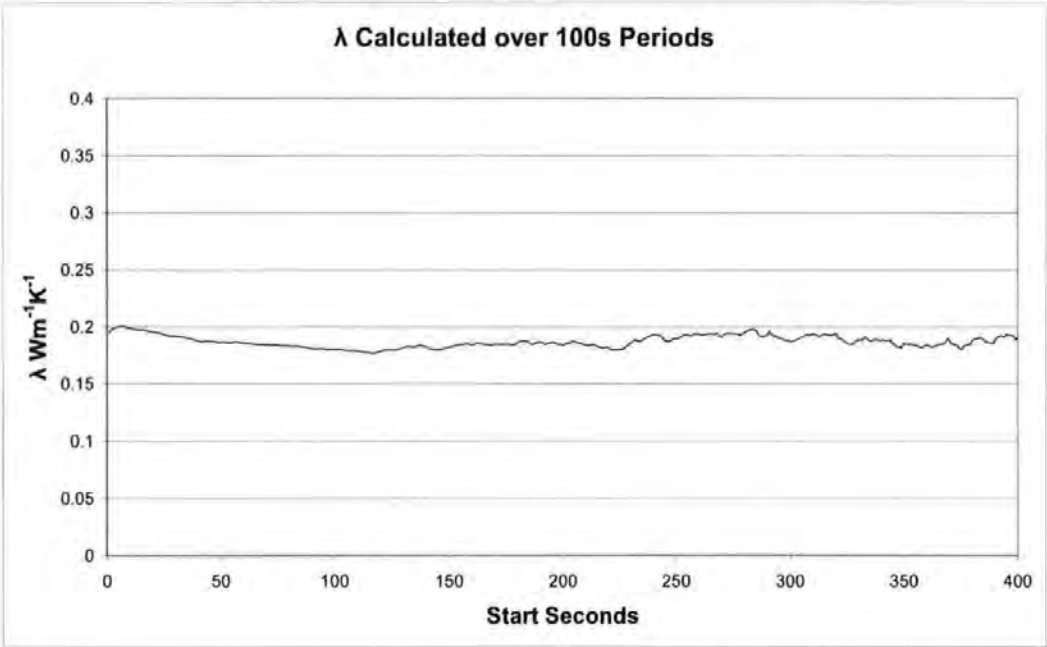

Chart 35: Thermal conductivity results for aerated concrete, 5% moisture content

Two series of thermal conductivity measurements were made in materials where the moisture content was varied over time. These were in standard,

rather than insulating, aerated concrete block, similar to that used for the moisture migration assessment, with dimensions 440mm x 250mm x 100mm, and in a block of oak with dimensions 250mm x 150mm x 152mm. Both these materials allowed close fitting holes and provided reasonably smooth, linear data after the initial heating period.

The concrete block was procured in a saturated state, having been left exposed to heavy rain for some time. Measurements were carried out over a period of 20 weeks, as the block gradually dried out in ambient room conditions. Chart 36 shows the clear correlation between moisture content, measured by weight, and thermal conductivity results achieved with the thermal probe. Measurement 5 in chart 36 was taken after the block had been oven dried at 67°C for 48 hours. Measurement 6 shows that thermal conductivity rose by approximately 2%, with 6 days between measurements, through atmospheric moisture absorption in an internal, dry, generally unoccupied room. This illustrates that, even in conditions normally thought of as dry, guarded hot plate measurements may not be representative of in situ thermal conductivity values.

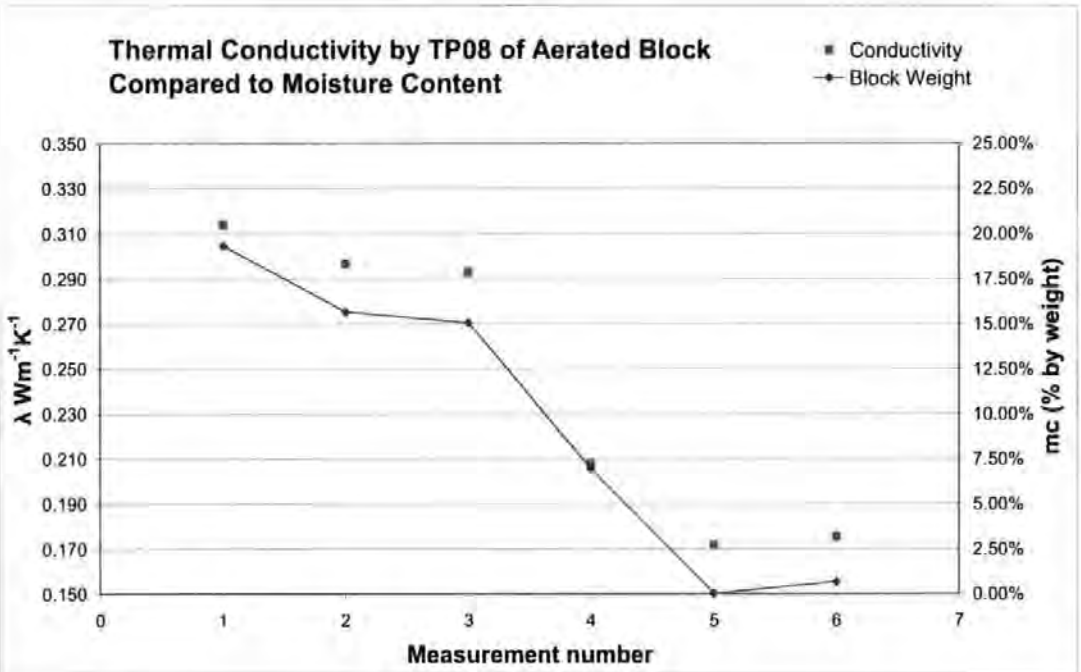

Chart 36: Thermal conductivity, aerated concrete, varied moisture content

Another group of measurements was taken in a sample of oak, both along and across the grain. The oak appeared dry when it was first measured at a density of 772 kg.m^{-3}. It was then left to season in a dry room for 4 months between the first and second set of measurements and a further 6 months before the last measurement at a density of 608 kg.m^{-3}, a fall of 21% from the original density. TP08 probes were used in 1.5mm holes with ArcticSilver5 thermal grease filler. Table 7 shows a summary of the results with the thermal conductivity falling by 40% for the measurement along the grain and 27% across the grain.

	Density (kg.m^{-3})	λ (Wm^{-1}K^{-1})	Variance Coefficient
Oak along the grain	772	0.253	2.33%
Oak along the grain	608	0.152	0.40%
Oak across the grain	772	0.349	1.68%
Oak across the grain	663	0.319	1.98%
Oak across the grain	608	0.256	1.38%

Table 7: Density and thermal conductivity compared in a sample of oak

Conclusions from the laboratory based measurements

The chapter concerning laboratory based measurements has provided a basis for in situ work, as well as reinforcing the significance of the work through identifying levels of error found when using contemporary and commercially available probe metering systems, and the potential for guarded hot plate measurements to not represent in situ values.

It has been found, through automated probe meter system checks, that calibration in one or two materials does not ensure valid results in diverse, or even similar materials. The evidence showed that fixed experimental and analytical parameters, such as length of measurement or chosen analysis time window, would not necessarily transfer from one material to another.

The TP08 probe, at 72mm x 1.2mm, was found to be appropriately dimensioned and robust for fieldwork in real buildings. Hole sizes were found suitable when as small as possible, ideally 1.5mm or 2.0mm, where the inclusion of a thermal paste could improve contact without their thermal properties significantly affecting results. 3.0mm and 4.0mm hole sizes were found able to produce indicative thermal conductivity results at later times with a contact paste but with less confidence. It was recognised that difficulties in obtaining fine masonry drills would restrict the range of materials that could be measured.

Probe temperature typically came into equilibrium with samples in under 20 minutes and, after a heating cycle, stabilised again after around an hour. However, as these times varied for different materials and temperature differences, it was found appropriate to use a live probe temperature read out on a laptop computer attached to the dt800. Temperature stability and trends

could then be visually assessed to ensure as small a drift as possible, 0.1°C over 200s being taken as the maximum acceptable.

Power level changes were not found to cause any significant changes in results but low inputs produced more scatter. As high inputs could potentially cause moisture migration, greater energy demands, and damage the equipment, power levels that produced temperature rises between in the order of 7°C to 15°C were considered appropriate.

Boundary conditions were discounted from being a significant problem for typical sample sizes with in situ building components, as long as holes were formed at least 50mm from material edges. Thermography showed that axial and end losses at and around the probe entry position were significant and prevented valid measurements for typical building insulations.

It was found that moisture migration was unlikely to introduce significant errors to thermal conductivity results at the power levels studied. The probe technique was capable of measuring thermal conductivity at the levels of moisture content that could typically be expected in occupied dwellings. Thus the potential is provided to obtain reasonable indications of increased heat transfer, and consequent loss of energy efficiency, caused by normal moisture contents, compared to dry or design values.

The next chapter concerns the transfer of the technique from laboratory based measurements to measurements in situ, of materials in real buildings.

Chapter 6: In situ measurements

Introduction to the in situ measurements

The preceding chapters have provided a background to the thermal probe technique, and explored its capabilities and potential with regard to measuring the real thermal properties of building components in situ. This chapter describes the development of a dedicated field apparatus to carry out such measurements, and reports on various case studies involving measurements in real buildings under varied climatic conditions.

Development of a field apparatus

Various objectives for the field apparatus were recognised at the design stage. These included:

- Robust and weather proof construction
- Time efficiency in measurements
- Reliable performance
- Stand alone capability
- Live data display
- Raw data storage

The robust construction, to allow the kit to be carried around and used on building sites, was achieved by hard wiring components in aluminium enclosures mounted on a steel plate within an Explorer 5822 case, conforming to IP67 dustproof and waterproof standards (IEC, 2001). It was considered to be unnecessary to pierce the case for cable entry. It was envisaged that sheltered and protected positions for the kit would be found during

measurements, so switch gear could be accessed and observations made with the case lid open. Figure 17 shows the field apparatus with the probe leads, hard wired to the datalogger, led out from the case.

Figure 17: The field apparatus

Measurement times had been estimated from the laboratory work, including temperature stabilisation periods after insertion and between heating cycles. To increase efficiency, four probes were connected to the datalogger so, with appropriate switching gear, each probe could be heated in turn and its temperature allowed to restabilise while the other three probes were engaged in turn. Two probes had leads of 2.5m and two were 5.0m, which had the occasional benefit of allowing measurements of building components to be taken internally and externally from one case position. The arrangement allowed up to four measurements to be taken per hour.

Several factors were considered regarding the reliable performance and precision of the equipment. Figure 18 shows the wiring diagram. An 18 V, sealed lead acid, rechargeable battery was used as the heater power supply, with a spare battery available to ensure at least 12 hours stand alone capability. A digital read out of the battery voltage was incorporated to avoid problems with losing charge during a measurement. To avoid voltage gradually reducing or

fluctuating during a measurement, a three terminal positive voltage regulator was placed in the circuit, an L7812ACV from ST Microelectronics.

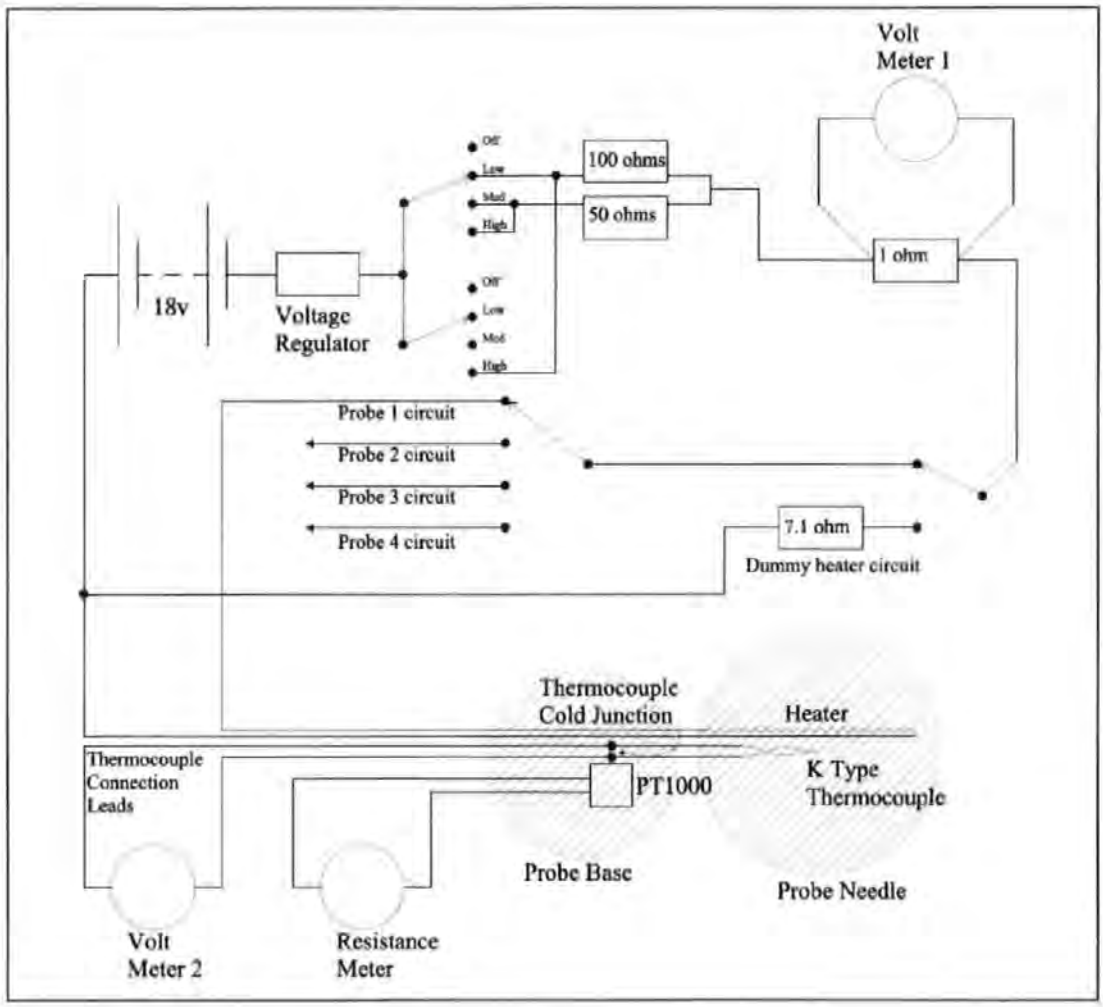

Figure 18: Field apparatus schematic

Thermal shocks to the circuit from fluctuating power levels were avoided by using a dummy heater, a resistor closely matching the resistance of a probe heating element. Power was directed to this resistor before and in between probe heating cycles. The power supply was regulated by two resistors, whereby the circuit passed through a 100 Ω resistor, a 50 Ω resistor or through both in parallel, giving powers in the region of 0.1 W, 0.25 W or 0.5 W respectively to the probes.

The power was measured using the voltage drop over a 1 Ω resistor. The resistor (Ra) was a wire wound Arcol HS25, mounted to the casing with a heat sink compound. The specified tolerance and temperature coefficient were 5% and 25ppm respectively. Discussion with Arcol technicians indicated that these values were exceptional worst case scenarios and unlikely to be encountered in practice. The resistance was checked at room temperature with a LCR 6401 Databridge from Tinsley Prism Instruments and found to measure 1.002 Ω, 0.2% higher than the marked value. The temperature coefficient indicated a potential maximum 0.00125 Ω difference across a 50°C temperature variation in Ra. This was assessed by carrying out measurements in agar-immobilised water and then heating the resistor to 54°C and remeasuring. No detectable difference in results occurred.

A dt800 datalogger from Grant Industries formed the heart of the apparatus. This had 16 digital channels, and up to 42 analogue channels. It was specified as capable of voltage and resistance measurement resolutions of 1 μV and 25 μΩ, dependent on the range being measured, and accuracies of 0.02% and 0.04% respectively at normal operating temperatures. 16 bit resolution was provided at sampling rates up to 12 Hz, with maximum sampling rates available up to 100 kHz. Frequency resolution was 0.01 Hz at 10 kHz.

The dt800 was powered with its own internal battery backed up by a 12V, sealed lead acid, rechargeable battery, also with a spare battery available to ensure at least 12 hours stand alone capability. The logger could also be run from a mains electricity connection, where available. It was attached to a laptop computer via an RS-232 serial port. The laptop had an internal battery life of

about 6 hours but could also be run and recharged from a mains connection, where available, or a cigarette lighter socket in a vehicle.

The dt800 was used with Delogger 4 Pro software. Sampling rate was set at 1 Hz, with a frequency resolution of 0.001s. Each of the four Hukseflux TP08 probes was attached to a separate channel which measured the resistance of the PT1000 at 1 mΩ resolution and the voltage across the needle thermocouple, the electromotive force (emf), at 10 μV. Another channel measured the potential difference across the 1 Ω resistor (Ra) and two channels had K type thermocouples attached so that ambient temperatures could be monitored using the dt800s built in conversion formula.

The software was set up to provide live graphical displays of:

- the voltage drop across the 1 Ω resistor, Ra, to assess power stability
- ambient temperatures in two positions
- the emf at all four probe needle thermocouples
- the resistance of all four PT1000 thermometers in the probe bases
- the four needle temperatures, calculated from PT1000 resistance and needle emf.

A further live window provided numerical values for these properties at 1 Hz. Figure 19 is a screenshot of the live window arrangement.

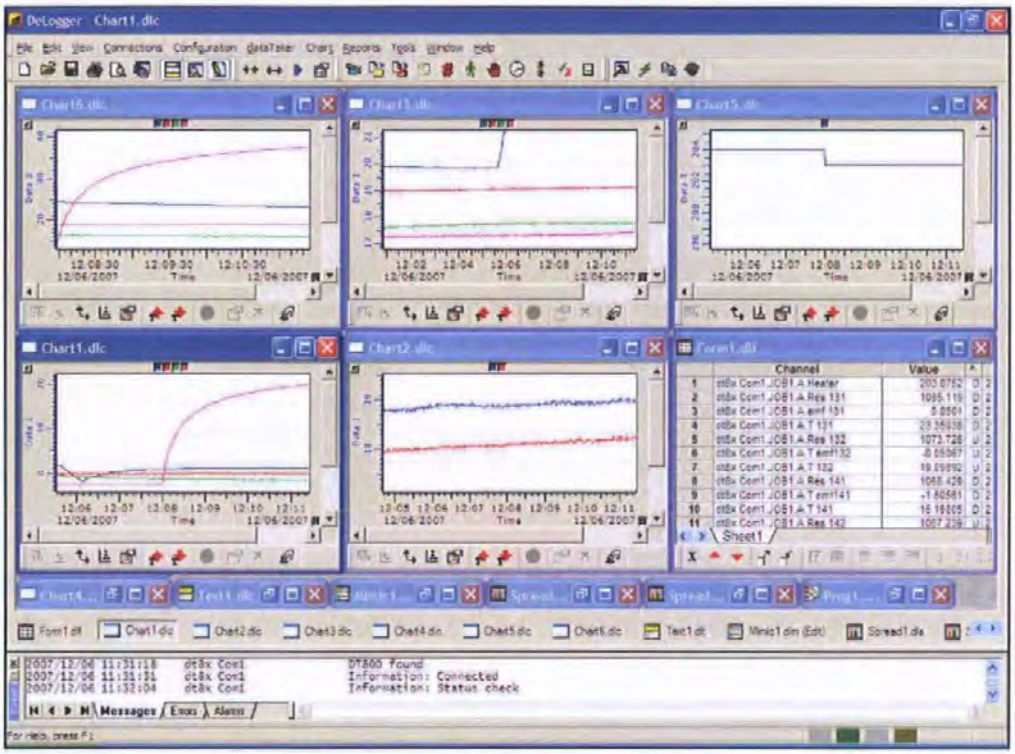

Figure 19: Screenshot of Delogger Pro

Experience with the commercially available probe meters, where there was no opportunity to carry out post measurement data analysis, and the pre-existing laboratory apparatus, where care had to be taken not to overwrite data before downloading, had shown the benefits of appropriate onboard data storage. The dt800 was fitted with additional flash memory which made available up to about 48 hours of onboard storage for all the parameters mentioned above at 1 Hz. In practice, data was usually downloaded to the laptop computer over smaller intervals and then stored as MS Excel files on a portable hard drive, both as complete sets of data and as individual sets for each probe heating cycle, which were similarly formatted for ease of future use with macros.

These arrangements allowed robust measurement and storage capabilities for on site, in situ work.

Probe temperature measurement

The thermal probes used for the experimental work reported here were commercially available Hukseflux TP08 stainless steel probes, designed and tested in collaboration with the Applied Physics Group of Wageningen University (Hukseflux, 2001).

These were single needle probes comprising a hairpin heater of known resistance per unit length, set in a crystalline surround, within a stainless steel tube, 72mm long and 1.2mm external diameter with walls approximately 0.185mm thick, referred to as the needle. A K type thermocouple (TK) was placed adjacent to the heater at around the needle's mid length point with its cold junction adjacent to a platinum resistance thermometer (PT1000) in the probe's base or handle.

This base was also constructed of stainless steel and was approximately 10mm in diameter and 100mm long. Cables exiting the base were the positive and negative feeds to and from the heater, positive and negative extensions to the TK cold junction, positive and negative current to the PT1000 with a sensor wire.

Previous researchers have usually attempted to create highly controlled thermal environments before undertaking measurements at stable, initial temperatures. This was generally the case with previous work at the University of Plymouth, where temperature stability had been assessed by the needle thermocouple, in bespoke and Hukseflux probes.

A number of problems with this methodology became apparent early in the work using the TP08. The datalogger used, a Datataker dt800, had initially been used to calculate thermocouple temperatures but was found to be unreliable with a remote cold junction. After switching on, the dt800 reported temperature rises of around 4°C over four hours, which temperature rise was found to be non-existent. This was assessed using two K type thermocouples, one with and one without a remote junction. Communications with the manufacturer did not resolve this anomaly.

A positive feedback mechanism was noticed whereby the heat generated by a measurement raised the temperature of the thermocouple cold junction, leading to progressive errors in temperature measurement data. This error increased with greater thermal isolation of the experimental area.

The dt800 was, however, capable of remotely measuring the electromotive force (emf) across the thermocouple, which could then be converted into a temperature difference using standard thermocouple calculations.

The two temperature measurement devices of the TP08 were found to allow a direct temperature measurement at the thermocouple position, following a methodology described by Childs (2001). Absolute temperatures at the base were calculated from resistance measurements of the PT1000 at 1Hz. The thermocouple emf, again measured at 1Hz, was converted to a temperature difference between the hot junction and the cold junction, assumed to be at the same temperature as the PT1000, being placed in close proximity. The temperature at the thermocouple position was then calculated as the sum of the PT1000 and TK temperature values.

This methodology produced a compound scatter, an example of which is shown in chart 37, where the temperature measurement was taken prior to any power being supplied to the probe.

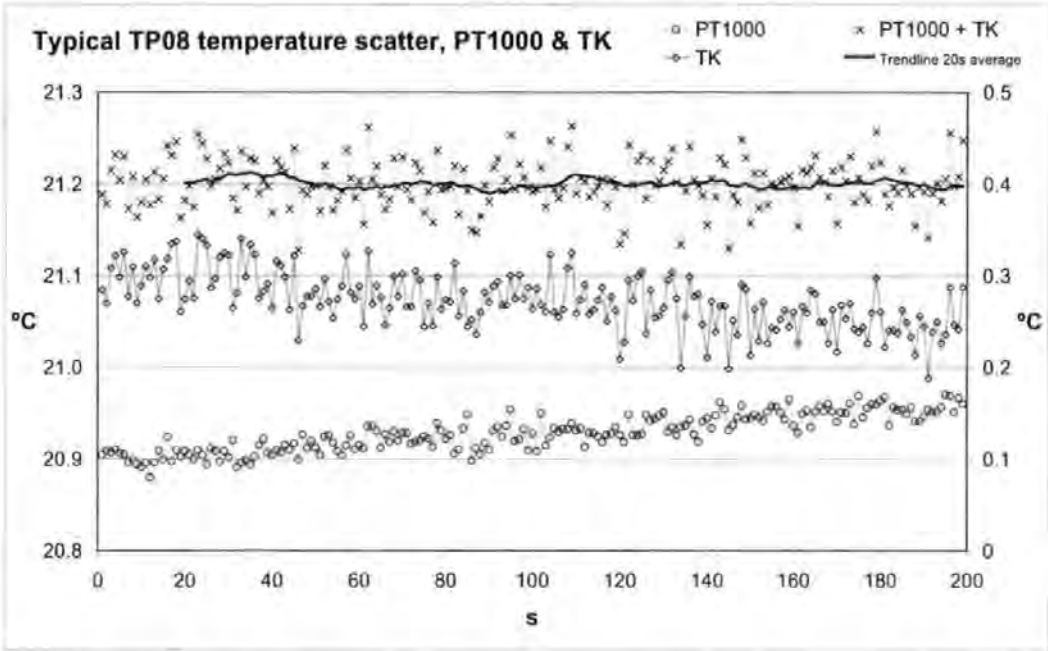

Chart 37: Data scatter in TP08 temperature measurements

The range of the thermocouple scatter, the middle band and right hand axis in chart 37, is approximately 0.1°C compared to that of the PT1000, lower band and left axis, same scale, which is less than 0.05°C. The sum of these two temperatures, the top band and also left axis, shows an increase in random scatter in the temperature measurement used for analyses. The scatter is discussed below.

The trendline added to the compound measurement is of particular interest in chart 37. The measurement shown was undertaken in an internal room of heavyweight construction creating a relatively stable thermal environment. The visible rise in the PT1000 temperature was caused by the author entering the

room, both raising the ambient temperature and radiating heat onto the probe base. The PT1000 temperature rise was not echoed at the thermocouple position in the probe needle because of: the thermal lag of the material in which it was embedded, in this case a sample cube of hemp and lime concrete; the small cross section of the needle which constricts the heat conduction path; and because of there being no direct radiation channel to the needle. This shows as a drop in the thermocouple temperature difference from the cold to hot junction, whereas the calculated temperature at the probe thermocouple position is shown by the trendline to be stable.

This effect was assessed using various heat sources on the probe base, including radiant heat from a light bulb and conducted heat from hand clasping the base, with similar results. Chart 38 shows the effect of touching the probe base with two fingers for two seconds at 10:50 and then again for five seconds at 11:03, the effects took approximately 20s to register, presumably the time taken for the heat to be conducted from the hand, through the probe base composition, to the PT1000 / TK cold junction position within the base. These results confirmed that combined, calculated temperatures could be used for analysis, when assessing temperature stabilisation periods or in situ measurements.

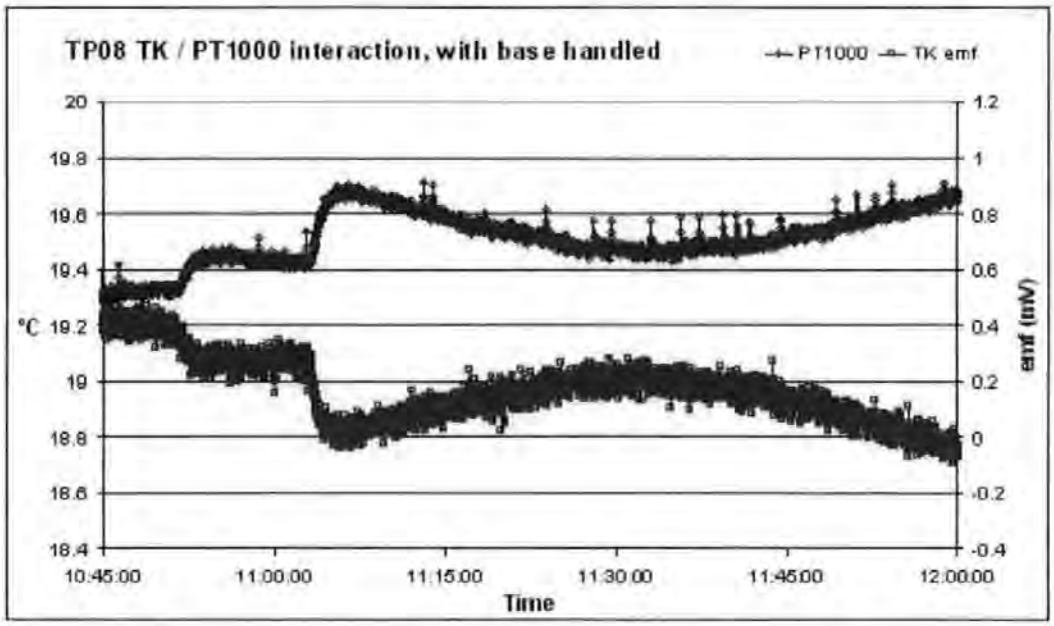

Chart 38: TP08 reactions of PT1000 and TK when probe base warmed

Measurement data scatter

The effect of the compound scatter was assessed using the software programme R (R Development Core Team, 2005). R is a statistical analysis software tool. It was used to carry out the locally weighted scatter plot smoothing process, Lowess. Data, previously converted to temperature equivalents for the PT1000 and TK, were imported from MS Excel analysis spreadsheets. The curves of the data were plotted and Lowess curves fitted. The resultant data from the Lowess curves were re-exported to the analyses spreadsheets and the effects on the $\Delta T/\ln t$ curves and subsequent thermal conductivity results assessed.

Lowess uses a linear polynomial analysis across a span of local data, referred to as the bandwidth, and weights the data within that span towards each data point considered. The bandwidth can be set to a value whereby the Lowess curve best fits the original data, using a visual appraisal and setting the desired

proportion of the data to be used. The early, steep part of the heating curves was best fitted using a small bandwidth, such as 0.01 (1% of data), whereas later parts of the curve fitted well at 0.1 (10% of data). Håkansson et al (1988) had previously used a similar methodology, employing an average value for the 10 data points either side of each data point under consideration, using fast sampling rates.

Charts 39 and 40 show the same part of a heating curve for a measurement in petroleum jelly with unsmoothed and smoothed data, *plotted firstly against* elapsed time and then the natural logarithm of elapsed time. Using a linear regression analysis between 100s and 300s and equation (6) on the unsmoothed and smoothed data gave a thermal conductivity value of 0.159 $Wm^{-1}K^{-1}$ for both datasets, although the retained scatter in the unsmoothed data gave an expectedly higher uncertainty, at ± 1.10% compared to ± 0.06%.

Similar effects were found using other datasets, in agar immobilised water and *in mineral wool insulation. The differences* were small enough to be considered negligible, giving confidence that the compound scatter effect was not significant, for thermal conductivity measurements.

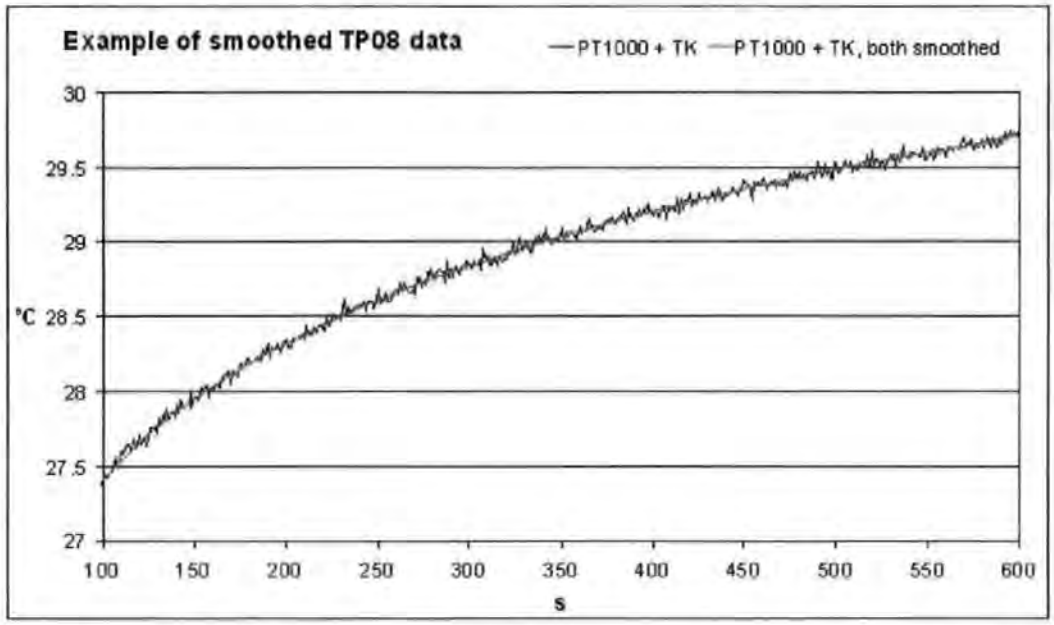

Chart 39: TP08 Δ*T*/*t* in petroleum jelly, with Lowess smoothing

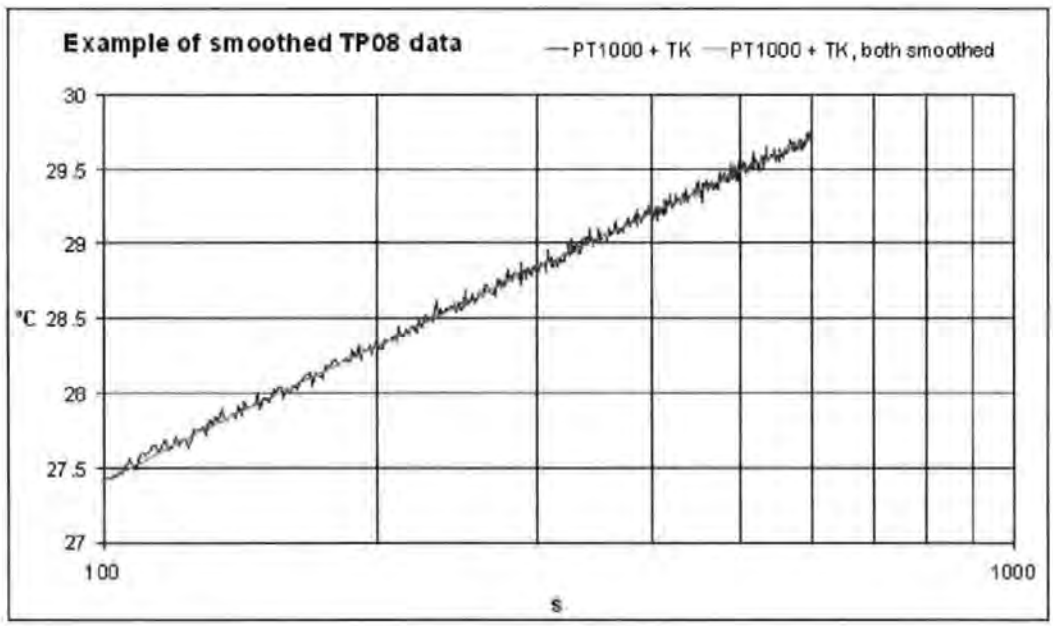

Chart 40: TP08 Δ*T*/ln*t* in petroleum jelly, with Lowess smoothing

In situ measurements using the field apparatus and measurement analysis routines are now described with the aid of five case studies.

Introduction to the case studies

This section continues with an assessment of in situ measurements. The conclusions arrived at from the literature review, the computer simulations and the laboratory work are used to inform the analyses of measurements in case study buildings.

The case study buildings were chosen for a number of reasons. The buildings had to be accessible. The materials to be measured had to be penetrable within the limits set by the drills available. The study would benefit from comparisons to similar materials measured in the laboratory situation, so that in situ results could be compared with those achieved under controlled conditions. As the ambient environmental effects were of key interest, it was advantageous to carry out measurements near the extremes of climatic conditions normal to the UK. Measurements were therefore undertaken during the height of summer in the south west of England and in the depths of winter in Scotland. The efficiency of the project was aided by the Scottish measurements coinciding with a demonstration of the equipment at the Building Research Establishment at East Kilbride.

The field apparatus was carried in an estate car, see Figure 26, along with a laptop computer, battery powered SDS drill and appropriate drill bits, a Rotronic S1 relative humidity meter, boom microphone stands to hold probes in position, surveyors' telescopic ladders, high visibility clothing, traffic cones, warning tape, fine surface Polyfilla, cleaning materials and various other small items such as heat sink paste, application syringe, etc.

Figure 20: Field apparatus packed for transit

A similar measurement methodology was used at each building, using a standard format to keep site notes of actions and events considered relevant. These notes were later transposed to typed experimental records, an example of which can be seen in appendix C.

Upon arrival, suitable positions for the case and measurements were identified. The case was positioned and connected to the laptop computer. The recording programme was then sent to the dt800, and logging commenced. Based on visual assessments of the material to be measured, the power output was set to one of the three available levels and directed to the dummy heater. Holes were then formed for the probes and the probes placed in situ. The needle temperatures were then followed visually on the laptop display.

Once temperatures appeared stable over 10 minutes, power was directed to each probe in turn with a minimum one minute interval between measurements, during which time power was redirected to the dummy heater. If necessary, adjustments to the power level could be made after the temperature rise of the first measurement had been assessed. In most cases, after each set of four

heating cycles, data were downloaded via the software to MS Excel files, which allowed onsite analysis to be ongoing during subsequent heating cycles.

Case study 1, Cob buildings

Measurements were carried out at two cob buildings. The first case study was a single storey bus shelter and toilet block known as The Body, at the Eden Project in Cornwall. Measurements took place over two hot days with broken cloud, on 27th June and the 11th July 2005. Ambient temperatures ranged from 23°C to 37°C and relative humidity from 22% to 62%. The layout of the building and the glazed roof areas meant that hole positions were sometimes exposed to direct solar irradiation and sometimes shaded (see Figure 21).

Walls were of mass cob, 450mm thick, comprising approximately 39% white china clay, 59% red Devon clay and 2% barley straw, by weight, with a reported dry density of 1,615 kg.m^{-3} (Abey and Smallcombe, 2005). The material was left exposed externally and finished with 10mm of clay plaster internally. The cob walls sat on 450mm high stone plinths, and were protected from water ingress at their head by wide projecting eaves. The building had permanent unglazed openings, allowing free ventilation. The roof was predominantly translucent Perspex sheet with some corrugated metal sheet. Measurements were taken externally at the foot and head of the north west-facing wall and internally at the foot and head of an internal partition wall of matching construction.

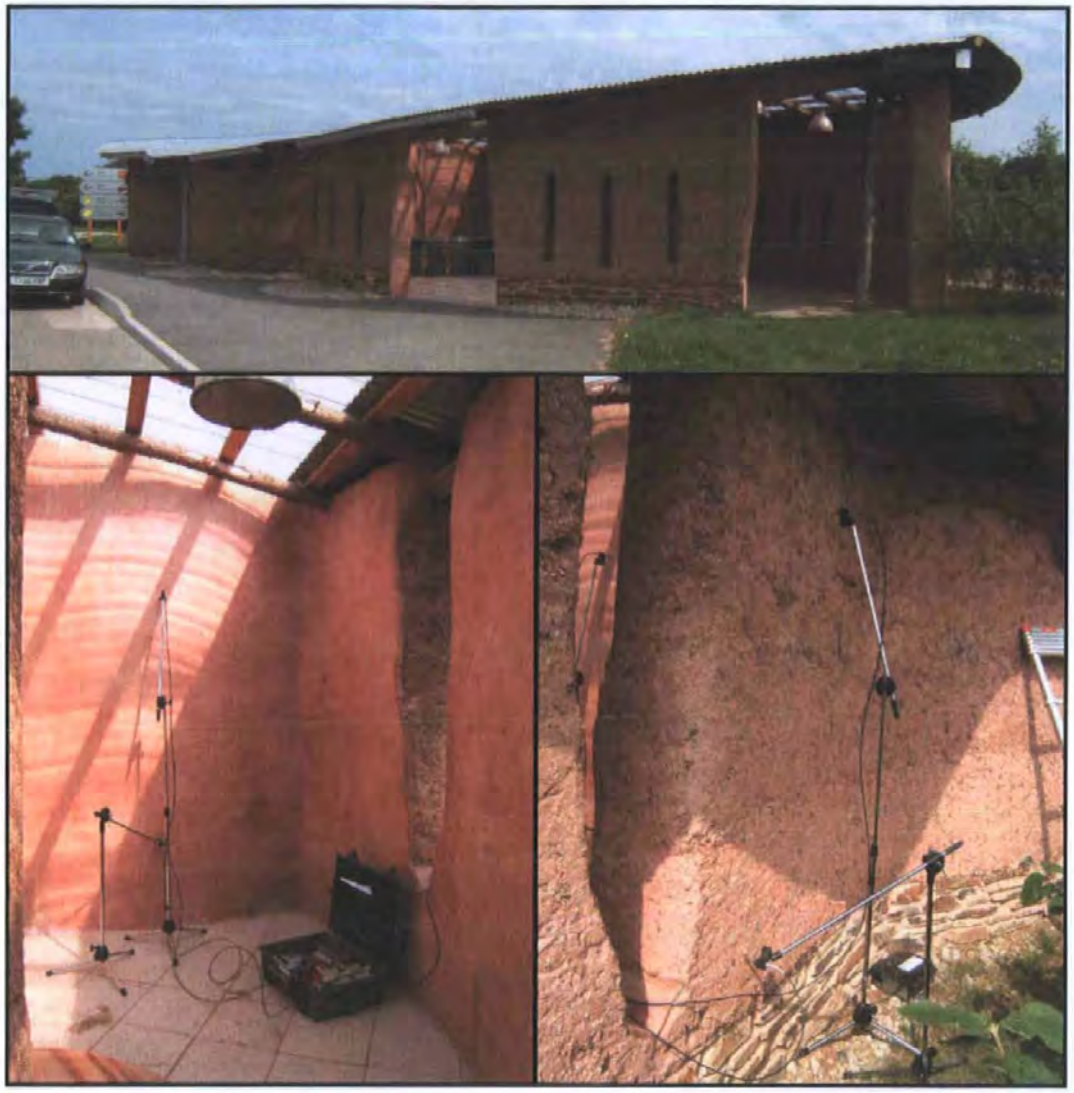

Figure 21: The Body and probe positions at the Eden Project, Cornwall

Chart 41 shows the temperature record from the probe base (PT1000) and needle (thermocouple) for one probe inserted at the internal wall head over most of the second day, including probe insertion at 08:20 and five of the heating cycles. The base record shows the more immediate effects of temperature changes and direct solar irradiation, whereas the needle record shows more gradual temperature change. Chart 42 shows the trend of the needle temperature for 200s before the second measurement rising by

approximately 0.035°C and chart 43 shows the reasonably consistent thermal conductivity results for 100s regression analyses of this second cycle.

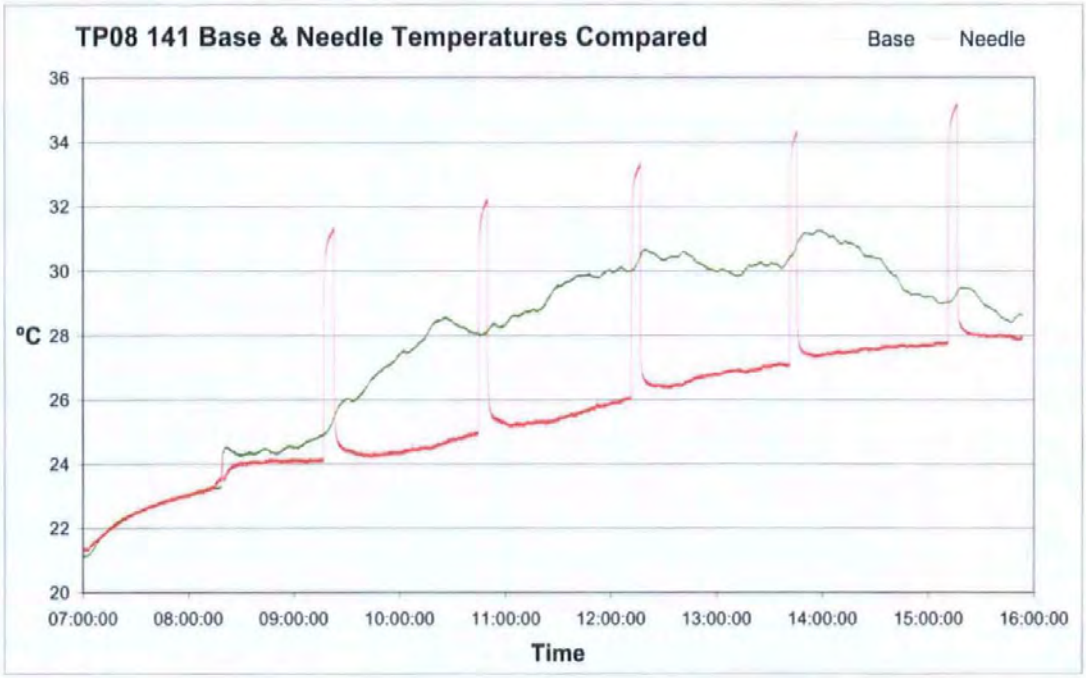

Chart 41: Temperature record of base and needle at internal wall head, the Body

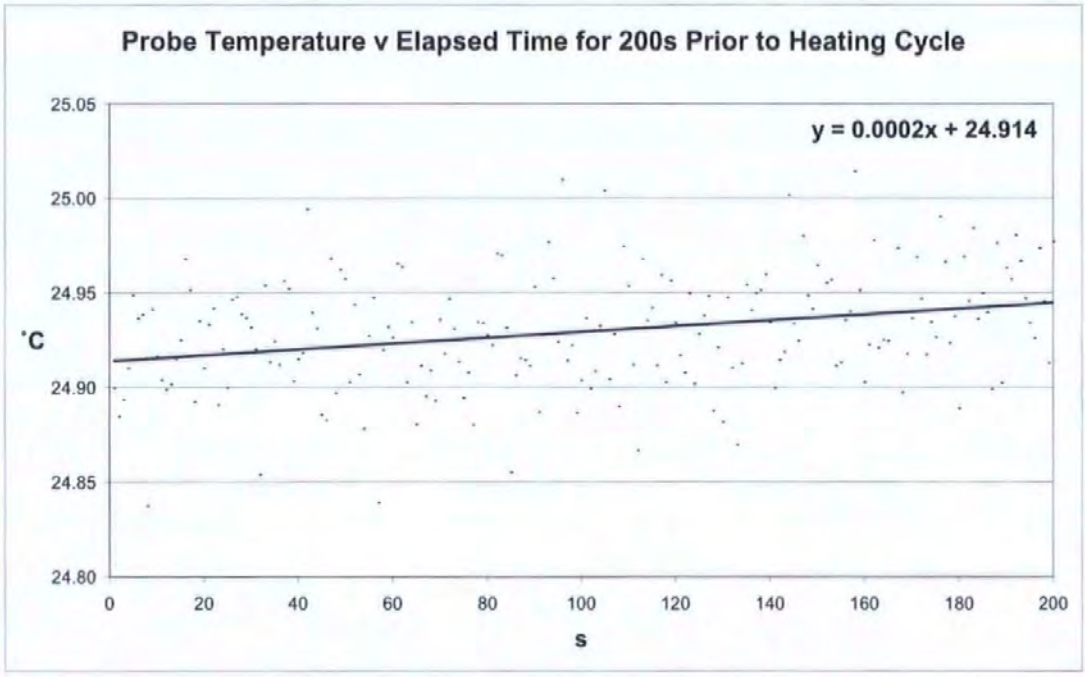

Chart 42: Temperature stability prior to the second measurement in chart 49

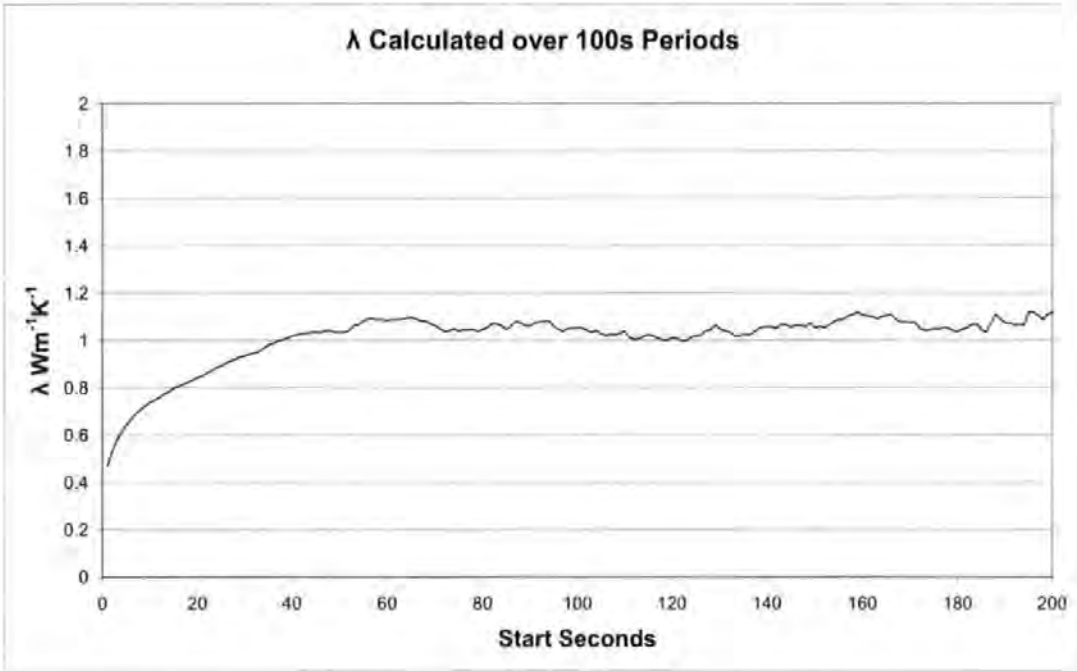

Chart 43: Thermal conductivity results for cob, internal wall head, the Body

Table 8 gives the combined thermal conductivity results of 10 measurements in each position over the two separate days, along with the standard deviation and variance coefficient. These were found by regression analyses carried out over visually assessed linear sections of $\Delta T/\ln t$, which appeared in all cases between 50s and 200s, using equation (6).

	External Wall head	Wall base	Internal Wall head	Wall base
Mean $Wm^{-1}K^{-1}$:	0.810	1.165	0.987	0.824
Standard deviation:	0.094	0.098	0.100	0.038
Variance coefficient:	11.60%	8.44%	10.09%	4.61%

Table 8: Thermal conductivity results for cob at the Body

The results show consistency better than 12% in all cases. While no alternative measurement methodology was employed to substantiate the values achieved and no samples taken, results were within the expected range for dense cob.

The second cob building was a small summerhouse in a sheltered area of south Devon. The walls under consideration were constructed from cob blocks, with those to the upper part containing a lambswool binder. The 240mm thick walls were left unplastered, over a stone plinth, under a projecting thatched roof. Internal and external measurements were taken below the wall head and at the wall foot above the plinth on an overcast day in September 2005. Ambient temperatures were in the region of 18°C and relative humidity 87%.

Chart 44 shows the temperature record of a probe needle and base, as well as the ambient temperature from a thermocouple suspended in the air near to the measurement position, before during and after a heating cycle. The ambient temperature changes were not so extreme as encountered at The Body and chart 45 shows the needle temperature to be comparatively stable for 200s prior to the measurement. Chart 46 shows reasonably consistent thermal conductivity results over time for one measurement each in a cob block and in a cob block with lambswool binder, albeit giving distinct values.

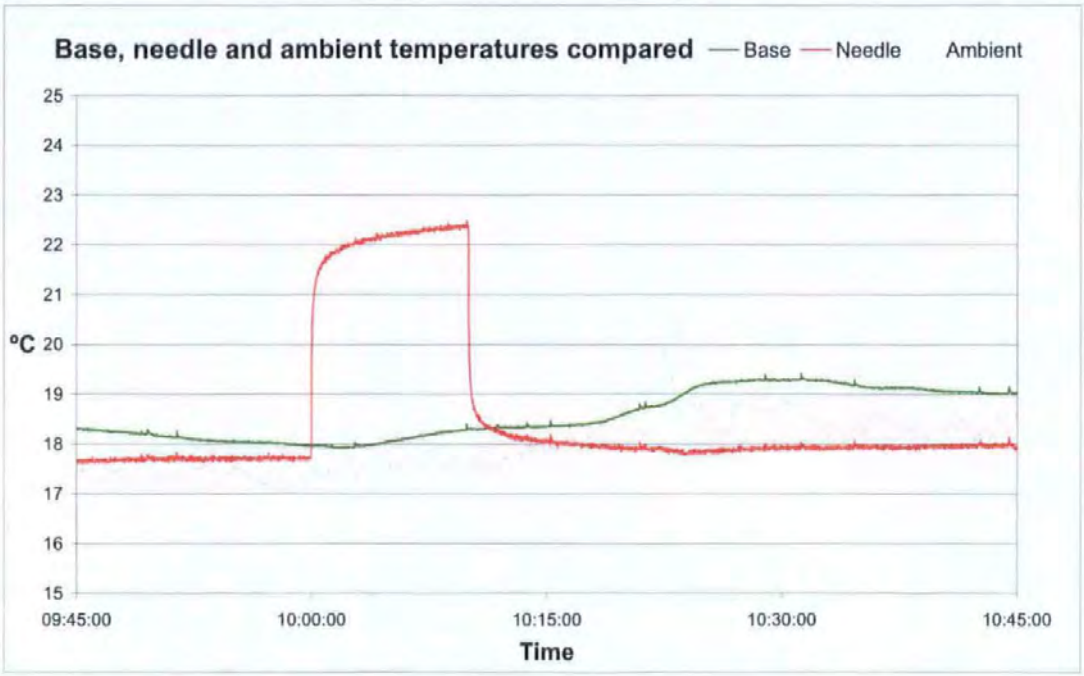

Chart 44: Temperature record of probe base and needle, cob summerhouse

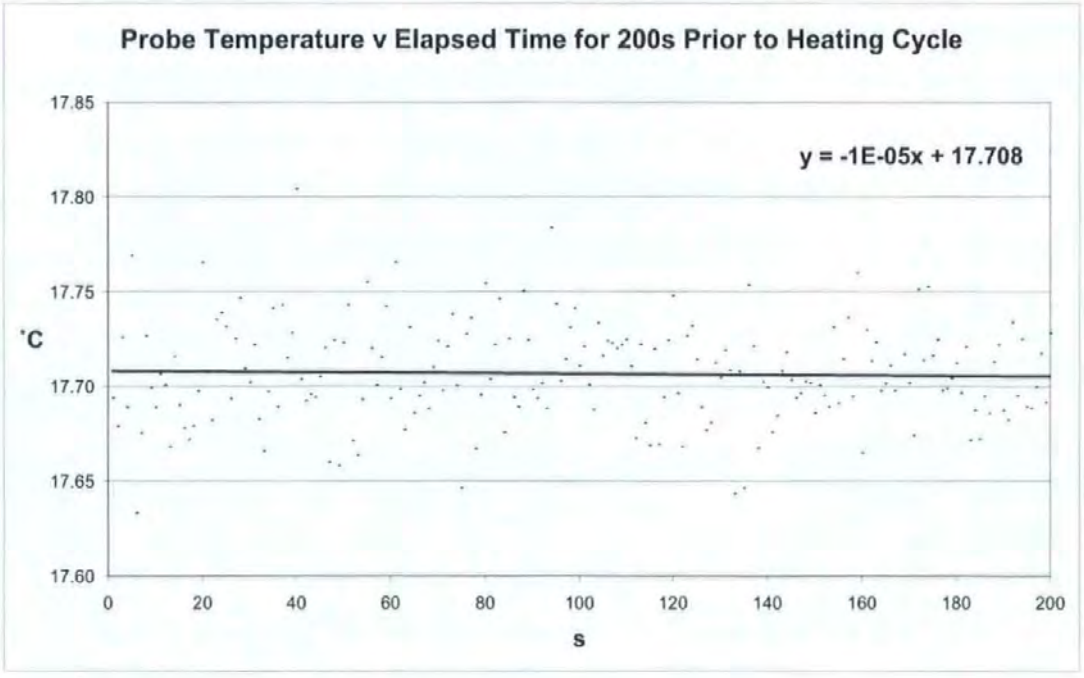

Chart 45: Temperature stability prior to the measurement in chart 52

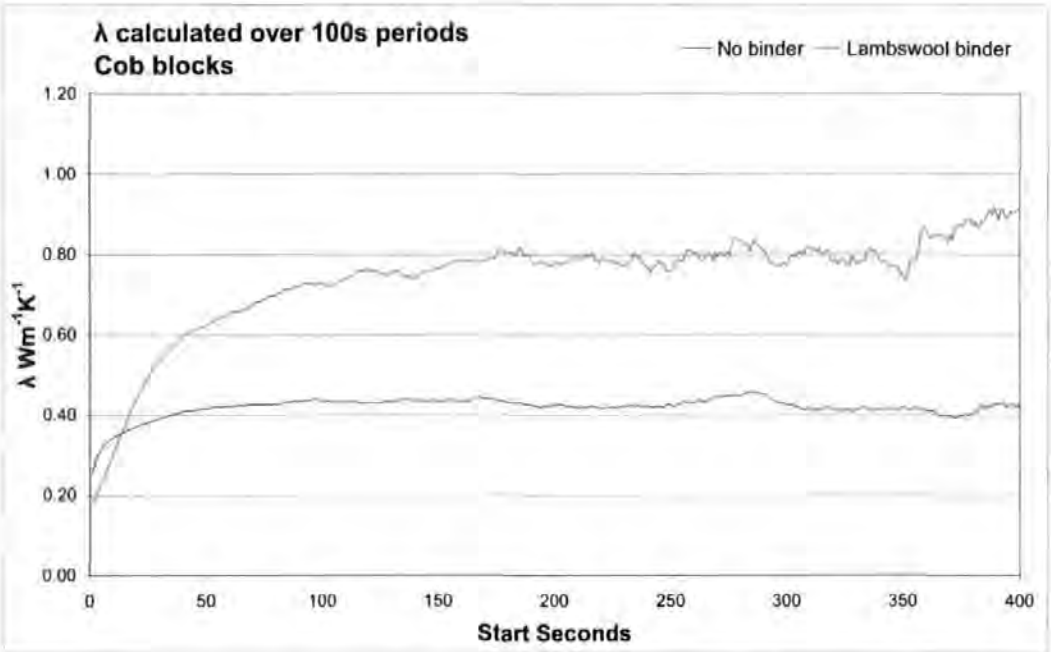

Chart 46: Thermal conductivity, cob blocks with and without lambswool binder

Table 9 gives thermal conductivity results for the four measurement positions using a regression analysis and equation (6) over visually assessed linear asymptotes from printed charts of $\Delta T/\ln t$, using a straight edge.

Probe positions were alternated between each of the four holes throughout the day to ensure measurements were not affected by any bias caused by probe construction. It was found that the time windows for linear asymptotes varied between measurements, from 50s – 150s to 200s – 500s. Linear asymptotes were also assessed onscreen while still on site. The results based on these time windows varied by up to ± 5% from those achieved later with the assessment of printed charts.

It is interesting to note that thermal conductivity results were higher for the external measurements for both block types, which could be expected from moisture level patterns in an unoccupied building with no guttering, with

unplastered walls, in a sheltered situation with a fairly high relative humidity. It is also interesting to note the difference in results between the two types of cob block. The manufacturer's expectation had been that the lambswool would provide additional insulation to the blocks, which expectation was contradicted by the results.

	Without lambswool		With lambswool	
	External	Internal	External	Internal
Mean $Wm^{-1}K^{-1}$:	0.556	0.467	0.889	0.761
Standard deviation:	0.017	0.027	0.051	0.075
Variance coefficient:	3.10%	5.71%	5.76%	9.83%

Table 9: Thermal conductivity results for cob blocks

Case study 2, Aerated concrete eco-house

This case study relates to a single storey, award-winning eco-house in North Cornwall. It was constructed of 250mm thick, solid walls of insulating, aerated concrete block, lime rendered internally, lime rendered and part timber clad externally. The building was set on a slope with aerated concrete foundation blocks exposed to the lower, south side. Internal and external measurements were taken at wall heads and wall feet, both above the damp proof course, and also externally below the damp proof course level. The building owners were happy to have small holes of 2mm diameter drilled in the walls, although they would not go so far as to consider the technique as non-destructive.

The measurements took place in June 2005, during hot, sunny weather. The house had been unoccupied for the previous two weeks. Measurements were taken externally in the morning on a west facing wall with ambient temperatures in the region of 19°C and relative humidity starting at 74% and dropping to 62%

through the morning. Internal measurements were taken during the afternoon in the kitchen area on a south facing wall, exposed to an expanse of east facing glazing, with ambient temperatures in the region of 29°C and relative humidity in the region of 48%. Figure 22 shows the house and measurement positions for the foundation blocks and kitchen.

Figure 22: North Cornwall eco-house showing various measurement positions

The manufacturer's literature had given guarded hot plate thermal conductivity values of 0.11 $Wm^{-1}K^{-1}$ and 0.15 $Wm^{-1}K^{-1}$ for the insulating and the foundation

blocks, respectively. Samples were measured with the thermal probe under laboratory conditions at various moisture contents, giving results for the insulating block from 0.193 $Wm^{-1}K^{-1}$ at 4.6% moisture content by weight to 0.113 $Wm^{-1}K^{-1}$ for a dry block.

Table 10 shows the results and variance coefficients for the six measurement positions. Chart 47 shows a typical probe needle temperature record, including stabilisation with the insulating block after probe insertion at 14:07. The record is shown with the temperature record of the probe base, which is affected by ambient conditions, before during and after one heating cycle. Chart 48 shows minimal temperature drift for 200s prior to the measurement.

	Mean λ $Wm^{-1}K^{-1}$	Standard Deviation	Variance coefficient
Foundation block, 120mm above ground level	0.509	0.0038	0.76%
Foundation block, 120mm below dpc.	0.239	0.0088	3.69%
Insulating block, 200mm above dpc. external	0.173	0.0085	4.90%
Insulating block, 1,400mm above dpc. external	0.153	0.0012	0.81%
Insulating block, 100mm above floor level, internal	0.136	0.0002	0.11%
Insulating block, 1,680mm above floor level, internal	0.132	0.0002	0.12%

Table 10: Thermal conductivity results, north Cornish eco-house

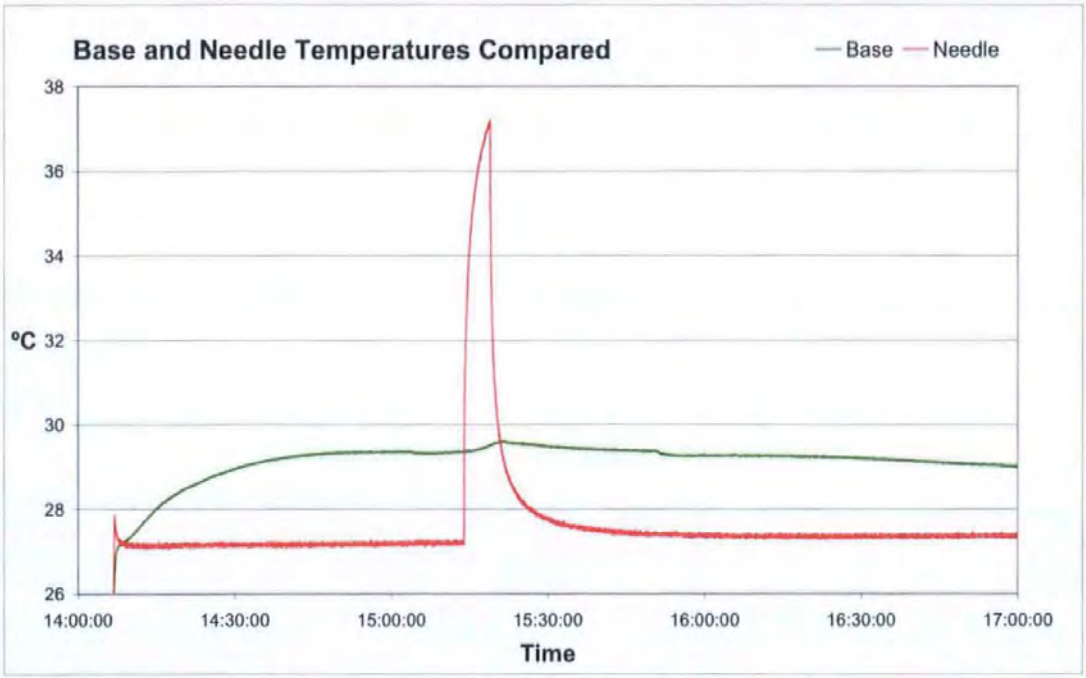

Chart 47: Temperature record of probe base and needle, aerated concrete, internal

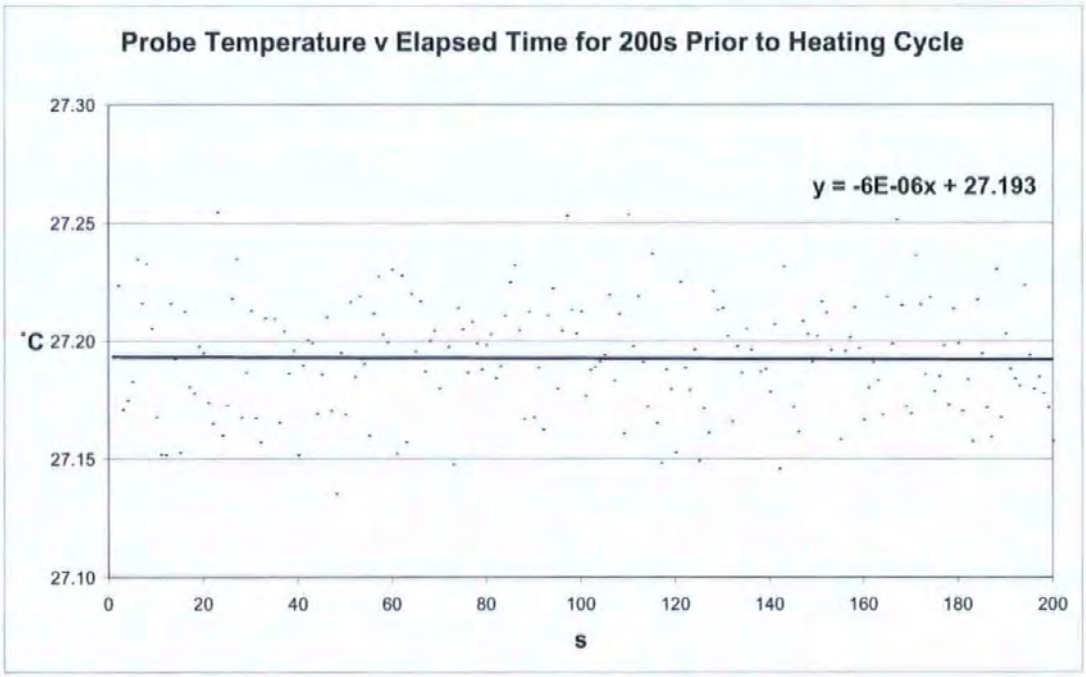

Chart 48: Temperature stability prior to the measurement in chart 56

Chart 49 shows the in situ thermal conductivity results over 100s periods for the internal measurements at the wall head and foot compared to the laboratory

based measurements of an oven dried sample. The internal face of the walls appeared dry and showed zero moisture content when tested with a resistance type moisture meter, an ETI 7000. The thermal conductivity results, being higher than the laboratory based measurements of an oven dried sample, suggest that some moisture was present, and slightly more at the foot than at the wall head.

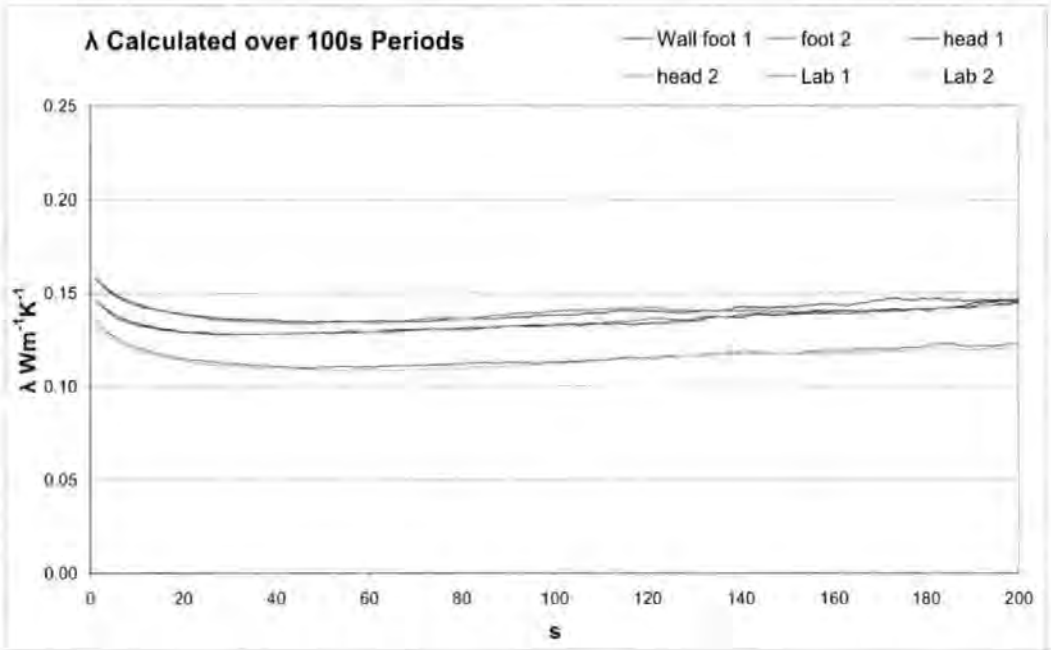

Chart 49: Thermal conductivity, aerated concrete in situ and laboratory results

The average thermal conductivity of all the above-dpc measurements, of the internal and external faces of the external walls, using visually assessed linear asymptotes for regression analyses, was 0.149 $Wm^{-1}K^{-1}$ compared to the design value of 0.11 $Wm^{-1}K^{-1}$. The averaged in situ results gave a U value of 0.51 $Wm^{-2}K^{-1}$ for the walls compared to the design value of 0.44 $Wm^{-2}K^{-1}$. This represents a potential 16% increase in heat transfer losses through the walls. The measurements were carried out in a dry period of mid summer while the house was unoccupied. It is to be expected that this difference from design

value would be significantly greater with an occupied house in a normally wet and humid Cornish winter, where penetrating damp and interstitial condensation would raise the thermal conductivity levels of the walls. This potentially greater heat loss would coincide with the time of year when heating would be more in demand.

The low variance coefficients in table 10 and the parallel results in chart 49 show that good levels of repeatability were obtained in situ and that they were comparable to those achieved with laboratory based measurements.

Case study 3, Unfired earth and woodshavings eco-house

Measurements at this award winning eco-house in Scotland took place during cold dry weather in November 2005. The walls were formed of earth plastered, 105mm thick, unfired earth and wood shaving bricks, an offset 100mm timber frame with 200mm cellulose insulation and larch cladding. The building had been designed to take advantage of solar gains, with the bricks envisaged as absorbing excess heat and providing thermal storage. There was minimal glazing to the north elevation and reasonably extensive glazing to the south side. The roof was formed of softwood trusses including 220mm cellulose insulation, with plasterboard under and natural slate over. The building had subsequently been found to overheat in summer (Morton et al, 2005). Figure 23 shows solar shading added to the south elevation to reduce this effect. The insert shows an example of the brick used in the wall construction.

Figure 23: Unfired earth and woodshaving brick house with an example brick

The house was an occupied family home, although unoccupied during the day of the measurements. External temperatures were between 0°C and 5°C through the day. Internal temperature was kept near to 22°C with oil fired central heating. Internal relative humidity was in the region of 44%.

Chart 50 shows typical results for thermal conductivity measurement results in situ and those taken in the laboratory at the University of Plymouth. It can be seen that the quality of data is at least as good for the in situ measurements, confirmed by table 11 which shows that the laboratory measurements had a higher variance coefficient.

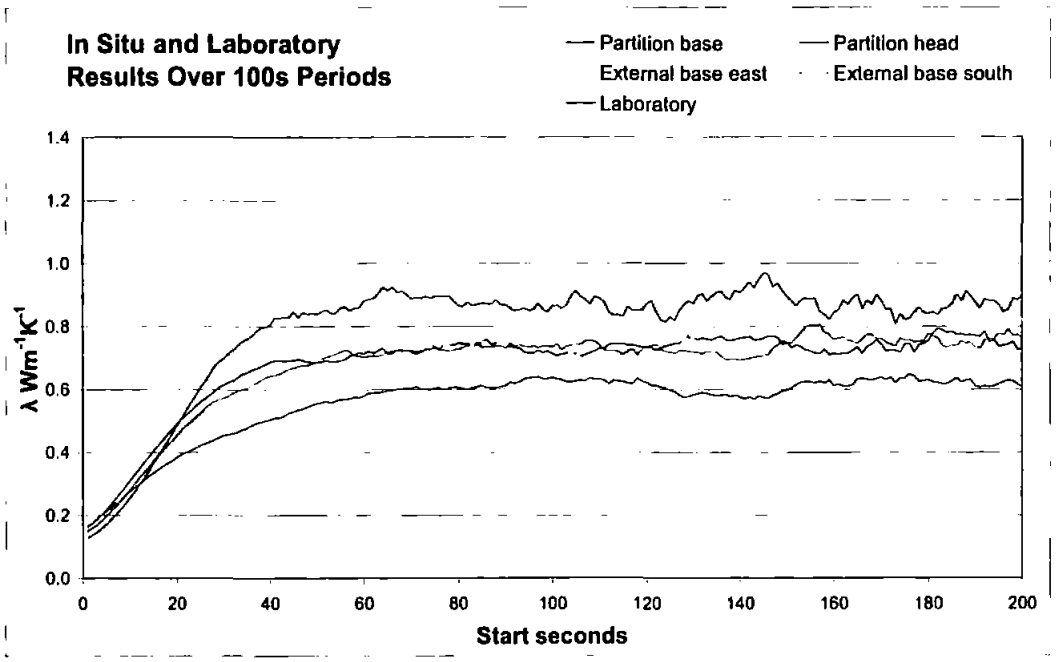

Chart 50: In situ and laboratory results for unfired earth and woodshaving bricks

It is interesting to note that all three in situ measurements at the wall bases gave similar results whereas the measurement at the wall head was found to be lower. This follows a similar pattern to that found in the aerated concrete house, and may be attributable to a pattern of higher moisture contents lower in the walls. This may be of interest for a future study.

The reasons for the higher thermal conductivity values found in the laboratory measurements are unclear. The brick was collected from a stack only partially protected from rain, with a tarpaulin. It was then stored in an occupied room at around 18°C and 70% relative humidity for two months, so may have retained some moisture or stabilised at a higher moisture level than in the case study building where the relative humidity at the time of measurements was 44%. The breathing wall technology and lower relative humidity of the house may have contributed towards lower moisture content and, hence, lower thermal conductivity values.

Some difficulties with the technique became apparent during this case study. It was not possible to be confident that boundary conditions had not been compromised with in situ measurements because of the holed bricks. Attempts were made to avoid this by identifying horizontal and vertical joints at ground level and, using brick dimensions, plotting the likely brick positions behind the plaster above. The low variance coefficients and apparent linearity in $\Delta T/\ln t$ curves would suggest the strategy had been successful in this case. The consistency of brick composition could not be verified, which could provide an alternative explanation for differences in results. It could make it possible to produce similar results for varied compositions at varied moisture contents.

The case study illustrated the probes' ability to identify differences in thermal conductivity from design values. Here it had been estimated at 0.65 $Wm^{-1}K^{-1}$, compared to the average measured value of 0.712 $Wm^{-1}K^{-1}$. It also showed the potential benefits to the engineering of passive heating and cooling strategies should it be found possible to obtain reliable volumetric heat capacity values with the probe in the future, as the initial overheating problem, from solar gains, would have been reduced with increased heat capacity in the internal, structural materials.

	Mean λ $Wm^{-1}K^{-1}$	Standard Deviation	Variance coefficient
Partition wall head	0.613	0.0126	2.05%
Partition wall base	0.748	0.0184	2.46%
External east wall, internal face, base	0.765	0.0185	2.42%
External south wall, internal face, base	0.721	0.0208	2.89%
Laboratory results	0.805	0.0230	3.09%

Table 11: In situ and laboratory results for unfired bricks with variance coefficients

Case study 4, Straw bale garages

Measurements were carried out to the walls of a garage in Stirlingshire, Scotland, on an overcast day in November 2005. Temperatures were in the region of 7°C and relative humidity in the region of 80%. The walls were constructed from straw bales with vertical 50mm x 50mm timber studwork set into the bales at 600mm centres internally, over a fired brick plinth (see Figure 24). The bales had been plastered internally and externally with a clay and lime mixture. Internally, this was between the studwork. Externally it was over wired reed cladding. The plaster depth was not measured and estimated to be around 15mm, plus 10mm externally for the reeds. The external render sounded hollow when tapped and may have come away from the straw in places.

Figure 24: Straw bale garages with probes in situ

Chart 51 shows average thermal conductivity results by equation (6) over 100s periods for internal and external in situ measurements at the wall head and base. Three measurements were taken at each location. The external base measurement, results not shown here, gave wildly fluctuating results after the first 30s and it was presumed that the probe had not been sufficiently inserted into the straw. A further measurement shown was carried out, to the same straw grain orientation, in a laboratory at the University of Plymouth. This was of a straw bale that had been purposely compressed beyond normal density and that had remained in the laboratory under dry room conditions for some months.

Consistent results were achieved for the internal measurements in situ, with low variance coefficients. A consistent pattern was found for the external measurement, albeit with higher thermal conductivity values. This may have been expected from weather conditions affecting the external wall face. The laboratory based sample also gave higher thermal conductivity values, which are likely to have been related to its higher density.

All measurements show, to a similar extent, a rise in calculated thermal conductivity values over time. From the laboratory based studies of insulating materials and the thermographic study, these have been seen to be expected in materials with lower thermal conductivities.

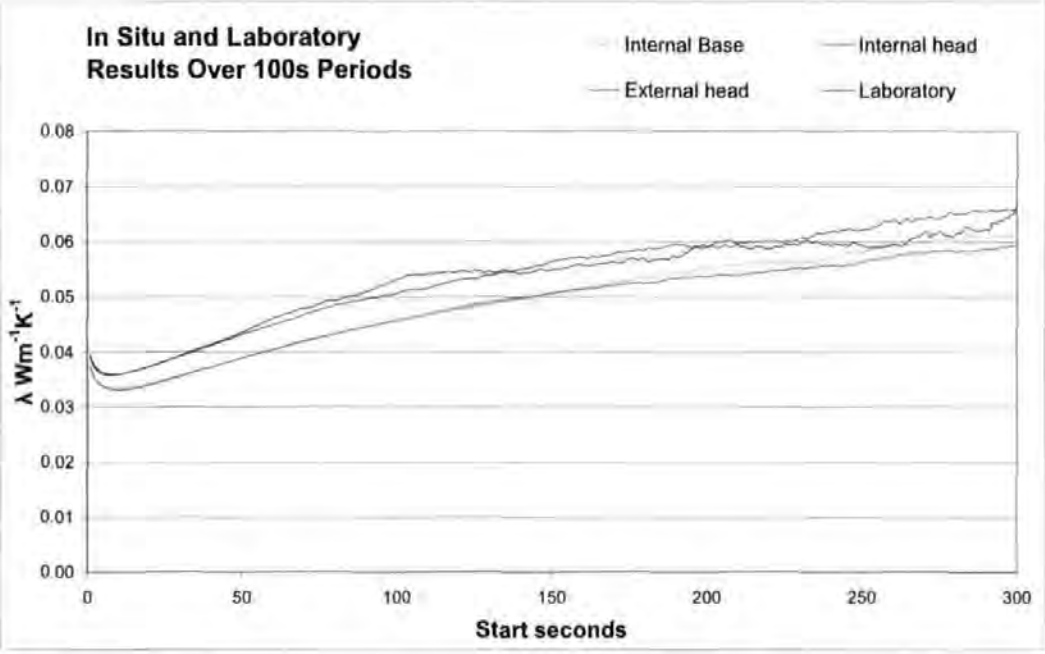

Chart 51: In situ and laboratory results for straw bale construction

Case study 5, Mass clay / straw studio

Wall measurements took place in November 2005 of a studio building in the Scottish Borders, containing a library, office and living accommodation (see *Figure 25*). Ambient temperatures fell during the night to around -8°C with 97% relative humidity, rising during the day to a maximum around 5°C with 60% relative humidity. Internal temperature was in the region of 19°C, heated by a system of hot water pipes embedded in both the floor and walls, with relative humidity around 40%.

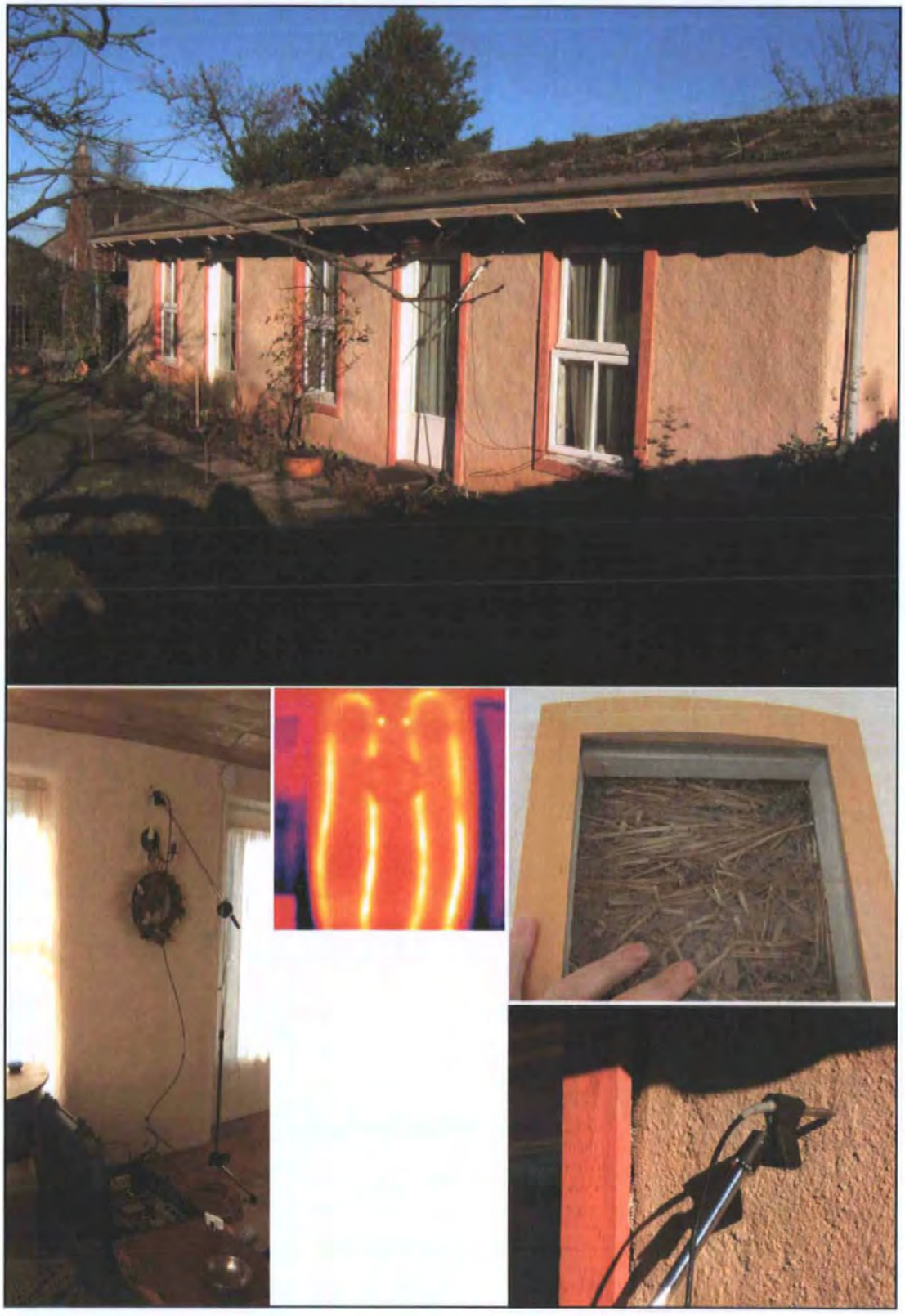

Figure 25: Clay straw studio, Scottish Borders

Measurements were taken internally and externally throughout the course of one day. Four probe positions were used. Chart 52 shows the results, where probe positions were:

Hole A: Internal, 200mm above floor level
Hole B: External, 200mm above floor level
Hole C: Internal, 1.8m above floor level
Hole D: External, 1.8m above floor level

Reasonable repeatability was found for holes A to C, although the rise in results over time presented the usual difficulty found with materials of low thermal conductivity. The external measurement at the wall head showed excessive fluctuations after about 60s for the first two runs. Probes were swapped between holes, and reasonably consistent measurements over time were achieved after reinsertion.

The higher thermal conductivity results at the external wall head, around 0.35 $Wm^{-1}K^{-1}$ compared to an estimated range of 0.06 $Wm^{-1}K^{-1}$ – 0.1 $Wm^{-1}K^{-1}$ for the other positions, were supported by thermal imaging (see Figure 26), which showed the external wall head to be significantly warmer on a cold morning than the greater part of the walls. The thermal image could indicate either greater heat loss through the building fabric or greater thermal storage in the building fabric, or a combination of these, at this position, possibly as a result of a denser mix being used. Figure 27 shows the method of construction whereby the lightweight clay straw mixture was placed in a studwork frame using shuttering. As can be seen from this, and the in situ sample shown in plate 12, it was not possible to assess variations in the mix consistency, which would lead

to varied thermal conductivity values, and so identify any potential effects from moisture ingress.

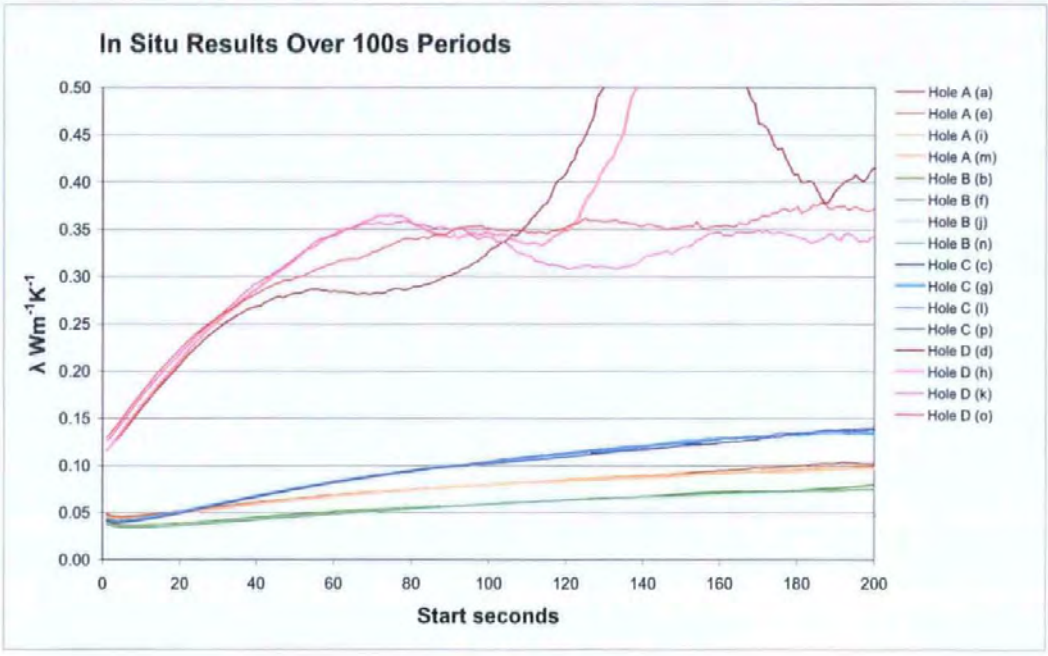

Chart 52: In situ results for clay straw wall construction

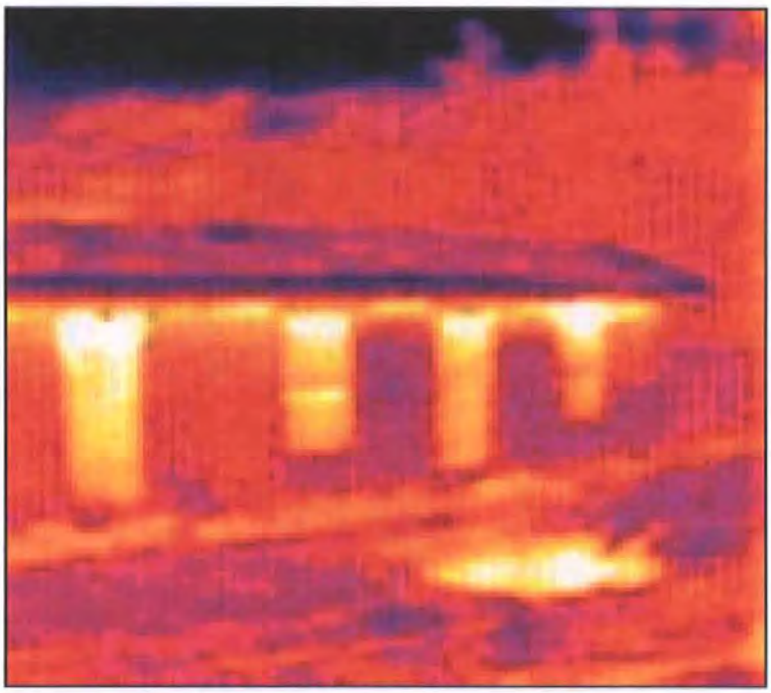

Figure 26: Thermal image of clay straw studio, ambient temperature -8°C

Photo courtesy of Chris Morgan

Figure 27: The clay straw studio under construction

The in situ conditions presented an opportunity to asses the effects of prior temperature instability against the 0.1°C maximum drift recommended in the ASTM standard (2005). Chart 53 shows two results for the external position 200mm above floor level. The needle temperature in the first measurement (b) rose gradually by 0.35°C for the 200s prior to the measurement. Prior to the second measurement (f), the needle temperature fell by just under 0.1°C. The difference in results, which also appeared in chart 60, was not significant, at less than 3%, compared to the rise in values over time.

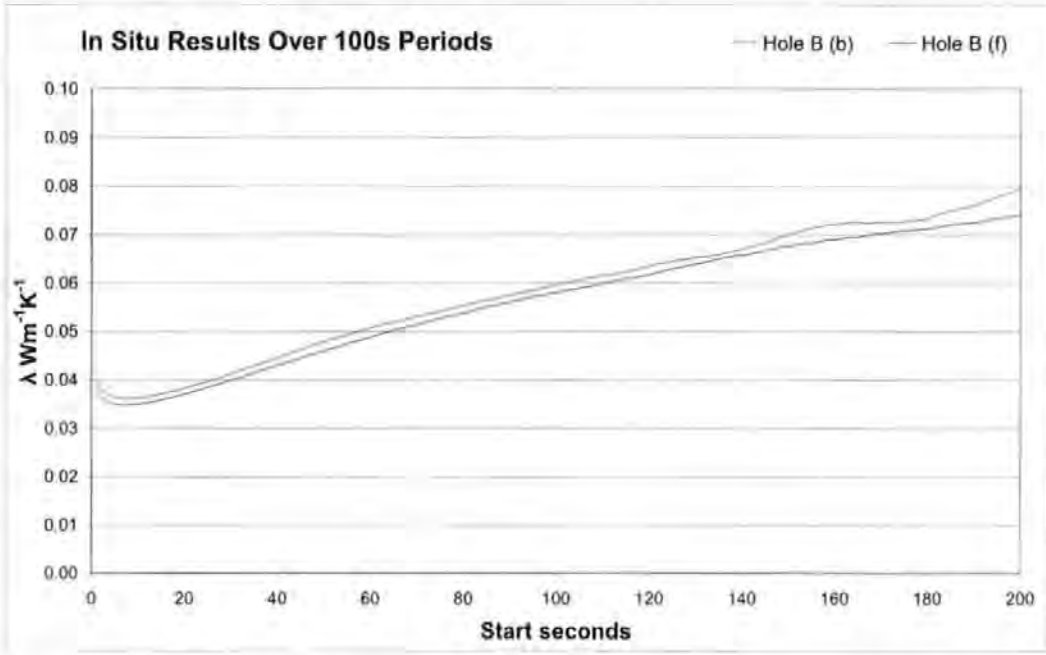

Chart 53: Two in situ clay straw results with varied prior temperature drifts

This case study has shown that reasonable measurement repeatability can be achieved in quite extreme temperature conditions. The variance coefficients for holes A – C were in the region of 2%. It has been shown that limitations to the technique, with low thermal conductivity materials, were more significant than the ambient environmental effects encountered.

A limitation to the technique was encountered in that the wall composition appeared to be quite varied, hence it was not possible to identify potential changes caused by moisture ingress. However, it is difficult to imagine any other current technique that could give representative values for walls with varied composition and varied moisture content. Monitoring over time, as was carried out by Boekwijt and Vos (1970), could provide more clarity on moisture changes.

The heating pipes in the wall were unmarked. Such matters could compromise the non-destructive nature of the technique in practice, as could any electrical circuits or plumbing installations accidentally encountered.

Summarised findings from the case studies

The field apparatus worked reliably and thermal conductivity results in the field showed similar levels of consistency and repeatability to those achieved in the laboratory, even when measurements were taken under fairly hostile conditions, such as under intermittent solar irradiation at over 35°C, as in the first part of case study 1, or at near freezing point, as in case study 5. It was usually possible to achieve appropriate levels of temperature stability over the measurement period, with prior thermal drifts less than 0.1°C over 200s, which could be confirmed in post measurement analysis.

Case study 1 showed that consistent results could be obtained in inhomogeneous materials. The random distribution of small stones in the cob did not cause discernible fluctuations or changes to thermal conductivity results throughout the duration of a measurement.

The second part of case study 1 showed that variations in thermal conductivity caused by changes in material composition were readily identifiable. Two types of similar earth block were measured, one incorporating a sheepswool binder. Contrary to expectations, the latter block was shown to have a higher thermal conductivity than the former.

The laboratory assessment of aerated concrete (see chart 36) showed that the thermal conductivity of an oven dried block rose after it had been left standing in

a notionally dry room for six days. A similar effect was shown in case study 2 where variations in thermal conductivity, and therefore 'U' values, caused by minimal moisture content were readily identified. The structural material of a wall, measured as having 0% moisture content by a resistance type moisture meter, in a house at the height of summer was found to have a thermal conductivity around 20% higher than its published design value. This created a 16% higher 'U' value for the wall element than its approved design value. The published design value for the insulating, aerated concrete blocks had been achieved by a UKAS accredited guarded hot plate apparatus, which method requires that materials are dried prior to a measurement being taken. The GHP results for the particular type of aerated concrete had also been replicated by thermal probe measurements in an oven dried sample.

Case study 3 showed consistent measurements for an inhomogeneous material, unfired earth with a randomly spread inclusion of wood shavings. It showed a difference in measured to design thermal conductivity values in a dry construction. The design had been based on a thermal conductivity value taken from generic data for similar materials, whereas the measured value was approximately 10% higher. Case study 3 also supported the case for future work in attempting to measure thermal diffusivity, and consequently volumetric heat capacity, by the thermal probe method, as the passive heating technology employed had been compromised by a lower thermal capacity than expected in the unfired earth and wood shaving bricks.

It was shown in the laboratory work that thermal conductivity results, rather than thermal conductivity, rose over the duration of a measurement in materials with low thermal conductivity, which rise increased as the thermal conductivity of

samples decreased. The thermographic assessment confirmed this was caused by increased heat losses from the probe and the sample material surrounding the probe entrance, these losses being to the surrounding air and to the probe base. The straw bale and clay straw case studies, 4 and 5, showed that the effects of these end, axial and entrance losses were a far greater problem than temperature drift in materials of low thermal conductivity, under quite extreme environmental conditions.

Other practical difficulties were identified, which anyone carrying out future work should be aware of. These included: the difficulty in identifying masonry joint positions under plaster, as in case studies 2 and 3; features such as hidden air voids, as in case studies 3 and 4; as well as wiring and plumbing locations, as in case study 5.

Chapter 7: Further work, discussion and conclusions

This section starts by suggesting areas for further work, where their significance has been identified through the project. This is followed by a critical appraisal of the project, highlighting where, with the benefit of hindsight, the methodologies might have been improved. The results of the current work are then discussed, which leads to the overall conclusions from the project.

Suggestions for further work

A guarded probe

The issues of asymmetric axial and end losses, which have been seen to significantly affect thermal conductivity measurements of insulants, and which are less of a problem in fully embedded hot wire techniques, may be addressed by a redesigned thermal probe. The problem occurs at the entrance to the sample medium with heat losses to the surroundings from the probe end, from the sample near the probe entry and through cable connections. It was found during the experimental work that insulating the external area did not improve results as the situation remained asymmetric. In some cases, insulating the external face made matters worse by allowing a greater build up of heat in the probe base and its components.

The redesigned probe would have a guarded end whereby the heater section, reduced to, say, 50mm long, would have a suggested 25mm unheated section at the end nearest the opening. The heater should be supplied with fine, low impedance cables through this section to avoid temperature rise through

electrical resistance and to avoid conduction losses from the heated section. The thermocouple cables should also be kept fine for this reason.

The material for the guarded section would need to be structurally strong and able to be finely machined, to form a connection with the heater, and to have fine holes to carry supply cables. It should be of low thermal conductivity and high thermal diffusivity to prevent heat losses and to quickly adjust to the sample temperature. The thermal and mechanical properties of various materials should be examined to assess which would best fit these criteria.

The shorter probe, if kept at the same diameter, would reduce the length to radius ratio from the current 120:1. Equation (21) showed that axial losses with the 72mm x 1.2mm hollow stainless steel probe, in an insulator such as phenolic foam with a thermal conductivity of 0.04 $Wm^{-1}K^{-1}$ and thermal diffusivity of 9.52 $x10^{-7}$ m^2s^{-1}, should be less than 1% up to 270s whereas charts of thermal conductivity results over time started to rise much earlier for such materials, because of entrance losses and end losses through attached cables.

A similarly constructed 50mm probe, if reduced to 1mm diameter, giving a length to radius ratio of 100:1, would have, by equation (21), less than 1% axial loss error up to 120s. While this time is shorter than for the longer probe, the potential reduction in entrance and asymmetric end losses should more than compensate. It is also of note that probe conductance *H* has no great effect on the results from equation (21), which may mean that such smaller diameter probes could still be viable in the hole sizes available by current drilling techniques. Equation (21) was also applied in the case of a 50mm x 1mm guarded probe for a sample with a thermal conductivity of 0.6 $Wm^{-1}K^{-1}$ and

thermal diffusivity of 1.4E-07 m^2s^{-1}. This gave less than 1% error from axial and end losses up to 1,200s.

Care should be taken with the redesigned probe that the thermocouple cold junction is placed such that its temperature can be reliably measured by the platinum resistance thermometer, possibly within a small insulated chamber within the probe base so as to dampen the effects of thermal changes brought about by environmental conditions, where they could produce a temperature gradient between the components.

Computer simulations

The computer simulations in Appendix A showed that, when representing the perfect model, linear asymptotes of $\Delta T/\ln t$ were not always achieved. This modelling should be carried forward with the introduction of a virtual probe made up of various components, such as a heater wire, a filler, and a casing, with thermal resistances between them and between the casing and the virtual sample medium. The effects of each of these thermal resistances should then be assessed against the standard theoretical solutions for thermal conductivity and thermal diffusivity.

The probe should then be modelled with axial, end and boundary losses, and curves compared to experimental curves. The aim would be to match curves where the model input values were those of real materials. The model should then be tested to see whether or not identical curves could arise for diverse properties, such as varied combinations of α and H, such as had been found by Jones (1988). If not, then the model may be able to show the different effects of

α and H on $\Delta T/\ln t$ so that they could be individually quantified, with the potential to obtain values for thermal diffusivity and volumetric heat capacity.

The effects of experimental data scatter should be borne in mind where this route may be taken. The comparisons to simulated data, in Appendix A, have shown that the extent of scatter when using a K type thermocouple to measure probe temperature may have a greater effect than the effects of α and H.

Data produced by computer simulations of the perfect model did not always fit the standard theoretical solutions for thermal conductivity and thermal diffusivity. This was especially true where thermal conductivity and thermal diffusivity values strayed from what appears to be the mid range of such values for common non-metallic materials, such as water at around 0.6 $Wm^{-1}K^{-1}$ and 1.4 $x10^{-7}$ m^2s^{-1}. It may be possible that thermal probe theory has not taken into account a sufficiently wide range of parameters to cover the eventualities that may be encountered when carrying out transient measurements of the range of building materials of interest.

New mathematical solutions for thermal diffusivity results may need to be sought as the standard equation does not appear to fit experimental curves in practice, which may or may not be borne out by the proposed computer simulations using a virtual probe. The consistency of the practical experimental curves achieved is excellent, giving the prospect that a solution based on these curves could prove valid. It seems possible, from the computer simulation work, that a thermal diffusivity solution might be found in the timing and extent of deviation from linearity in $\Delta T/\ln t$. Removing deviations from linearity caused by

entrance losses, as proposed with the guarded probe, may go some way towards assisting such a thermal diffusivity solution.

Calibration

A selection of materials should be developed to be used in calibration for thermal conductivity and thermal diffusivity measurements. These should have diverse thermal properties, across a range of thermal conductivities at various thermal diffusivities. Perhaps six materials would be a minimum requirement, with two each at three thermal conductivity values with different thermal diffusivities, such as:

A = 0.03 $Wm^{-1}K^{-1}$ and 1.00 $x10^{-7}$ m^2s^{-1}
B = 0.03 $Wm^{-1}K^{-1}$ and 9.00 $x10^{-7}$ m^2s^{-1}
C = 0.60 $Wm^{-1}K^{-1}$ and 1.00 $x10^{-7}$ m^2s^{-1}
D = 0.60 $Wm^{-1}K^{-1}$ and 9.00 $x10^{-7}$ m^2s^{-1}
E = 1.50 $Wm^{-1}K^{-1}$ and 1.00 $x10^{-7}$ m^2s^{-1}
F = 1.50 $Wm^{-1}K^{-1}$ and 9.00 $x10^{-7}$ m^2s^{-1}

Calibration would be further enhanced for in situ measurements where these materials could be provided with varied textural forms, such as smooth, cellular or granular solids.

It is suggested that the calibration materials may not need to be of the quality required for precise work. Should it be ensured that these values were within say 5% for thermal conductivity and 10% for thermal diffusivity, they should ensure that errors in the orders of magnitude identified in various previous works did not reoccur.

Forming holes for the thermal probe in hard materials

One of the more difficult and unresolved aspects of the project was finding a practical solution to forming small holes in hard materials. The ideal solution was considered to be a slow rotating masonry drill bit, so as not to raise temperatures through friction, as this could alter moisture contents of materials being measured. The target drill bit diameter was a maximum of 2mm with a cutting depth of 72mm. The smallest SDS drill bits normally available and of sufficient length were found to be 5mm diameter and the smallest standard masonry bits, which could be used with an adaptor chuck in an SDS drill, were 4mm.

Various local, national and international drill manufacturers and suppliers were contacted with requests to provide more suitable drill bits. Most requests were declined although a local manufacturer attempted to braze a 2mm tungsten tip to a slightly smaller, fluted shaft. The flutes were too shallow and the drill bit clogged in a stone sample and broke. A national supplier eventually supplied a batch of 3mm, extended masonry bits but the cutting edges failed to perform and it was found impossible to penetrate hard materials such as granite or Plymouth limestone with these.

Minute diameter, but very short, masonry type bits are available and commonly used by such as jewellers using semi precious stones. With this in mind, it would seem possible that suitable drill bits could be manufactured, although this may require stress calculations of the pressures exerted on and by a 2mm tungsten cutting blade mounted in a fluted shaft sufficiently smaller than the cutter to allow dust to be brought out from the hole during drilling. Any future

work where it is envisaged that small probes may be used in hard materials should allow sufficient time and resources to resolve this difficult and potentially pivotal issue.

Critical appraisal of the project

There were a great many unknowns at the start of this project and the strategy adopted could be likened to throwing a number of balls in the air, and juggling as many as possible until they formed a coherent pattern. While various either previously unrecognised or previously unconnected factors became apparent and related by this method, in hindsight, various improvements could have been made. Chief among these would have been the earlier use of more reference materials.

The lack of reference materials had been reported by Banaszkiewicz et al (1997), and highlighted in a workshop at the 15th European Conference on Thermophysical Properties (Kubicar, 1999). However, the levels of accuracy required for the absolute values being sought could have been reduced for the current work, where it was being attempted to avoid errors sometimes amounting to hundreds of percent. In this case, it would have been prudent to build a guarded hot plate apparatus and obtain or build a drop calorimeter, as described by Touloukian and Buyco (1970), to check the validity of laboratory based measurements and analysis routines. Laboratory compliance to BS EN 1946-2 (BSI, 1999a) for the guarded hot plate apparatus would have been an advantage but cost prohibitive, although the validity of future work may require this.

Contact with contemporary researchers in the field could have been expanded during the project, as could the output of peer reviewed articles. Although researchers in the particular field are few and far between, contact or conference attendance with contemporary researchers involved with the pure and applied physics of heat transfer may have made some issues clearer, earlier.

At the inception of this work, the thermal probe technique to measure thermal conductivity and thermal diffusivity to good levels of approximation was considered to be reliable under controlled laboratory conditions. The initial purpose of the work was then to transfer the methodology to in situ measurements, identifying and carrying out the work needed to allow for the diverse environmental conditions encountered. The applied physics of heat transfer in transient line source measurement was a new area of study for the author and hence much initial work was undertaken before it was confirmed that the laboratory based technique had unresolved issues regarding thermal conductivity measurements, and that a reliable thermal diffusivity measurement methodology by the thermal probe technique in granular materials was lacking from the literature. This was apart from the difficulties found with in situ measurements, and despite the various publications that had claimed the method had moved from an experimental technique to use as a practical engineering tool.

Discussion

The aim of this project was to assess the transfer of the thermal probe technique, as a means of measuring the thermal conductivity and thermal diffusivity of construction materials, from laboratory to in situ measurements. This assessment has been carried out through: a literature review; evaluations of the previous work carried out at the University of Plymouth and the solutions reported in the literature; and three further areas of scientific research. These were: computer simulations; laboratory studies; and in situ studies. The introductory chapter presented the rationale for the work, the environmental and economic benefits that could be gained and illustrated the lack of robust alternative sources for in situ thermal conductivity and thermal diffusivity data.

Peer reviewed articles had suggested that the method was already sufficiently advanced to use as an engineering tool. The evidence of a wider ranging literature review was contradictory and it was found there was not a consensual agreement on a comprehensive or reliable methodology for thermal conductivity of thermal diffusivity measurements by the thermal probe. This meant that laboratory techniques required investigation before in situ measurements could be undertaken with confidence.

Formulae, generally deriving from Fourier's heat conduction equation via the work of Carslaw and Jaeger in the early and mid 20th century, described the theoretical solution to the transient line heat source problem. These formulae included avoidance of errors during the initial heating period of a physical probe, where the thermal properties of the probe itself exerted more influence on the temperature rise, and strategies to avoid significant axial and end losses along

and from the probe at later times. Further formulae were given to ensure avoidance of errors arising from losses or reflections at the sample boundary.

These formulae depended on a knowledge of the thermal conductivity and thermal diffusivity of the samples under consideration. Where these were known, a time window from the heating curve could be identified, after the early probe influences were sufficiently reduced, and before the axial, end or boundary losses caused significant errors. This time window, at least in homogenous materials, was then said to provide a linear asymptote of $\Delta T/\ln t$, to which solutions could be fitted. In the practical case, where thermal diffusivity was unknown, it was held that conditions were met in any case where a linear asymptote occurred. The slope of this asymptote was used to calculate thermal conductivity, and the intercept to calculate thermal diffusivity. A complication arose as the intercept shifted depending on the extent of thermal contact, or probe conductance, between the probe and sample.

Previous researchers at the University of Plymouth had developed an iterative optimisation procedure based on Solver spreadsheet solutions in MS Excel to simultaneously calculate the three unknowns: thermal conductivity; thermal diffusivity; and probe conductance, from $\Delta T/\ln t$. This solution required estimated values to be entered for the three unknowns. The sensitivity to these input values was tested in chapter 4. It was found that widely varying results for thermal diffusivity, and therefore volumetric heat capacity, could result from small changes of input estimates, while meeting all the other conditions of the routine. The sensitivity of the equation used in the standard solution was tested and it was found that it was not possible to differentiate between the

temperature rise effects of thermal diffusivity and probe conductance, or contact resistance, by this method.

Computer simulations were carried out to model the temperature rise of a line source. This was done to assess the matching of simulated curves to experimental curves and to assess solutions from the literature using a perfect model. The perfect model comprised an infinitely thin and long line source in an infinite, homogenous material. In such a case, no effects should occur as a result of physical probe presence, such as axial and end losses, probe conductance or thermal contact, and probe thermal capacity. The modelling of an infinitely large, homogenous sample should remove effects from boundary losses or reflections. In this perfect model, S and U shaped curves of $\Delta T/\ln t$ were found at early times similar to those encountered with a physical probe. It was also found that the slope of $\Delta T/\ln t$ did not achieve linearity at all in most cases, giving rise to errors in thermal conductivity and volumetric heat capacity calculations of up to 8% and 20% respectively, at the extents of the wide ranging combinations of these values studied. The Solver solution was also found to remain sensitive to input estimates for the perfect model used in the computer simulations.

A series of laboratory based measurements were carried out using a pre-existing apparatus and, later, a robust apparatus developed during the project for field work applications. Two currently marketed thermal properties probe meter systems were also borrowed and trialled. Results from the borrowed probes showed that calibration in one material, for either thermal conductivity or thermal diffusivity, could not be relied upon to transfer to other materials. Work with both sets of project apparatus showed that, for thermal conductivity

measurements, the time windows for near linearity in $\Delta T/\ln t$ varied from material to material. No solution to measure thermal diffusivity, transferable between diverse materials, was found reliable for any of the practical methods undertaken.

It was seen that calibration in one or two materials, as suggested in the relevant international and American standards, was not sufficient to allow the assumption of reliable measurements in other materials. There are a number of reasons for this. One example would be where the appropriate time window changed between materials with different thermal properties. In such a case, a simple numerical factor applied to a result achieved from the linear asymptote in one material, to meet a reference value, could not be assumed to transpose to another material over the same time period, as the same time period in other materials may not coincide with linear sections of $\Delta T/\ln t$. The same problem would arise where experimental parameters were changed in the measurement of one material, such as creating a theoretical radius for the measurement position from the line source to achieve a reference thermal conductivity value. No basis has been found that the same adjustment would be appropriate for other materials with different thermal properties. It should be emphasised that these differences would be predominantly dependent on the unknown thermal properties of the materials being studied rather than the properties of the probe itself.

The laboratory work assessed such factors as hole size, contact fillers, power levels, and temperature stabilisation periods. It was found that reliable data could be obtained where hole sizes were as small as possible and high thermal conductivity contact filler used. Power levels were found appropriate where they

produced temperature rises in the region of 7°C to 15°C, and Charts 24 (PTFE) and 27 (aerated concrete) showed that, where axial, end, entrance and boundary losses were avoided, power levels did not affect thermal conductivity results.

The probes used were normally found to stabilise their temperature with that of the samples in less than 30 minutes, which could be assessed by observing live display charts, which assessment was then confirmed during post measurement analysis (see Chart 18 for an example in aerated concrete). The temperature change over time as residual heat dissipated from a previous measurement, for all those carried out in the project, became insignificant, that is less than 0.1°C over 200s, within an hour (see Chart 20 for an example in aerated concrete). Again, this could be assessed from the live display charts and then confirmed during post measurement analysis.

The probe technique was found able to measure differences in thermal conductivity dependent on moisture levels, with the repeatability of results, as in Table 6 for aerated concrete, showing that moisture migration effects were imperceptible.

The linearity of $\Delta T/\ln t$ curves was assessed by carrying out regression analyses over 10s, 50s, 100s and 150s time windows for the whole measurement period at 1 Hz to give experimental values for thermal conductivity. A study of over 700 measurements carried out during the project showed that $\Delta T/\ln t$ curves moved farther from linearity with samples of lower thermal conductivity, where values steadily increased over time. This showed that considerable errors must have been occurring as the sample thermal conductivity could not be changing to

such extents. A thermographic study in chapter 5 showed that significant but unquantifiable heat losses were occurring from the sample and the probe at and around the point of insertion. These particular combinations of end, axial and boundary losses, may, for want of a better term, be called the entrance losses. Such heat losses would be consistent with thermal conductivity results appearing to rise over time.

Håkansson et al (1988) had observed that relative end losses to connecting cables increased with lower thermal conductivity samples. Here, the entrance loss effect was noticeable with materials below around 0.13 $Wm^{-1}K^{-1}$, although some linearity was still detectable at this level immediately after the early, probe heating period. Below around 0.07 $Wm^{-1}K^{-1}$, no appreciable linearity existed and it was not found possible to measure the thermal conductivity of such materials as building insulations. These limits varied slightly dependent on the thermal diffusivity of the samples.

It is of note that Blackwell's (1956) article describing axial and end loss calculations, the results of which were later relied upon by many researchers, had considered the case of axial symmetry, where Jaeger (1955) and others had considered heat losses through attached heater supply and thermocouple cables. Blackwell's article, and his subsequent publications, despite describing inserted probes, did not discuss the challenge to this symmetry caused by the open ends of both the insertion hole and the adjacent surface area of the volume of sample being heated. It has not been discussed whether it would be possible to confidently distinguish axial and end losses, which would occur with a fully embedded probe, from entrance losses. It may have been that such matters were of minor import where probes used in geophysics were in the

region of 0.8m long. However, with the small probes used here, and appropriately sized for construction materials, the entrance loss effects in more insulting materials appear to be greater by orders of magnitude than those caused by normal measurement data scatter and slight variations in hole size, power level, temperature stability, etc.

The laboratory work provided the basis to carry out in situ measurements. It was found that the methodology transferred well. With precautions, and with thermal drift compensation built into analysis spreadsheets, levels of repeatability matched those already achieved in the laboratory, while under fairly extreme climatic conditions, and was often better than ± 2%. It is of particular note that equivalent linearity was achieved with $\Delta T/\ln t$ curves, at similar thermal conductivity levels, with in situ and laboratory based measurements.

The case studies showed that in situ values for thermal conductivity could be substantially different to design values, whether through varied moisture content or varied or unknown material composition. Significant rises in the thermal conductivity of building materials were found with moisture content variation to internal walls during hot dry weather, as a result of occupancy patterns and relative humidity levels. Thermal conductivity levels may reasonably be expected to increase further during heating seasons coincident with wetter weather, with higher relative humidity and moisture ingress, where greater heat losses through the building fabric would lead to increased energy consumption. It was shown that the thermal probe technique had the ability to measure these real in situ values to reasonable levels of accuracy, although not as yet for the low thermal conductivity building insulation materials of greater interest.

Conclusions

This section provides a summary of the main conclusions reached during the project.

It was found that, with simple precautions, the technique described could provide reliable thermal conductivity results for construction materials, whether as samples or in situ, where their thermal conductivity values were above around 1.3 $Wm^{-1}K^{-1}$. Indicative results were achievable for materials with thermal conductivity values between 0.07 $Wm^{-1}K^{-1}$ and 1.3 $Wm^{-1}K^{-1}$. The technique was currently found unsuitable for materials with values below around 0.07 $Wm^{-1}K^{-1}$, which includes the majority of building insulation materials. Repeatability levels for these measurements were often better than ± 2% but results were compromised by an increase in asymmetric axial losses from the probe and surrounding sample material. The guarded probe described earlier in this chapter will potentially overcome this difficulty in the future and allow the thermal conductivity measurement of building insulations as found in situ, including the effects of moisture content.

Sufficient levels of thermal stability were readily achieved in variable outdoor environments, between around 3°C and 35°C, that allowed the technique to be used for in situ measurements, across a similar range of materials to those studied in controlled environments, without any perceptible loss of accuracy.

It was found that, despite typical levels of repeatability for thermal diffusivity values being better than ± 5%, it was not yet possible to establish these, and hence volumetric heat capacity, reliably by the technique. This was because unknown levels of thermal resistance between the probe and sample occurred,

along with the effects of temperature gradients across the probe components and the thermal resistances between them. The combined effects of these resistances could not yet be distinguished from the effect of thermal diffusivity on the curve of $\Delta T/\ln t$, using traditional or contemporary thermal probe solutions.

Thermal conductivity results were found to be dependent on recognition of the appropriate time window chosen for analysis, which varied for different materials. Theoretical calculations and predictions of this time window were found to be dependent on thermal diffusivity values, which were usually unknown. Recognition was achieved in the current work by carrying out multiple automated thermal conductivity calculations over successive periods and observing the longest sequence of periods over which values remained relatively constant, indicating linear asymptotes of $\Delta T/\ln t$. It was found that the prediction of an appropriate time window was not necessary in achieving reliable thermal conductivity results as the methodology allowed the time window to be identified following a measurement. This post measurement assessment of linearity in $\Delta T/\ln t$ would need to be undertaken with any fully automated analysis routines, such as may be envisaged for a probe based thermal conductivity meter.

Calibration in one or two materials was not found to be sufficient to allow the assumption of reliable measurements in other materials. Should calibration be relied upon, or the checking of accuracy be required, between five and ten materials, with distinct and wide ranging physical and thermal properties, should be used. The precision of these reference materials only needs to be as good

as the results required, which, for building materials, may be within around ± 2.5%. These values could be achieved with a guarded hot plate apparatus.

Limitations were found with the practical application of the in situ technique, such as difficulties in establishing the nature, thickness and location of wall materials under decorative or plastered finishes. These issues should be borne in mind in future work.

This work confirmed that in situ thermal conductivity values can vary significantly from design values, even where this may not be previously have been suspected. The thermal probe technique can measure the thermal conductivity of materials as used in real buildings, before or after their placement and during building occupation. Currently, this is only within the range of thermal conductivity values described above. The differences to design values were found to have two causes: moisture content and material composition.

Materials may appear dry by visual inspection and by resistance type damp meters, but their interstitial moisture content can result in higher thermal conductivity. As shown by Chart 36, this can be the case when no moisture ingress has occurred, where the hygroscopic nature of materials has caused moisture to be taken up as a result only of atmospheric relative humidity. It may be borne in mind that the relative humidity inside occupied buildings is often higher than that found in ambient conditions, and more so in bathrooms and kitchens. The thermal conductivities of building materials, for buildings in occupation, must now be thought to often be higher than their design values, which compromises the aims of the Building Regulations and the good efforts of

designers wishing to reduce energy in use, fuel poverty and potential carbon dioxide emissions.

Thermal conductivity values used in design may not be representative where material composition is different from that originally measured or assumed from the literature, as was found in the earth building case studies. This may be through varied manufacturing processes, including variations to the proportions of ingredients used, variations to the grain sizes in granular materials, and variations to the densities of finished products. It may also be through materials being of a different composition than those for which values have been found in the literature, for example, different earth or rock types may have different thermal conductivities. The thermal probe technique provides a relatively quick and economical way of measuring the thermal conductivity of particular materials, as samples in the design stage or as in situ components. Thus, where material dimensions are sufficient to avoid boundary losses during measurements, the insulating properties of various thermal elements in a building can be predicted or measured.

This thesis makes a significant contribution to knowledge in that it has:

- Shown the successful transfer of the thermal conductivity probe technique from laboratory to in situ measurements
- Confirmed that the effective thermal conductivity of materials containing moisture can be measured by the technique
- Confirmed that heat loss through building materials in situ is often significantly greater than that predicted using guarded hot plate thermal conductivity values, even in notionally dry buildings

- Described a new methodology to assess the reliability of thermal conductivity results, based on the semi-automated assessment of linearity in charts of temperature rise against the natural logarithm of elapsed time
- Identified that heat losses at and around the probe entry position have prevented reliable thermal conductivity results from being obtained for building insulations, and described a potential solution using a guarded probe
- Described and justified essential improvements to calibration and corroboration methods
- Improved the speed of thermal conductivity measurements of building materials by the thermal probe technique, whether as samples or in situ, whether dry or containing moisture, from many hours to a few minutes
- Shown that thermal diffusivity and volumetric heat capacity values achieved by the technique are currently unreliable and influenced by initial estimates used in calculations

Appendix A: Computer simulation

The assessment of traditional solutions in chapter 3 showed the difficulty in differentiating between the various influences that gave rise to particular rates and levels of probe temperature rise recorded from a probe heated within a sample medium. The transient line source theory used in the thermal probe technique was mostly developed in the middle of the 20th century, and based on empirical deductions made from the results of experimental measurements. This could provide a clue as to why thermal probe technology remained unreliable, as evidenced by the literature review and the assessment. In a pre-digital age, the time taken to undertake and analyse measurements may have limited the number that could be undertaken to substantiate empirical conclusions. For this reason, it appeared sensible to assess the theory by using computer simulations to examine measurements where normal causes of experimental error were removed.

Computer simulation would have to be able to carry out adiabatic modelling of a perfect line source in an infinite, homogenous medium. This would allow virtual measurements to be undertaken without the practical sources of error identified in the literature review and previous work at the University of Plymouth. This included the difficulty noted in the conclusion to chapter 3 concerning the differentiation between contact resistance and thermal diffusivity effects. Measurements needed to be undertaken independently from the effects of:

- Contact resistance
- Boundary conditions
- Probe thermal properties: heat capacity, thermal conductivity and internal resistances

- Axial and end losses
- Convection and radiation, within the sample and between the probe and sample
- Moisture migration, changes in density and phase changes
- Power fluctuations

The author is indebted to Dr. Pieter de Wilde, who is experienced in simulation tools, for identifying the software programme Voltra from Physibel as being capable of finite element calculations of this three dimensional transient heat transfer problem (Physibel, 2007). Further details of this software are given in the publication bound into this thesis (de Wilde et al, 2007). Two series of computer simulations were designed. The first series used a range of thermal properties unrelated to real materials and included extremes of thermal conductivity and volumetric heat capacity values. This was with the view that increased levels of error might occur and their causes be identified where such errors may not have been obvious in practical measurements. The second series used published thermal values for a range of construction related materials.

The thermal data for sample materials were input to the models as was the power level to be released by the line source, over time. After a temperature stabilisation period to ensure all components were in thermal equilibrium, virtual power was applied to the line source and the temperature rise recorded at 1Hz, on the line source and at various radii from it. The data were then exported and treated in a similar way to practical experimental data.

The author is further indebted to Dr. Pieter de Wilde for building the Voltra model, arranging the input of data supplied by the author, and returning the resulting temperature rise records.

The first series – theoretical values

The first series of simulations used thermal conductivity input values from 0.01 $Wm^{-1}K^{-1}$ to 100 $Wm^{-1}K^{-1}$ combined with volumetric heat capacity values between 1 $kJm^{-3}K^{-1}$ to 60 $MJm^{-3}K^{-1}$, giving rise to approximately 250 raw data sets. The resultant temperature rise data were then analysed using equation (6) for thermal conductivity and equation (34) for volumetric heat capacity. This was done without the final term as no contact resistance existed between the line source and material, theoretically making *H* infinitely large and therefore the final term infinitely small.

Initial trials showed that Voltra results were not affected where the same volumetric heat capacity value was created using varied combinations of density and specific heat capacity, hence a nominal density of 1,000 $kg.m^{-3}$ was used for the theoretical materials with their volumetric heat capacity adjusted by altering specific heat capacity inputs only.

Chart 54 shows the temperature rise measured on the line source plotted over time on a logarithmic scale for simulations at thermal conductivity 0.1 $Wm^{-1}K^{-1}$ and volumetric heat capacity values between 100 $kJm^{-3}K^{-1}$ to 6 $MJm^{-3}K^{-1}$. S curves were formed within the first 20s to 40s with their shape dependent on the single variable, the volumetric heat capacity of the sample. This shows that S curves at early times are not solely caused by internal and external contact resistance, and the probe heat capacity, as described by previous researchers.

This draws into question the means of achieving valid results where adjustments had been made on the basis of the probe causing early S curves, and the use of that means in calibration measurements.

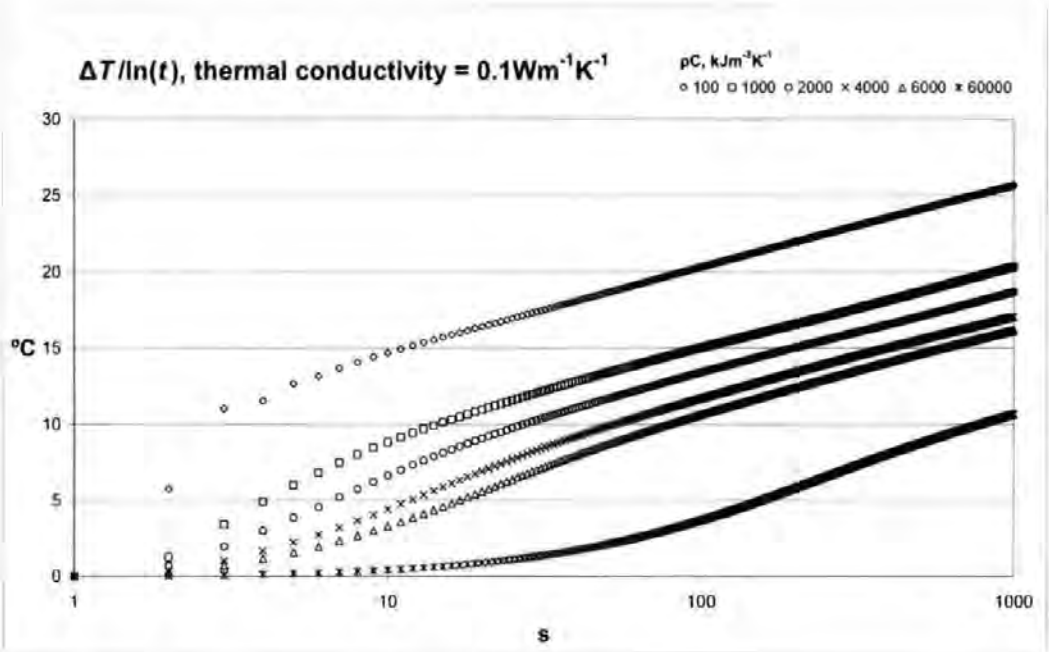

Chart 54: Voltra temperature rises for 0.1 $Wm^{-1}K^{-1}$ thermal conductivity

Thermal conductivity values for the data in chart 54, and for similar data where the thermal conductivity input was 0.6 $Wm^{-1}K^{-1}$, were calculated over time windows of 60s – 160s, as these sections appeared to be reasonably linear. Charts 55 and 56 show that thermal conductivity results at these later times, unaffected by boundary conditions or probe heating times, and calculated using equation (6), were not independent of volumetric heat capacity and that the proportional difference to input values varied dependent on the relationship between thermal conductivity and volumetric heat capacity. Such differences were observed over the range of input values.

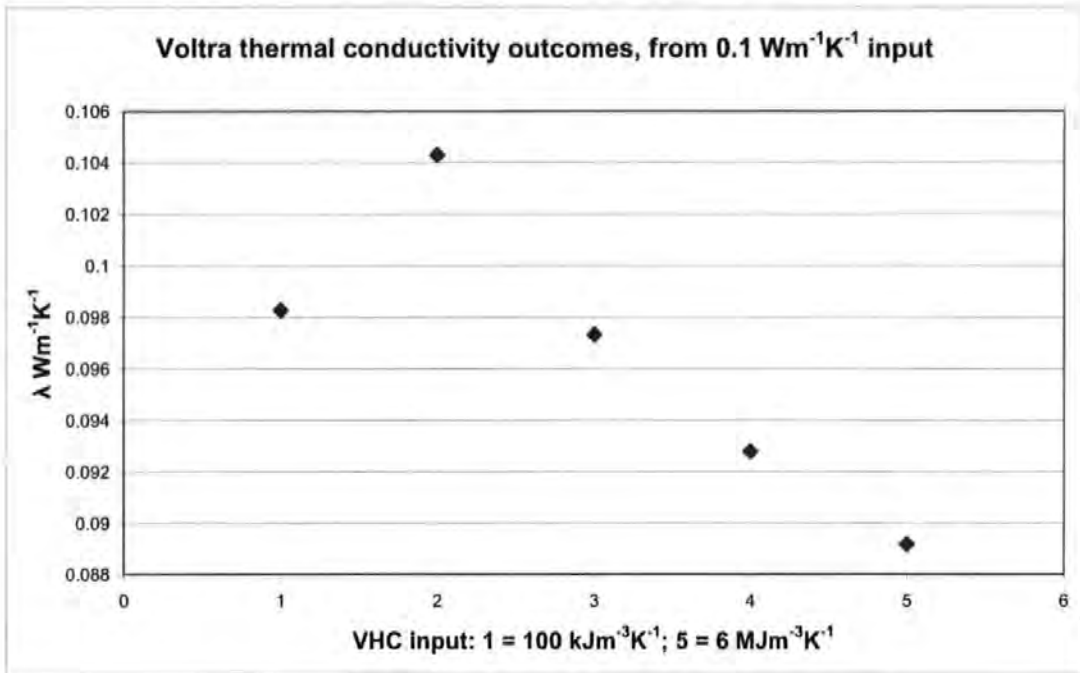

Chart 55: Voltra thermal conductivity outcomes for 0.1 $Wm^{-1}K^{-1}$ input, varied ρC

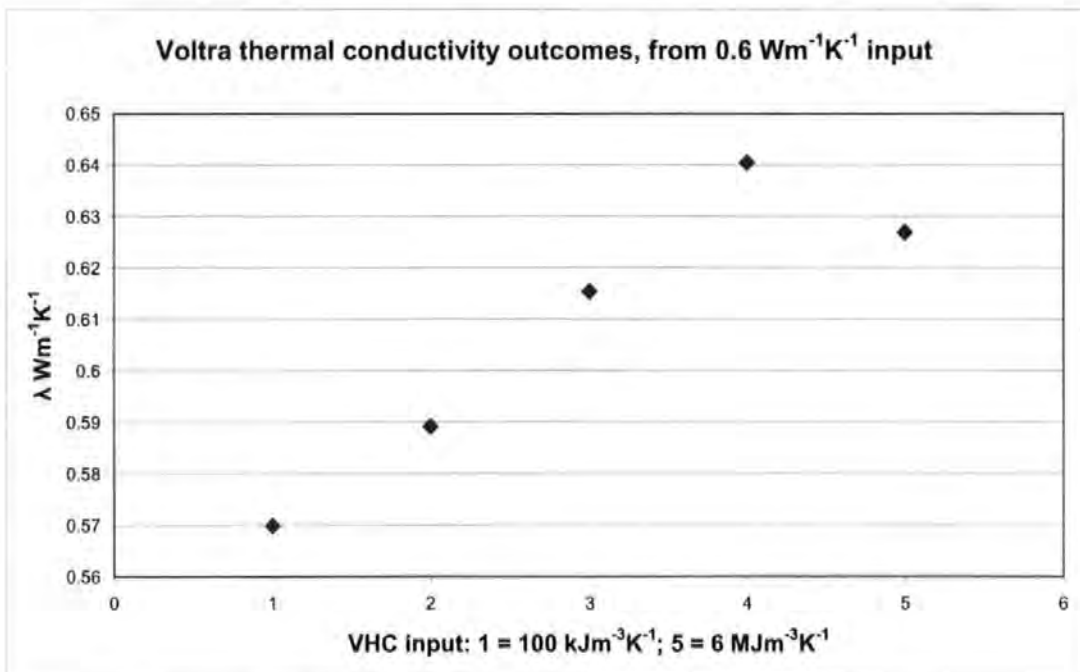

Chart 56: Voltra thermal conductivity outcomes for 0.6 $Wm^{-1}K^{-1}$ input, varied ρC

The slope assessment methodology as applied to charts 6 and 8 was applied to the Voltra data to assess whether linear sections existed in plots of $\Delta T/\ln t$. Chart 57 shows an example of thermal conductivity results by equation (6) for successive 100s time windows where the input data was 0.01 $Wm^{-1}K^{-1}$ and 100 $kJm^{-3}K^{-1}$, giving a thermal diffusivity value of 1.00 $x10^{-7}$ m^2s^{-1}. This shows that no linear section existed, which was confirmed when using shorter time windows. The input value, which may be taken to represent the known value in practical experiments, was only achieved at around 550s – 650s and 1,025s – 1,125s, which time windows varied for other combinations of thermal conductivity and volumetric heat capacity.

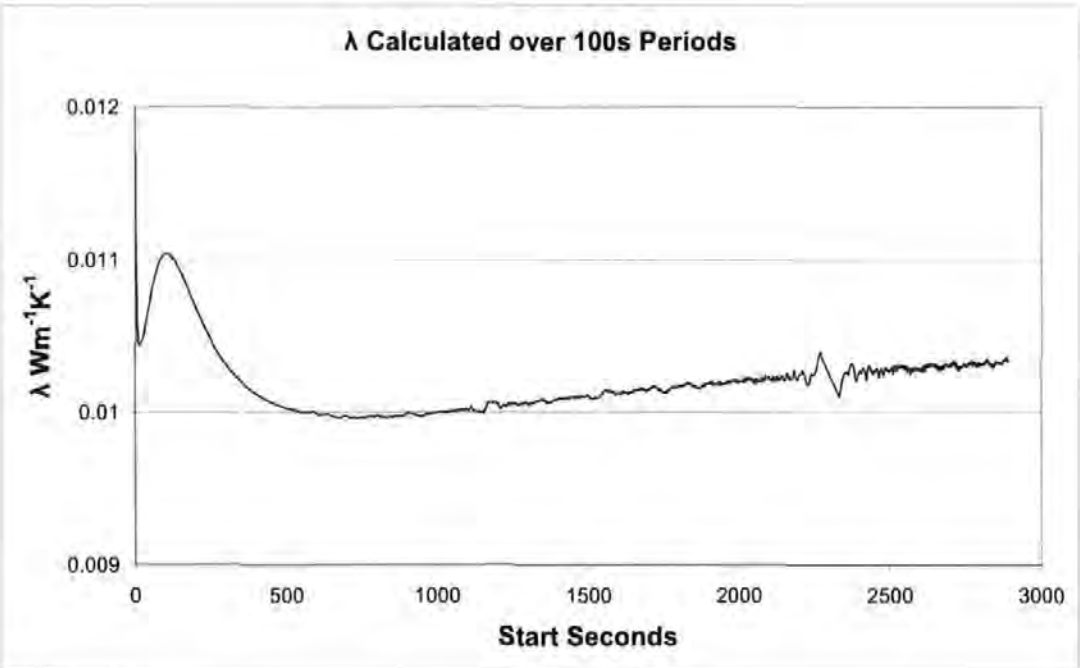

Chart 57: Voltra 100s results for 0.01 $Wm^{-1}K^{-1}$, 100 $kJm^{-3}K^{-1}$

These other combinations sometimes generated more pronounced fluctuations. Chart 58 shows the effect with volumetric heat capacity at 100 $kJm^{-3}K^{-1}$ and thermal conductivity at 1.0 $Wm^{-1}K^{-1}$. Chart 59 is given for comparison, being

based on real experimental data for a sample cube of hemp and hydraulic lime. Charts 60 and 61 show results for the theoretical input of 1.0 $kJm^{-3}K^{-1}$ and 0.01 $Wm^{-1}K^{-1}$, and experimental data for a sample of phenolic foam measured with the TP08 thermal probe, respectively.

The similarity of these curves suggests the extent to which volumetric heat capacity of the sample material has an effect on thermal conductivity results when measured with a transient line source, whether as a perfect model or in real situations with the experimental limitations of contact resistance, boundary effects, etc. of a physical probe. It must be emphasised that this is a difficulty with the measurement method rather than an indication of fluctuating thermal values.

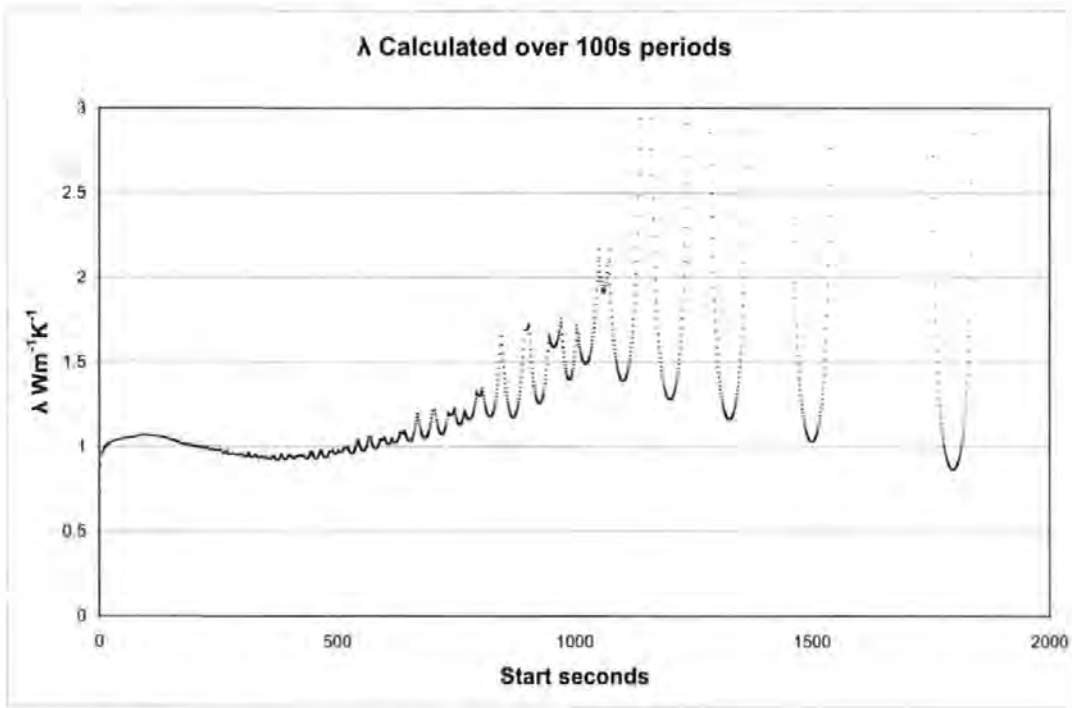

Chart 58: Voltra 100s results for 1.0 $Wm^{-1}K^{-1}$, 100 $kJm^{-3}K^{-1}$

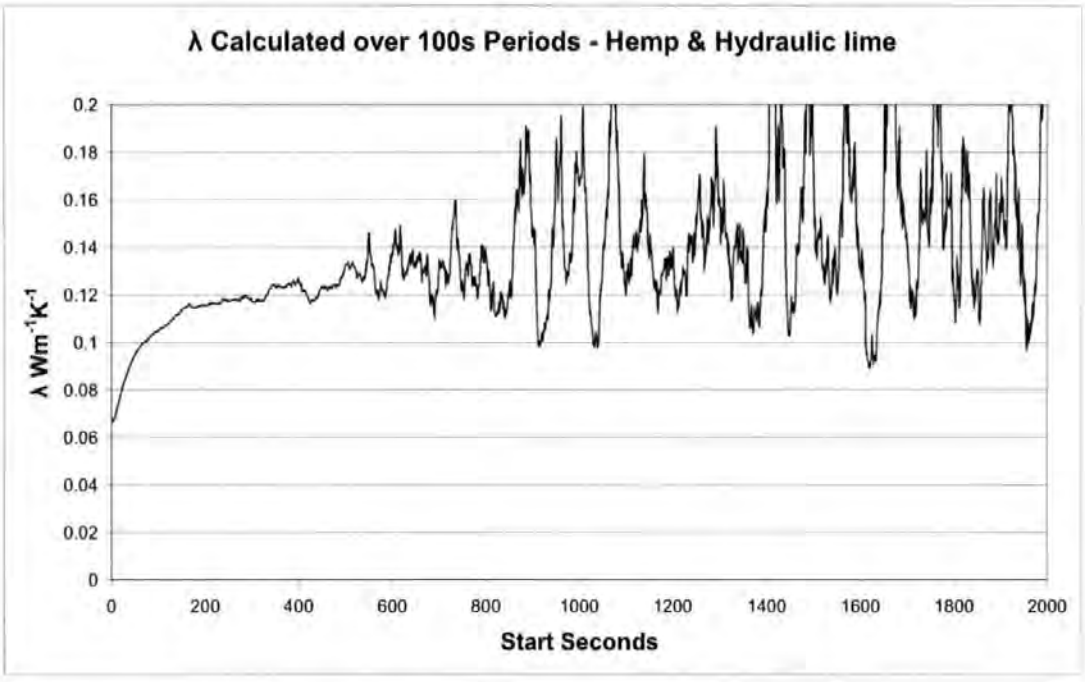

Chart 59: Thermal conductivity 100s results for hemp lime sample

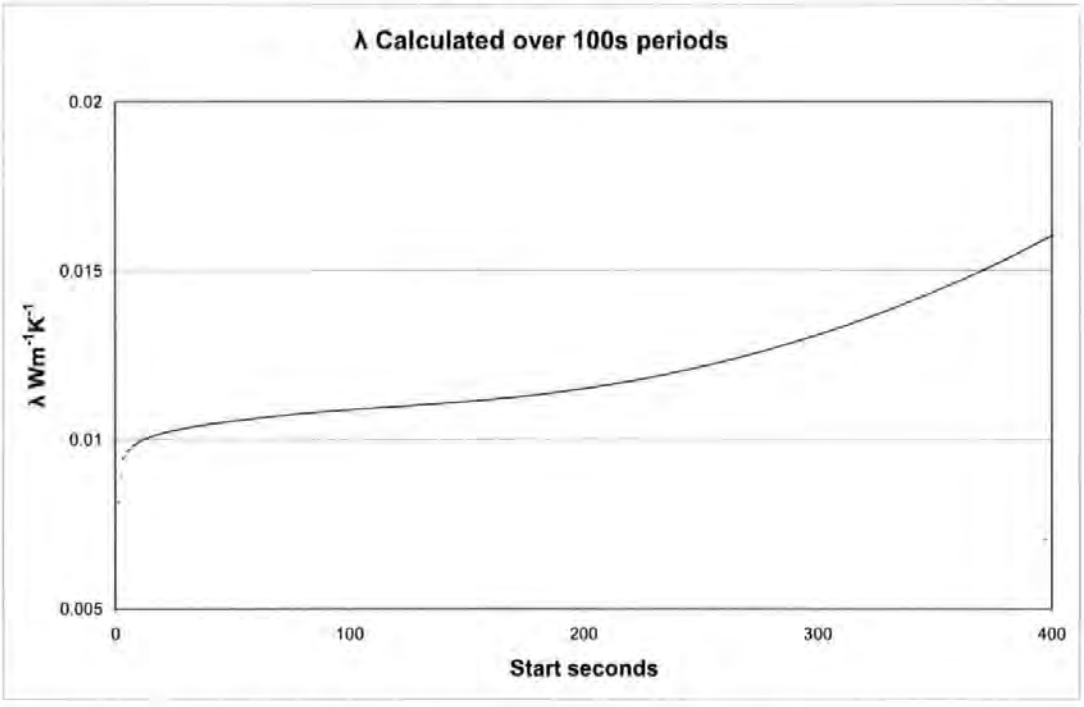

Chart 60: Voltra 100s results by for 0.01 $Wm^{-1}K^{-1}$, 1.0 $kJm^{-3}K^{-1}$ input

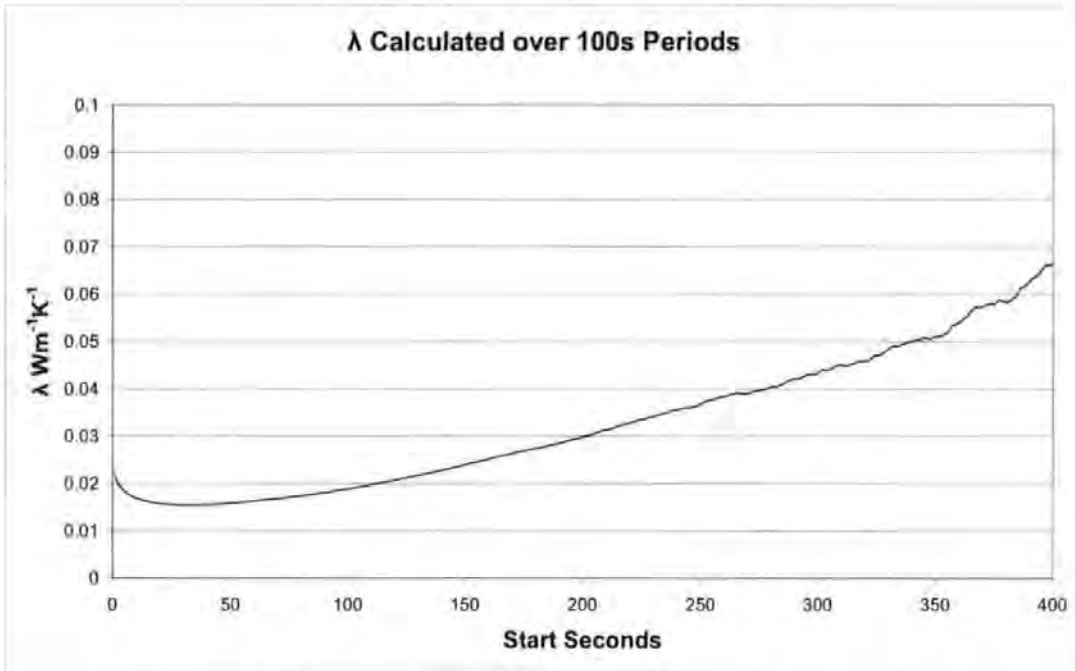

Chart 61: Thermal conductivity 100s results for a phenolic foam sample

Thermal diffusivity values were calculated from the first series data using equation (34), with the calculated thermal conductivity values from visually assessed linear sections of $\Delta T/\ln t$. The results were used to achieve output values for volumetric heat capacity. 98 of these results are presented in appendix D. The variance coefficient is shown for each measurement and the resultant error levels given.

It can be seen from these results that the error level does not form a consistent pattern related to either thermal conductivity or volumetric heat capacity, apart from the very large error levels at the higher thermal conductivity values. Measurements at greater radii consistently show greater error levels. However, error levels for both thermal conductivity and volumetric heat capacity achieved at 1mm radius in all but the most extreme cases would be within acceptable levels for construction applications.

The second series – virtual construction materials

The second series of Voltra simulations used the same methodology as the first series, with input thermal values selected for a range of construction materials from the Ashrae handbook (Parsons, 2005). The error levels achieved for thermal conductivity, calculated by equation (6), and for volumetric heat capacity, calculated by equation (34), are given in appendix E.

It should be borne in mind that, where the error in volumetric heat capacity is less than that in thermal conductivity, the error in thermal diffusivity must be greater, through the relationship $\rho C = \lambda / \alpha$. However, the results show that error levels at lower radii were within around 8% for thermal conductivity and 20% for volumetric heat capacity, which may be thought acceptable for most construction applications.

Conclusions from the computer simulation

Four potentially significant factors were identified through various analyses of around 500 computer simulations:

1) It was seen that S and U curves over the first 0s – 40s of $\Delta T/\ln t$ exist independently of any physical probe presence
2) Thermal conductivity calculated by traditional regression analysis, equation (6), varied from the known value depending on the material volumetric heat capacity
3) Visually assessed linear asymptotes of $\Delta T/\ln t$, generated without practical experimental error or physical line source, gave varied results over time, which variation was similar to that found in practical experiments

4) Despite the three issues above, values achieved by equations (6) and (34) for a visually assessed linear asymptote of $\Delta T/\ln t$ were within around 8% for thermal conductivity and 20% for volumetric heat capacity

The Solver spreadsheets were used to analyse various of the data sets, with a large H input to represent no contact resistance. Similar errors occurred for thermal conductivity and values achieved for volumetric heat capacity were usually lower than input values, although often dependent on initial input estimates. It is of note that the spreadsheets still produced start and end times as if a physical probe with a distinct heat capacity, and producing axial and end losses, existed.

Appendix B: The experiment log

Below is an extract from the experiment log, listing the measurements done and indicating some of the analyses carried out. The working version used hyperlinks to access each and any of the data sets or analysis routines.

Ref	Date	Material	Probe	Heat	Lab In situ	Raw Data Location	Descriptions	Miscellaneous Analyses	ATv10
BP-0006	13/01/2005	Straw Bale	TP08 131	Low	Lab	bp-0006.csv			
BP-0007	13/01/2005	Straw Bale	TP08 131	Low	Lab	bp-0007.csv			
BP-0008	13/01/2005	Straw Bale	TP08 131	Low	Lab	No data			
BP-0009	13/01/2005	Straw Bale	TP08 131	Low	Lab	bp-0009.csv			
BP-0010a	24/01/2005	Straw Bale	TP08 132	Low	Lab	BP-0010a.xls	BP-0010 description.doc		BP-0010a ATv10.xls
BP-0010b	24/01/2005	Aerated concrete Shield	TP08 131	Low	Lab	BP-0010b.xls	BP-0010 description.doc		BP-0010b ATv10.xls
BP-0011a	26/01/2005	Straw Bale	TP08 131	Low	Lab	BP-0011.csv	BP-0011 description.doc		
BP-0011b	26/01/2005	Cob Block	TP08 132	Low	Lab	BP-0011b.xls	BP-0011 description.doc		BP-0011b ATv10.xls
BP-0011c	26/01/2005	Cob Block	TP08 132	Med	Lab	BP-0011.csv	BP-0011 description.doc		BP-0011c ATv10.xls
BP-0012a	27/01/2005	Straw Bale	TP08 131	Low	Lab	BP-0012b.csv	BP-0012 description.doc		BP-0012a ATv10.xls
BP-0012b	27/01/2005	Cob Block	TP08 132	Med	Lab	BP-0012b.csv	BP-0012 description.doc		BP-0012b ATv10.xls
BP-0012c	27/01/2005	Polystyrene	TP08 131	Low	Lab	BP-0012c.csv	BP-0012 description.doc		BP-0012c ATv10.xls
BP-0012d	27/01/2005	Cob Block	TP08 132	Low	Lab	BP-0012c.csv	BP-0012 description.doc		BP-0012d ATv10.xls
BP-0013a	02/02/2005	Aerated concrete Shield	TP08 132	Low	Lab	BP-0013.xls	BP-0013 description.doc		BP-0013a ATv10.xls
BP-0013b	02/02/2005	Cob Block	TP08 131	Med	Lab	BP-0013b.xls	BP-0013 description.doc		BP-0013b ATv10.xls
BP-0014a	09/02/2005	Aerated concrete Shield	TP08 132	Low	Lab	BP-0014a.xls	BP-0014 description.doc	BP-0014 Charts.xls	BP-0014a ATv10.xls
BP-0014b	09/02/2005	Aerated concrete Shield	TP08 131	Low	Lab	BP-0014b.xls	BP-0014 description.doc	Volumes probe & Vaseline in Aerated concrete Shield 01.xls	BP-0014b ATv10.xls
BP-0014c	09/02/2005	Aerated concrete Shield	TP08 132	Low	Lab	BP-0014c.xls	BP-0014 description.doc		BP-0014c ATv10.xls
BP-0014d	09/02/2005	Aerated concrete Shield	TP08 131	Low	Lab	BP-0014d.xls	BP-0014 description.doc		BP-0014d ATv10.xls
BP-0015a	15/02/2005	Aerated concrete Shield	TP08 132	Med	Lab	BP-0015a.xls	BP-0015 description.doc		BP-0015a ATv10.xls
BP-0015b	15/02/2005	Aerated concrete Shield	TP08 131	Med	Lab	BP-0015b.xls	BP-0015 description.doc		BP-0015b ATv10.xls
BP-0015c	15/02/2005	Aerated concrete Shield	TP08 131	Med	Lab	BP-0015c.xls	BP-0015 description.doc		BP-0015c ATv10.xls
BP-0015d	15/02/2005	Aerated concrete Shield	TP08 132	Med	Lab	BP-0015d.xls	BP-0015 description.doc		BP-0015d ATv10.xls
BP-0016a	16/02/2005	Aerated concrete Shield	TP08 132	Med	Lab	BP-0016a.xls	BP-0016 description.doc		bad data
BP-0016b	16/02/2005	Aerated concrete Shield	TP08 131	Med	Lab	BP-0016b.xls	BP-0016 description.doc		BP-0016b ATv10.xls
BP-0016c	16/02/2005	Aerated concrete Shield	TP08 132	Med	Lab	BP-0016c.xls	BP-0016 description.doc		BP-0016c ATv10.xls
BP-0016d	16/02/2005	Aerated concrete Shield	TP08 131	Med	Lab	BP-0016d.xls	BP-0016 description.doc	BP-0017 Charts emf drop, PT1000 reconnected.xls	BP-0016d ATv10.xls
BP-0017a	23/02/2005	Aerated concrete Shield	TP08 132	Med	Lab	BP-0017a.xls	BP-0017 description.doc	BP-0017 Charts PT1000 disconnection & base warming.xls	BP-0017a ATv10.xls
BP-0017b	23/02/2005	Aerated concrete Shield	TP08 131	Med	Lab	BP-0017b.xls	BP-0017 description.doc		BP-0017b ATv10.xls
BP-0017c	23/02/2005	Aerated concrete Shield	TP08 132	Med	Lab	BP-0017c.xls	BP-0017 description.doc		BP-0017c ATv10.xls
BP-0017d	23/02/2005	Aerated concrete Shield	TP08 131	Med	Lab	BP-0017d.xls	BP-0017 description.doc		BP-0017d ATv10.xls
BP0018a	24/02/2005	Aerated concrete Shield	TP08 132	Med	Lab	BP-0018a.xls	BP-0018 description.doc		BP-0018a ATv10.xls
BP0018b	24/02/2005	Aerated concrete Shield	TP08 131	Med	Lab	BP-0018b.xls	BP-0018 description.doc		BP-0018b ATv10.xls
BP0018c	24/02/2005	Aerated concrete Shield	TP08 132	Med	Lab	BP-0018c.xls	BP-0018 description.doc		BP-0018c ATv10.xls
BP0018d	24/02/2005	Aerated concrete Shield	TP08 131	Med	Lab	BP-0018d.xls	BP-0018 description.doc		BP-0018d ATv10.xls
BP0018e	24/02/2005	Aerated concrete Shield	TP08 132	Med	Lab	BP-0018e.xls	BP-0018 description.doc		BP-0018e ATv10.xls

Ref	Date	Material	Probe	Heat	Lab In situ	Raw Data Location	Descriptions	Miscellaneous Analyses	ATv10
BP-0019a	25/02/2005	Aerated concrete Shield	TP08 132	Med	Lab	BP-0019a.xls	BP-0019 description.doc		BP-0019a ATv10.xls
BP-0019b	25/02/2005	Aerated concrete Shield	TP08 131	Med	Lab	BP-0019b.xls	BP-0019 description.doc		BP-0019b ATv10.xls
BP-0019c	25/02/2005	Aerated concrete Shield	TP08 132	Med	Lab	BP-0019c.xls	BP-0019 description.doc		BP-0019c ATv10.xls
BP-0019d	25/02/2005	Aerated concrete Shield	TP08 131	Med	Lab	BP-0019d.xls	BP-0019 description.doc		BP-0019d ATv10.xls
BP-0019e	25/02/2005	Aerated concrete Shield	TP08 132	Med	Lab	BP-0019e.xls	BP-0019 description.doc		BP-0019e ATv10.xls
BP-0019f	25/02/2005	Aerated concrete Shield	TP08 131	Med	Lab	BP-0019f.xls	BP-0019 description.doc		BP-0019f ATv10.xls
BP-0019g	25/02/2005	Aerated concrete Shield	TP08 132	Med	Lab	BP-0019g.xls	BP-0019 description.doc	BP-0019g PT1000 & emf scatter compared.xls	BP-0019g ATv10.xls
BP-0019h	25/02/2005	Aerated concrete Shield	TP08 131	Med	Lab	BP-0019h.xls	BP-0019 description.doc		BP-0019h ATv10.xls
BP-0020a	02/03/2005	Aerated concrete Shield	TP08 132	Med	Lab	BP-0020a.xls	BP-0020 description.doc		BP-0020a ATv10.xls
BP-0020b	02/03/2005	Aerated concrete Shield	TP08 131	Med	Lab	BP-0020b.xls	BP-0020 description.doc		BP-0020b ATv10.xls
BP-0020c	02/03/2005	Aerated concrete Shield	TP08 132	Med	Lab	BP-0020c.xls	BP-0020 description.doc		BP-0020c ATv10.xls
BP-0020d	02/03/2005	Aerated concrete Shield	TP08 131	Med	Lab	BP-0020d.xls	BP-0020 description.doc		BP-0020d ATv10.xls
BP-0021a	08/03/2005	Aerated concrete Shield	TP08 132	Med	Lab	BP-0021a.xls	BP-0021 description.doc	BP-0021 Charts thermal drift & temp stabilisation.xls	BP-0021a ATv10.xls
BP-0021b	08/03/2005	Aerated concrete Shield	TP08 131	Med	Lab	BP-0021b.xls	BP-0021 description.doc		BP-0021b ATv10.xls
BP-0021c	08/03/2005	Aerated concrete Shield	TP08 132	Med	Lab	BP-0021c.xls	BP-0021 description.doc		BP-0021c ATv10.xls
BP-0021d	08/03/2005	Aerated concrete Shield	TP08 131	Med	Lab	BP-0021d.xls	BP-0021 description.doc		BP-0021d ATv10.xls
BP-0021e	08/03/2005	Aerated concrete Shield	TP08 131	Med	Lab	No data	BP-0021 description.doc		
BP-0021f	08/03/2005	Aerated concrete Shield	TP08 132	Med	Lab	No data	BP-0021 description.doc		
BP-0021g	08/03/2005	Aerated concrete Shield	TP08 132	Med	Lab	No data	BP-0021 description.doc		
BP-0021h	08/03/2005	Aerated concrete Shield	TP08 131	Med	Lab	No data	BP-0021 description.doc		
BP-0022a	09/03/2005	Aerated concrete Shield	TP08 132	Med	Lab	BP-0022a.xls	BP-0022 description.doc	BP-0022 Charts all temperatures & drift.xls	BP-0022a ATv10.xls
BP-0022b	09/03/2005	Aerated concrete Shield	TP08 131	Med	Lab	BP-0022b.xls	BP-0022 description.doc	BP-0022 Charts base temp drift with needle heating.xls	BP-0022b ATv10.xls
BP-0022c	09/03/2005	Aerated concrete Shield	TP08 132	Med	Lab	BP-0022c.xls	BP-0022 description.doc		BP-0022c ATv10.xls
BP-0022d	09/03/2005	Aerated concrete Shield	TP08 131	Med	Lab	BP-0022d.xls	BP-0022 description.doc		BP-0022d ATv10.xls
BP-0022e	09/03/2005	Aerated concrete Shield	TP08 132	Med	Lab	BP-0022e.xls	BP-0022 description.doc		BP-0022e ATv10.xls
BP-0022f	09/03/2005	Aerated concrete Shield	TP08 131	Med	Lab	BP-0022f.xls	BP-0022 description.doc	BP-0023f Charts needle temp difference by dt800 & by calculation.xls	BP-0022f ATv10.xls
BP-0022g	09/03/2005	Aerated concrete Shield	TP08 132	Med	Lab	BP-0022g.xls	BP-0022 description.doc		BP-0022g ATv10.xls
BP-0022h	09/03/2005	Aerated concrete Shield	TP08 131	Med	Lab	BP-0022h.xls	BP-0022 description.doc		BP-0022h ATv10.xls
BP-0023a	10/03/2005	Aerated concrete Shield	TP08 132	Med	Lab	BP-0023a.xls	BP-0023 description.doc		BP-0023a ATv10.xls
BP-0023b	10/03/2005	Aerated concrete Shield	TP08 131	Med	Lab	BP-0023b.xls	BP-0023 description.doc		BP-0023b ATv10.xls
BP-0023c	10/03/2005	Aerated concrete Shield	TP08 132	Med	Lab	BP-0023c.xls	BP-0023 description.doc		BP-0023c ATv10.xls
BP-0023d	10/03/2005	Aerated concrete Shield	TP08 131	Med	Lab	BP-0023d.xls	BP-0023 description.doc		BP-0023d ATv10.xls
BP-0023e	10/03/2005	Aerated concrete Shield	TP08 132	Med	Lab	BP-0023e.xls	BP-0023 description.doc		BP-0023e ATv10.xls
BP-0023f	10/03/2005	Aerated concrete Shield	TP08 131	Med	Lab	BP-0023f.xls	BP-0023 description.doc	BP-0023f ATv10 VHC.xls	BP-0023f ATv10.xls
BP-0024a	16/03/2005	Aerated concrete Shield	TP08 132	Med	Lab	BP-0024a.xls	BP-0024 description.doc		BP-0024a ATv10.xls
BP-0025a	17/03/2005	Aerated concrete Shield	TP08 132	Med	Lab	BP-0025a.xls	BP-0025 description.doc	BP-0025 REFT drift in dt800.xls	BP-0025a ATv10.xls
BP-0025b	17/03/2005	Aerated concrete Shield	TP08 132	Med	Lab	BP-0025b.xls	BP-0025 description.doc		BP-0025b ATv10.xls
BP-0025c	17/03/2005	Aerated concrete Shield	TP08 131	Med	Lab	BP-0025c.xls	BP-0025 description.doc	Summary Solver 4-3 Aerated concrete Shield 01.xls	BP-0025c ATv10.xls
BP-0025d	17/03/2005	Aerated concrete Shield	TP08 132	Med	Lab	BP-0025d.xls	BP-0025 description.doc	Summary Main Values Aerated concrete Shield 01.xls	BP-0025d ATv10.xls
BP-0025e	17/03/2005	Aerated concrete Shield	TP08 131	Med	Lab	BP-0025e.xls	BP-0025 description.doc	BP-0025e oscillations PT1000 & emf compared.xls	BP-0025e ATv10.xls
BP-0026						No data			
BP-0027	31/03/2005				Lab	No data			

Ref	Date	Material	Probe	Heat	Lab In situ	Raw Data Location	Descriptions	Miscellaneous Analyses	ATv10
BP-0028a	27/04/2005	Vaseline	TP08 132	Med	Lab	BP-0028a.xls	BP-0028 description.doc	Summary Main Values Aerated concrete Shield 02.xls	BP-0028a ATv10.xls
BP-0028b	27/04/2005	Vaseline	TP08 132	Med	Lab	BP-0028b.xls	BP-0028 description.doc		N/A
BP-0028c	27/04/2005	Aerated concrete Shield	TP08 131	Med	Lab	BP-0028c.xls	BP-0028 description.doc		BP-0028c ATv10.xls
BP-0028d	27/04/2005	Vaseline	TP08 132	Med	Lab	BP-0028d.xls	BP-0028 description.doc		BP-0028d ATv10.xls
BP-0028e	27/04/2005	Aerated concrete Shield	TP08 131	Med	Lab	BP-0028e.xls	BP-0028 description.doc		BP-0028e ATv10.xls
BP-0028f	27/04/2005	Vaseline	TP08 132	Med	Lab	BP-0028f.xls	BP-0028 description.doc		BP-0028f ATv10.xls
BP-0028g	27/04/2005	Vaseline	TP08 132	Med	Lab	BP-0028g.xls	BP-0028 description.doc	Regressions	BP-0028g ATv10.xls
BP-0028h	27/04/2005	Aerated concrete Shield	TP08 131	Med	Lab	BP-0028h.xls	BP-0028 description.doc	Summary Moisture BP-0028, 29, 30, 34, 35, 36, 45, 43 & 50	BP-0028h ATv10.xls
BP-0029a	04/05/2005	Vaseline	TP08 132	Med	Lab	BP-0029a.xls	BP-0029 description.doc		BP-0029a ATv10.xls
BP-0029b	04/05/2005	Aerated concrete Shield	TP08 131	Med	Lab	BP-0029b.xls	BP-0029 description.doc		BP-0029b ATv10.xls
BP-0029c	04/05/2005	Aerated concrete Shield	TP08 131	Med	Lab	BP-0029c.xls	BP-0029 description.doc		BP-0029c ATv10.xls
BP-0029d	04/05/2005	Vaseline	TP08 132	Med	Lab	BP-0029d.xls	BP-0029 description.doc	Summary Moisture BP-0028, 29, 30, 34, 35, 36, 45, 43 & 50	BP-0029d ATv10.xls
BP-0030a	05/05/2005	Aerated concrete Shield	TP08 131	Med	Lab	BP-0030a.xls	BP-0030 description.doc		BP-0030a ATv10.xls
BP-0030b	05/05/2005	Vaseline	TP08 132	Med	Lab	BP-0030b.xls	BP-0030 description.doc		BP-0030b ATv10.xls
BP-0030c	05/05/2005	Aerated concrete Shield	TP08 131	Med	Lab	BP-0030c.xls	BP-0030 description.doc		BP-0030c ATv10.xls
BP-0030d	05/05/2005	Vaseline	TP08 132	Med	Lab	BP-0030d.xls	BP-0030 description.doc		BP-0030d ATv10.xls
BP-0030e	05/05/2005	Aerated concrete Shield	TP08 131	Med	Lab	BP-0030e.xls	BP-0030 description.doc		BP-0030e ATv10.xls
BP-0030f	05/05/2005	Vaseline	TP08 132	Med	Lab	BP-0030f.xls	BP-0030 description.doc	Summary Vaseline 01.xls	BP-0030f ATv10.xls
BP-0030g	05/05/2005	Aerated concrete Shield	TP08 131	Med	Lab	BP-0030g.xls	BP-0030 description.doc		BP-0030g ATv10.xls
BP-0030h	05/05/2005	Vaseline	TP08 132	Med	Lab	BP-0030h.xls	BP-0030 description.doc	Summary Moisture BP-0028, 29, 30, 34, 35, 36, 45, 43 & 50	BP-0030h ATv10.xls
BP-0031a	23/05/2005	Agar	TP08 131	Med	Lab	BP-0031a.xls	BP-0031 description.doc		BP-0031a ATv10.xls
BP-0031b	23/05/2005	Agar	TP08 132	Med	Lab	BP-0031b.xls	BP-0031 description.doc		BP-0031b ATv10.xls
BP-0031c	23/05/2005	Agar	TP08 131	High	Lab	BP-0031c.xls	BP-0031 description.doc		BP-0031c ATv10.xls
BP-0031d	23/05/2005	Agar	TP08 132	High	Lab	BP-0031d.xls	BP-0031 description.doc		BP-0031d ATv10.xls
BP-0032a	24/05/2005	Agar	TP08 132	High	Lab	BP-0032a.xls	BP-0032 description.doc		BP-0032a ATv10.xls
BP-0032b	24/05/2005	Agar	TP08 131	High	Lab	BP-0032b.xls	BP-0032 description.doc		BP-0032b ATv10.xls
BP-0033a	25/05/2005	Agar	TP08 132	High	Lab	BP-0033a.xls	BP-0033 description.doc		BP-0033a ATv10.xls
BP-0033b	25/05/2005	Agar	TP08 131	High	Lab	BP-0033b.xls	BP-0033 description.doc		BP-0033b ATv10.xls
BP-0034a	06/06/2005	Vaseline	TP08 131	High	Lab	BP-0034a.xls	BP-0034 description.doc		BP-0034a ATv10.xls
BP-0034b	06/06/2005	Agar	TP08132	High	Lab	BP-0034b.xls	BP-0034 description.doc		BP-0034b ATv10.xls
BP-0034c	06/06/2005	Vaseline	TP08 131	High	Lab	BP-0034c.xls	BP-0034 description.doc		BP-0034c ATv10.xls
BP-0034d	06/06/2005	Aerated concrete Shield	TP08 132	Med	Lab	BP-0034d.xls	BP-0034 description.doc		BP-0034d ATv10.xls
BP-0034e	06/06/2005	Aerated concrete Shield	TP08 131	Med	Lab	BP-0034e.xls	BP-0034 description.doc	Summary Moisture BP-0028, 29, 30, 34, 35, 36, 45, 43 & 50	BP-0034e ATv10.xls
BP-0035a	08/06/2005	Aerated concrete Shield	TP08 132	Med	Lab	BP-0035a.xls	BP-0035 description.doc		BP-0035a ATv10.xls
BP-0035b	08/06/2005	Aerated concrete Shield	TP08 131	Med	Lab	BP-0035b.xls	BP-0035 description.doc	Summary Moisture BP-0028, 29, 30, 34, 35, 36, 45, 43 & 50	BP-0035b ATv10.xls
BP-0036a	14/06/2005	Aerated concrete Shield	TP08 131	Med	Lab	BP-0036a.xls	BP-0036 description.doc		BP-0036a ATv10.xls
BP-0036b	14/06/2005	Aerated concrete Shield	TP08 141	Med	Lab	BP-0036b.xls	BP-0036 description.doc		BP-0036b ATv10.xls
BP-0036c	14/06/2005	Aerated concrete Shield	TP08 132	Med	Lab	BP-0036c.xls	BP-0036 description.doc		BP-0036c ATv10.xls
BP-0036d	14/06/2005	Aerated concrete Shield	TP08 142	Med	Lab	BP-0036d.xls	BP-0036 description.doc	Summary Moisture BP-0028, 29, 30, 34, 35, 36, 45, 43 & 50	BP-0036d ATv10.xls
BP-0037a	21/06/2005	Agar	TP08 131	High	Lab	BP-0037a.xls	BP-0037 description.doc	BP-0037a-p probe resistance results in agar at 0.6.xls	BP-0037a ATv10.xls
BP-0037b	21/06/2005	Agar	TP08 132	High	Lab	BP-0037b.xls	BP-0037 description.doc	BP-0037 Summary H Values.xls	BP-0037b ATv10.xls

Ref	Date	Material	Probe	Heat	Lab In situ	Raw Data Location	Descriptions	Miscellaneous Analyses	ATv10
BP-0037c	21/06/2005	Agar	TP08 141	High	Lab	BP-0037c.xls	BP-0037 description.doc	BP-0037c Alpha Equation 02.xls	BP-0037c ATv10.xls
BP-0037d	21/06/2005	Agar	TP08 142	High	Lab	BP-0037d.xls	BP-0037 description.doc		BP-0037d ATv10.xls
BP-0037e	21/06/2005	Agar	TP08 131	High	Lab	BP-0037e.xls	BP-0037 description.doc		BP-0037e ATv10.xls
BP-0037f	21/06/2005	Agar	TP08 132	High	Lab	BP-0037f.xls	BP-0037 description.doc		BP-0037f ATv10.xls
BP-0037g	21/06/2005	Agar	TP08 141	High	Lab	BP-0037g.xls	BP-0037 description.doc	BP-0037g Analysis Template v06 Slope assessment.xls	BP-0037g ATv10.xls
BP-0037h	21/06/2005	Agar	TP08 142	High	Lab	BP-0037h.xls	BP-0037 description.doc		BP-0037h ATv10.xls
BP-0037i	22/06/2005	Agar	TP08 131	High	Lab	BP-0037i.xls	BP-0037 description.doc		BP-0037i ATv10.xls
BP-0037j	22/06/2005	Agar	TP08 132	High	Lab	BP-0037j.xls	BP-0037 description.doc		BP-0037j ATv10.xls
BP-0037k	22/06/2005	Agar	TP08 141	High	Lab	BP-0037k.xls	BP-0037 description.doc		BP-0037k ATv10.xls
BP-0037l	22/06/2005	Agar	TP08 142	High	Lab	BP-0037l.xls	BP-0037 description.doc		BP-0037l ATv10.xls
BP-0037m	22/06/2005	Agar	TP08 131	High	Lab	BP-0037m.xls	BP-0037 description.doc	BP-0037m Analysis Template v06 Slope assessment.xls	BP-0037m ATv10.xls
BP-0037n	22/06/2005	Agar	TP08 132	High	Lab	BP-0037n.xls	BP-0037 description.doc	BP-0037n Analysis Template v06 Slope assessment.xls	BP-0037n ATv10.xls
BP-0037o	22/06/2005	Agar	TP08 141	High	Lab	BP-0037o.xls	BP-0037 description.doc		BP-0037o ATv10.xls
BP-0037p	22/06/2005	Agar	TP08 142	High	Lab	BP-0037p.xls	BP-0037 description.doc	Summary Agar Regression, Res Calibration.xls	BP-0037p ATv10.xls
BP-0037q	22/06/2005	Agar	TP08 131/132/141/142	High	Lab	BP-0037q.xls	BP-0037 description.doc	BP-0037q emf TK PT1000 interaction TP08 131.xls	
BP-0038a	23/06/2005	Aerated concrete Foundation	TP08 131	Med	In situ	BP-0038a.xls	BP-0038 description.doc	BP-0038 PT1000 & TK compared, external.xls	BP-0038a ATv10.xls
BP-0038b	23/06/2005	Aerated concrete Foundation	TP08 132	Med	In situ	BP-0038b.xls	BP-0038 description.doc	BP-0038 PT1000 & TK compared, internal.xls	BP-0038b ATv10.xls
BP-0038c	23/06/2005	Aerated concrete Solar Block	TP08 141	Med	In situ	BP-0038c.xls	BP-0038 description.doc		BP-0038c ATv10.xls
BP-0038d	23/06/2005	Aerated concrete Solar Block	TP08 142	Med	In situ	BP-0038d.xls	BP-0038 description.doc		BP-0038d ATv10.xls
BP-0038e	23/06/2005	Aerated concrete Foundation	TP08 131	Med	In situ	BP-0038e.xls	BP-0038 description.doc		BP-0038e ATv10.xls
BP-0038f	23/06/2005	Aerated concrete Foundation	TP08 132	Med	In situ	BP-0038f.xls	BP-0038 description.doc		BP-0038f ATv10.xls
BP-0038g	23/06/2005	Aerated concrete Solar Block	TP08 141	Med	In situ	BP-0038g.xls	BP-0038 description.doc		BP-0038g ATv10.xls
BP-0038h	23/06/2005	Aerated concrete Solar Block	TP08 142	Med	In situ	BP-0038h.xls	BP-0038 description.doc		BP-0038h ATv10.xls
BP-0038i	23/06/2005	Aerated concrete Solar Block	TP08 131	Med	In situ	BP-0038i.xls	BP-0038 description.doc		BP-0038i ATv10.xls
BP-0038j	23/06/2005	Aerated concrete Solar Block	TP08 132	Med	In situ	BP-0038j.xls	BP-0038 description.doc		BP-0038j ATv10.xls
BP-0038k	23/06/2005	Aerated concrete Solar Block	TP08 131	Med	In situ	BP-0038k.xls	BP-0038 description.doc	Internal lambda curves compared.xls	BP-0038k ATv10.xls
BP-0038l	23/06/2005	Aerated concrete Solar Block	TP08 132	Med	In situ	BP-0038l.xls	BP-0038 description.doc	Summary BP-0038 Puffins, Aerated concrete in-situ.xls	BP-0038l ATv10.xls
BP-0039a	27/06/2005	Cob	TP08 131	Med	In situ	BP-0039a.xls	BP-0039 description.doc	BP-0039 Base & Needle Temperatures Compared.xls	BP-0039a ATv10.xls
BP-0039b	27/06/2005	Cob	TP08 132	Med	In situ	BP-0039b.xls	BP-0039 description.doc		BP-0039b ATv10.xls
BP-0039c	27/06/2005	Cob	TP08 141	Med	In situ	BP-0039c.xls	BP-0039 description.doc		BP-0039c ATv10.xls
BP-0039d	27/06/2005	Cob	TP08 142	Med	In situ	BP-0039d.xls	BP-0039 description.doc		Bad data
BP-0039e	27/06/2005	Cob	TP08 131	Med	In situ	BP-0039e.xls	BP-0039 description.doc		BP-0039e ATv10.xls
BP-0039f	27/06/2005	Cob	TP08 132	Med	In situ	BP-0039f.xls	BP-0039 description.doc		BP-0039f ATv10.xls
BP-0039g	27/06/2005	Cob	TP08 141	Med	In situ	BP-0039g.xls	BP-0039 description.doc		BP-0039g ATv10.xls
BP-0039h	27/06/2005	Cob	TP08 142	Med	In situ	BP-0039h.xls	BP-0039 description.doc		BP-0039h ATv10.xls
BP-0039i	27/06/2005	Cob	TP08 131	High	In situ	BP-0039i.xls	BP-0039 description.doc		BP-0039i ATv10.xls
BP-0039j	27/06/2005	Cob	TP08 132	High	In situ	BP-0039j.xls	BP-0039 description.doc		BP-0039j ATv10.xls
BP-0039k	27/06/2005	Cob	TP08 141	High	In situ	BP-0039k.xls	BP-0039 description.doc		BP-0039k ATv10.xls
BP-0039l	27/06/2005	Cob	TP08 142	High	In situ	BP-0039l.xls	BP-0039 description.doc		BP-0039l ATv10.xls
BP-0039m	27/06/2005	Cob	TP08 131	High	In situ	BP-0039m.xls	BP-0039 description.doc		BP-0039m ATv10.xls
BP-0039n	27/06/2005	Cob	TP08 132	High	In situ	BP-0039n.xls	BP-0039 description.doc		BP-0039n ATv10.xls

Ref	Date	Material	Probe	Heat	Lab In situ	Raw Data Location	Descriptions	Miscellaneous Analyses	ATv10
BP-0039o	27/06/2005	Cob	TP08 141	High	In situ	BP-0039o.xls	BP-0039 description.doc		BP-0039o ATv10.xls
BP-0039p	27/06/2005	Cob	TP08 142	High	In situ	BP-0039p.xls	BP-0039 description.doc		BP-0039p ATv10.xls
BP-0040a	11/07/2005	Cob	TP08 131	High	In situ	BP-0040a.xls	BP-0040 description.doc	BP-0040 Base, Needle, dl800 & Ambient Compared.xls	BP-0040a ATv10.xls
BP-0040b	11/07/2005	Cob	TP08 132	High	In situ	BP-0040b.xls	BP-0040 description.doc		BP-0040b ATv10.xls
BP-0040c	11/07/2005	Cob	TP08 141	High	In situ	BP-0040c.xls	BP-0040 description.doc		BP-0040c ATv10.xls
BP-0040d	11/07/2005	Cob	TP08 142	High	In situ	BP-0040d.xls	BP-0040 description.doc		BP-0040d ATv10.xls
BP-0040e	11/07/2005	Cob	TP08 131	High	In situ	BP-0040e.xls	BP-0040 description.doc		BP-0040e ATv10.xls
BP-0040f	11/07/2005	Cob	TP08 132	High	In situ	BP-0040f.xls	BP-0040 description.doc		Bad data
BP-0040g	11/07/2005	Cob	TP08 141	High	In situ	BP-0040g.xls	BP-0040 description.doc		BP-0040g ATv10.xls
BP-0040h	11/07/2005	Cob	TP08 142	High	In situ	BP-0040h.xls	BP-0040 description.doc		BP-0040h ATv10.xls
BP-0040i	11/07/2005	Cob	TP08 131	High	In situ	BP-0040i.xls	BP-0040 description.doc		BP-0040i ATv10.xls
BP-0040j	11/07/2005	Cob	TP08 132	High	In situ	BP-0040j.xls	BP-0040 description.doc		BP-0040j ATv10.xls
BP-0040k	11/07/2005	Cob	TP08 141	High	In situ	BP-0040k.xls	BP-0040 description.doc		BP-0040k ATv10.xls
BP-0040l	11/07/2005	Cob	TP08 142	High	In situ	BP-0040l.xls	BP-0040 description.doc		BP-0040l ATv10.xls
BP-0040m	11/07/2005	Cob	TP08 131	High	In situ	BP-0040m.xls	BP-0040 description.doc		BP-0040m ATv10.xls
BP-0040n	11/07/2005	Cob	TP08 132	High	In situ	BP-0040n.xls	BP-0040 description.doc		BP-0040n ATv10.xls
BP-0040o	11/07/2005	Cob	TP08 141	High	In situ	BP-0040o.xls	BP-0040 description.doc		BP-0040o ATv10.xls
BP-0040p	11/07/2005	Cob	TP08 142	High	In situ	BP-0040p.xls	BP-0040 description.doc		BP-0040p ATv10.xls
BP-0040q	11/07/2005	Cob	TP08 131	High	In situ	BP-0040q.xls	BP-0040 description.doc		BP-0040q ATv10.xls
BP-0040r	11/07/2005	Cob	TP08 132	High	In situ	BP-0040r.xls	BP-0040 description.doc		BP-0040r ATv10.xls
BP-0040s	11/07/2005	Cob	TP08 141	High	In situ	BP-0040s.xls	BP-0040 description.doc		BP-0040s ATv10.xls
BP-0040t	11/07/2005	Cob	TP08 142	High	In situ	BP-0040t.xls	BP-0040 description.doc		BP-0040t ATv10.xls
BP-0040u	11/07/2005	Cob	TP08 131	High	In situ	BP-0040u.xls	BP-0040 description.doc		BP-0040u ATv10.xls
BP-0040v	11/07/2005	Cob	TP08 132	High	In situ	BP-0040v.xls	BP-0040 description.doc		BP-0040v ATv10.xls
BP-0040w	11/07/2005	Cob	TP08 141	High	In situ	BP-0040w.xls	BP-0040 description.doc	Summary Eden Cob.xls	BP-0040w ATv10.xls
BP-0040x	11/07/2005	Cob	TP08 142	High	In situ	BP-0040x.xls	BP-0040 description.doc	Regression summary 01.xls	BP-0040x ATv10.xls
BP-0041a	14/07/2005	PTFE	TP08 131	Med	Lab	BP-0041a.xls	BP-0041 description.doc		BP-0041a ATv10.xls
BP-0041b	14/07/2005	PTFE	TP08 131	Med	Lab	BP-0041b.xls	BP-0041 description.doc		BP-0041b ATv10.xls
BP-0041c	14/07/2005	PTFE	TP08 131	Med	Lab	BP-0041c.xls	BP-0041 description.doc		BP-0041c ATv10.xls
BP-0041d	14/07/2005	PTFE	TP08 131	High	Lab	BP-0041d.xls	BP-0041 description.doc		BP-0041d ATv10.xls
BP-0041e	14/07/2005	PTFE	TP08 131	Low	Lab	BP-0041e.xls	BP-0041 description.doc		BP-0041e ATv10.xls
BP-0041f	14/07/2005	PTFE	TP08 131	Med	Lab	BP-0041f.xls	BP-0041 description.doc	3 Power levels PTFE.xls	BP-0041f ATv10.xls
BP-0041g	14/07/2005	PTFE	TP08 131	Med	Lab	BP-0041g.xls	BP-0041 description.doc		BP-0041g ATv10.xls
BP-0041h	14/07/2005	PTFE	TP08 131	Med	Lab	BP-0041h.xls	BP-0041 description.doc		BP-0041h ATv10.xls
BP-0041i	14/07/2005	PTFE	TP08 131	Med	Lab	BP-0041i.xls	BP-0041 description.doc	BP-0041i Analysis Template v06 slope assessment.xls	BP-0041i ATv10.xls
BP-0041j	15/07/2005	PTFE	TP08 132	Med	Lab	BP-0041j.xls	BP-0041 description.doc	BP-0041 TP08-132 needle to sample stabilisaion.xls	BP-0041j ATv10.xls
BP-0041k	15/07/2005	PTFE	TP08 132	Med	Lab	BP-0041k.xls	BP-0041 description.doc	BP-0041k Analysis Template v06 slope assessment.xls	BP-0041k ATv10.xls
BP-0041l	15/07/2005	PTFE	TP08 132	Med	Lab	BP-0041l.xls	BP-0041 description.doc	BP-0041l Analysis Template v06 long time slope assessment.xls	BP-0041l ATv10.xls
BP-0041m	15/07/2005	PTFE	TP08 132	Med	Lab	BP-0041m.xls	BP-0041 description.doc	BP-0041m Analysis Template v06 slope assessment.xls	BP-0041m ATv10.xls
BP-0041n	16/07/2005	PTFE	TP08 141	Med	Lab	BP-0041n.xls	BP-0041 description.doc		BP-0041n ATv10.xls
BP-0041o	16/07/2005	PTFE	TP08 141	Med	Lab	BP-0041o.xls	BP-0041 description.doc		BP-0041o ATv10.xls
BP-0041p	16/07/2005	PTFE	TP08 141	Med	Lab	BP-0041p.xls	BP-0041 description.doc		BP-0041p ATv10.xls

Ref	Date	Material	Probe	Heat	Lab In situ	Raw Data Location	Descriptions	Miscellaneous Analyses	ATv10
BP-0041q	16/07/2005	PTFE	TP08 141	Med	Lab	BP-0041q.xls	BP-0041 description.doc		BP-0041q ATv10.xls
BP-0041r	17/07/2005	PTFE	TP08 142	Med	Lab	BP-0041r.xls	BP-0041 description.doc		BP-0041r ATv10.xls
BP-0041s	17/07/2005	PTFE	TP08 142	Med	Lab	BP-0041s.xls	BP-0041 description.doc		BP-0041s ATv10.xls
BP-0041t	17/07/2005	PTFE	TP08 142	Med	Lab	BP-0041t.xls	BP-0041 description.doc		BP-0041t ATv10.xls
BP-0041u	17/07/2005	PTFE	TP08 142	Med	Lab	BP-0041u.xls	BP-0041 description.doc		BP-0041u ATv10.xls
BP-0042	######								
BP-0042a	28/07/2005	PTFE	TP08 131	Med	Lab	BP-0042a.xls	BP-0042 description.doc	Power chart of BP-0042a regression ATy07.xls	BP-0042a ATv10.xls
BP-0042b	28/07/2005	PTFE	TP08 132	Med	Lab	BP-0042b.xls	BP-0042 description.doc		BP-0042b ATv10.xls
BP-0042c	28/07/2005	PTFE	TP08 141	Med	Lab	BP-0042c.xls	BP-0042 description.doc		BP-0042c ATv10.xls
BP-0042d	28/07/2005	PTFE	TP08 142	Med	Lab	BP-0042d.xls	BP-0042 description.doc		BP-0042d ATv10.xls
BP-0042e	29/07/2005	PTFE	TP08 142	Med	Lab	BP-0042e.xls	BP-0042 description.doc		BP-0042e ATv10.xls
BP-0042f	29/07/2005	PTFE	TP08 142	Med	Lab	BP-0042f.xls	BP-0042 description.doc		BP-0042f ATv10.xls
BP-0042g	29/07/2005	PTFE	TP08 142	Med	Lab	BP-0042g.xls	BP-0042 description.doc		BP-0042g ATv10.xls
BP-0042h	30/07/2005	PTFE	TP08 141	Med	Lab	BP-0042h.xls	BP-0042 description.doc		BP-0042h ATv10.xls
BP-0042i	30/07/2005	PTFE	TP08 141	Med	Lab	BP-0042i.xls	BP-0042 description.doc		BP-0042i ATv10.xls
BP-0042j	30/07/2005	PTFE	TP08 141	Med	Lab	BP-0042j.xls	BP-0042 description.doc		BP-0042j ATv10.xls
BP-0042k	30/07/2005	PTFE	TP08 132	Med	Lab	BP-0042k.xls	BP-0042 description.doc		BP-0042k ATv10.xls
BP-0042-KD2	12/01/2006	PTFE	KD2	N/A	Lab	Summary KD2			
BP-0042l	30/07/2005	PTFE	TP08 132	Med	Lab	BP-0042l.xls	BP-0042 description.doc		BP-0042l ATv10.xls
BP-0042m	30/07/2005	PTFE	TP08 132	Med	Lab	BP-0042m.xls	BP-0042 description.doc		BP-0042m ATv10.xls
BP-0042n	31/07/2005	PTFE	TP08 131	Med	Lab	BP-0042n.xls	BP-0042 description.doc		BP-0042n ATv10.xls
BP-0042o	31/07/2005	PTFE	TP08 131	Med	Lab	BP-0042o.xls	BP-0042 description.doc	BP-0042p data smoothing trial 01 averages	BP-0042o ATv10.xls
BP-0042p	31/07/2005	PTFE	TP08 131	Med	Lab	BP-0042p.xls	BP-0042 description.doc	BP-0041 & 42 Summary PTFE Regression.xls	BP-0042p ATv10.xls
BP-0043a	01/08/2005	Aerated concrete Solar Block	TP08 131	Med	Lab	BP-0043a.xls	BP-0043 description.doc		BP-0043a ATv10.xls
BP-0043b	01/08/2005	Aerated concrete Block - unidentified	TP08 132	Med	Lab	BP-0043b.xls	BP-0043 description.doc		BP-0043b ATv10.xls
BP-0043c	01/08/2005	Aerated concrete Solar Block	TP08 141	Med	Lab	BP-0043c.xls	BP-0043 description.doc		BP-0043c ATv10.xls
BP-0043d	01/08/2005	Aerated concrete Foundation	TP08 142	Med	Lab	BP-0043d.xls	BP-0043 description.doc		BP-0043d ATv10.xls
BP-0043e	01/08/2005	Aerated concrete Solar Block	TP08 131	Med	Lab	BP-0043e.xls	BP-0043 description.doc		BP-0043e ATv10.xls
BP-0043f	01/08/2005	Aerated concrete Block - unidentified	TP08 132	Med	Lab	BP-0043f.xls	BP-0043 description.doc		BP-0043f ATv10.xls
BP-0043g	01/08/2005	Aerated concrete Solar Block	TP08 141	Med	Lab	BP-0043g.xls	BP-0043 description.doc		BP-0043g ATv10.xls
BP-0043h	01/08/2005	Aerated concrete Foundation	TP08 142	Med	Lab	BP-0043h.xls	BP-0043 description.doc		BP-0043h ATv10.xls
BP-0043i	02/08/2005	Aerated concrete Solar Block	TP08 131	Med	Lab	BP-0043i.xls	BP-0043 description.doc		BP-0043i ATv10.xls
BP-0043j	02/08/2005	Aerated concrete Block - unidentified	TP08 132	Med	Lab	BP-0043j.xls	BP-0043 description.doc		BP-0043j ATv10.xls
BP-0043k	02/08/2005	Aerated concrete Solar Block	TP08 141	Med	Lab	BP-0043k.xls	BP-0043 description.doc		BP-0043k ATv10.xls
BP-0043l	02/08/2005	Aerated concrete Foundation	TP08 142	Med	Lab	BP-0043l.xls	BP-0043 description.doc		BP-0043l ATv10.xls
BP-0043m	02/08/2005	Aerated concrete Foundation	TP08 131	Med	Lab	BP-0043m.xls	BP-0043 description.doc		BP-0043m ATv10.xls
BP-0043n	02/08/2005	Aerated concrete Solar Block	TP08 132	Med	Lab	BP-0043n.xls	BP-0043 description.doc		BP-0043n ATv10.xls
BP-0043o	02/08/2005	Aerated concrete Block - unidentified	TP08 141	Med	Lab	BP-0043o.xls	BP-0043 description.doc		BP-0043o ATv10.xls
BP-0043p	02/08/2005	Aerated concrete Solar Block	TP08 142	Med	Lab	BP-0043p.xls	BP-0043 description.doc		BP-0043p ATv10.xls
BP-0043q	02/08/2005	Aerated concrete Foundation	TP08 131	Med	Lab	BP-0043q.xls	BP-0043 description.doc		BP-0043q ATv10.xls
BP-0043r	02/08/2005	Aerated concrete Solar Block	TP08 132	Med	Lab	BP-0043r.xls	BP-0043 description.doc		BP-0043r ATv10.xls
BP-0043s	02/08/2005	Aerated concrete Block - unidentified	TP08 141	Med	Lab	BP-0043s.xls	BP-0043 description.doc	Summary Moisture BP-0028, 29, 30, 34, 35, 36, 45, 43 & 50	BP-0043s ATv10.xls
BP-0043t	02/08/2005	Aerated concrete Solar Block	TP08 142	Med	Lab	BP-0043t.xls	BP-0043 description.doc	Summary BP-0043 Aerated concrete Home Office.xls	BP-0043t ATv10.xls
BP-0044a	02/08/2005	Agar	TP08 131	Med	Lab	BP-0044a.xls	BP-0044 description.doc		BP-0044a ATv10.xls

Ref	Date	Material	Probe	Heat	Lab In situ	Raw Data Location	Descriptions	Miscellaneous Analyses	ATv10
BP-0044b	02/08/2005	Agar	TP08 132	High	Lab	BP-0044b.xls	BP-0044 description.doc		BP-0044b ATv10.xls
BP-0044c	02/08/2005	Agar	TP08 141	High	Lab	BP-0044c.xls	BP-0044 description.doc		BP-0044c ATv10.xls
BP-0044d	02/08/2005	Agar	TP08 142	High	Lab	BP-0044d.xls	BP-0044 description.doc		BP-0044d ATv10.xls
BP-0044e	02/08/2005	Agar	TP08 131	High	Lab	BP-0044e.xls	BP-0044 description.doc		BP-0044e ATv10.xls
BP-0044f	03/08/2005	Agar	TP08 131	High	Lab	BP-0044f.xls	BP-0044 description.doc		BP-0044f ATv10.xls
BP-0044g	03/08/2005	Agar	TP08 132	High	Lab	BP-0044g.xls	BP-0044 description.doc		BP-0044g ATv10.xls
BP-0044h	03/08/2005	Agar	TP08 141	High	Lab	BP-0044h.xls	BP-0044 description.doc		BP-0044h ATv10.xls
BP-0044i	03/08/2005	Agar	TP08 142	High	Lab	BP-0044i.xls	BP-0044 description.doc		BP-0044i ATv10.xls
BP-0044j	03/08/2005	Agar	TP08 131	High	Lab	BP-0044j.xls	BP-0044 description.doc	BP-0044jklm Resistor Box Temps.xls	BP-0044j ATv10.xls
BP-0044k	03/08/2005	Agar	TP08 132	High	Lab	BP-0044k.xls	BP-0044 description.doc		BP-0044k ATv10.xls
BP-0044l	03/08/2005	Agar	TP08 141	High	Lab	BP-0044l.xls	BP-0044 description.doc		BP-0044l ATv10.xls
BP-0044m	03/08/2005	Agar	TP08 142	High	Lab	BP-0044m.xls	BP-0044 description.doc	BP-0042&44 H using fixed & measured Lambda.xls	BP-0044m ATv10.xls
BP-0044n	04/08/2005	Agar	TP08 131	High	Lab	BP-0044n.xls	BP-0044 description.doc	BP-0044nopq Resistor Temperature Check.xls	BP-0044n ATv10.xls
BP-0044o	04/08/2005	Agar	TP08 132	High	Lab	BP-0044o.xls	BP-0044 description.doc	BP-0044o regression ATv07.xls	BP-0044o ATv10.xls
BP-0044p	04/08/2005	Agar	TP08 141	High	Lab	BP-0044p.xls	BP-0044 description.doc	BP-0044p regression ATv07 plus alpha H.xls	BP-0044p ATv10.xls
BP-0044q	04/08/2005	Agar	TP08 142	High	Lab	BP-0044q.xls	BP-0044 description.doc	H from Calibration Sheets.xls	BP-0044q ATv10.xls
BP-0044r	04/08/2005	Agar	TP08 142	High	Lab	BP-0044r.xls	BP-0044 description.doc	Summary Agar Regression, Res Calibration.xls	BP-0044r ATv10.xls
BP-0044s	04/08/2005	Agar	TP08 141	High	Lab	BP-0044s.xls	BP-0044 description.doc	BP-0044u Lambda Live Power not Mean Power ATv07.xls	BP-0044s ATv10.xls
BP-0044t	04/08/2005	Agar	TP08 132	High	Lab	BP-0044t.xls	BP-0044 description.doc	BP-0044u Power Chart ATv07.xls	BP-0044t ATv10.xls
BP-0044u	04/08/2005	Agar	TP08 131	High	Lab	BP-0044u.xls	BP-0044 description.doc	Calibration Sheets.xls	BP-0044u ATv10.xls
BP-0045a	15/08/2005	Aerated concrete Solar Block	TP08 131	Med	Lab	BP-0045a.xls	BP-0045 description.doc		BP-0045a ATv10.xls
BP-0045b	15/08/2005	Aerated concrete Solar Block	TP08 132	Med	Lab	BP-0045b.xls	BP-0045 description.doc		BP-0045b ATv10.xls
BP-0045c	15/08/2005	Aerated concrete Block - unidentified	TP08 141	Med	Lab	BP-0045c.xls	BP-0045 description.doc		BP-0045c ATv10.xls
BP-0045d	15/08/2005	Aerated concrete Foundation	TP08 142	Med	Lab	BP-0045d.xls	BP-0045 description.doc		BP-0045d ATv10.xls
BP-0045e	15/08/2005	Aerated concrete Solar Block	TP08 131	Med	Lab	BP-0045e.xls	BP-0045 description.doc		BP-0045e ATv10.xls
BP-0045f	15/08/2005	Aerated concrete Solar Block	TP08 132	Med	Lab	BP-0045f.xls	BP-0045 description.doc		BP-0045f ATv10.xls
BP-0045g	15/08/2005	Aerated concrete Block - unidentified	TP08 141	Med	Lab	BP-0045g.xls	BP-0045 description.doc		BP-0045g ATv10.xls
BP-0045h	15/08/2005	Aerated concrete Foundation	TP08 142	Med	Lab	BP-0045h.xls	BP-0045 description.doc		BP-0045h ATv10.xls
BP-0045i	15/08/2005	Aerated concrete Solar Block	TP08 131	Med	Lab	BP-0045i.xls	BP-0045 description.doc		BP-0045i ATv10.xls
BP-0045j	15/08/2005	Aerated concrete Block - unidentified	TP08 132	Med	Lab	BP-0045j.xls	BP-0045 description.doc		BP-0045j ATv10.xls
BP-0045k	15/08/2005	Aerated concrete Foundation	TP08 141	Med	Lab	BP-0045k.xls	BP-0045 description.doc		BP-0045k ATv10.xls
BP-0045l	15/08/2005	Aerated concrete Solar Block	TP08 142	Med	Lab	BP-0045l.xls	BP-0045 description.doc		BP-0045l ATv10.xls
BP-0045m	15/08/2005	Aerated concrete Solar Block	TP08 131	Med	Lab	BP-0045m.xls	BP-0045 description.doc		BP-0045m ATv10.xls
BP-0045n	15/08/2005	Aerated concrete Block - unidentified	TP08 132	Med	Lab	BP-0045n.xls	BP-0045 description.doc		BP-0045n ATv10.xls
BP-0045o	15/08/2005	Aerated concrete Foundation	TP08 141	Med	Lab	BP-0045o.xls	BP-0045 description.doc		BP-0045o ATv10.xls
BP-0045p	15/08/2005	Aerated concrete Solar Block	TP08 142	Med	Lab	BP-0045p.xls	BP-0045 description.doc		BP-0045p ATv10.xls
BP-0045q	16/08/2005	Aerated concrete Block - unidentified	TP08 131	Med	Lab	BP-0045q.xls	BP-0045 description.doc		BP-0045q ATv10.xls
BP-0045r	16/08/2005	Aerated concrete Foundation	TP08 132	Med	Lab	BP-0045r.xls	BP-0045 description.doc		BP-0045r ATv10.xls
BP-0045s	16/08/2005	Aerated concrete Solar Block	TP08 141	Med	Lab	BP-0045s.xls	BP-0045 description.doc		BP-0045s ATv10.xls
BP-0045t	16/08/2005	Aerated concrete Solar Block	TP08 142	Med	Lab	BP-0045t.xls	BP-0045 description.doc		BP-0045t ATv10.xls

Ref	Date	Material	Probe	Heat	Lab In situ	Raw Data Location	Descriptions	Miscellaneous Analyses	ATv10
BP-0045u	17/08/2005	Aerated concrete Block - unidentified	TP08 131	Med	Lab	BP-0045u.xls	BP-0045 description.doc		BP-0045u ATv10.xls
BP-0045v	17/08/2005	Aerated concrete Foundation	TP08 132	Med	Lab	BP-0045v.xls	BP-0045 description.doc		BP-0045v ATv10.xls
BP-0045w	17/08/2005	Aerated concrete Solar Block	TP08 141	Med	Lab	BP-0045w.xls	BP-0045 description.doc		BP-0045w ATv10.xls
BP-0045x	17/08/2005	Aerated concrete Solar Block	TP08 142	Med	Lab	BP-0045x.xls	BP-0045 description.doc		BP-0045x ATv10.xls
BP-0045y	17/08/2005	Aerated concrete Foundation	TP08 131	Med	Lab	BP-0045y.xls	BP-0045 description.doc		BP-0045y ATv10.xls
BP-0045za	17/08/2005	Aerated concrete Solar Block	TP08 132	Med	Lab	BP-0045za.xls	BP-0045 description.doc		BP-0045za ATv10.xls
BP-0045zb	17/08/2005	Aerated concrete Solar Block	TP08 141	Med	Lab	BP-0045zb.xls	BP-0045 description.doc		BP-0045zb ATv10.xls
BP-0045zc	17/08/2005	Aerated concrete Block - unidentified	TP08 142	Med	Lab	BP-0045zc.xls	BP-0045 description.doc		BP-0045zc ATv10.xls
BP-0045zd	18/08/2005	Aerated concrete Foundation	TP08 131	Med	Lab	BP-0045zd.xls	BP-0045 description.doc		BP-0045zd ATv10.xls
BP-0045ze	18/08/2005	Aerated concrete Solar Block	TP08 132	Med	Lab	BP-0045ze.xls	BP-0045 description.doc	Summary Moisture BP-0028, 29, 30, 34, 35, 36, 45, 43 & 50	BP-0045ze ATv10.xls
BP-0045zf	18/08/2005	Aerated concrete Solar Block	TP08 141	Med	Lab	BP-0045zf.xls	BP-0045 description.doc	Regressions	BP-0045zf ATv10.xls
BP-0045zg	18/08/2005	Aerated concrete Block - unidentified	TP08 142	Med	Lab	BP-0045zg.xls	BP-0045 description.doc	Summary BP-0045 & 43 Aerated concrete Home Office.xls	BP-0046zg ATv10.xls
BP-0046a	22/08/2005	Agar	TP08 131	High	Lab	BP-0046a.xls	BP-0046 description.doc		BP-0046a ATv10.xls
BP-0046b	22/08/2005	Agar	TP08 132	High	Lab	BP-0046b.xls	BP-0046 description.doc		BP-0046b ATv10.xls
BP-0046c	22/08/2005	Agar	TP08 141	High	Lab	BP-0046c.xls	BP-0046 description.doc		BP-0046c ATv10.xls
BP-0046d	22/08/2005	Agar	TP08 142	High	Lab	BP-0046d.xls	BP-0046 description.doc	BP-0046d ATv08 resistor check.xls	BP-0046d ATv10.xls
BP-0046e	22/08/2005	Agar	TP08 131	High	Lab	BP-0046e.xls	BP-0046 description.doc		BP-0046e ATv10.xls
BP-0046f	22/08/2005	Agar	TP08 132	High	Lab	BP-0046f.xls	BP-0046 description.doc		BP-0046f ATv10.xls
BP-0046g	22/08/2005	Agar	TP08 141	High	Lab	BP-0046g.xls	BP-0046 description.doc	Regressions	BP-0046g ATv10.xls
BP-0046h	22/08/2005	Agar	TP08 142	High	Lab	BP-0046h.xls	BP-0046 description.doc	Summary BP-0046.xls	BP-0046h ATv10.xls
BP-0047a	25/08/2005	Dupre Vermiculite	TP08 131	Low	Lab	BP-0047a.xls	BP-0047 description.doc		BP-0047a ATv10.xls
BP-0047b	25/08/2005	Phenolic foam	TP08 132	Low	Lab	BP-0047b.xls	BP-0047 description.doc		BP-0047b ATv10.xls
BP-0047c	25/08/2005	Multi foil insulation	TP08 141	Low	Lab	BP-0047c.xls	BP-0047 description.doc	U Value calcs.xls	BP-0047c ATv10.xls
BP-0047d	25/08/2005	Sheeps Wool, with the 'grain'	TP08 142	Low	Lab	BP-0047d.xls	BP-0047 description.doc		BP-0047d ATv10.xls
BP-0047e	25/08/2005	Dupre Vermiculite	TP08 131	Low	Lab	BP-0047e.xls	BP-0047 description.doc		BP-0047e ATv10.xls
BP-0047f	25/08/2005	Phenolic foam	TP08 132	Low	Lab	BP-0047f.xls	BP-0047 description.doc		BP-0047f ATv10.xls
BP-0047g	25/08/2005	Multi foil insulation	TP08 141	Low	Lab	BP-0047g.xls	BP-0047 description.doc		BP-0047g ATv10.xls
BP-0047h	25/08/2005	Sheeps Wool, with the 'grain'	TP08 142	Low	Lab	BP-0047h.xls	BP-0047 description.doc		BP-0047h ATv10.xls
BP-0047i	26/08/2005	Dupre Vermiculite	TP08 131	Low	Lab	BP-0047i.xls	BP-0047 description.doc		BP-0047i ATv10.xls
BP-0047j	26/08/2005	Phenolic foam	TP08 132	Low	Lab	BP-0047j.xls	BP-0047 description.doc		BP-0047j ATv10.xls
BP-0047k	26/08/2005	Multi foil insulation	TP08 141	Low	Lab	BP-0047k.xls	BP-0047 description.doc		BP-0047k ATv10.xls
BP-0047l	26/08/2005	Sheeps Wool, with the 'grain'	TP08 142	Low	Lab	BP-0047l.xls	BP-0047 description.doc		BP-0047l ATv10.xls
BP-0047m	26/08/2005	Dupre Vermiculite	TP08 131	Med	Lab	BP-0047m.xls	BP-0047 description.doc		BP-0047m ATv10.xls
BP-0047n	26/08/2005	Phenolic foam	TP08 132	Med	Lab	BP-0047n.xls	BP-0047 description.doc		BP-0047n ATv10.xls
BP-0047o	26/08/2005	Multi foil insulation	TP08 141	Med	Lab	BP-0047o.xls	BP-0047 description.doc		BP-0047o ATv10.xls
BP-0047p	26/08/2005	Sheeps Wool, with the 'grain'	TP08 142	Med	Lab	BP-0047p.xls	BP-0047 description.doc		BP-0047p ATv10.xls
BP-0047q	26/08/2005	Glass wool across the grain	TP08 131	Low	Lab	BP-0047q.xls	BP-0047 description.doc		BP-0047q ATv10.xls
BP-0047r	26/08/2005	Glass wool with the grain	TP08 132	Low	Lab	BP-0047r.xls	BP-0047 description.doc		BP-0047r ATv10.xls
BP-0047s	26/08/2005	Multi foil insulation in roll	TP08 141	Low	Lab	BP-0047s.xls	BP-0047 description.doc		BP-0047s ATv10.xls
BP-0047t	26/08/2005	Sheep's Wool, across the 'grain'	TP08 142	Low	Lab	BP-0047t.xls	BP-0047 description.doc		BP-0047t ATv10.xls
BP-0047u	26/08/2005	Glass wool across the grain	TP08 131	Low	Lab	BP-0047u.xls	BP-0047 description.doc		BP-0047u ATv10.xls
BP-0047v	26/08/2005	Glass wool with the grain	TP08 132	Low	Lab	BP-0047v.xls	BP-0047 description.doc		BP-0047v ATv10.xls
BP-0047w	26/08/2005	Multi foil insulation in roll	TP08 141	Low	Lab	BP-0047w.xls	BP-0047 description.doc		BP-0047w ATv10.xls
BP-0047x	26/08/2005	Sheep's Wool, across the 'grain'	TP08 142	Low	Lab	BP-0047x.xls	BP-0047 description.doc		BP-0047x ATv10.xls

Ref	Date	Material	Probe	Heat	Lab In situ	Raw Data Location	Descriptions	Miscellaneous Analyses	ATv10
BP-0047y	27/08/2005	Glass wool across the grain	TP08 131	Low	Lab	BP-0047y.xls	BP-0047 description.doc		BP-0047y ATv10.xls
BP-0047za	27/08/2005	Glass wool with the grain	TP08 132	Low	Lab	BP-0047za.xls	BP-0047 description.doc		BP-0047za ATv10.xls
BP-0047zb	27/08/2005	Multi foil insulation in roll	TP08 141	Low	Lab	BP-0047zb.xls	BP-0047 description.doc		BP-0047zb ATv10.xls
BP-0047zc	27/08/2005	Sheep's Wool, across the 'grain'	TP08 142	Low	Lab	BP-0047zc.xls	BP-0047 description.doc		BP-0047zc ATv10.xls
BP-0047zd	27/08/2005	Glass wool across the grain	TP08 131	Low	Lab	BP-0047zd.xls	BP-0047 description.doc		BP-0047zd ATv10.xls
BP-0047ze	27/08/2005	Glass wool with the grain	TP08 132	Low	Lab	BP-0047ze.xls	BP-0047 description.doc		BP-0047ze ATv10.xls
BP-0047zf	27/08/2005	Multi foil insulation in roll	TP08 141	Low	Lab	BP-0047zf.xls	BP-0047 description.doc		BP-0047zf ATv10.xls
BP-0047zg	27/08/2005	Sheep's Wool, across the 'grain'	TP08 142	Low	Lab	BP-0047zg.xls	BP-0047 description.doc		BP-0047zg ATv10.xls
BP-0047zh	29/08/2005	Phenolic foam	TP08 131	Low	Lab	BP-0047zh.xls	BP-0047 description.doc		BP-0047zh ATv10.xls
BP-0047zi	29/08/2005	Glass wool rolled	TP08 132	Low	Lab	BP-0047zi.xls	BP-0047 description.doc		BP-0047zi ATv10.xls
BP-0047zj	29/08/2005	Dupre Vermiculite	TP08 141	Low	Lab	BP-0047zj.xls	BP-0047 description.doc		BP-0047zj ATv10.xls
BP-0047zk	29/08/2005	Sheep's Wool, rolled	TP08 142	Low	Lab	BP-0047zk.xls	BP-0047 description.doc		BP-0047zk ATv10.xls
BP-0047zl	29/08/2005	Phenolic foam	TP08 131	Low	Lab	BP-0047zl.xls	BP-0047 description.doc		BP-0047zl ATv10.xls
BP-0047zm	29/08/2005	Glass wool rolled	TP08 132	Low	Lab	BP-0047zm.xls	BP-0047 description.doc		BP-0047zm ATv10.xls
BP-0047zn	29/08/2005	Dupre Vermiculite	TP08 141	Low	Lab	BP-0047zn.xls	BP-0047 description.doc		BP-0047zn ATv10.xls
BP-0047zo	29/08/2005	Sheep's Wool, rolled	TP08 142	Low	Lab	BP-0047zo.xls	BP-0047 description.doc		BP-0047zo ATv10.xls
BP-0047zp	29/08/2005	Phenolic foam	TP08 131	Low	Lab	BP-0047zp.xls	BP-0047 description.doc		BP-0047zp ATv10.xls
BP-0047zq	29/08/2005	Glass wool rolled	TP08 132	Low	Lab	BP-0047zq.xls	BP-0047 description.doc		BP-0047zq ATv10.xls
BP-0047zr	29/08/2005	Dupre Vermiculite	TP08 141	Low	Lab	BP-0047zr.xls	BP-0047 description.doc		BP-0047zr ATv10.xls
BP-0047zs	29/08/2005	Sheep's Wool, rolled	TP08 142	Low	Lab	BP-0047zs.xls	BP-0047 description.doc		BP-0047zs ATv10.xls
BP-0047zt	29/08/2005	Phenolic foam	TP08 131	Low	Lab	BP-0047zt.xls	BP-0047 description.doc		BP-0047zt ATv10.xls
BP-0047zu	29/08/2005	Glass wool rolled	TP08 132	Low	Lab	BP-0047zu.xls	BP-0047 description.doc	2 powers & boundary assessment Phenolic foam.xls	BP-0047zu ATv10.xls
BP-0047zv	29/08/2005	Dupre Vermiculite	TP08 141	Low	Lab	BP-0047zv.xls	BP-0047 description.doc	Regressions	BP-0047zv ATv10.xls
BP-0047zw	29/08/2005	Sheep's Wool, rolled	TP08 142	Low	Lab	BP-0047zw.xls	BP-0047 description.doc	Summary BP-0047.xls	BP-0047zw ATv10.xls
BP-0048a	07/09/2005	Straw Bale	TP08 131	Low	Lab	BP-0048a.xls	BP-0048 description.doc		BP-0048a ATv10.xls
BP-0048b	07/09/2005	Straw Bale	TP08 132	Low	Lab	BP-0048b.xls	BP-0048 description.doc		BP-0048b ATv10.xls
BP-0048c	07/09/2005	Straw Bale	TP08 141	Low	Lab	BP-0048c.xls	BP-0048 description.doc	Regressions	BP-0048c ATv10.xls
BP-0048d	07/09/2005	Straw Bale	TP08 142	Low	Lab	BP-0048d.xls	BP-0048 description.doc	Summary BP-0048.xls	BP-0048d ATv10.xls
BP-0049a	08/09/2005	Cob block with lambswool	TP08 131	Med	In situ	BP-0049a.xls	BP-0049 description.doc		BP-0049a ATv10.xls
BP-0049b	08/09/2005	Cob block	TP08 132	Med	In situ	BP-0049b.xls	BP-0049 description.doc		BP-0049b ATv10.xls
BP-0049c	08/09/2005	Cob block with lambswool	TP08 141	Med	In situ	BP-0049c.xls	BP-0049 description.doc		BP-0049c ATv10.xls
BP-0049d	08/09/2005	Cob block	TP08 142	Med	In situ	BP-0049d.xls	BP-0049 description.doc		BP-0049d ATv10.xls
BP-0049e	08/09/2005	Cob block with lambswool	TP08 131	High	In situ	BP-0049e.xls	BP-0049 description.doc		BP-0049e ATv10.xls
BP-0049f	08/09/2005	Cob block	TP08 132	High	In situ	BP-0049f.xls	BP-0049 description.doc		BP-0049f ATv10.xls
BP-0049g	08/09/2005	Cob block with lambswool	TP08 141	High	In situ	BP-0049g.xls	BP-0049 description.doc		BP-0049g ATv10.xls
BP-0049h	08/09/2005	Cob block	TP08 142	High	In situ	BP-0049h.xls	BP-0049 description.doc		BP-0049h ATv10.xls
BP-0049i	08/09/2005	Cob block	TP08 131	High	In situ	BP-0049i.xls	BP-0049 description.doc		BP-0049i ATv10.xls
BP-0049j	08/09/2005	Cob block with lambswool	TP08 132	High	In situ	BP-0049j.xls	BP-0049 description.doc		BP-0049j ATv10.xls
BP-0049k	08/09/2005	Cob block	TP08 141	High	In situ	BP-0049k.xls	BP-0049 description.doc		BP-0049k ATv10.xls

Ref	Date	Material	Probe	Heat	Lab In situ	Raw Data Location	Descriptions	Miscellaneous Analyses	ATv10
BP-0049l	08/09/2005	Cob block with lambswool	TP08 142	High	In situ	BP-0049l.xls	BP-0049 description.doc		BP-0049l ATv10.xls
BP-0049m	08/09/2005	Cob block	TP08 131	High	In situ	BP-0049m.xls	BP-0049 description.doc		BP-0049m ATv10.xls
BP-0049n	08/09/2005	Cob block with lambswool	TP08 132	High	In situ	BP-0049n.xls	BP-0049 description.doc		BP-0049n ATv10.xls
BP-0049o	08/09/2005	Cob block	TP08 141	High	In situ	BP-0049o.xls	BP-0049 description.doc		Jump in heating curve
BP-0049p	08/09/2005	Cob block with lambswool	TP08 142	High	In situ	BP-0049p.xls	BP-0049 description.doc	BP-0049abcd with temp stabilisation chart.xls	BP-0049p ATv10.xls
BP-0049q	08/09/2005	Cob block with lambswool	TP08 131	High	In situ	BP-0049q.xls	BP-0049 description.doc	BP-0049mnop with temp stabilisation chart.xls	BP-0049q ATv10.xls
BP-0049r	08/09/2005	Cob block	TP08 132	High	In situ	BP-0049r.xls	BP-0049 description.doc	Regressions	BP-0049r ATv10.xls
BP-0049s	08/09/2005	Cob block with lambswool	TP08 141	High	In situ	BP-0049s.xls	BP-0049 description.doc	Summary BP-0049 onsite & print results compared.xls	BP-0049s ATv10.xls
BP-0049t	08/09/2005	Cob block	TP08 142	High	In situ	BP-0049t.xls	BP-0049 description.doc	Summary BP-0049.xls	BP-0049t ATv10.xls
BP-0050a	10/09/2005	Aerated concrete Standard	TP08 131	Med	Lab	BP-0050a.xls	BP-0050 description.doc	BP-0050a power curve.xls	BP-0050a ATv10.xls
BP-0050b	10/09/2005	Aerated concrete Solar	TP08 132	Med	Lab	BP-0050b.xls	BP-0050 description.doc	BP-0050b power curve.xls	BP-0050b ATv10.xls
BP-0050c	10/09/2005	Aerated concrete Solar	TP08 141	Med	Lab	BP-0050c.xls	BP-0050 description.doc	BP-0050c power curve.xls	BP-0050c ATv10.xls
BP-0050d	10/09/2005	Aerated concrete Foundation	TP08 142	Med	Lab	BP-0050d.xls	BP-0050 description.doc	BP-0050d power curve.xls	BP-0050d ATv10.xls
BP-0050e	10/09/2005	Aerated concrete Standard	TP08 131	Med	Lab	BP-0050e.xls	BP-0050 description.doc		BP-0050e ATv10.xls
BP-0050f	10/09/2005	Aerated concrete Solar	TP08 132	Med	Lab	BP-0050f.xls	BP-0050 description.doc		BP-0050f ATv10.xls
BP-0050g	10/09/2005	Aerated concrete Solar	TP08 141	Med	Lab	BP-0050g.xls	BP-0050 description.doc		BP-0050g ATv10.xls
BP-0050h	10/09/2005	Aerated concrete Foundation	TP08 142	Med	Lab	BP-0050h.xls	BP-0050 description.doc		BP-0050h ATv10.xls
BP-0050i	10/09/2005	Aerated concrete Solar	TP08 131	Med	Lab	BP-0050i.xls	BP-0050 description.doc		BP-0050i ATv10.xls
BP-0050j	10/09/2005	Aerated concrete Solar	TP08 132	Med	Lab	BP-0050j.xls	BP-0050 description.doc		BP-0050j ATv10.xls
BP-0050k	10/09/2005	Aerated concrete Foundation	TP08 141	Med	Lab	BP-0050k.xls	BP-0050 description.doc		BP-0050k ATv10.xls
BP-0050l	10/09/2005	Aerated concrete Standard	TP08 142	Med	Lab	BP-0050l.xls	BP-0050 description.doc		BP-0050l ATv10.xls
BP-0050m	10/09/2005	Aerated concrete Solar	TP08 131	Med	Lab	BP-0050m.xls	BP-0050 description.doc		BP-0050m ATv10.xls
BP-0050n	10/09/2005	Aerated concrete Solar	TP08 132	Med	Lab	BP-0050n.xls	BP-0050 description.doc		BP-0050n ATv10.xls
BP-0050o	10/09/2005	Aerated concrete Foundation	TP08 141	Med	Lab	BP-0050o.xls	BP-0050 description.doc		BP-0050o ATv10.xls
BP-0050p	10/09/2005	Aerated concrete Standard	TP08 142	Med	Lab	BP-0050p.xls	BP-0050 description.doc		BP-0050p ATv10.xls
BP-0050q	11/09/2005	Aerated concrete Solar	TP08 131	Med	Lab	BP-0050q.xls	BP-0050 description.doc		BP-0050q ATv10.xls
BP-0050r	11/09/2005	Aerated concrete Foundation	TP08 132	Med	Lab	BP-0050r.xls	BP-0050 description.doc		BP-0050r ATv10.xls
BP-0050s	11/09/2005	Aerated concrete Standard	TP08 141	Med	Lab	BP-0050s.xls	BP-0050 description.doc		BP-0050s ATv10.xls
BP-0050t	11/09/2005	Aerated concrete Solar	TP08 142	Med	Lab	BP-0050t.xls	BP-0050 description.doc		BP-0050t ATv10.xls
BP-0050u	11/09/2005	Aerated concrete Solar	TP08 131	Med	Lab	BP-0050u.xls	BP-0050 description.doc		BP-0050u ATv10.xls
BP-0050v	11/09/2005	Aerated concrete Foundation	TP08 132	Med	Lab	BP-0050v.xls	BP-0050 description.doc		BP-0050v ATv10.xls
BP-0050w	11/09/2005	Aerated concrete Standard	TP08 141	Med	Lab	BP-0050w.xls	BP-0050 description.doc		BP-0050w ATv10.xls
BP-0050x	11/09/2005	Aerated concrete Solar	TP08 142	Med	Lab	BP-0050x.xls	BP-0050 description.doc		BP-0050x ATv10.xls
BP-0050y	11/09/2005	Aerated concrete Foundation	TP08 131	Med	Lab	BP-0050y.xls	BP-0050 description.doc		BP-0050y ATv10.xls
BP-0050za	11/09/2005	Aerated concrete Standard	TP08 132	Med	Lab	BP-0050za.xls	BP-0050 description.doc		BP-0050za ATv10.xls
BP-0050zb	11/09/2005	Aerated concrete Solar	TP08 141	Med	Lab	BP-0050zb.xls	BP-0050 description.doc		BP-0050zb ATv10.xls
BP-0050zc	11/09/2005	Aerated concrete Solar	TP08 142	Med	Lab	BP-0050zc.xls	BP-0050 description.doc		BP-0050zc ATv10.xls
BP-0050zd	12/09/2005	Aerated concrete Foundation	TP08 131	Med	Lab	BP-0050zd.xls	BP-0050 description.doc		BP-0050zd ATv10.xls
BP-0050ze	12/09/2005	Aerated concrete Standard	TP08 132	Med	Lab	BP-0050ze.xls	BP-0050 description.doc	Regressions	BP-0050ze ATv10.xls
BP-0050zf	12/09/2005	Aerated concrete Solar	TP08 141	Med	Lab	BP-0050zf.xls	BP-0050 description.doc	Summary Moisture BP-0028, 29, 30, 34, 35, 36, 45, 43 & 50	BP-0050zf ATv10.xls
BP-0050zg	12/09/2005	Aerated concrete Solar	TP08 142	Med	Lab	BP-0050zg.xls	BP-0050 description.doc		BP-0050zg ATv10.xls
BP-0051a	24/09/2005	Spruce across	TP08 131	Med	Lab	BP-0051a.xls	BP-0051 description.doc		BP-0051a ATv10.xls

Ref	Date	Material	Probe	Heat	Lab In situ	Raw Data Location	Descriptions	Miscellaneous Analyses	ATv10
BP-0051b	24/09/2005	Spruce across	TP08 132	Med	Lab	BP-0051b.xls	BP-0051 description.doc		BP-0051b ATv10.xls
BP-0051c	24/09/2005	Spruce along	TP08 141	Med	Lab	BP-0051c.xls	BP-0051 description.doc		BP-0051c ATv10.xls
BP-0051d	24/09/2005	Oak across	TP08 142	Med	Lab	BP-0051d.xls	BP-0051 description.doc		BP-0051d ATv10.xls
BP-0051e	25/09/2005	Spruce across	TP08 131	Med	Lab	BP-0051e.xls	BP-0051 description.doc		BP-0051e ATv10.xls
BP-0051f	25/09/2005	Spruce across	TP08 132	Med	Lab	BP-0051f.xls	BP-0051 description.doc		BP-0051f ATv10.xls
BP-0051g	25/09/2005	Spruce along	TP08 141	Med	Lab	BP-0051g.xls	BP-0051 description.doc		BP-0051g ATv10.xls
BP-0051h	25/09/2005	Oak across	TP08 142	Med	Lab	BP-0051h.xls	BP-0051 description.doc		BP-0051h ATv10.xls
BP-0051i	25/09/2005	Spruce across	TP08 131	Med	Lab	BP-0051i.xls	BP-0051 description.doc		BP-0051i ATv10.xls
BP-0051j	25/09/2005	Spruce across	TP08 132	Med	Lab	BP-0051j.xls	BP-0051 description.doc		BP-0051j ATv10.xls
BP-0051k	25/09/2005	Spruce along	TP08 141	Med	Lab	BP-0051k.xls	BP-0051 description.doc		BP-0051k ATv10.xls
BP-0051l	25/09/2005	Oak across	TP08 142	Med	Lab	BP-0051l.xls	BP-0051 description.doc		BP-0051l ATv10.xls
BP-0051m	25/09/2005	Spruce along	TP08 131	Med	Lab	BP-0051m.xls	BP-0051 description.doc		BP-0051m ATv10.xls
BP-0051n	25/09/2005	Oak across	TP08 132	Med	Lab	BP-0051n.xls	BP-0051 description.doc		BP-0051n ATv10.xls
BP-0051o	25/09/2005	Spruce across	TP08 141	Med	Lab	BP-0051o.xls	BP-0051 description.doc		BP-0051o ATv10.xls
BP-0051p	25/09/2005	Spruce across	TP08 142	Med	Lab	BP-0051p.xls	BP-0051 description.doc		BP-0051p ATv10.xls
BP-0051q	25/09/2005	Spruce along	TP08 131	Med	Lab	BP-0051q.xls	BP-0051 description.doc		BP-0051q ATv10.xls
BP-0051r	25/09/2005	Oak across	TP08 132	Med	Lab	BP-0051r.xls	BP-0051 description.doc		BP-0051r ATv10.xls
BP-0051s	25/09/2005	Spruce across	TP08 141	Med	Lab	BP-0051s.xls	BP-0051 description.doc		BP-0051s ATv10.xls
BP-0051t	25/09/2005	Spruce across	TP08 142	Med	Lab	BP-0051t.xls	BP-0051 description.doc		BP-0051t ATv10.xls
BP-0051u	25/09/2005	Spruce along	TP08 131	Med	Lab	BP-0051u.xls	BP-0051 description.doc		BP-0051u ATv10.xls
BP-0051v	25/09/2005	Oak across	TP08 132	Med	Lab	BP-0051v.xls	BP-0051 description.doc		BP-0051v ATv10.xls
BP-0051w	25/09/2005	Spruce across	TP08 141	Med	Lab	BP-0051w.xls	BP-0051 description.doc		BP-0051w ATv10.xls
BP-0051x	25/09/2005	Spruce across	TP08 142	Med	Lab	BP-0051x.xls	BP-0051 description.doc		BP-0051x ATv10.xls
BP-0051y	26/09/2005	Spruce across	TP08 131	Med	Lab	BP-0051y.xls	BP-0051 description.doc		BP-0051y ATv10.xls
BP-0051za	26/09/2005	Spruce across	TP08 132	Med	Lab	BP-0051za.xls	BP-0051 description.doc		BP-0051za ATv10.xls
BP-0051zb	26/09/2005	Spruce along	TP08 141	Med	Lab	BP-0051zb.xls	BP-0051 description.doc		BP-0051zb ATv10.xls
BP-0051zc	26/09/2005	Oak across	TP08 142	Med	Lab	BP-0051zc.xls	BP-0051 description.doc		BP-0051zc ATv10.xls
BP-0051zd	26/09/2005	Spruce across	TP08 131	Med	Lab	BP-0051zd.xls	BP-0051 description.doc		BP-0051zd ATv10.xls
BP-0051ze	26/09/2005	Spruce across	TP08 132	Med	Lab	BP-0051ze.xls	BP-0051 description.doc		BP-0051ze ATv10.xls
BP-0051zf	26/09/2005	Spruce along	TP08 141	Med	Lab	BP-0051zf.xls	BP-0051 description.doc		BP-0051zf ATv10.xls
BP-0051zg	26/09/2005	Oak across	TP08 142	Med	Lab	BP-0051zg.xls	BP-0051 description.doc		BP-0051zg ATv10.xls
BP-0051zh	26/09/2005	Chestnut across	TP08 131	Med	Lab	BP-0051zh.xls	BP-0051 description.doc		BP-0051zh ATv10.xls
BP-0051zi	26/09/2005	Chestnut across	TP08 132	Med	Lab	BP-0051zi.xls	BP-0051 description.doc		BP-0051zi ATv10.xls
BP-0051zj	26/09/2005	Chestnut along	TP08 141	Med	Lab	BP-0051zj.xls	BP-0051 description.doc		BP-0051zj ATv10.xls
BP-0051zk	26/09/2005	Oak along	TP08 142	Med	Lab	BP-0051zk.xls	BP-0051 description.doc		BP-0051zk ATv10.xls
BP-0051zl	26/09/2005	Chestnut across	TP08 131	Med	Lab	BP-0051zl.xls	BP-0051 description.doc		BP-0051zl ATv10.xls
BP-0051zm	26/09/2005	Chestnut across	TP08 132	Med	Lab	BP-0051zm.xls	BP-0051 description.doc		BP-0051zm ATv10.xls
BP-0051zn	26/09/2005	Chestnut along	TP08 141	Med	Lab	BP-0051zn.xls	BP-0051 description.doc		BP-0051zn ATv10.xls
BP-0051zo	26/09/2005	Oak along	TP08 142	Med	Lab	BP-0051zo.xls	BP-0051 description.doc		BP-0051zo ATv10.xls
BP-0051zp	26/09/2005	Chestnut along	TP08 131	Med	Lab	BP-0051zp.xls	BP-0051 description.doc		BP-0051zp ATv10.xls
BP-0051zq	26/09/2005	Oak along	TP08 132	Med	Lab	BP-0051zq.xls	BP-0051 description.doc		BP-0051zq ATv10.xls
BP-0051zr	26/09/2005	Chestnut across	TP08 141	Med	Lab	BP-0051zr.xls	BP-0051 description.doc		BP-0051zr ATv10.xls

Ref	Date	Material	Probe	Heat	Lab In situ	Raw Data Location	Descriptions	Miscellaneous Analyses	ATv10
BP-0051zs	26/09/2005	Chestnut across	TP08 142	Med	Lab	BP-0051zs.xls	BP-0051 description.doc		BP-0051zs ATv10.xls
BP-0051zt	27/09/2005	Chestnut along	TP08 131	Med	Lab	BP-0051zt.xls	BP-0051 description.doc		BP-0051zt ATv10.xls
BP-0051zu	27/09/2005	Oak along	TP08 132	Med	Lab	BP-0051zu.xls	BP-0051 description.doc		BP-0051zu ATv10.xls
BP-0051zv	27/09/2005	Chestnut across	TP08 141	Med	Lab	BP-0051zv.xls	BP-0051 description.doc		BP-0051zv ATv10.xls
BP-0051zw	27/09/2005	Chestnut across	TP08 142	Med	Lab	BP-0051zw.xls	BP-0051 description.doc		BP-0051zw ATv10.xls
BP-0051zx	27/09/2005	Douglas Fir across	TP08 131	Med	Lab	BP-0051zx.xls	BP-0051 description.doc		BP-0051zx ATv10.xls
BP-0051zy	27/09/2005	Larch across	TP08 132	Med	Lab	BP-0051zy.xls	BP-0051 description.doc		BP-0051zy ATv10.xls
BP-0051zza	27/09/2005	Douglas Fir along	TP08 141	Med	Lab	BP-0051zza.xls	BP-0051 description.doc		BP-0051zza ATv10.xls
BP-0051zzb	27/09/2005	Larch along	TP08 142	Med	Lab	BP-0051zzb.xls	BP-0051 description.doc		BP-0051zzb ATv10.xls
BP-0051zzc	30/09/2005	Douglas Fir across	TP08 131	Med	Lab	BP-0051zzc.xls	BP-0051 description.doc		BP-0051zzc ATv10.xls
BP-0051zzd	30/09/2005	Larch across	TP08 132	Med	Lab	BP-0051zzd.xls	BP-0051 description.doc		BP-0051zzd ATv10.xls
BP-0051zze	30/09/2005	Douglas Fir along	TP08 141	Med	Lab	BP-0051zze.xls	BP-0051 description.doc		BP-0051zze ATv10.xls
BP-0051zzf	30/09/2005	Larch along	TP08 142	Med	Lab	BP-0051zzf.xls	BP-0051 description.doc		BP-0051zzf ATv10.xls
BP-0051zzg	30/09/2005	Douglas Fir across	TP08 131	Med	Lab	BP-0051zzg.xls	BP-0051 description.doc		BP-0051zzg ATv10.xls
BP-0051zzh	30/09/2005	Larch across	TP08 132	Med	Lab	BP-0051zzh.xls	BP-0051 description.doc		BP-0051zzh ATv10.xls
BP-0051zzi	30/09/2005	Douglas Fir along	TP08 141	Med	Lab	BP-0051zzi.xls	BP-0051 description.doc		BP-0051zzi ATv10.xls
BP-0051zzj	30/09/2005	Larch along	TP08 142	Med	Lab	BP-0051zzj.xls	BP-0051 description.doc		BP-0051zzj ATv10.xls
BP-0051zzk	30/09/2005	Larch along	TP08 131	Med	Lab	BP-0051zzk.xls	BP-0051 description.doc		BP-0051zzk ATv10.xls
BP-0051zzl	30/09/2005	Douglas Fir along	TP08 132	Med	Lab	BP-0051zzl.xls	BP-0051 description.doc		BP-0051zzl ATv10.xls
BP-0051zzm	30/09/2005	Larch across	TP08 141	Med	Lab	BP-0051zzm.xls	BP-0051 description.doc		BP-0051zzm ATv10.xls
BP-0051zzn	30/09/2005	Douglas Fir across	TP08 142	Med	Lab	BP-0051zzn.xls	BP-0051 description.doc		BP-0051zzn ATv10.xls
BP-0051zzo	30/09/2005	Larch along	TP08 131	Med	Lab	BP-0051zzo.xls	BP-0051 description.doc		BP-0051zzo ATv10.xls
BP-0051zzp	30/09/2005	Douglas Fir along	TP08 132	Med	Lab	BP-0051zzp.xls	BP-0051 description.doc		BP-0051zzp ATv10.xls
BP-0051zzq	30/09/2005	Larch across	TP08 141	Med	Lab	BP-0051zzq.xls	BP-0051 description.doc	Timber Moisture Content.xls	BP-0051zzq ATv10.xls
BP-0051zzr	30/09/2005	Douglas Fir across	TP08 142	Med	Lab	BP-0051zzr.xls	BP-0051 description.doc	Summary Timber HL Office.xls	BP-0051zzr ATv10.xls
BP-0052a	15/11/2005	Straw bale	TP08 131	Med	In situ	BP-0052a.xls	BP-0052 description.doc		BP-0052a ATv10.xls
BP-0052b	15/11/2005	Straw bale	TP08 132	Med	In situ	BP-0052b.xls	BP-0052 description.doc		BP-0052b ATv10.xls
BP-0052c	15/11/2005	Straw bale	TP08 141	Med	In situ	BP-0052c.xls	BP-0052 description.doc		Bad data 52c
BP-0052d	15/11/2005	Straw bale	TP08 142	Med	In situ	BP-0052d.xls	BP-0052 description.doc		BP-0052d ATv10.xls
BP-0052e	15/11/2005	Straw bale	TP08 131	Low	In situ	BP-0052e.xls	BP-0052 description.doc		BP-0052e ATv10.xls
BP-0052f	15/11/2005	Straw bale	TP08 132	Low	In situ	BP-0052f.xls	BP-0052 description.doc		BP-0052f ATv10.xls
BP-0052g	15/11/2005	Straw bale	TP08 141	Low	In situ	BP-0052g.xls	BP-0052 description.doc		Bad data 52g
BP-0052h	15/11/2005	Straw bale	TP08 142	Low	In situ	BP-0052h.xls	BP-0052 description.doc		BP-0052h ATv10.xls
BP-0052i	15/11/2005	Straw bale	TP08 131	Med	In situ	BP-0052i.xls	BP-0052 description.doc		BP-0052i ATv10.xls
BP-0052j	15/11/2005	Straw bale	TP08 132	Med	In situ	BP-0052j.xls	BP-0052 description.doc		BP-0052j ATv10.xls
BP-0052k	15/11/2005	Straw bale	TP08 141	Med	In situ	BP-0052k.xls	BP-0052 description.doc	In situ and lab curves compared Straw.xls	Bad data 52k

Ref	Date	Material	Probe	Heat	Lab In situ	Raw Data Location	Descriptions	Miscellaneous Analyses	ATv10
BP-0052l	15/11/2005	Straw bale	TP08 142	Med	In situ	BP-0052l.xls	BP-0052 description.doc	Summary Scotland Results.xls	BP-0052l ATv10.xls
BP-0053a	16/11/2005	Unfired earth wood shaving bricks	TP08 131	Med	In situ	BP-0053a.xls	BP-0053 description.doc		BP-0053a ATv10.xls
BP-0053b	16/11/2005	Unfired earth wood shaving bricks	TP08 132	Med	In situ	BP-0053b.xls	BP-0053 description.doc	Solver and VHC example	BP-0053b ATv10.xls
BP-0053c	16/11/2005	Unfired earth wood shaving bricks	TP08 141	Med	In situ	BP-0053c.xls	BP-0053 description.doc		BP-0053c ATv10.xls
BP-0053d	16/11/2005	Unfired earth wood shaving bricks	TP08 142	Med	In situ	BP-0053d.xls	BP-0053 description.doc		BP-0053d ATv10.xls
BP-0053e	16/11/2005	Unfired earth wood shaving bricks	TP08 131	Med	In situ	BP-0053e.xls	BP-0053 description.doc		BP-0053e ATv10.xls
BP-0053f	16/11/2005	Unfired earth wood shaving bricks	TP08 132	Med	In situ	BP-0053f.xls	BP-0053 description.doc		BP-0053f ATv10.xls
BP-0053g	16/11/2005	Unfired earth wood shaving bricks	TP08 141	Med	In situ	BP-0053g.xls	BP-0053 description.doc		BP-0053g ATv10.xls
BP-0053h	16/11/2005	Unfired earth wood shaving bricks	TP08 142	Med	In situ	BP-0053h.xls	BP-0053 description.doc		BP-0053h ATv10.xls
BP-0053i	16/11/2005	Unfired earth wood shaving bricks	TP08 131	Med	In situ	BP-0053i.xls	BP-0053 description.doc		BP-0053i ATv10.xls
BP-0053j	16/11/2005	Unfired earth wood shaving bricks	TP08 132	Med	In situ	BP-0053j.xls	BP-0053 description.doc		BP-0053j ATv10.xls
BP-0053k	16/11/2005	Unfired earth wood shaving bricks	TP08 141	Med	In situ	BP-0053k.xls	BP-0053 description.doc	In situ and lab curves compared, Eol.xls	BP-0053k ATv10.xls
BP-0053l	16/11/2005	Unfired earth wood shaving bricks	TP08 142	Med	In situ	BP-0053l.xls	BP-0053 description.doc	Summary Scotland Results.xls	BP-0053l ATv10.xls
BP-0054a	17/11/2005	Mass clay straw	TP08 131	Med	In situ	BP-0054a.xls	BP-0054 description.doc		BP-0054a ATv10.xls
BP-0054b	17/11/2005	Mass clay straw	TP08 132	Med	In situ	BP-0054b.xls	BP-0054 description.doc		BP-0054b ATv10.xls
BP-0054c	17/11/2005	Mass clay straw	TP08 141	Med	In situ	BP-0054c.xls	BP-0054 description.doc		BP-0054c ATv10.xls
BP-0054d	17/11/2005	Mass clay straw	TP08 142	Med	In situ	BP-0054d.xls	BP-0054 description.doc		BP-0054d ATv10.xls
BP-0054e	17/11/2005	Mass clay straw	TP08 131	Med	In situ	BP-0054e.xls	BP-0054 description.doc		BP-0054e ATv10.xls
BP-0054f	17/11/2005	Mass clay straw	TP08 132	Med	In situ	BP-0054f.xls	BP-0054 description.doc		BP-0054f ATv10.xls
BP-0054g	17/11/2005	Mass clay straw	TP08 141	Med	In situ	BP-0054g.xls	BP-0054 description.doc		BP-0054g ATv10.xls
BP-0054h	17/11/2005	Mass clay straw	TP08 142	Med	In situ	BP-0054h.xls	BP-0054 description.doc		BP-0054h ATv10.xls
BP-0054i	17/11/2005	Mass clay straw	TP08 131	Med	In situ	BP-0054i.xls	BP-0054 description.doc		BP-0054i ATv10.xls
BP-0054j	17/11/2005	Mass clay straw	TP08 132	Med	In situ	BP-0054j.xls	BP-0054 description.doc		BP-0054j ATv10.xls
BP-0054k	17/11/2005	Mass clay straw	TP08 141	Med	In situ	BP-0054k.xls	BP-0054 description.doc		BP-0054k ATv10.xls
BP-0054l	17/11/2005	Mass clay straw	TP08 142	Med	In situ	BP-0054l.xls	BP-0054 description.doc		BP-0054l ATv10.xls
BP-0054m	17/11/2005	Mass clay straw	TP08 131	Med	In situ	BP-0054m.xls	BP-0054 description.doc		BP-0054m ATv10.xls
BP-0054n	17/11/2005	Mass clay straw	TP08 132	Med	In situ	BP-0054n.xls	BP-0054 description.doc		BP-0054n ATv10.xls
BP-0054o	17/11/2005	Mass clay straw	TP08 141	Med	In situ	BP-0054o.xls	BP-0054 description.doc	In situ curves compared, clay straw.xls	BP-0054o ATv10.xls
BP-0054p	17/11/2005	Mass clay straw	TP08 142	Med	In situ	BP-0054p.xls	BP-0054 description.doc	Summary Scotland Results.xls	BP-0054p ATv10.xls
BP-0055a	25/11/2005	Aerated concrete Shield	TP08 131	Med	Lab	BP-0055a.xls	BP-0055 description.doc		BP-0055a ATv10.xls
BP-0055b	25/11/2005	cased probe	TP08 132	Med	Lab	BP-0055b.xls	BP-0055 description.doc		BP-0055b ATv10.xls
BP-0055c	25/11/2005	Unfired earth wood shaving bricks	TP08 141	Med	Lab	BP-0055c.xls	BP-0055 description.doc		spikey!
BP-0055d	25/11/2005	Unfired earth wood shaving bricks	TP08 142	Med	Lab	BP-0055d.xls	BP-0055 description.doc		spikey!
BP-0055e	25/11/2005	Aerated concrete Shield	TP08 131	Med	Lab	BP-0055e.xls	BP-0055 description.doc		BP-0055e ATv10.xls
BP-0055f	25/11/2005	Unfired earth wood shaving bricks	TP08 141	Med	Lab	BP-0055f.xls	BP-0055 description.doc		BP-0055f ATv10.xls
BP-0055g	25/11/2005	Unfired earth wood shaving bricks	TP08 142	Med	Lab	BP-0055g.xls	BP-0055 description.doc		BP-0055g ATv10.xls
BP-0055h	25/11/2005	Aerated concrete Shield	TP08 131	Med	Lab	BP-0055h.xls	BP-0055 description.doc		BP-0055h ATv10.xls
BP-0055i	25/11/2005	Unfired earth wood shaving bricks	TP08 141	Med	Lab	BP-0055i.xls	BP-0055 description.doc		spikey!
BP-0055j	25/11/2005	Unfired earth wood shaving bricks	TP08 142	Med	Lab	BP-0055j.xls	BP-0055 description.doc		BP-0055j ATv10.xls

Ref	Date	Material	Probe	Heat	Lab In situ	Raw Data Location	Descriptions	Miscellaneous Analyses	ATv10
BP-0055k	25/11/2005	Aerated concrete Shield	TP08 131	Med	Lab	BP-0055k.xls	BP-0055 description.doc		BP-0055k ATv10.xls
BP-0055l	25/11/2005	Unfired earth wood shaving bricks	TP08 141	Med	Lab	BP-0055l.xls	BP-0055 description.doc		BP-0055l ATv10.xls
BP-0055m	25/11/2005	Unfired earth wood shaving bricks	TP08 142	Med	Lab	BP-0055m.xls	BP-0055 description.doc	Summary Scotland Results.xls	BP-0055m ATv10.xls
BP-0056a	14/01/2006	Oak across	TP08131	Med	Lab	BP-0056a.xls	BP-0056 description.doc	Summary Timber HL Office.xls	spikey!
BP-0056b	14/01/2006	Oak across	TP08131	Med	Lab	BP-0056b.xls	BP-0056 description.doc		spikey!
BP-0056c	14/01/2006	Oak across	TP08131	Med	Lab	BP-0056c.xls	BP-0056 description.doc		BP-0056c ATv10.xls
BP-0056d	15/01/2006	Spruce across	TP08131	Med	Lab	BP-0056d.xls	BP-0056 description.doc		BP-0056d ATv10.xls
BP-0056e	15/01/2006	Spruce across	TP08131	Med	Lab	BP-0056e.xls	BP-0056 description.doc		BP-0056e ATv10.xls
BP-0056f	15/01/2006	Spruce across	TP08131	Med	Lab	BP-0056f.xls	BP-0056 description.doc		Battery failure
BP-0056g	15/01/2006	Spruce across	TP08131	Med	Lab	BP-0056g.xls	BP-0056 description.doc		BP-0056g ATv10.xls
BP-0056h	15/01/2006	Oak across	TP08131	Med	Lab	BP-0056h.xls	BP-0056 description.doc		BP-0056h ATv10.xls
BP-0056i	15/01/2006	Oak across	TP08131	Med	Lab	BP-0056i.xls	BP-0056 description.doc		BP-0056i ATv10.xls
BP-0056j	15/01/2006	Oak across	TP08131	Med	Lab	BP-0056j.xls	BP-0056 description.doc		BP-0056j ATv10.xls
BP-0056k	15/01/2006	Spruce across	TP08131	Med	Lab	BP-0056k.xls	BP-0056 description.doc		BP-0056k ATv10.xls
BP-0056l	15/01/2006	Spruce across	TP08131	Med	Lab	BP-0056l.xls	BP-0056 description.doc		BP-0056l ATv10.xls
BP-0056m	15/01/2006	Spruce across	TP08131	Med	Lab	BP-0056m.xls	BP-0056 description.doc		BP-0056m ATv10.xls
BP-0057a	17/01/2006	Aerated concrete Solar	TP08131	Med	Lab	BP-0057a.xls	BP-0057 description.doc		BP-0057a ATv10.xls
BP-0057b	17/01/2006	Aerated concrete Standard	TP08132	Med	Lab	BP-0057b.xls	BP-0057 description.doc		BP-0057b ATv10.xls
BP-0057c	17/01/2006	Aerated concrete Foundation	TP08141	Med	Lab	BP-0057c.xls	BP-0057 description.doc		BP-0057c ATv10.xls
BP-0057d	17/01/2006	Unfired earth wood shaving bricks	TP08142	Med	Lab	BP-0057d.xls	BP-0057 description.doc		spikey!
BP-0057e	17/01/2006	Aerated concrete Solar	TP08131	Med	Lab	BP-0057e.xls	BP-0057 description.doc		BP-0057e ATv10.xls
BP-0057f	17/01/2006	Aerated concrete Standard	TP08132	Med	Lab	BP-0057f.xls	BP-0057 description.doc		BP-0057f ATv10.xls
BP-0057g	17/01/2006	Aerated concrete Foundation	TP08141	Med	Lab	BP-0057g.xls	BP-0057 description.doc		BP-0057g ATv10.xls
BP-0057h	17/01/2006	Unfired earth wood shaving bricks	TP08142	Med	Lab	BP-0057h.xls	BP-0057 description.doc		BP-0057h ATv10.xls
BP-0057i	17/01/2006	Aerated concrete Solar	TP08131	Med	Lab	BP-0057i.xls	BP-0057 description.doc		BP-0057i ATv10.xls
BP-0057j	17/01/2006	Aerated concrete Standard	TP08132	Med	Lab	BP-0057j.xls	BP-0057 description.doc		BP-0057j ATv10.xls
BP-0057k	17/01/2006	Aerated concrete Foundation	TP08141	Med	Lab	BP-0057k.xls	BP-0057 description.doc		BP-0057k ATv10.xls
BP-0057l	17/01/2006	Unfired earth wood shaving bricks	TP08142	Med	Lab	BP-0057l.xls	BP-0057 description.doc		BP-0057l ATv10.xls
BP-0057m	17/01/2006	Aerated concrete Solar (thesis)	TP08131	Med	Lab	BP-0057m.xls	BP-0057 description.doc		BP-0057m ATv10.xls
BP-0057n	17/01/2006	Aerated concrete Standard	TP08132	Med	Lab	BP-0057n.xls	BP-0057 description.doc		BP-0057n ATv10.xls
BP-0057o	17/01/2006	Aerated concrete Foundation	TP08141	Med	Lab	BP-0057o.xls	BP-0057 description.doc	Internal lambda curves compared.xls	BP-0057o ATv10.xls
BP-0057p	17/01/2006	Unfired earth wood shaving bricks	TP08142	Med	Lab	BP-0057p.xls	BP-0057 description.doc	Summary BP-0057 Aerated concrete EoI Home Office.xls	BP-0057p ATv10.xls
BP-0058a	24/01/2006	Portland Stone	TP08131	Med	Lab	BP-0058a.xls	BP-0058 description.doc		BP-0058a ATv10.xls
BP-0058b	24/01/2006	Portland Stone	TP08131	High	Lab	BP-0058b.xls	BP-0058 description.doc		BP-0058b ATv10.xls
BP-0058c	24/01/2006	Portland Stone	TP08131	High	Lab	BP-0058c.xls	BP-0058 description.doc	Summary Stone.xls	BP-0058c ATv10.xls
BP-0058-KD2	24/01/2006	Portland Stone	KD2	N/A	Lab	Summary KD2	BP-0058 description.doc	BP-0058-KD2.xls	
BP-0059a	22/02/2006	Lime / hemp block	TP08131	Med	Lab	BP-0059a.xls	BP-0059 description.doc		BP-0059a ATv10.xls
BP-0059b	22/02/2006	Lime / hemp block	TP08132	Med	Lab	BP-0059b.xls	BP-0059 description.doc		BP-0059b ATv10.xls
BP-0059c	22/02/2006	Lime / glass block	TP08141	Med	Lab	BP-0059c.xls	BP-0059 description.doc		BP-0059c ATv10.xls
BP-0059d	22/02/2006	Portland Stone	TP08142	Med	Lab	BP-0059d.xls	BP-0059 description.doc		BP-0059d ATv10.xls
BP-0059e	23/02/2006	Lime / hemp block	TP08131	Med	Lab	BP-0059e.xls	BP-0059 description.doc		BP-0059e ATv10.xls
BP-0059f	23/02/2006	Lime / hemp block	TP08132	Med	Lab	BP-0059f.xls	BP-0059 description.doc		BP-0059f ATv10.xls
BP-0059g	23/02/2006	Lime / glass block	TP08141	Med	Lab	BP-0059g.xls	BP-0059 description.doc		BP-0059g ATv10.xls
BP-0059h	23/02/2006	Portland Stone	TP08142	Med	Lab	BP-0059h.xls	BP-0059 description.doc		BP-0059h ATv10.xls

Ref	Date	Material	Probe	Heat	Lab In situ	Raw Data Location	Descriptions	Miscellaneous Analyses	ATv10
BP-0059i	23/02/2006	Lime / hemp block	TP08131	Med	Lab	BP-0059i.xls	BP-0059 description.doc		BP-0059i ATv10.xls
BP-0059j	23/02/2006	Lime / hemp block	TP08132	Med	Lab	BP-0059j.xls	BP-0059 description.doc		BP-0059j ATv10.xls
BP-0059k	23/02/2006	Lime / glass block	TP08141	Med	Lab	BP-0059k.xls	BP-0059 description.doc		BP-0059k ATv10.xls
BP-0059l	23/02/2006	Portland Stone	TP08142	Med	Lab	BP-0059l.xls	BP-0059 description.doc		BP-0059l ATv10.xls
BP-0059m	23/02/2006	Lime / hemp block	TP08131	Med	Lab	BP-0059m.xls	BP-0059 description.doc		BP-0059m ATv10.xls
BP-0059n	23/02/2006	Lime / hemp block	TP08132	Med	Lab	BP-0059n.xls	BP-0059 description.doc		BP-0059n ATv10.xls
BP-0059o	23/02/2006	Lime / glass block	TP08141	Med	Lab	BP-0059o.xls	BP-0059 description.doc		BP-0059o ATv10.xls
BP-0059p	23/02/2006	Portland Stone	TP08142	Med	Lab	BP-0059p.xls	BP-0059 description.doc		BP-0059p ATv10.xls
BP-0059q	23/02/2006	Lime / hemp block	TP08131	Med	Lab	BP-0059q.xls	BP-0059 description.doc		BP-0059q ATv10.xls
BP-0059r	23/02/2006	Lime / hemp block	TP08132	Med	Lab	BP-0059r.xls	BP-0059 description.doc		BP-0059r ATv10.xls
BP-0059s	23/02/2006	Lime / glass block	TP08141	Med	Lab	BP-0059s.xls	BP-0059 description.doc		BP-0059s ATv10.xls
BP-0059t	23/02/2006	Portland Stone	TP08142	Med	Lab	BP-0059t.xls	BP-0059 description.doc		BP-0059t ATv10.xls
BP-0059u	23/02/2006	Lime / hemp block	TP08131	Med	Lab	BP-0059u.xls	BP-0059 description.doc		BP-0059u ATv10.xls
BP-0059v	23/02/2006	Lime / hemp block	TP08132	Med	Lab	BP-0059v.xls	BP-0059 description.doc		BP-0059v ATv10.xls
BP-0059w	23/02/2006	Lime / glass block	TP08141	Med	Lab	BP-0059w.xls	BP-0059 description.doc		BP-0059w ATv10.xls
BP-0059x	23/02/2006	Portland Stone	TP08142	Med	Lab	BP-0059x.xls	BP-0059 description.doc	Summary Hemp & Glass blocks.xls	BP-0059x ATv10.xls
BP-0060a	22/06/2006	Oak across	TP08131	High	Lab	BP-0060a.xls	BP-0060 description.doc	Oak Alpha Trial, H modelled and charted.xls	BP-0060a ATv10.xls
BP-0060a	22/06/2006	Oak along	TP08132	High	Lab	BP-0060b.xls	BP-0060 description.doc		BP-0060b ATv10.xls
BP-0060a	22/06/2006	Oak across	TP08131	High	Lab	Lost	BP-0060 description.doc		
BP-0060a	22/06/2006	Oak along	TP08132	High	Lab	Lost	BP-0060 description.doc		
BP-0061	######								
BP-0061a	20/07/2006	Oak across	TP08131	Med	Lab	BP-0061a.xls	BP-0061 description.doc		BP-0061a ATv10.xls
BP-0061b	20/07/2006	Oak along	TP08132	Med	Lab	BP-0061b.xls	BP-0061 description.doc		BP-0061b ATv10.xls
BP-0061c	20/07/2006	Portland Stone	TP08141	Med	Lab	BP-0061c.xls	BP-0061 description.doc		BP-0061c ATv10.xls
BP-0061d	20/07/2006	Portland Stone	TP08142	High	Lab	BP-0061d.xls	BP-0061 description.doc		BP-0061d ATv10.xls
BP-0061e	20/07/2006	Oak across	TP08131	Med	Lab	BP-0061e.xls	BP-0061 description.doc		BP-0061e ATv10.xls
BP-0061f	20/07/2006	Oak along	TP08132	Med	Lab	BP-0061f.xls	BP-0061 description.doc		BP-0061f ATv10.xls
BP-0061g	20/07/2006	Portland Stone	TP08141	High	Lab	BP-0061g.xls	BP-0061 description.doc		BP-0061g ATv10.xls
BP-0061h	20/07/2006	Portland Stone	TP08142	High	Lab	BP-0061h.xls	BP-0061 description.doc		BP-0061h ATv10.xls
BP-0061i	20/07/2006	Oak across	TP08131	Med	Lab	BP-0061i.xls	BP-0061 description.doc		BP-0061i ATv10.xls
BP-0061j	20/07/2006	Oak along	TP08132	Med	Lab	BP-0061j.xls	BP-0061 description.doc		BP-0061j ATv10.xls
BP-0061k	20/07/2006	Portland Stone	TP08141	High	Lab	BP-0061k.xls	BP-0061 description.doc		BP-0061k ATv10.xls
BP-0061l	20/07/2006	Portland Stone	TP08142	High	Lab	BP-0061l.xls	BP-0061 description.doc	BP-0061 Timber Portland stone Summary 01.xls	BP-0061l ATv10.xls
BP-0062a	24/07/2006	Lime hemp block	TP08131	Low	Lab	BP-0062a.xls	BP-0062 description.doc		BP-0062a ATv10.xls
BP-0062b	24/07/2006	Lime hemp block	TP08132	Low	Lab	BP-0062b.xls	BP-0062 description.doc		BP-0062b ATv10.xls
BP-0062c	24/07/2006	Lime hemp block	TP08131	Low	Lab	BP-0062c.xls	BP-0062 description.doc		BP-0062c ATv10.xls
BP-0062d	24/07/2006	Lime hemp block	TP08132	Low	Lab	BP-0062d.xls	BP-0062 description.doc	Summary Lime Hemp 01.xls	BP-0062d ATv10.xls
BP-0063a	31/07/2006	Lime perlite cube	TP08131	Low	Lab	BP-0063a.xls	BP-0063 description.doc		BP-0063a ATv10.xls
BP-0063b	31/07/2006	Lime hemp cube	TP08132	Low	Lab	BP-0063b.xls	BP-0063 description.doc	BP-0063b data scatter compounded to linear.xls	BP-0063b ATv10.xls
BP-0063c	31/07/2006	Hemp pith	TP08141	Low	Lab	BP-0063c.xls	BP-0063 description.doc		BP-0063c ATv10.xls
BP-0063d	31/07/2006	Perlite granules	TP08142	Med	Lab	BP-0063d.xls	BP-0063 description.doc		BP-0063d ATv10.xls
BP-0063e	01/08/2006	Lime perlite cube	TP08131	Med	Lab	BP-0063e.xls	BP-0063 description.doc		BP-0063e ATv10.xls
BP-0063f	01/08/2006	Lime hemp cube	TP08132	Med	Lab	BP-0063f.xls	BP-0063 description.doc		BP-0063f ATv10.xls
BP-0063g	01/08/2006	Hemp pith	TP08141	Med	Lab	BP-0063g.xls	BP-0063 description.doc		BP-0063g ATv10.xls
BP-0063h	01/08/2006	Perlite granules	TP08142	Med	Lab	BP-0063h.xls	BP-0063 description.doc		BP-0063h ATv10.xls
BP-0063i	01/08/2006	Lime perlite cube	TP08131	Med	Lab	BP-0063i.xls	BP-0063 description.doc		BP-0063i ATv10.xls

Ref	Date	Material	Probe	Heat	Lab In situ	Raw Data Location	Descriptions	Miscellaneous Analyses	ATv10
BP-0063j	01/08/2006	Lime hemp cube	TP08132	Med	Lab	BP-0063j.xls	BP-0063 description.doc		BP-0063j ATv10.xls
BP-0063k	01/08/2006	Hemp pith	TP08141	Med	Lab	BP-0063k.xls	BP-0063 description.doc		BP-0063k ATv10.xls
BP-0063l	01/08/2006	Perlite granules	TP08142	Med	Lab	BP-0063l.xls	BP-0063 description.doc	Summary Lime, Hemp & Perlite samples.xls	BP-0063l ATv10.xls
BP-0064a	03/08/2006	Phenolic foam	TP08131	Low	Lab	BP-0064a.xls	BP-0064 description.doc	BP-0064a ATv08 Phenolic foam log shift.xls	BP-0064a ATv10.xls
BP-0064b	03/08/2006	Dupre Vermiculite	TP08132	Low	Lab	BP-0064b.xls	BP-0064 description.doc	BP-0064a fringe temperature.xls	BP-0064b ATv10.xls
BP-0065a	08/08/2006	Lime hemp cube	TP08131	Med	Lab	BP-0065a.xls	BP-0065 description.doc		BP-0065a ATv10.xls
BP-0065b	08/08/2006	Lime perlite cube	TP08132	Med	Lab	BP-0065b.xls	BP-0065 description.doc		BP-0065b ATv10.xls
BP-0065c	08/08/2006	Hemp perlite lime	TP08141	Med	Lab	BP-0065c.xls	BP-0065 description.doc		BP-0065c ATv10.xls
BP-0065d	08/08/2006	Hemp putty cment	TP08142	Med	Lab	BP-0065d.xls	BP-0065 description.doc	Summary Lime, Hemp & Perlite samples.xls	BP-0065d ATv10.xls
BP-0066a	21/08/2006	Hemcrete	TP08131	Med	In situ	BP-0066a.xls	BP-0066 description.doc		BP-0066a ATv10.xls
BP-0066b	21/08/2006	Hemcrete	TP08132	Med	In situ	BP-0066b.xls	BP-0066 description.doc		BP-0066b ATv10.xls
BP-0066c	21/08/2006	Hemcrete	TP08141	Med	In situ	BP-0066c.xls	BP-0066 description.doc		BP-0066c ATv10.xls
BP-0066d	21/08/2006	Hemcrete	TP08142	Med	In situ	BP-0066d.xls	BP-0066 description.doc		BP-0066d ATv10.xls
BP-0066e	21/08/2006	Hemcrete	TP08131	Med	In situ	BP-0066e.xls	BP-0066 description.doc		BP-0066e ATv10.xls
BP-0066f	21/08/2006	Hemcrete	TP08132	Med	In situ	BP-0066f.xls	BP-0066 description.doc		BP-0066f ATv10.xls
BP-0066g	21/08/2006	Hemcrete	TP08141	Med	In situ	BP-0066g.xls	BP-0066 description.doc		BP-0066g ATv10.xls
BP-0066h	21/08/2006	Hemcrete	TP08142	Med	In situ	BP-0066h.xls	BP-0066 description.doc	Summary Lime Hemp 02.xls	BP-0066h ATv10.xls
BP-0066i	22/08/2006	Hemcrete	TP08131	Med	Lab	BP-0066i.xls	BP-0066 description.doc		BP-0066i ATv10.xls
BP-0066j	22/08/2006	Hemcrete	TP08132	Med	Lab	BP-0066j.xls	BP-0066 description.doc		BP-0066j ATv10.xls
BP-0066k	22/08/2006	Compressed earth	TP08141	High	Lab	BP-0066k.xls	BP-0066 description.doc		BP-0066k ATv10.xls
BP-0066l	22/08/2006	Compressed earth	TP08142	High	Lab	BP-0066l.xls	BP-0066 description.doc		BP-0066l ATv10.xls
BP-0066m	22/08/2006	Hemcrete	TP08131	Med	Lab	BP-0066m.xls	BP-0066 description.doc		BP-0066m ATv10.xls
BP-0066n	22/08/2006	Hemcrete	TP08132	Med	Lab	BP-0066n.xls	BP-0066 description.doc		BP-0066n ATv10.xls
BP-0066o	22/08/2006	Compressed earth	TP08141	High	Lab	BP-0066o.xls	BP-0066 description.doc		BP-0066o ATv10.xls
BP-0066p	22/08/2006	Compressed earth	TP08142	High	Lab	BP-0066p.xls	BP-0066 description.doc		BP-0066p ATv10.xls
BP-0066q	29/08/2006	Hemcrete	TP08131	Med	Lab	BP-0066q.xls	BP-0066 description.doc		BP-0066q ATv10.xls
BP-0066r	29/08/2006	Hemcrete	TP08131	Med	Lab	BP-0066r.xls	BP-0066 description.doc		BP-0066r ATv10.xls
BP-0066s	29/08/2006	Hemcrete	TP08131	Med	Lab	BP-0066s.xls	BP-0066 description.doc	Summary Lime Hemp 02.xls	BP-0066s ATv10.xls
BP-0067a	01/09/2006	Agar	TP08131	Med	Lab	BP-0067a.xls	BP-0067 description.doc	BP-0067a ATv10 with scatter.xls	BP-0067a ATv10.xls
BP-0067b	01/09/2006	Vaseline	TP08132	Med	Lab	BP-0067b.xls	BP-0067 description.doc		BP-0067b ATv10.xls
BP-0067c	01/09/2006	Agar	TP08141	Med	Lab	BP-0067c.xls	BP-0067 description.doc		Unknown problem
BP-0067d	01/09/2006	Water	TP08142	Med	Lab	BP-0067d.xls	BP-0067 description.doc		BP-0067d ATv10.xls
BP-0067e	01/09/2006	Agar	TP08131	High	Lab	BP-0067e.xls	BP-0067 description.doc	BP-0067e ATv10 H assessment.xls	BP-0067e ATv10.xls
BP-0067f	01/09/2006	Vaseline	TP08132	High	Lab	BP-0067f.xls	BP-0067 description.doc		BP-0067f ATv10.xls
BP-0067g	01/09/2006	Agar	TP08141	High	Lab	BP-0067g.xls	BP-0067 description.doc	Summary H values 01.xls	Unknown problem
BP-0067h	01/09/2006	Water	TP08142	High	Lab	BP-0067h.xls	BP-0067 description.doc		BP-0067h ATv10.xls
BP-0068a	12/09/2006	Agar	TP08 131	High	Lab	BP-0068a.xls	BP-0068 description.doc	BP-0068a ATv10 H.xls	BP-0068a ATv10.xls
BP-0068b	12/09/2006	Agar	TP08 132	High	Lab	BP-0068b.xls	BP-0068 description.doc	BP-0068b ATv10 H.xls	BP-0068b ATv10.xls
BP-0068c	12/09/2006	Agar	TP08 141	High	Lab	BP-0068c.xls	BP-0068 description.doc	BP-0068c ATv10 H.xls	BP-0068c ATv10.xls
BP-0068d	12/09/2006	Agar	TP08 142	High	Lab	Bad data	BP-0068 description.doc	BP-0068c ATv10 H.xls	Bad data
BP-0068e	12/09/2006	Vaseline	TP08 131	High	Lab	BP-0068e.xls	BP-0068 description.doc	BP-0068e ATv10 H.xls	BP-0068e ATv10.xls
BP-0068f	12/09/2006	Agar	TP08 132	High	Lab	BP-0068f.xls	BP-0068 description.doc	BP-0068f ATv10 H.xls	BP-0068f ATv10.xls
BP-0068g	12/09/2006	Agar	TP08 141	High	Lab	BP-0068g.xls	BP-0068 description.doc	BP-0068g ATv10 H.xls	BP-0068g ATv10.xls
BP-0068h	12/09/2006	Agar	TP08 142	High	Lab	BP-0068h.xls	BP-0068 description.doc	BP-0068h ATv10 H.xls	BP-0068h ATv10.xls
BP-0068i	12/09/2006	Agar (V)	TP08 131	High	Lab	BP-0068i.xls	BP-0068 description.doc	BP-0068i ATv10 H.xls	BP-0068i ATv10.xls
BP-0068j	12/09/2006	Vaseline	TP08 132	High	Lab	BP-0068j.xls	BP-0068 description.doc	BP-0068j ATv10 H.xls	BP-0068j ATv10.xls

Ref	Date	Material	Probe	Heat	Lab In situ	Raw Data Location	Descriptions	Miscellaneous Analyses	ATv10
BP-0068k	12/09/2006	Agar	TP08 141	High	Lab	BP-0068k.xls	BP-0068 description.doc	BP-0068k ATv10 H.xls	BP-0068k ATv10.xls
BP-0068l	12/09/2006	Agar	TP08 142	High	Lab	BP-0068l.xls	BP-0068 description.doc	BP-0068l ATv10 H.xls	BP-0068l ATv10.xls
BP-0068m	12/09/2006	Agar (V)	TP08 131	High	Lab	BP-0068m.xls	BP-0068 description.doc	BP-0068m ATv10 H.xls	BP-0068m ATv10.xls
BP-0068n	12/09/2006	Agar (V)	TP08 132	High	Lab	BP-0068n.xls	BP-0068 description.doc	BP-0068n ATv10 H.xls	BP-0068n ATv10.xls
BP-0068o	12/09/2006	Vaseline	TP08 141	High	Lab	BP-0068o.xls	BP-0068 description.doc	BP-0068o ATv10 H.xls	BP-0068o ATv10.xls
BP-0068p	12/09/2006	Agar	TP08 142	High	Lab	BP-0068p.xls	BP-0068 description.doc	BP-0068p ATv10 H.xls	BP-0068p ATv10.xls
BP-0068q	12/09/2006	Agar	TP08 131	High	Lab	BP-0068q.xls	BP-0068 description.doc	BP-0068q ATv10 H.xls	BP-0068q ATv10.xls
BP-0068r	12/09/2006	Agar (V)	TP08 132	High	Lab	BP-0068r.xls	BP-0068 description.doc	BP-0068r ATv10 H.xls	BP-0068r ATv10.xls
BP-0068s	12/09/2006	Agar (V)	TP08 141	High	Lab	BP-0068s.xls	BP-0068 description.doc	BP-0068s ATv10 H.xls	BP-0068s ATv10.xls
BP-0068t	12/09/2006	Vaseline	TP08 142	High	Lab	BP-0068t.xls	BP-0068 description.doc	BP-0068t ATv10 H.xls	BP-0068t ATv10.xls
BP-0068u	13/09/2006	Agar	TP08 131	High	Lab	BP-0068u.xls	BP-0068 description.doc	BP-0068u ATv10 H.xls	BP-0068u ATv10.xls
BP-0068v	13/09/2006	Agar	TP08 132	High	Lab	BP-0068v.xls	BP-0068 description.doc	BP-0068v ATv10 H.xls	BP-0068v ATv10.xls
BP-0068w	13/09/2006	Agar (V)	TP08 141	High	Lab	BP-0068w.xls	BP-0068 description.doc	BP-0068w ATv10 H.xls	BP-0068w ATv10.xls
BP-0068x	13/09/2006	Agar (V)	TP08 142	High	Lab	BP-0068x.xls	BP-0068 description.doc	BP-0068x ATv10 H.xls	BP-0068x ATv10.xls
BP-0068y	13/09/2006	Agar	TP08 131	High	Lab	BP-0068y.xls	BP-0068 description.doc	BP-0068y ATv10 H.xls	BP-0068y ATv10.xls
BP-0068za	13/09/2006	Agar	TP08 132	High	Lab	BP-0068za.xls	BP-0068 description.doc	BP-0068za ATv10 H.xls	BP-0068za ATv10.xls
BP-0068zb	13/09/2006	Agar	TP08 141	High	Lab	BP-0068zb.xls	BP-0068 description.doc	BP-0068zd ATv10 with alpha from Greg et al.xls	BP-0068rb ATv10.xls
BP-0068zc	13/09/2006	Agar (V)	TP08 142	High	Lab	BP-0068zc.xls	BP-0068 description.doc	BP-0068zd ATv10 Morabito test.xls	BP-0068zc ATv10.xls
BP-0068zd	13/09/2006	Agar	TP08 131	High	Lab	BP-0068zd.xls	BP-0068 description.doc	BP-0068zd ATv10 BS EN 993-14 test.xls	BP-0068zd ATv10.xls
BP-0068ze	13/09/2006	Agar	TP08 132	High	Lab	BP-0068ze.xls	BP-0068 description.doc	BP-0068 summary with H goalseek & direct.xls	BP-0068ze ATv10.xls
BP-0068zf	13/09/2006	Agar	TP08 141	High	Lab	BP-0068zf.xls	BP-0068 description.doc	BP-0068 summary with H.xls	BP-0068zf ATv10.xls
BP-0068zg	13/09/2006	Agar	TP08 142	High	Lab	BP-0068zg.xls	BP-0068 description.doc	Summary H values 01.xls	BP-0068zg ATv10.xls
SMG-101a	07/11/2006	Hemcrete	TP08 142	?	In situ	SMG-101a.xls	BP-0069 description.doc		SMG-101a ATv10.xls
BP-0069a	05/12/2006	Cast lime & hemp	TP08 131	MED	In situ	BP-0069a.xls	BP-0069 description.doc	Summary Hartest 01.xls	BP-0069a ATv10.xls
BP-0069b	05/12/2006	Cast lime & hemp	TP08 132	MED	In situ	BP-0069b.xls	BP-0069 description.doc		BP-0069b ATv10.xls
BP-0069c	05/12/2006	Cast lime & hemp	TP08 141	MED	In situ	BP-0069c.xls	BP-0069 description.doc		BP-0069c ATv10.xls
BP-0069d	05/12/2006	Cast lime & hemp	TP08 142	MED	In situ	BP-0069d.xls	BP-0069 description.doc		BP-0069d ATv10.xls
BP-0069e	05/12/2006	Cast lime & hemp	TP08 131	MED	In situ	BP-0069e.xls	BP-0069 description.doc		BP-0069e ATv10.xls
BP-0069f	05/12/2006	Cast lime & hemp	TP08 132	MED	In situ	BP-0069f.xls	BP-0069 description.doc		BP-0069f ATv10.xls
BP-0069g	05/12/2006	Cast lime & hemp	TP08 141	MED	In situ	BP-0069g.xls	BP-0069 description.doc		BP-0069g ATv10.xls
BP-0069h	05/12/2006	Cast lime & hemp	TP08 142	MED	In situ	BP-0069h.xls	BP-0069 description.doc		BP-0069h ATv10.xls
BP-0069i	05/12/2006	Cast lime & hemp	TP08 131	MED	In situ	BP-0069i.xls	BP-0069 description.doc		BP-0069i ATv10.xls
BP-0069j	05/12/2006	Cast lime & hemp	TP08 132	MED	In situ	BP-0069j.xls	BP-0069 description.doc		BP-0069j ATv10.xls
BP-0069k	05/12/2006	Cast lime & hemp	TP08 141	MED	In situ	BP-0069k.xls	BP-0069 description.doc		BP-0069k ATv10.xls
BP-0069l	05/12/2006	Cast lime & hemp	TP08 142	MED	In situ	BP-0069l.xls	BP-0069 description.doc		BP-0069l ATv10.xls
BP-0069m	05/12/2006	Cast lime & hemp	TP08 131	MED	In situ	BP-0069m.xls	BP-0069 description.doc		BP-0069m ATv10.xls
BP-0069n	05/12/2006	Cast lime & hemp	TP08 132	MED	In situ	BP-0069n.xls	BP-0069 description.doc		BP-0069n ATv10.xls
BP-0069o	05/12/2006	Cast lime & hemp	TP08 141	MED	In situ	BP-0069o.xls	BP-0069 description.doc		BP-0069o ATv10.xls
BP-0069p	05/12/2006	Cast lime & hemp	TP08 142	MED	In situ	BP-0069p.xls	BP-0069 description.doc		BP-0069p ATv10.xls
BP-0069q	05/12/2006	Cast lime & hemp	TP08 131	MED	In situ	BP-0069q.xls	BP-0069 description.doc		BP-0069q ATv10.xls
BP-0069r	05/12/2006	Cast lime & hemp	TP08 132	MED	In situ	BP-0069r.xls	BP-0069 description.doc		BP-0069r ATv10.xls
BP-0069s	05/12/2006	Cast lime & hemp	TP08 141	MED	In situ	BP-0069s.xls	BP-0069 description.doc		BP-0069s ATv10.xls
BP-0069t	05/12/2006	Cast lime & hemp	TP08 142	MED	In situ	BP-0069t.xls	BP-0069 description.doc		BP-0069t ATv10.xls
BP-0069u	05/12/2006	Cast lime & hemp	TP08 131	MED	In situ	BP-0069u.xls	BP-0069 description.doc		BP-0069u ATv10.xls
BP-0069v	05/12/2006	Cast lime & hemp	TP08 132	MED	In situ	BP-0069v.xls	BP-0069 description.doc		BP-0069v ATv10.xls

Ref	Date	Material	Probe	Heat	Lab In situ	Raw Data Location	Descriptions	Miscellaneous Analyses	ATv10
BP-0069w	05/12/2006	Cast lime & hemp	TP08 141	MED	In situ	BP-0069w.xls	BP-0069 description.doc		BP-0069w ATv10.xls
BP-0069x	05/12/2006	Cast lime & hemp	TP08 142	MED	In situ	BP-0069x.xls	BP-0069 description.doc		BP-0069x ATv10.xls
BP-VHC-001	12/12/2006	Unfired earth wood shaving bricks	TK100/11	N/A	Lab		BP-VHC-001 description.doc	SHC drop calorimeter model & results.xls	BP-0053h ATv10.xls
BP-VHC-002	14/12/2006	Vaseline & Hemcrete	TK100/11	N/A	Lab		BP-VHC-002 description.doc	SHC drop calorimeter model & results.xls	BP-0068l ATv10 H.xls
BP-0070a	14/02/2007	Hemcrete	TP08 131	MED	Lab	BP-0070a.xls	BP-0070 description.doc		BP-0070a ATv10.xls
BP-0070b	14/02/2007	Hemcrete	TP08 132	MED	Lab	BP-0070b.xls	BP-0070 description.doc		BP-0070b ATv10.xls
BP-0070c	14/02/2007	Hemcrete	TP08 141	MED	Lab	BP-0070c.xls	BP-0070 description.doc		BP-0070c ATv10.xls
BP-0070d	14/02/2007	Hemcrete	TP08 142	MED	Lab	BP-0070d.xls	BP-0070 description.doc		BP-0070d ATv10.xls
BP-0070e	14/02/2007	Hemcrete	TP08 131	MED	Lab	BP-0070e.xls	BP-0070 description.doc	Summary Hemcrete samples AG - 12G.xls	BP-0070e ATv10.xls
BP-0071a	24/10/2007	Aerated concrete Solar	TP08 131	LOW	Lab	BP-0071a.xls	BP-0071 description.doc	BP-0071 all slopes.xls	BP-0071a ATv10.xls
BP-0071b	24/10/2007	Aerated concrete Solar	TP08 132	LOW	Lab	BP-0071b.xls	BP-0071 description.doc		BP-0071b ATv10.xls
BP-0071c	24/10/2007	Aerated concrete Solar	TP08 141	LOW	Lab	BP-0071c.xls	BP-0071 description.doc		BP-0071c ATv10.xls
BP-0071d	24/10/2007	Aerated concrete Solar	TP08 142	LOW	Lab	BP-0071d.xls	BP-0071 description.doc		BP-0071d ATv10.xls
BP-0071e	24/10/2007	Aerated concrete Solar	TP08 131	MED	Lab	BP-0071e.xls	BP-0071 description.doc		BP-0071e ATv10.xls
BP-0071f	24/10/2007	Aerated concrete Solar	TP08 132	MED	Lab	BP-0071f.xls	BP-0071 description.doc		BP-0071f ATv10.xls
BP-0071g	24/10/2007	Aerated concrete Solar	TP08 141	MED	Lab	BP-0071g.xls	BP-0071 description.doc		BP-0071g ATv10.xls
BP-0071h	24/10/2007	Aerated concrete Solar	TP08 142	MED	Lab	BP-0071h.xls	BP-0071 description.doc		BP-0071h ATv10.xls
BP-0071i	24/10/2007	Aerated concrete Solar	TP08 131	High	Lab	BP-0071i.xls	BP-0071 description.doc		BP-0071i ATv10.xls
BP-0071j	24/10/2007	Aerated concrete Solar	TP08 132	High	Lab	BP-0071j.xls	BP-0071 description.doc		BP-0071j ATv10.xls
BP-0071k	24/10/2007	Aerated concrete Solar	TP08 141	High	Lab	BP-0071k.xls	BP-0071 description.doc		BP-0071k ATv10.xls
BP-0071l	24/10/2007	Aerated concrete Solar	TP08 142	High	Lab	BP-0071l.xls	BP-0071 description.doc		BP-0071l ATv10.xls
BP-0071m	24/10/2007	Aerated concrete Solar	TP08 131	LOW	Lab	BP-0071m.xls	BP-0071 description.doc		BP-0071m ATv10.xls
BP-0071n	24/10/2007	Aerated concrete Solar	TP08 132	LOW	Lab	BP-0071n.xls	BP-0071 description.doc		BP-0071n ATv10.xls
BP-0071o	24/10/2007	Aerated concrete Solar	TP08 141	LOW	Lab	BP-0071o.xls	BP-0071 description.doc		BP-0071o ATv10.xls
BP-0071p	24/10/2007	Aerated concrete Solar	TP08 142	LOW	Lab	BP-0071p.xls	BP-0071 description.doc		BP-0071p ATv10.xls
BP-0071q	24/10/2007	Aerated concrete Solar	TP08 131	MED	Lab	BP-0071q.xls	BP-0071 description.doc		BP-0071q ATv10.xls
BP-0071r	24/10/2007	Aerated concrete Solar	TP08 132	MED	Lab	BP-0071r.xls	BP-0071 description.doc		BP-0071r ATv10.xls
BP-0071s	24/10/2007	Aerated concrete Solar	TP08 141	MED	Lab	BP-0071s.xls	BP-0071 description.doc		BP-0071s ATv10.xls
BP-0071t	24/10/2007	Aerated concrete Solar	TP08 142	MED	Lab	BP-0071t.xls	BP-0071 description.doc		BP-0071t ATv10.xls
BP-0071u	24/10/2007	Aerated concrete Solar	TP08 131	High	Lab	BP-0071u.xls	BP-0071 description.doc		BP-0071u ATv10.xls
BP-0071v	24/10/2007	Aerated concrete Solar	TP08 132	High	Lab	BP-0071v.xls	BP-0071 description.doc	Blackwells axial eqn.xls	BP-0071v ATv10.xls
BP-0071w	24/10/2007	Aerated concrete Solar	TP08 141	High	Lab	BP-0071w.xls	BP-0071 description.doc	Base rises, entrance losses v01.xls	BP-0071w ATv10.xls
BP-0071x	24/10/2007	Aerated concrete Solar	TP08 142	High	Lab	BP-0071x.xls	BP-0071 description.doc	BP-0071x ATv10 lambda rise assessment.xls	BP-0071x ATv10.xls
BP-0072	25/10/2007	Aerated concrete Solar	Four TP08	None	Lab		BP-0072 description.doc	BP-0072 temperature stabilisation.xls	
BP-0072a	25/10/2007	Aerated concrete Solar	Four TP08	None	Lab		BP-0072 description.doc	BP-0072a ALL 142 stabilisation.xls	
BP-0073a	28/10/2007	Phenolic foam	TP08 131	MED	Lab	BP-0073a.xls	BP-0073 Boundary assessment Phenolic foam.doc	2 powers & boundary assessment Phenolic foam.xls	BP-0073a ATv10.xls
BP-0073a	28/10/2007	Phenolic foam	TP08 131	MED	Lab	BP-0073all 131 (with charts).xls	BP-0073 Boundary assessment Phenolic foam.doc	Boundary for Phenolic foam from Vos.xls	

Appendix C: Example of experiment record

Below is an example of an experimental record, kept for each group of measurements. This, along with site notes and digital photographs, circumstances to be checked where anomalies may have been found in the data.

BP-0054
17/11/05
Property:
Architect:
Contact:
Field kit v01 with Delogger v4 on Ergo laptop
Probes in cases. TP08s – 131 & 132 with 2.5m cable, base marked as 80.75Ω/m, 141 & 142 with 5.0m cable, base marked as 75.56Ω/m.
Thermocouples: Channel 10 , Channel 11, exposed to ambient air

Aims
1) Assess measurement of clay straw mass construction on site
2) Assess effects of taking measurements in extreme weather conditions, i.e. very cold outside.

Notes
A recently constructed (completed 2002) detached annexe. Various wall types. Here mass clay straw, incorporating piped hot water heating system, with clay plaster was measured. The section of wall was 1.1m long, between door and window openings and faced 10° south of west (260°).

12:15	Probes in-situ: Hole A: Internal, ≈ 200mm above finished floor level (FFL) Hole B: External, ≈ 200mm above FFL Hole C: Internal, ≈ 1.8m above FFL Hole D: External, ≈ 1.8m above FFL
12:25	MED/DUMMY
12:37	(a) MED/131 (hole A)
12:47	MED/DUMMY
12:48	(b) MED/132 (hole B)
12:58	MED/DUMMY
12:59	(c) MED/141 (hole C)
13:09	MED/DUMMY
12:59	(d) MED/142 (hole D) Rotronic S1 18.9° and 39.5% internally
13:09	MED/DUMMY
	Unload to BP-0054abcd
13:40	(e) MED/131 (hole A) Rotronic S1 4.8° and 60.0% externally
13:50	MED/DUMMY

13:51	(f) MED/132 (hole B)
14:01	MED/DUMMY
14:02	(g) MED/141 (hole C)
14:12	MED/DUMMY
14:13	(h) MED/142 (hole D)
14:23	MED/DUMMY
14:33	Swapped 141 and 142 around to check inconsistent behaviour
	Unload to BP-0054efgh
14:51	(i) MED/131 (hole A)
15:01	MED/DUMMY
15:02	(j) MED/132 (hole B)
15:12	MED/DUMMY
15:13	(k) MED/141 (hole D)
15:23	MED/DUMMY
15:24	(l) MED/142 (hole C) Rotronic S1 19.9° and 35.8% internally
15:34	MED/DUMMY
	External drop in temperature, 3.8° and 62.4% to 0.4° and 79.6% whilst taking thermal images
	Unload to BP-0054ijkl
15:58	(m) MED/131 (hole A)
16:08	MED/DUMMY
16:09	(n) MED/132 (hole B)
16:19	MED/DUMMY
16:20	(o) MED/141 (hole D)
16:30	MED/DUMMY
16:31	(p) MED/142 (hole C)
16:41	MED/DUMMY
	Unload to BP-0054mnop
18/11/05	
08:00	Taking thermal images, Rotronic S1 -8.0° and 96.2%

Comments

1) What are the connotations of the base being at sub zero temperatures? The prior 200s compensation seems to work as the results are similar with different drift patterns, up and down

2) There may be a heating gradient on the internal side of the wall because of the heating pipes embedded.

Appendix D: Voltra summary, series one

Input thermal properties and radii	Start s	End s	Mean λ $Wm^{-1}K^{-1}$	SD / mean	Mean ρC (ρ= 1000) $Jm^{-3}K^{-1}$	SD / mean	Output λ ± Input λ	Output ρC ± Input ρC
λ0.01 C100 r1	100	2000	0.010	0.06%	96,494	1.01%	**1.57%**	**-3.51%**
λ0.01 C100 r2	300	2000	0.010	0.02%	103,043	0.19%	**1.19%**	**3.04%**
λ0.01 C100 r5	1000	2500	0.011	0.01%	102,362	0.03%	**5.25%**	**2.36%**
λ0.01 C100 r10	1500	2500	0.012	0.04%	83,504	0.10%	**16.57%**	**-16.50%**
λ0.01 C100 r50	2200	2800	0.185	0.64%	288,929	0.56%	**1751%**	**188.93%**
λ0.01 C1000 r1	200	2000	0.011	0.07%	802,125	0.86%	**7.18%**	**-19.79%**
λ0.01 C1000 r2	700	2000	0.012	0.04%	769,901	0.21%	**17.74%**	**-23.01%**
λ0.01 C1000 r5	2000	2800	0.013	0.10%	893,233	0.14%	**34.55%**	**-10.68%**
λ0.01 C1000 r10	2200	2800	0.030	0.28%	899,817	0.24%	**199.72%**	**-10.02%**
λ0.01 C2000 r1	300	2800	0.011	0.04%	1,633,254	0.58%	**6.02%**	**-18.34%**
λ0.01 C2000 r2	1000	2800	0.012	0.02%	1,512,339	0.12%	**19.47%**	**-24.38%**
λ0.01 C2000 r5	1500	2800	0.021	0.33%	1,843,899	1.09%	**105.32%**	**-7.81%**
λ0.01 C4000 r1	1000	2800	0.010	0.01%	3,338,916	0.05%	**4.36%**	**-16.53%**
λ0.01 C4000 r2	1500	2800	0.012	0.05%	2,958,930	0.17%	**23.04%**	**-26.03%**
λ0.01 C4000 r5	2400	2800	0.033	0.26%	4,463,071	0.12%	**226.41%**	**11.58%**
λ0.01 C6000 r1	1000	2800	0.011	0.03%	4,952,487	0.18%	**5.22%**	**-17.46%**
λ0.01 C6000 r2	2400	2800	0.013	0.05%	4,393,826	0.02%	**26.00%**	**-26.77%**
λ0.01 C6000 r5	2400	2800	0.061	0.40%	9,314,752	0.18%	**508.99%**	**55.25%**
λ0.01 C60000 r1	2400	2800	0.018	0.16%	46,694,903	0.07%	**83.01%**	**-22.18%**
λ0.01 C60000 r2	2400	2800	0.087	0.41%	77,999,290	0.18%	**771.60%**	**30.00%**
λ0.6 C100 r1	60	400	0.634	0.18%	77,674	0.85%	**5.66%**	**-22.33%**
λ0.6 C100 r2	60	400	0.635	0.18%	86,792	0.83%	**5.81%**	**-13.21%**
λ0.6 C100 r5	60	400	0.639	0.17%	100,950	0.82%	**6.45%**	**0.95%**
λ0.6 C100 r10	60	400	0.651	0.17%	93,025	0.82%	**8.55%**	**-6.98%**
λ0.6 C100 r50	400	800	0.750	0.45%	89,295	0.91%	**25.05%**	**-10.71%**
λ0.6 C1000 r1	60	400	0.598	0.16%	1,059,353	0.77%	**-0.31%**	**5.94%**
λ0.6 C1000 r2	60	400	0.603	0.16%	1,062,874	0.75%	**0.45%**	**6.29%**
λ0.6 C1000 r5	200	1000	0.632	0.12%	1,027,824	0.77%	**5.25%**	**2.78%**
λ0.6 C1000 r10	600	2000	0.660	0.13%	894,001	0.80%	**10.04%**	**-10.60%**
λ0.6 C1000 r50	2000	2800	0.983	0.86%	880,266	1.20%	**63.79%**	**-11.97%**
λ0.6 C2000 r1	60	400	0.604	0.19%	2,024,532	0.91%	**0.63%**	**1.23%**
λ0.6 C2000 r2	100	400	0.605	0.23%	2,087,995	0.77%	**0.90%**	**4.40%**
λ0.6 C2000 r5	200	1000	0.633	0.12%	2,043,911	0.78%	**5.43%**	**2.20%**
λ0.6 C2000 r10	1000	2800	0.662	0.13%	1,776,640	0.81%	**10.37%**	**-11.17%**
λ0.6 C4000 r1	60	1000	0.612	0.13%	3,816,792	1.37%	**1.92%**	**-4.58%**
λ0.6 C4000 r2	200	1000	0.607	0.12%	4,138,067	0.76%	**1.09%**	**3.45%**
λ0.6 C4000 r5	700	2000	0.631	0.14%	4,099,101	0.76%	**5.22%**	**2.48%**
λ0.6 C4000 r10	1200	2800	0.679	0.17%	3,431,629	0.84%	**13.22%**	**-14.21%**

Input thermal properties and radii	Start s	End s	Mean λ $Wm^{-1}K^{-1}$	SD / mean	Mean ρC (ρ= 1000) $Jm^{-3}K^{-1}$	SD / mean	Output λ ± Input λ	Output ρC ± Input ρC
λ0.6 C6000 r1	60	2000	0.613	0.09%	5,649,015	1.51%	**2.12%**	**-5.85%**
λ0.6 C6000 r2	4000	2000	0.606	0.08%	6,222,264	0.74%	**0.99%**	**3.70%**
λ0.6 C6000 r5	700	2800	0.633	0.09%	6,117,005	0.77%	**5.47%**	**1.95%**
λ0.6 C6000 r10	1500	2800	0.695	0.26%	5,032,475	0.84%	**15.90%**	**-16.13%**
λ0.6 C60000 r1	200	1000	0.629	0.13%	49,880,019	0.81%	**4.88%**	**-16.87%**
λ0.6 C60000 r2	800	2800	0.692	0.12%	47,481,123	0.97%	**15.40%**	**-20.86%**
λ0.6 C60000 r5	1500	2800	0.849	0.35%	53,042,986	1.13%	**41.50%**	**-11.60%**
λ1.0 C100 r1	60	200	1.056	0.64%	78,145	1.30%	**5.62%**	**-21.86%**
λ2.0 C100 r1	20	120	2.070	1.04%	91,537	2.55%	**3.50%**	**-8.46%**
λ2.0 C100 r2	20	120	2.072	1.05%	99,403	2.56%	**3.61%**	**-0.60%**
λ2.0 C100 r5	20	120	2.082	1.04%	111,678	2.54%	**4.08%**	**11.68%**
λ2.0 C100 r10	20	120	2.116	1.07%	100,790	2.62%	**5.80%**	**0.79%**
λ2.0 C100 r50	200	500	1.730	0.92%	94,420	2.11%	**-13.48%**	**-5.58%**
λ2.0 C1000 r1	20	120	1.952	0.99%	1,189,260	2.42%	**-2.39%**	**18.93%**
λ2.0 C1000 r2	20	120	1.964	1.00%	1,163,259	2.45%	**-1.79%**	**16.33%**
λ2.0 C1000 r5	20	120	2.078	1.05%	1,066,528	2.58%	**3.89%**	**6.65%**
λ2.0 C1000 r10	200	1000	2.186	0.42%	909,568	2.67%	**9.32%**	**-9.04%**
λ2.0 C1000 r50	1800	2800	1.819	1.09%	918,851	2.23%	**-9.05%**	**-8.11%**
λ2.0 C2000 r1	20	200	1.978	0.59%	2,208,082	2.39%	**-1.10%**	**10.40%**
λ2.0 C2000 r2	20	200	1.997	0.61%	2,177,411	2.45%	**-0.15%**	**8.87%**
λ2.0 C2000 r5	80	1000	2.107	0.26%	2,058,324	2.54%	**5.37%**	**2.92%**
λ2.0 C2000 r10	1000	2800	2.114	0.42%	1,982,207	2.63%	**5.72%**	**-0.89%**
λ2.0 C2000 r50	1000	2800	2.856	0.62%	1,690,226	3.91%	**42.80%**	**-15.49%**
λ2.0 C4000 r1	30	1000	2.020	0.20%	3,999,599	2.53%	**1.00%**	**-0.01%**
λ2.0 C4000 r2	30	1000	2.035	0.20%	4,083,137	2.52%	**1.74%**	**2.08%**
λ2.0 C4000 r5	100	1000	2.109	0.28%	4,091,758	2.55%	**5.46%**	**2.29%**
λ2.0 C4000 r10	600	2800	2.202	0.27%	3,570,701	2.69%	**10.12%**	**-10.73%**
λ2.0 C4000 r50	1800	2800	3.946	2.32%	3,610,135	4.78%	**97.31%**	**-9.75%**
λ2.0 C6000 r1	50	1000	2.013	0.22%	6,069,875	2.46%	**0.65%**	**1.16%**
λ2.0 C6000 r2	50	1000	2.031	0.22%	6,139,372	2.49%	**1.55%**	**2.32%**
λ2.0 C6000 r5	500	2000	2.113	0.34%	6,108,029	2.58%	**5.63%**	**1.80%**
λ2.0 C6000 r10	500	2000	2.242	0.36%	5,206,228	2.74%	**12.08%**	**-13.23%**
λ2.0 C60000 r1	50	1000	2.144	0.24%	48,539,108	2.73%	**7.18%**	**-19.10%**
λ2.0 C60000 r2	1000	2800	2.047	0.40%	60,121,399	2.47%	**2.33%**	**0.20%**
λ2.0 C60000 r5	1000	2800	2.242	0.44%	57,358,734	2.73%	**12.12%**	**-4.40%**
λ100 C100 r1	200	400	3.400	2.87%	265,163,054	4.10%	**-96.60%**	**265,063%**
λ100 C100 r2	200	400	3.418	2.98%	69,273,618	4.24%	**-96.58%**	**69,173%**
λ100 C100 r5	200	400	3.513	2.89%	11,467,626	4.12%	**-96.49%**	**11,367%**
λ100 C100 r10	200	400	3.383	2.89%	3,116,810	4.12%	**-96.62%**	**3016.81%**
Λ100 C1000 r1	1500	2800	3.525	1.35%	2,543,322,928	4.45%	**-96.48%**	**254,232%**

Appendix E: Voltra summary, construction materials

Input thermal properties, from Parsons (2005)	Output λ ± Input λ	Output ρC ± Input ρC
Brick: λ 0.7, ρ 1970, Cp 800, ρCp 1,576,000, r 1	**0.00%**	**4.64%**
Brick: λ 0.7, ρ 1970, Cp 800, ρCp 1,576,000, r 2	**3.56%**	**-5.41%**
Brick: λ 0.7, ρ 1970, Cp 800, ρCp 1,576,000, r 5	**6.61%**	**-0.95%**
Brick: λ 0.7, ρ 1970, Cp 800, ρCp 1,576,000, r 10	**10.13%**	**-10.80%**
Brick: λ 0.7, ρ 1970, Cp 800, ρCp 1,576,000, r 50	**98.60%**	**-8.84%**
Cellular Glass: λ 0.05, ρ 136, Cp 750, ρCp 102,000, r 1	**-0.45%**	**6.43%**
Cellular Glass: λ 0.05, ρ 136, Cp 750, ρCp 102,000, r 2	**3.89%**	**-6.70%**
Cellular Glass: λ 0.05, ρ 136, Cp 750, ρCp 102,000, r 5	**6.89%**	**-1.77%**
Cellular Glass: λ 0.05, ρ 136, Cp 750, ρCp 102,000, r 10	**10.73%**	**-11.84%**
Cellular Glass: λ 0.05, ρ 136, Cp 750, ρCp 102,000, r 50	**94.06%**	**-8.08%**
Cellulose: λ 0.057, ρ 54, Cp 1300, ρCp 70,200, r 1	**-1.59%**	**12.12%**
Cellulose: λ 0.057, ρ 54, Cp 1300, ρCp 70,200, r 2	**5.26%**	**-12.17%**
Cellulose: λ 0.057, ρ 54, Cp 1300, ρCp 70,200, r 5	**9.07%**	**-8.49%**
Cellulose: λ 0.057, ρ 54, Cp 1300, ρCp 70,200, r 10	**11.85%**	**-14.13%**
Cellulose: λ 0.057, ρ 54, Cp 1300, ρCp 70,200, r 15	**59.37%**	**-9.35%**
Concrete/stone: λ 0.93, ρ 2300, Cp 653, ρCp 1,501,900, r 1	**-1.27%**	**10.21%**
Concrete/stone: λ 0.93, ρ 2300, Cp 653, ρCp 1,501,900, r 2	**4.36%**	**-8.55%**
Concrete/stone: λ 0.93, ρ 2300, Cp 653, ρCp 1,501,900, r 5	**7.66%**	**-4.14%**
Concrete/stone: λ 0.93, ρ 2300, Cp 653, ρCp 1,501,900, r 10	**9.52%**	**-9.54%**
Concrete/stone: λ 0.93, ρ 2300, Cp 653, ρCp 1,501,900, r 50	**62.18%**	**-12.44%**
Fireclay brick: λ 1.0, ρ 1790, Cp 829, ρCp 1,483,910, r 1	**-1.30%**	**10.53%**
Fireclay brick: λ 1.0, ρ 1790, Cp 829, ρCp 1,483,910, r 2	**4.58%**	**-9.39%**
Fireclay brick: λ 1.0, ρ 1790, Cp 829, ρCp 1,483,910, r 5	**7.93%**	**-4.97%**
Fireclay brick: λ 1.0, ρ 1790, Cp 829, ρCp 1,483,910, r 10	**9.01%**	**-8.44%**
Fireclay brick: λ 1.0, ρ 1790, Cp 829, ρCp 1,483,910, r 50	**49.26%**	**-13.12%**
Limestone: λ 0.93, ρ 1650, Cp 909, ρCp 1,499,850, r 1	**-1.28%**	**10.27%**
Limestone: λ 0.93, ρ 1650, Cp 909, ρCp 1,499,850, r 2	**4.30%**	**-8.29%**
Limestone: λ 0.93, ρ 1650, Cp 909, ρCp 1,499,850, r 5	**7.55%**	**-3.79%**
Limestone: λ 0.93, ρ 1650, Cp 909, ρCp 1,499,850, r 10	**9.58%**	**-9.68%**
Limestone: λ 0.93, ρ 1650, Cp 909, ρCp 1,499,850, r 50	**62.01%**	**-12.47%**
Marble: λ 2.6, ρ 2600, Cp 880, ρCp 2,288,000, r 1	**-0.88%**	**9.20%**
Marble: λ 2.6, ρ 2600, Cp 880, ρCp 2,288,000, r 2	**5.28%**	**-12.01%**
Marble: λ 2.6, ρ 2600, Cp 880, ρCp 2,288,000, r 5	**7.98%**	**-5.30%**
Marble: λ 2.6, ρ 2600, Cp 880, ρCp 2,288,000, r 10	**-1.51%**	**21.00%**
Marble: λ 2.6, ρ 2600, Cp 880, ρCp 2,288,000, r 50	**4.64%**	**-12.62%**
Portland cement: λ 0.029, ρ 1920, Cp 670, ρCp 1,286,400, r 1	**5.28%**	**-16.46%**
Portland cement: λ 0.029, ρ 1920, Cp 670, ρCp 1,286,400, r 2	**15.50%**	**-20.59%**
Portland cement: λ 0.029, ρ 1920, Cp 670, ρCp 1,286,400, r 5	**23.23%**	**-8.90%**
Portland cement: λ 0.029, ρ 1920, Cp 670, ρCp 1,286,400, r 10	**74.89%**	**-23.04%**

Input thermal properties, from Parsons (2005)	Output λ ± Input λ	Output ρC ± Input ρC
Sand: λ 0.33, ρ 1520, Cp 800, ρCp 1,216,000, r 1	**4.48%**	**-10.58%**
Sand: λ 0.33, ρ 1520, Cp 800, ρCp 1,216,000, r 2	**2.11%**	**0.04%**
Sand: λ 0.33, ρ 1520, Cp 800, ρCp 1,216,000, r 5	**5.79%**	**1.37%**
Sand: λ 0.33, ρ 1520, Cp 800, ρCp 1,216,000, r 10	**10.08%**	**-10.59%**
Sand: λ 0.33, ρ 1520, Cp 800, ρCp 1,216,000, r 50	**225.67%**	**8.78%**
Steel: λ 45.3, ρ 7830, Cp 500, ρCp 3,915,000, r 1	**Non linear**	
Wood (fir): λ 0.12, ρ 540, Cp 1210, ρCp 653,400, r 1	**7.70%**	**-19.24%**
Wood (fir): λ 0.12, ρ 540, Cp 1210, ρCp 653,400, r 2	**1.05%**	**3.55%**
Wood (fir): λ 0.12, ρ 540, Cp 1210, ρCp 653,400, r 5	**5.32%**	**2.29%**
Wood (fir): λ 0.12, ρ 540, Cp 1210, ρCp 653,400, r 10	**11.32%**	**-12.29%**
Wood (fir): λ 0.12, ρ 540, Cp 1210, ρCp 653,400, r 50	**474.18%**	**43.12%**
Wood (oak): λ 0.176, ρ 750, Cp 2390, ρCp 1,792,500, r 1	**7.41%**	**-19.62%**
Wood (oak): λ 0.176, ρ 750, Cp 2390, ρCp 1,792,500, r 2	**0.77%**	**4.39%**
Wood (oak): λ 0.176, ρ 750, Cp 2390, ρCp 1,792,500, r 5	**5.35%**	**2.21%**
Wood (oak): λ 0.176, ρ 750, Cp 2390, ρCp 1,792,500, r 10	**15.93%**	**-16.17%**
Wood (oak): λ 0.176, ρ 750, Cp 2390, ρCp 1,792,500, r 50	**1884.70%**	**200.03%**

References

Abey J, Smallcombe J (2005) *Abey Smallcoombe, earth art and architecture,* available at www.abeysmallcombe.com on 11/07/2005

Abramowitz M, Stegun IA (eds) (1972) *Handbook of mathematical tables,* AMS 55, New York. Cited in: BSI (2005) *Methods of test for dense shaped refractory products. Determination of thermal conductivity by the hot-wire (parallel) method,* BS EN 993-15

Agrawal MP, Bhandari RC (1970) *Simultaneous determination of thermal conductivity and diffusivity of porous materials,* Applied Scientific Research, v.23, nr.1, pp.113-120

Albrecht F (1932) *Ein messgaraet fur die messung des warmeumsatzes im erdboden,* Met. Zs. V.49, pp.294-299, cited in Buettner K (1955) *Evaluation of soil heat conductivity with cylindrical test bodies,* Transactions, American Geophysical Union, v.36, nr.5, pp.831-837

Alexander LV et al (2006) *Global observed changes in daily climate extremes of temperature and precipitation,* Journal of Geophysical Research (Atmospheres), v.111, nr.D5, citation number D05109

Alley R et al (2007) *Climate change 2007: the physical science basis - summary for policymakers,* Intergovernmental Panel on Climate Change

American Society of Heating (2003) *Handbook 2003: HVAC applications. Chapter 34 - Thermal storage,* Ashrae

Anderson B (2005) *Thermal conductivity of building materials,* private communication, BRE, East Kilbride

Andersson P, Backstrom G (1976) *Thermal conductivity of solids under pressure by the transient hot-wire method,* Rev. Sci. Instr. V.47, nr.2, pp.205-209

Anon (1981) *Insulation handbook,* Comprint ltd. Watford, UK. Cited in: Batty WJ, O'Callaghan PW, Probert SD (1984a) *Assessment of the thermal-probe technique for rapid, accurate measurements of effective thermal conductivities,* Applied Energy, v.16, pp.83-113

Assael MJ, Dix M, Gialou K, Vozar L, Wakeham WA (2002) *Application of the transient hot-wire technique to the measurement of the thermal conductivity of solids,* International Journal of Thermophysics, v23, nr.3, pp. 615-633

ASTM Committee D18 (2000) *Standard test method for determination of thermal conductivity of soil and soft rock by thermal needle probe procedure,* ASTM International, designation D 5334-00

ASTM Committee D20 (2005) *Standard test method for thermal conductivity of plastics by means of a transient line-source technique,* ASTM International, designation D 5930-01

ASTM Committee E37.01 (2005) *E1269-05 Standard Test Method for Determining Specific Heat Capacity by Differential Scanning Calorimetry,* ASTM International

Baggott SL, Brown L, Milne R, Murrells TP, Passant N, Thistlethwaite G, Watterson JD (2005) *UK Greenhouse Gas Inventory, 1990 to 2003 Annual Report for submission under the Framework Convention on Climate Change,* AEA Technology plc. for Department for Environment, Food and Rural Affairs. Accessed at:
http://www.airquality.co.uk/archive/reports/cat07/0509161559_ukghgi_90-03_Issue_1.1.doc
on 12/04/2006

Banaszkiewicz M, Seiferlin K, Spohn T, Kargl G, Kömle N (1997) *A new method for the determination of thermal conductivity and thermal diffusivity from linear heat source measurements,* Rev. Sci. Instruments, v.68, nr.11, pp.4184-4190

Banaszkiewicz M, Seweryn K, Wawrzaszek R (2007) *A sensor to perform in-situ thermal conductivity determination of cometary and asteroid material,* Advances in Space Research, v.40, pp.226–237

Barrett LR, Vyse J, Green AT (1946) *Heat transfer in refractory insulating materials. Part III. Thermal conductivity and permeability as related directional properties,* Bull. BRRA, v.70, pp.109...cited in Davis WR, Downs A (1980) *The hot wire test - a critical review and comparison with the BS 1902 panel test,* Transactions British Ceramic Society, v.79, pp.44-52

Batty WJ, O'Callaghan PW, Probert SD (1984a) *Assessment of the thermal-probe technique for rapid, accurate measurements of effective thermal conductivities,* Applied Energy, v.16, pp.83-113

Batty WJ, Probert SD, Ball M, O'Callaghan PW (1984b) *Use of the thermal probe technique for the measurement of the apparent thermal conductivities of moist materials,* Applied Energy, v.18, pp.301-317

Blackwell JH, Misener AD (1951) *Approximate Solution of a Transient Heat Flow Problem,* Proc. Phys. Soc. A 64, pp.1132-1133

Blackwell JH (1953) *Radial-axial heat flow in regions bounded internally by circular cylinders,* Canadian Journal of Physics, v.31, nr.4, pp.472-479

Blackwell JH (1954) *A transient-flow method for determination of thermal constants of insulating materials in bulk. Part 1-Theory,* Journal of Applied Physics, v.25, nr.2, pp.137-144

Blackwell JH (1956) *The axial-flow error in the thermal-conductivity probe,* Canadian Journal of Physics, v.34, nr.4, pp.412-417

Blair ACL (2004) *Prime Minister's speech on climate change,* 14/09/2004, accessed at: http://www.number-10.gov.uk/output/page6333.asp on 30/01/2007

Boekwijt WO, Vos BH (1970) *Measuring Method for Determining Moisture Content and Moisture Distribution in Monuments,* Studies in Conservation, v.15, nr.2, pp. 81-93

Bohac V, Kubicar L, Vretenar V (2003) *Use of the pulse transient method to investigate the thermal properties of two porous materials,* High Temperatures - High Pressures, 2003-2004, v.35/36, pp.67-74

BREEAM Office (2006) *EcoHomes 2006 – the environmental rating for homes: the Guidance – 2006 / Issue1.2,* BRE Press

Bruijn PJ, van Haneghem IA, Schenk J (1983) *An improved nonsteady state probe method for measurements in granular materials, part 1: theory,* High Temperatures, High Pressures, v.15, pp.359-366

BSI (1973) *Methods for determining thermal insulating properties with definitions of thermal insulating terms,* BS 874:1973. Cited in: Batty WJ, O'Callaghan PW, Probert SD (1984a) *Assessment of the thermal-probe technique for rapid, accurate measurements of effective thermal conductivities,* Applied Energy, v.16, pp.83-113

BSI (1996) *Thermal insulation — Physical quantities and definitions,* BS EN ISO 7345:1996

BSI (1998) *Methods of testing dense shaped refractory products. Part 14: Determination of thermal conductivity by the hot-wire (cross-array) method,* BB EN 993-14:1998

BSI (1999a) *Thermal performance of building products and components. Specific criteria for the assessment of laboratories measuring heat transfer properties. Measurements by guarded hot plate method,* BS EN 1946-2:1999

BSI (1999b) *Building materials and products - Procedures for determining declared and design thermal values,* BS EN ISO 10456:2000

BSI (2001a) *Thermal performance of building materials and products — Determination of thermal resistance by means of guarded hot plate and heat flow meter methods — Products of high and medium thermal resistance,* BS EN 12667:2001

BSI (2001b) *Thermal performance of building materials and products — Determination of thermal resistance by means of guarded hot plate and*

heat flow meter methods — Dry and moist products of medium and low thermal resistance, BS EN 12664:2001

BSI (2001c) *Thermal performance of building materials and products — Determination of thermal resistance by means of guarded hot plate and heat flow meter methods — Thick products of high and medium thermal resistance*, BS EN 12939:2001

BSI (2005) *Methods of test for dense shaped refractory products. Determination of thermal conductivity by the hot-wire (parallel) method*, BS EN 993-15

Buettner K (1955) *Evaluation of soil heat conductivity with cylindrical test bodies*, Transactions, American Geophysical Union, v.36, nr.5, pp.831-837

California Energy Commission (2005) *Residential Compliance Manual for California's 2005 Energy Efficiency Standards*, Publication Number: CEC-400-2005-005-CMF

Campbell GS, Calissendorff C, Williams JH (1991) *Probe for measuring soil specific heat using a heat-pulse method*, Soil Sci. Soc. Am. J. v.55 pp. 291-293

Campbell GS, Huffaker EM, Wacker BT, Wacker KC (2004) *Use of the line heat source method to measure thermal conductivity of insulation and other porous materials*, in: Thermal Conductivity 27 / Thermal Expansion 15, Proceedings of the 27th International Thermal Conductivity Conference and the 15th International Thermal Expansion Symposium 2003, p.ix, DEStech Publications Inc., Pensylvania, eds. Wang H, Porter W, pp.187-195

Carslaw HS (1921) *Conduction of heat*, 2nd edtn. Macmillan, London, cited in: Carslaw HS, Jaeger JC (1940) *Some two-dimensional problems in conduction of heat with circular symmetry*, Proceedings of the London Mathematical Society, s2-46(1) pp.361-388

Carslaw HS, Jaeger JC (1940) *Some two-dimensional problems in conduction of heat with circular symmetry*, Proceedings of the London Mathematical Society, s2-46(1) pp.361-388

Carslaw HS, Jaeger JC (1947) *Conduction of heat in solids*, University Press, Oxford, cited in Blackwell JH, Misener AD (1951) *Approximate Solution of a Transient Heat Flow Problem*, Proc. Phys. Soc. A 64 1132-1133

Carslaw HS, Jaeger JC (1948) *Conduction of heat in solids*, University Press, Oxford, 2nd impression

Carslaw HS, Jaeger JC (1959) *Conduction of heat in solids*, 2nd edtn. Oxford University Press

Chambers N, Child R, Jenkin N, Lewis K, Vergoulas G, Whiteley M (2005) *Stepping Forward: A resource flow and ecological footprint analysis of the South West of England - Summary report*, Best Foot Forward Ltd, Oxford

Cheng SX, Jiang YF, Liang XG (1994) *A tiny heat probe for measuring the thermal conductivities of non-rigid materials*, Meas. Sci. Technol. 5 pp. 1339-1344

Childs PRN (2001) *Practical Temperature Measurement*, Butterworth Heinemann

Cull JP (1978) *Thermal contact resistance in transient conductivity measurements*, J. Phys. E: Sci. Instrum. v.11, pp.323-326

Davies M, Tirovic M, Ye Z, Baker PH (2004) *A low cost, accurate instrument to measure the moisture content of building envelopes in situ: a modelling study*, Building Ser. Eng. Technol. v,25, nr.4, pp.295-304

Davis WR, Downs A (1980) *The hot wire test - a critical review and comparison with the BS 1902 panel test*, Transactions British Ceramic Society, v.79, pp.44-52

Davis WR in Maglic KD, Cezairliyan A, Peletsky VE (editors) (1984) *Compendium of thermophysical property measurement methods, v.1 Survey of measurement techniques*, Plenum Press, New York and London, pp.231-254

DCLG (2006) *Code for Sustainable Homes - A step-change in sustainable home building practice*, Department for Communities and Local Government: London

DCLG (2007) *Code for sustainable homes technical guide*, Department for Communities and Local Government: London

DEFRA (2005) *The Government's Standard Assessment Procedure for Energy Rating of Dwellings - 2005 edtn.* BRE

Dedrick DE, Kanouff MP, Replogle BC, Gross KJ (2005) *Thermal properties characterisation of sodium alanates*, Journal of Alloys and Compounds, v.389, pp.299-305

Department of the Environment and the Welsh Office (1995) Approved document L to the Building Regulations - Conservation of Fuel and Power, HMSO

Department of Trade and Industry (2005) *UK Energy in Brief* - July 2005, National Statistics

Department of Trade and Industry (2006a) *Energy Trends, last quarter 2006,* dti

Department of Trade and Industry (2006b) *Energy - its impact on the environment and society,* dti

DESA: Dept. of Economic and Social Affairs - population division (2004) *World population prospects - the 2004 revision,* v.3 analytical report, United Nations publication

Doran S (2000) *DETR Framework Project Report: Field investigations of the thermal performance of construction elements as built,* Building Research Establishment Client Report No. 78132. BRE East Kilbride. Scotland, 2001 revision

Drury MJ (1988) *A simple needle-probe method for measuring thermal diffusivity of unconsolidated materials,* Geothermics, v.17, nr.5-6, pp.757-763

DuPont (2007) *Material safety data sheet,* available at http://www.ifa.hawaii.edu/instr-shop/MSDS/Delrin.pdf on 20/10/2007

Energie-Atlas GmbH (2007) Atlas of renewable energy - solar radiation, Available at:
http://www.energie-atlas.ch/so-100.htm#1-1-101 on 17/04/07

Energy Saving Trust (1997) *Report GIR27: Passive solar estate layout,* EST (reprinted 2006)

Eschner A, GrosskopfB, Jeschke P (1974) *Experiences with the hot-wire method for the measurement of thermal conductivity of refractories,* Tonind-Ztg, v.98, nr.9, pp.212... in German – cited in Davis WR, Downs A (1980) *The hot wire test - a critical review and comparison with the BS 1902 panel test,* Transactions British Ceramic Society, v.79, pp.44-52

European Parliament and Council (2002) *Directive 2002/91/EC of the European Parliament and of the Council of 16 December 2002 on the energy performance of buildings,* Official Journal of the European Communities

D'Eustachio D, Schreiner RE (1952) *A study of a transient heat method for measuring thermal conductivity,* Transactions of ASHVE, v.58, pp.331-342

Fourier J, translated by Freeman A with corrections by Baynes RE & Woolcombe WG (1888) *The analytical theory of heat,* G.E. Stechert & Co. New York (reprint approx. 1945)

Frontline Systems, Inc. (2007) *Solver tutorial for optimization users,* available at: http://www.solver.com/tutorial.htm on 24/04/2007

FPAG - Fuel Poverty Advisory Group (for England) (2007) Fifth annual report - 2006, DTI/Pub 8535/0.3k/04/07NP available at: http://www.defra.gov.uk/environment/energy/fuelpov/fpag/pdf/fpag-annualreport0607.pdf on 17/04/07

Garcia-Gutierrez A, Espinosa-Paredes G (2004) *Thermal conductivity measurement of geothermal cementing systems: an experimental comparison between the line source and Jaeger methods*, Energy Conversion and Management, v.45, nr.5, pp.755-764

van Ginkel JT, van Haneghem IA, Raats PAC (2002) *Physical properties of composting material: gas permeability, oxygen diffusion coefficient and thermal conductivity,* Biosystems Engineering (2002) v.81, nr.1, pp.113-125

Goodhew SM (2000) *The thermal properties of cob buildings of Devon*, PhD Thesis. University of Plymouth (unpublished)

Goodhew SM, Griffiths R (2003) *Handbook giving practical details for thermal probe studies with iterative methods for data analysis using Solver routines,* University of Plymouth, Joint Schools of the Built Environment, internal report, unpublished

Goodhew SM, Griffiths R (2004) *Analysis of thermal probe measurements using an iterative method to give sample conductivity and diffusivity data*, Applied Energy, v.77, pp.205-224

Goodhew SM, Griffiths R (2005) *Sustainable walls to meet the building regulations*, Energy and Buildings, v.37, pp.451-459

Greg C, Glatzmaier GC, Ramirez WF (1985) *Simultaneous measurement of the thermal conductivity and thermal diffusivity of unconsolidated materials by the transient hot wire method,* Rev. Sci. Instruments 56 (7)1394-1398. American Institute of Physics

de Groot JJ, Kestin J, Sookiazian H (1974) *Instrument to measure the thermal conductivity of gases*, Physica, v.75, pp.454-482

Grosskopf B, Kilian B (1980) Table book with Ei(-x) and $\Delta\theta(2t)/\Delta\theta(t)$ values, Kubel-Druck, Wiesbaden, FRG. Cited in: BSI (2005) *Methods of test for dense shaped refractory products. Determination of thermal conductivity by the hot-wire (parallel) method,* BS EN 993-15

Gustafsson SE, Karawacki E, Khan MN (1979) *Transient hot-strip method for simultaneously measuring thermal conductivity and thermal diffusivity of solids and fluids,* J. Phys. D: Appl. Phys. v.12, nr.9, pp.1411-1421

Haarman, J. W. (1971) *A contribution to the theory of the transient hot-wire method*, Physica, v.52, nr.4, p.605-619

Hacker J, Holmes M, Belcher S, Davies G (2005) *Climate change and the indoor environment: impacts and adaptation, TM36*, The Chartered Institution of Building Services Engineers (CIBSE)

Håkansson B, Andersson P, Bäckström G (1988) *Improved hot-wire procedure for thermophysical measurements under pressure*, Review of Scientific Instruments, v.59, nr.10, pp.2269-2275

Hammerschmidt U (2003) *A quasi-steady state technique to measure the thermal conductivity*, International Journal of Thermophysics, v.24, nr.5, pp.1291-1312

van Haneghem IA (1981) *Een niet-stationaire naaldmethode (warmtegeleiding, warmtecapaciteit, contactweerstand)*, Wageningen UR internal publication, dissertation abstract, nr.875

van Haneghem IA, Schenk T, Boshoven PA (1983) *An improved nonsteady-state probe method for measurements in granular materials. II: Experimental results*, High Temperatures, High Pressures, v.15, nr.4, pp.367-374

van Haneghem IA, van Asselt CJ, van Loon WKP, Boshoven HP (1998) *A portable device to measure thermal conductivity in porous media*, High Temperatures - High Pressures v.30, nr.5, pp.593-597 (14 ECTP Proceedings pp.847-851)

Hansen Dr JE (2005) *Is there still time to avoid 'dangerous anthropogenic interference' with global climate?* Presentation on December 6, 2005 at the American Geophysical Union, San Francisco, California

Healy JJ, De Groot JJ, Kestin J (1976) *The theory of the transient hot-wire method for measuring thermal conductivity*, Physica 82C, pp.392-408

Van der Held (1932), Warmte-Techniek, cited in: Van der Held EFM, Van Drunen FG (1949). *A method of measuring the thermal conductivity of liquids*. Physica A, v.15, nr.10, pp.865-881

Van der Held EFM; Van Drunen FG (1949). *A method of measuring the thermal conductivity of liquids*. Physica A, v.15, nr.10, pp.865-881

Van der Held EFM, Hardebol J, Kalshoven J (1953) *On the Measurement of the Thermal Conductivity of Liquids by a Non-Stationary Method*, Physica, v.19, nr.1-12, pp.208-216

Hitchin R (2007) *Decarbonising buildings*, Ingenia, issue 31, pp.31-36, The Royal Academy of Engineering

Hockstad L et al (2005) *Inventory of U.S. greenhouse gas emissions and sinks 1990 - 2003*, U.S. Environmental Protection Agency

Holman JP (1981) *Heat Transfer*, 5th edtn, McGraw-Hill, New York, pp.48-51, cited in: Batty WJ, O'Callaghan PW, Probert SD (1984a) *Assessment of the thermal-probe technique for rapid, accurate measurements of effective thermal conductivities*, Applied Energy, v.16, pp.83-113

Hooper FC, Chang SC (1953) *Development of the thermal conductivity probe*, ASHVE Transactions, v.59, pp. 463-472

Hooper FC, Lepper FR (1950) *Transient heat flow apparatus for the determination of thermal conductivities*, Transactions American Society of Heating and Ventilation Engineers v.56, pp.309-324

Hukseflux (2001) *TP08 small size non-steady-state probe for thermal conductivity measurement*, Hukseflux Thermal Sensors – available by email request at info@hukseflux.com on 1/03/2005

Hukseflux (2007) *Thermal Conductivity Science*, available at http://www.hukseflux.com/thermal%20conductivity/thermal.htm on 18/09/07

Hust JG, Smith DR (1989) *Interlaboratory comparison of two types of line-source thermal-conductivity apparatus measuring five insulating materials*, National Institute of Standards and Technology, report nr. 89/3908, for U.S Dept. of Energy, Oak Ridge National Laboratory

IEC (2001) *International Standard 60529: Degrees of protection provided by enclosures (IP code)*, International Electrical Commission 2001

Incropera FP, DeWitt DP (1996) *Introduction to heat transfer*, John Wiley and Sons, 3rd edtn.

Ingersoll LR, Zobel OJ, Ingersoll AC (1954) *Heat conduction with engineering and geological applications*, McGraw Hill, New York, pp. 143-147, cited in: Nix GH, Lowery GW, Vachon RI, Tanqer GE (1967) *Direct determination of thermal diffusivity and conductivity with a refined line-source technique*, Process in Astronautics and Aeronautics, v.20, pp. 865-878

Jaeger JC (1944) *Some problems involving line sources in conduction of heat*, Philosophical magazine, S.7 35, pp. 169-179

Jaeger JC (1955) *Conduction of heat in a solid in contact with a thin layer of a good conductor*, The Quarterly Journal of Mechanics and Applied Mathematics, v.8, nr.1, pp.101-106

Jaeger JC (1956) *Conduction of heat in an infinite region bounded internally by a circular cylinder of a perfect conductor*, Australian J. Phys. v.9, pp.167-179

Jaeger JC (1958) *The measurement of thermal conductivity and diffusivity with cylindrical probes,* Transactions, American Geophysical Union, v.39, nr.4, pp.708-710

Jaeger JC, Sass JH (1964) *A line source method for measuring the thermal conductivity and diffusivity of cylindrical specimens of rock and other poor conductors,* Brit. J. Appl. Phys. v.15. pp.1187-1194

Jespersen HB (1953) *Thermal conductivity of moist materials and its measurement,* J. Inst. Heat. Vent. Eng., v.21, pp.157-174

Jones BW (1988) *Thermal conductivity probe: development of method and application to a coarse granular medium,* J. Phys. E: Sci. Instrum. v.21, pp.832-839

Joy FA (1957) *Thermal conductivity of insulation containing moisture,* ASTM Symposium on Thermal Conductivity Measurements, pp.65-80

Kelly R (MP) (2006) *Shaping a low carbon future - our environmental vision,* Speech by Ruth Kelly MP at the 'Towards Zero Carbon Development' event hosted by WWF on 13 December 2006, available at http://www.communities.gov.uk/index.asp?id=1505202 0n 17/04/07

Kluitenberg GJ, Ham JM, Bristow KL (1993) *Error analysis of the heat pulse method for measuring soil volumetric heat capacity,* Soil Sci. Soc. Am. J. v.57, pp.1444-1451

Knibbe PG (1986) *The end-effect error in the determination of thermal conductivity using a hot-wire apparatus,* International journal of heat and mass transfer, v.29, nr.3, pp.463-473

Knibbe PG (1987) *An accurate instrument for fast thermal-conductivity and thermal-diffusivity measurements at elevated temperatures and pressures,* J. Phys. E: Sci. Instrum. v.20, pp.1205-1211

Krishnaiah S, Singh DN (2004) *A device for determination of thermal properties of soil,* Journal of Testing and Evaluation, v.32, nr.2, pp.1-6

Krishnaiah S, Singh DN, Jadhav GN (2004) *A methodology for determining thermal properties of rocks,* International Journal of Rock Mechanics and Mining Sciences, v.41, nr.5, pp.877-882

Kubicar L (1999) *Transient methods for measuring thermophysical parameters,* Minutes of Workshop W III, 15th European Conference on Thermophysical Properties, Wurzburg, September 5-9

Kubicár L, Bohác V, Vretenár V (2005) *Thermophysical parameters of phenolic foam measured by pulse transient method: Methodology for low thermal conductivity materials,* Thermal Conductivity, v.27, pp.328-337

Lavelle M (2006) Personal communication

Lazarus N (2003) *Beddington zero (fossil) energy development - toolkit for carbon neutral developments, part II*, Bioregional Development Group

Lide DR et al (2004) *Handbook of chemistry & physics*, CRC press 85th edtn

Lindsay RW, Zhang J (2005) *The Thinning of Arctic Sea Ice, 1988-2003: Have We Passed a Tipping Point?* Journal of Climate, accessed at: http://psc.apl.washington.edu/zhang/Pubs/tipping_point.pdf on 6/03/2007

Lockmuller N (2007) Private communication, NPL Management Ltd

van Loon WKP, van Haneghem IA, Schenk J (1989) *A new model for the non-steady-state probe method to measure thermal properties of porous media*, Int. J. Heat Mass Transfer, v.32, nr.8, pp.1473-1481

Lovelock J (2006) *The Revenge of Gaia: Why the Earth Is Fighting Back - and How We Can Still Save Humanity*, Allen Lane

Lutz W, Sanderson WC, Scherbov S (2004) *The end of population growth in the 21st century*, IIASA & Earthscan

Manohar K, Yarbrough DW, Booth JR (2000) *Measurement of apparent thermal conductivity by the thermal probe method*, ASTM Journal of Testing and Evaluation, v.28, nr.5, pp.345-351

Marland G, Boden TA, Andres RJ (2005) *Global, Regional, and National CO2 Emissions*. In Trends: A Compendium of Data on Global Change. Carbon Dioxide Information Analysis Center, Oak Ridge National Laboratory, U.S. Department of Energy, Oak Ridge, Tenn., U.S.A.

Mastin DE (1964) *A method for determining the thermal diffusivity of solid propellants*, Report P-63-27, Rohm and Haas Company Huntsville, Alabama, cited in: Nix GH, Lowery GW, Vachon RI, Tanqer GE (1967) *Direct determination of thermal diffusivity and conductivity with a refined line-source technique*, Process in Astronautics and Aeronautics, v.20, pp. 865-878

McMullan R (1992) *Environmental science in building*, Macmillan Press ltd, 3rd edtn.

Middleton GF, revised by Schneider LM (1987) *Bulletin 5: Earth-wall construction*, CSIRO, Division of building, construction and engineering, Australia, 4th edtn.

Morabito P (1989) *Thermal conductivity and diffusivity measurements by the transient two linear and parallel probe method*, Thermochimica Acta, 148, pp. 513-520

Morton T, Stevenson F, Taylor B, Smith NC (2005) *Low cost earth brick construction: 2 Kirk Park, Dalguise: monitoring & evaluation,* Arc, Auchtermuchty

NASA (2007) *Astrophysics Data System – physics abstract service,* available at: http://adsabs.harvard.edu/abs/1952PhDT.....2B on 25/04/2007

National Physical Laboratory (2007a) *Standard test protocol for measurement of thermophysical properties of materials using contact transient methods based on a common principle*, available at: http://www.npl.co.uk/thermal/ctm/draft_transient_standard.doc on 7/09/07

National Physical Laboratory (2007b) *Annex 3A: non-steady state probe technique, to Standard test protocol for measurement of thermophysical properties of materials using contact transient methods based on a common principle*, available at http://www.npl.co.uk/thermal/ctm/3a.doc on 7/09/07

Niven C (1905) *On a Method of Finding the Conductivity for Heat,* Proceedings of the Royal Society of London. Series A, Containing Papers of a Mathematical and Physical Character, v.76, nr.507 (Apr. 22, 1905), pp.34-48

Nix GH, Lowery GW, Vachon RI, Tanqer GE (1967) *Direct determination of thermal diffusivity and conductivity with a refined line-source technique,* Process in Astronautics and Aeronautics, v.20, pp. 865-878

Norton J (1997) *Building with Earth - a handbook,* Intermediate Technology Publications, London

Novichenok LN, Pikus Yu M (1975) *Joint determination of thermal properties by a probe method,* Journal of Engineering Physics and Thermophysics v.29, pt.3, pp.1116-1118

Oughton RJ et al (1986) *CIBSE guide, volume A: design data,* The Chartered Institution of Building Services Engineers, London, 5th edtn.

Ozisik MN, Hughes D (1966) *Thermal contact conductance of smooth-to-rough contact joints,* ASME 66-WA/HT-54, presented at the Winter Annual Meeting and Energy Systems Exposition, New York, cited in: Batty WJ, O'Callaghan PW, Probert SD (1984a) *Assessment of the thermal-probe technique for rapid, accurate measurements of effective thermal conductivities*, Applied Energy, v.16, pp.83-113

Pande RN, Saxena NS, Chaudhary DR (1984) *Measurement of effective thermal conductivity of building construction materials at different interstitial air pressures,* Ind. J. Tech. v.22, pp.66-69

Parkpoom S, Harrison GP, Bialek JW (2004) *Climate change impacts on electricity demand*, 39th International Universities Power Engineering Conference, v.3, pp.1342-1346 vol.2

Parsons R ed (2005) *Handbook 2005: Fundamentals. Chapter 25 - Thermal and water vapor transmission data*, American Society of Heating, Refrigerating and Air-Conditioning Engineers

Patten HE (1909) *Heat transference in soils*, US Dept. of Agriculture, Bureau of Soils - bulletin nr.59, pp.1-54

Patterson DE, Riseborough DW, Smith MW (1987) *Analysis of Norman Wells core samples*, Geotech. Science Laboratory Report, Carleton University, Ottawa, Canada, 128pp. Cited in: Drury MJ (1988) *A simple needle-probe method for measuring thermal diffusivity of unconsolidated materials*, Geothermics, v.17, nr.5-6, pp.757-763

Physibel home page (2007) available at: http://www.physibel.be/index.htm on 18/10/2007

Picot JC, Fredrickson AG (1968) *Interfacial and electrical effects on thermal conductivity of nematic liquid crystals*, Industrial & Engineering Chemistry Fundamentals, v.2, nr.1, pp. 84-89

Powell RW, Ho CY, Liley PE (1966) *Thermal conductivity of selected materials*, National Standard Reference Data Series - National Bureau of Standards, Washington D.C.

Powell-Smith V, Billington MJ (1995) *The building regulations explained and illustrated*, Blackwell Science, 10th edtn.

R Development Core Team (2005) *R: A language and environment for statistical computing*, R Foundation for Statistical Computing, Vienna

Ratcliffe EH (1959) *Thermal conductivities of fused and crystalline quartz*, British Journal of Applied Physics, v.10, pp.22-25, cited in: Woodside W, Messmer JH (1961) *Thermal conductivity of porous media. I: Unconsolidated sands*, Journal of Applied Physics, v.32, nr.9, pp.1688-1699

Ren T, Noborio K, Horton R (1999) *Measuring soil water content, electrical conductivity, and thermal properties with a thermo-time domain reflectometry probe*, Soil Sci. Soc. Am. J. v.63, pp.450-457

Riseborough DW, Smith MW, Halliwell DH (1983) *Determination of the thermal properties of frozen soils*, Permafrost, Proceedings of the 4th International Conference, Fairbanks, Alaska, July 1983. National Academy Press, Washington D.C., v.1, pp.1072-1077

Ross T (2001) *The last word on Part L*, Building Magazine, issue 19 available at:

http://www.building.co.uk/story.asp?sectioncode=71&storycode=1007119 on 17/04/07

Salmon DR, Williams RG, Tye RP (2002) *Thermal conductivity and moisture measurements on masonry materials,* Insulation materials: testing and applications: 4th volume, ASTM STP 1426, A.O. Desjarlais and R.R. Zarr, Eds., American Society for Testing and Materials, West Conshohocken, PA, 2002

Sandberg O, Andersson P, Backstrom G (1977) *Heat capacity and thermal conductivity from pulsed wire probe measurements under pressure,* J. Phys. E: Sci. Instrum. v.10, pp.474-477

de Saulles T (2005) *Thermal mass - a concrete solution for the changing climate,* The Concrete Centre, Camberley, Surrey, accessed at: http://www.concretecentre.com/PDF/MB_Thermal%20Mass_May05.pdf on 17/04/2007

Schleiermacher A (1888) *On the thermal conduction of gas,* Wiedeman Ann. Phys. V34 pp. 623-646 (in German)

Schwarze W (1903) *Determination of the thermal conductivity of argon and helium by the Method of Schleiermacher,* Ann. Physik v.11, pp.303-330 cited in: Hall LA, Hust JG, Gosman AL (1964) *A bibliography of thermophysical properties of argon from 0 to 300°C,* National Bureau of Standards, technical note 217, US Department of Commerce

Scripps Institution of Oceanography (2007) *The Keeling Curve,* data available at http://scrippsco2.ucsd.edu/data/in_situ_co2/monthly_mlo.csv on 21/11/2007

Seiferlin K (1990) *Die Warmeleitfahigkeit synthetischer poroser Eis-proben-Messungen und einfache* Modelle, Diploma thesis, Institut fur Planetologie der Westfalischen Wilhelms-Universitat Cited in: Seiferlin K, Komle NI, Kargl G, Spohn T (1996) *Line heat-source measurements of the thermal conductivity of porous H2O ice, CO2 ice and mineral powders under space conditions,* Planet. Space Sci., v.44, nr.7, pp.691-704

Seiferlin K, Komle NI, Kargl G, Spohn T (1996) *Line heat-source measurements of the thermal conductivity of porous H2O ice, CO2 ice and mineral powders under space conditions,* Planet. Space Sci., v.44, nr.7, pp.691-704

Sharma RG, Pande RN, Chaudhary DR (1984a) Indian Journal of Pure and Applied Physics, not found, cited as "in press" by: Singh R, Saxena NS, Chaudhary DR (1985) *Simultaneous measurement of thermal conductivity and thermal diffusivity of some building materials using the transient hot strip method,* J. Phys. D: Appl. Phys. v.18, nr.1, pp.1-8

Singh R, Saxena NS, Chaudhary DR (1985) *Simultaneous measurement of thermal conductivity and thermal diffusivity of some building materials using the transient hot strip method*, J. Phys. D: Appl. Phys. v.18, nr.1, pp.1-8

Smoluchowski M: (1910) Bull. Intern. de Cracovie, p.295; (1911a) Ann. Phys. Chem. v.35, p.983; (1911b) Bull. Intern. de Cracovie, p.432; (1953) Phil. Mag. v.21, p.472, cited by: Haarman, J. W. (1971) *A contribution to the theory of the transient hot-wire method*, Physica, v.52, nr.4, p.605-619

Spanos I, Simons M, Holmes KL (2005) *Cost savings by application of passive solar heating*, Structural Survey, v.23, nr.2, pp.111-130

Spiess EL, Walz E, Nesvabda P, Morley M, van Haneghem IA, Salmon DR (2001) *Thermal conductivity of food materials at elevated temperatures*, High Temperatures - High Pressures v.33, nr.6, pp.693-697 (15 ECTP Proceedings pp.1197-1201)

Spohn T, Seiferlin K, Benkhoff J (1989) *Thermal conductivities and diffusivities of porous ice samples at low pressures and temperatures and possible modes of heat transfer in near surface layers of comets*, Proc. Int. Workshop on Physics and Mechanics of Cometry Material, ESA SP-302, pp.81. Cited in: Seiferlin K, Komle NI, Kargl G, Spohn T (1996) *Line heat-source measurements of the thermal conductivity of porous H2O ice, CO2 ice and mineral powders under space conditions*, Planet. Space Sci., v.44, nr.7, pp.691-704

Spohn T, Seiferlin K, Hagermann A, Knollenberg J, Ball AJ, Banaszkiewicz M, Benkhoff J, Gadomski S, Gregorczyk W, Grygorczuk J, Hlond M, Kargl G, Kührt E, Kömle N, Krasowski J, Marczewski W, Zarnecki J C (2007) *MUPUS - a Thermal and Mechanical Properties Probe for the Rosetta Lander Philae*. Space Sci. Rev. v.128, nr.1-4, pp.339-362

Stalhane B and Pyk S (1931) *New method for measuring the thermal conductivity coefficients*, Teknisk Tidskrift. 51. 389-96 (in Swedish)

Steinhagen HP (1977) *Thermal conductive properties of wood, green or dry, from -40 to + 100°C: a literature review*, USDA Forest Service, general technical report, FPL-9

Stern N (2007) *The economics of climate change: the Stern review*, Cambridge University Press

Svincek P (1999) History of other NIST thermal conductivity equipment, available at http://www.bfrl.nist.gov/863/hotplate/webdoc4.htm on 18/04/2007

Szokolay SV (2004) *Introduction to Architectural science - The basis of sustainable design*, Architectural Press, Oxford

Todd S (2006) *A review of the proposals for amending the energy efficiency provisions in the building regulations for dwellings*, Structural Survey, v.24, nr.3, pp.181-200

Touloukian YS, Powell RW, HO CY, Klemens PG (1970a) *Thermophysical properties of matter, volume 2: Thermal conductivity nonmetallic solids*, Thermophysical Properties Research Center (TPRC), Purdue University, IFI/Plenum, New York

Touloukian YS, Buyco EH (1970) *Thermophysical properties of matter, volume 5: Specific heat nonmetalic solids*, Thermophysical Properties Research Center (TPRC), Purdue University, IFI/Plenum, New York

Touloukian YS, Liley PF, Sanena SC (1970b) *Thermophysical properties of matter, volume 3: Thermal Conductivity - Nonmetallic Liquids and Gases*, Thermophysical Properties Research Center (TPRC), Purdue University, IFI/Plenum, New York. Cited in Xie H, Cheng S (2001) *A fine needle probe for determining the thermal conductivity of penetrable materials*, Meas. Sci. Technol. v.12, pp.58-62, IOP Publishing Ltd.

Touloukian YS, Powell RW, HO CY, Nicolaou MC (1973) *Thermophysical properties of matter, volume 10: Thermal diffusivity*, Thermophysical Properties Research Center (TPRC), Purdue University, IFI/Plenum, New York

Twinn C (2003) *BedZED*, The Arup Journal, 1/2003, pp.10-16

Tye R, Kubičár L, Lockmuller N (2005) *The development of a standard for contact transient methods of measurement of thermophysical properties*, International Journal of Thermophysics, v.26, nr.6, November 2005, pp.1917-1938

Underwood WM, McTaggart RB (1960) *The thermal conductivity of several plastics, measured by an unsteady state method*, Chem. Eng. Progr. Sym. v.56, nr.30, pp. 261-268

UKAS (2007) *Welcome to UKAS websites*, available at http://www.ukas.org/ on 19/04/2007

UK-GBC (2007) *UK Green Building Council – Mission*, available at http://www.ukgbc.org/index.jsp on 17/04/07

UNEP (2007) *Global Environment Outlook: environment for development, GEO-4*, United Nations Environment Programme

Venart JES, Krishnamurthy C (1968) Thermal conductivity, proceedings of the seventh conference, eds. Flyn DR, Peavy BA Jr, NBS special publication nr. 302, p.659...; cited in: Greg C, Glatzmaier GC, Ramirez WF (1985) *Simultaneous measurement of the thermal conductivity and thermal diffusivity of unconsolidated materials by the transient hot wire*

method, Rev. Sci. Instruments, v.56, nr.7, pp.1394-1398. American Institute of Physics

Veziroglu TN (1967) *Correlation of thermal contact conductance experimental results*, Prog. Astronaut. Aeronaut. v.20, pp.879-907, Academic Press, NY

Vos BH (1955) *Measurements of thermal conductivity by a non-steady-state method*, Appl. Sci. Res. Section A, v.5, pp.425-438

de Vries DA (1952a) *The thermal conductivity of soil*, Mededelingen van de Landbouwhogeschool te Wageningen, v.52, nr.1, pp.1-73 (in Dutch)

de Vries DA (1952b) *A nonstationary method for determining thermal conductivity of soil in situ*, Soil Sci. v.73, nr.2, pp.83–89

de Vries DA, Peck AJ (1958) *On the cylindrical probe method of measuring thermal conductivity with special reference to soils.* 1. Extension of theory and discussion of probe characteristics, Australian Journal of Physics, v.11, pp.255-271

Waite WF, Gilbert LY, Winters WJ, Mason DH (2006) Estimating thermal diffusivity and specific heat from needle probe thermal conductivity data, Rev. Sci. Instrum. v.77, 044904, 5pp.

Waite WF, Stern LA, Kirby SH, Winters WJ, Mason DH (2007) *Simultaneous determination of thermal conductivity, thermal diffusivity and specific heat in sI methane hydrate*, Geophys. J. Int. v.169, pp.767–774

Whitehead S, Hutchings EE (1938) *Current rating of cables for transmission and distribution*, J. Inst. Elect. Engrs. v.83, pp.517-565

Whitehead S (1944) *An approximate method for calculating heat flow in an infinite medium heated by a cylinder*, The Proceedings of the Physical Society, v.56, part 6, nr.318, pp. 357-366

de Wilde P, Griffiths R, Pilkington B, Goodhew SM (2007) *Simulation of heat flow from a line source in support of development of a thermal probe.* In: Jiang, Zhu, Yang and Li, eds. Building Simulation '07, 10th International IBPSA Conference, Beijing, China, September 3-6 2007, 1858-1865

Witte HJL, van Gelder GJ, Spitler JD (2002) *In situ measurement of ground thermal conductivity: the Dutch perspective*, ASHRAE Transactions, v.108, nr.1, pp.263-272

Woodside W (1958) *Probe for thermal conductivity measurement of dry and moist materials*, Heating, Piping & Air Conditioning, September 1958, pp.163-170

Woodside W, Messmer JH (1961a) *Thermal conductivity of porous media. I: Unconsolidated sands*, Journal of Applied Physics, v.32, nr.9, pp.1688-1699

Woodside W, Messmer JH (1961b) *Thermal conductivity of porous media. II: Consolidated rocks*, Journal of Applied Physics, v.32, nr.9, pp.1699-1706

Xie H, Cheng S (2001) *A fine needle probe for determining the thermal conductivity of penetrable materials*, Meas. Sci. Technol. v.12, pp.58-62. IOP Publishing Ltd.

Zarr RR et al (2000) *NIST Standard Reference Database 81 - Heat Transmission Properties of Insulating and Building Materials*, National Institute of Standards and Technology, Gaithersburg, USA, available at: http://srdata.nist.gov/insulation/ on 18/04/2007

Zarr RR, Filliben JJ (2002) *An international study of guarded hot plate laboratories using fibrous glass and expanded polystyrene reference materials*, Insulation materials: testing and applications: 4th volume, ASTM STP 1426, A.O. Desjarlais and R.R. Zarr, Eds., American Society for Testing and Materials, West Conshohocken, PA, 2002

Bibliography

Asher GB, Sloan ED, Graboski MS (1986) *A computer-controlled transient needle-probe thermal conductivity instrument for liquids.* International Journal of Thermophysics, v.7, nr.2, pp.285-294. Cited in Yang W, Sokhansanj S, Tang J, Winter P (2002) *Determination of Thermal Conductivity, Specific Heat and Thermal Diffusivity of Borage Seeds,* Biosystems Engineering, v.82, nr.2, pp.169–176

Assael MJ, Gialou K (2003a) *A transient hot-wire instrument for the measurement of the thermal conductivity of solids up to 590 K,* International Journal of Thermophysics, v.24, nr.3, pp.667-674

Assael MJ, Gialou K (2003b) *Measurement of the thermal conductivity of stainless steel AISI 304L up to 550 K,* International Journal of Thermophysics, v.24, nr.4, pp.1145-1153

Assael MJ, Gialou K, Kakosimos K, Metaxa I (2004) *Thermal conductivity of reference solid materials,* International Journal of Thermophysics, v.25, nr.2, pp.397-408

ASTM Committee C-8 (2004) *C 1113-99 Standard test method for thermal conductivity of refractories by hot wire (platinum resistance thermometer technique),* Annual book of ASTM standards 2004, v.15.01, pp.209-214, ASTM International

ASTM Committee C-8 (2004) *C 182-88 (reapproved 1998) Standard test for thermal conductivity of insulating firebrick,* Annual book of ASTM standards 2004, v.15.01, pp.46-48, ASTM International

Ball, EF (1968) *Measurements of thermal conductivity of building materials,* J. Inst. Heating Ventilating Engrs., v.36, pp.51-56

Bates DM, Watts DG (1988) *Nonlinear regression analysis and its applications,* John Wiley & Sons, Inc.

BSI (2003) *Building components and building elements - Thermal resistance and thermal transmittance - Calculation method,* BS EN ISO 6946:1997 Incorporating Amendment No.1

BSI (2003) *Thermal performance of building materials and components — Principles for the determination of thermal properties of moist materials and components,* PD CEN/TR 14613:2003

Bullard E (1954) *The flow of heat through the floor of the Atlantic Ocean,* Proceedings of the Royal Society, London, v.222, pt.1150, pp.408-429

Carpentier O, Defer D, Antczak E, Chauchois A, Duthoit B (2007) *In situ thermal properties characterization using frequential methods,* Energy and Buildings, 8 pp. - accepted manuscript

Carwile LCK, Hoge HJ (1966) *Thermal conductivity of polystyrene: selected values*, US Army Natick laboratories, pioneering research division, technical report 66-27-PR

Clifford AA, Kestin J, Wakeham WA (1980) *A further contribution to the theory of the transient hot-wire technique for thermal conductivity measurements*, Physica 100A pp. 370-374

Demirboga R, Gul R (2003) *The effects of expanded perlite aggregate, silica fume and fly ash on the thermal conductivity of lightweight concrete*, Cement and Concrete Research, v.33, nr.5, pp.723-727

Doebelin EO (1990) *Measurement systems, application and design*, 4th edtn, McGraw Hill

Dowding KJ, Blackwell BF (1998) *Joint experimental / computational techniques to measure thermal properties of solids*, Meas. Sci. Technol. v.9, pp.877-887

Draper RD, Smith H (1998) *Applied regression analysis*, John Wiley and Sons, Inc. Third edtn.

Evrard A (2006) *Sorption behaviour of lime-hemp concrete and its relation to indoor comfort and energy demand*, Compagnon, Haefeli and Weber, ed. PLEA'06, 23rd International Conference, Geneva, Switzerland, September 6-8 2006, v.1, pp.553-558

Evrard A, De Herde A, Minet J (2006) *Dynamical interactions between heat and mass flows in lime-hemp concrete*. In: Research in Building Physics and Building Engineering: 3rd International Conference in Building Physics (Montreal, Canada, 27-31 August 2006) Editor(s) - Paul Fazio, Hua Ge, Jiwu Rao, Guylaine Desmarais, Taylor and Francis. Pp. 69-76

Franco A (2007) *An apparatus for the routine measurement of thermal conductivity of materials for building application based on a transient hot-wire method*, Applied Thermal Engineering, v.27, nr.14-15, pp.2495-2504

Fylstra D et al (1998) *Design and use of the Microsoft Excel Solver*, Interfaces, v.28, nr.5, September-October 1998 pp.29-55

Gafner G (1957) *The application of a transient method to the measurment of the thermal conductivity of rocks and building materials*, British Journal of Physics, v.8, nr.10, pp.393-397

Gendelis S, Jakovics A (2005) *Heat transfer measurements in non-stationary conditions for building structures*, 14th International Conference on Thermal Engineering and Thermogrammetry (THERMO), 22-24 June, 2005, Budapest, Hungary, p.69

Gilbo CF (1985) *Thermal conductivity measurement using a thin-heater apparatus,* Journal of Thermal Insulation, v.9, pp.92-101

Glassmeier KH, Boehnhardt H, Koschny D, Kuhrt E, Richter I (2007) *The Rosetta Mission: flying towards the origin of the solar system,* Space Science Reviews, v.128, pp.1-21

Glaser PE, Wechsler AE, Germeles AE (1965) *Thermal properties of postulated lunar surface materials,* Annals of the New York Academy of Science, v.123, nr.2, pp.656-670

Gori F, Marino C, Pietrafesa M (2001) *Experimental measurements and theoretical predictions of the thermal conductivity of two phases glass beads,* International Communications in Heat Mass Transfer, v.28, nr.8, pp.1091-1102

Gunerhan H, Hepbasli A (2005) *Utilisation of basalt stone as a sensible heat storage material,* Energy Sources, v.27, pt.14, pp.1357-1366

Haran EN, Wakeham WA (1982) *A transient hot-wire cell for thermal conductivity measurements over a wide temperature range,* J. Phys. E: Sci. Instrum.. v.15, pp.839-842

Ingersoll LR, Zobel OJ, Ingersoll AC (1948) *Heat conduction with engineeering and geological applications,* McGraw Hill, reprinted by Lightning Source UK Ltd. 2007

Jaeger JC (1959) *The Use of Complete Temperature-Time Curves for Determination of Thermal Conductivity with particular Reference to Rocks,* Australian Journal of Physics, v.12, pp.203-217

James N, Desai P (2003) *A study into the development of sustainability rating for homes,* Bioregional Development Group

Krishnaiah S, Singh DN (2006) *Determination of thermal properties of some supplementary cementing materials used in cement and concrete,* Construction and Building Materials, v.20, nr.3, pp.193-198

Kubicár L, Bohác V, Vretenár V (2005) *Thermophysical parameters of phenolic foam measured by pulse transient method: Methodology for low thermal conductivity materials,* Thermal Conductivity, v.27, pp.328-337

Kumaran MK (1996) *Heat, air and moisture transfer through new and retrofitted insulated envelope parts (Hamtie),* International Energy Agency, IEA, Annex 24, Final report v.3, Task 3: Material properties

Levett R (1998) *Sustainability indicators - integrating quality of life and environmental protection,* Journal of the Royal Statistical Society, Series A, v.161, Pt.3, pp.291-302

Lovins AB (1996) Negawatts: *Twelve transitions, eight improvements and one distraction,* Energy Policy, v.24, nr.4, pp.331-343

E. McLaughlin, J. F. T. Pittman (1971) *Determination of the Thermal Conductivity of Toluene-A Proposed Data Standard-from 180 to 400k under Saturation Pressure by the Transient Hot-Wire Method II. New Measurements and a Discussion of Existing Data,* Philosophical Transactions of the Royal Society of London. Series A, Mathematical and Physical Sciences, v. 270, nr.1209 (Dec. 16, 1971), pp. 579-602

Nagasaka Y, Nagashima A (1981) *Absolute measurement of the thermal conductivity of electrically conducting liquids by the transient hot-wire method,* J. Phys. E: Sci. Instrum. v.14, pp.1435-1440

Norminton EJ, Blackwell JH (1964) *Transient heat flow from constant temperature spheroids and the thin circular disk,* Quart. Journ. Mech. And Applied Math., v17, pt.1, pp. 65-72

Opoku A, Tabil LG, Crerar B, Shaw MD (2006) *Thermal conductivity and thermal diffusivity of timothy hay,* Canadian Biosystems Engineering, v.48, pp.3.1-3.7, available online at http://engrwww.usask.ca/oldsite/societies/csae/protectedpapers/c0515.pdf on 29/03/2007

Parsons R ed. (2001) *Fundamentals: 2001 Ashrae Handbook : Si Edition,* American Society of Heating, Refrigerating and Air-Conditioning Engineers, Atlanta

Pollock DD (1991) *Thermocouples: Theory and Properties,* CRC Press

Potienko NF, Tsymarnyi VA (1972) *Application of a nonstationary method for temperature conduction research in liquids,* Measurement techniques, v.15, nr.3, pp.410-413, translated from Izmeritel'naya Tekhnika, nr.3, pp.40-42 March 1972

R Development Core Team (2005). *R: A language and environment for statistical computing.* R Foundation for Statistical Computing, Vienna, Austria. ISBN 3-900051-07-0, available at URL http://www.R-project.org on 7/09/07

Reason L, Olivier D (2006) *Minimising CO2 emissions from new homes,* AECB, accessed at http://www.aecb.net/PDFs/NewHomesCO2Savings25May06.pdf on 5/03/2007

River BH, Vick CB, Gillespie RH (1991) *Wood as an adherend,* Marcel Dekker, Inc. New York

Sachs W, Santarius T, eds. (2007) *Fair future - resource conflicts, security and global justice,* Zed Books and Fernwood Publishing

Sharma RG, Pande RN, Chaudhary DR (1984b) *Estimation of thermal diffusivity in an isotropic homogenous two phase system,* Japanese Journal of Applied Physics, v.23, nr.1, pp.34-39

Spitler JD, Yavuzturk C, Rees SJ (2000) *In situ measurement of ground thermal properties,* Proceedings of Terrastock 2000, v.1, Stuttgart, August 28-September 1, 2000, pp.165-170

Takahashi H, Hiki Y, Kogure Y (1994) *An improved transient hot-wire method for studying thermal transport in condensed matter,* Review of Scientific Instruments, v.65, nr.9, pp.2901-2907

Trevisan OV, Mohanty S, Miller MA (1993) *Transient method for measuring thermal properties of saturated porous media,* International Journal of Heat and Mass Transfer, v. 36, nr. 10, pp. 2565-2573

Unal O, Uygunoglu T, Yildiz A (2005) *Investigation of properties of low-strength lightweight concrete for thermal insulation,* Building and Environment, v.42, nr.2, pp.584-590

Vendrick AJH, Vos JJ (1957) *A method for the measurement of the thermal conductivity of human skin,* Journal of Applied Physiology, v.11, nr.2, pp.211-215

Wagner R, Clauser C (2005) *Evaluating thermal response tests using parameter estimation for thermal conductivity and thermal capacity,* J. Geophys. Eng. v.2 pp.349-356

Wang J, Hayakawa K (1993) *Maximum Slope Method for Evaluating Thermal Conductivity Probe Data,* Journal of Food Science, v.58, nr.6. pp.1340-1345. Cited in Yang W, Sokhansanj S, Tang J, Winter P (2002) *Determination of Thermal Conductivity, Specific Heat and Thermal Diffusivity of Borage Seeds,* Biosystems Engineering, v.82, nr.2, pp.169–176

Wang Z, Zhang Y, Liang X, Ge X (1994) *Long/short hot-probe method for determining thermophysical properties,* Meas. Sci. Technol. v.5, pp.964-968

Weber S (2006) *Comparison of in-situ measured ground heat fluxes within a heteorogeneous urban ballast layer,* Theor. Appl. Climatol. v.83, pp.169–179

Welch SM, Kluitenberg GJ, Bristow KL (1996) *Rapid numerical estimation of soil thermal properties for a broad class of heat-pulse emitter geometries,* Measurement Science and Technology, v.7, pp.932-938. IOP Publishing Ltd.

Westfold KC (1981) *Obituary: JC Jaeger,* Royal Astronomical Society Quaterly Journal, v.22, pp.84-5

Woodside W (1958) *Calculation of the thermal conductivity of porous media,* Canadian Journal of Physics, v.36, nr.7, pp.815-823

Woodside W, Kuzmak JM (1959) *Authors' Reply to De Vries and Philip's Discussion of `Effect of Temperature Distribution on Moisture Flow in Porous Materials',* Journal of Geophysical Research, Vol. 64, p.2035

Xing L, Hongyan L, Shujun W, Lu Z, Hua C (2006) *Preparation and thermal properties of form-stable paraffin phase change material encapsulation,* Solar Energy v.80, pp.1561–1567

Yang W, Sokhansanj S, Tang J, Winter P (2002) *Determination of Thermal Conductivity, Specific Heat and Thermal Diffusivity of Borage Seeds,* Biosystems Engineering, v.82, nr.2, pp.169–176

Zarr RR (1997) *Expanded polystyrene board as a standard reference material for thermal resistance measurement systems,* Insulation materials: testing and applications: 3rd volume, ASTM STP 1320, Graves RS and Zarr RR, eds. American Society for Testing and Materials, 1997

Zhang X, Fujii M (2003) *Measurements of the thermal conductivity and thermal diffusivity of polymers,* Polymer Engineering and Science, November 2003 v43 nr.11 pp.1755-1764

Zhang X, Hendro W, Fujii M, Tomimura T, Imaishi N (2002) *Measurements of the thermal conductivity and thermal diffusivity of polymer melts with the short-hot-wire method,* International Journal of Thermophysics, v.23, nr.4, pp.1077-1090

SIMULATION OF HEAT FLOW FROM A LINE SOURCE IN SUPPORT OF DEVELOPMENT OF A THERMAL PROBE

P. de Wilde, R. Griffiths, B. Pilkington and S. Goodhew

School of Engineering, University of Plymouth
PL4 8AA, United Kingdom

ABSTRACT

The use of a thermal probe allows a range of in-situ conditions to be taken into account that impact upon the properties of building materials (λ, α) as encountered in reality. In this study, the transient thermal simulation of a model representing a line source in an infinite material sample has been used to guide the development of an experimental thermal probe apparatus. Simulation produced a series of datasets that have been used to test the data analysis routines used with the experimental probe. Findings show that by careful application of these routines close agreement (errors of less than 1 percent) with input values can be achieved. This validates the analysis routines and provides a deeper appreciation of the behaviour a theoretical line source model. The model provides valuable insights into the level of error and uncertainty in in-situ measurements.

KEYWORDS

Material properties, thermal probe, transient simulation, experiments

INTRODUCTION

Reliable data concerning the thermal properties of building materials, in particular the thermal conductivity (λ) and thermal diffusivity (α), is needed for the proper simulation of the thermal behavior of buildings, whether in a design stage, refurbishment project, or research context. However, much of the data currently used in building performance simulation is obtained under laboratory conditions, which results in two main problems. Firstly, material properties established using techniques like the guarded hot box method might reflect a dried-out condition, which differs from material properties in actual use. Secondly, actual material properties might be hard to obtain from a handbook due to the multitude of variants of any material, resulting for instance from different manufacturing processes and differences in ingredients.

An alternative to the use of laboratory data is the use of in-situ measurements, allowing the capture of actual thermal properties of materials in buildings in use. One technique for measuring such data on site is the use of a thermal probe apparatus. Thermal probes have been developed and used in other industries, such as geotechnics, food and plastic manufacturing; it is only recently being applied to buildings. The technique is based on the measurement of transient heat flow from a line source. A needle is inserted into the material; a constant power per unit length (Q) is then applied to the needle, with the temperature rise ΔT monitored and plotted against the natural logarithm of elapsed time ln(t). For the resulting graph of the rise in temperature ΔT versus the natural logarithm of the elapsed heating time (t), where the slope of the straight section is S, the intercept I, the thermal conductivity (λ) and thermal diffusivity (α) can then be calculated by equations (1) and (2):

$$\lambda = Q / (4 \pi S) \quad (1)$$

$$\alpha = (r^2/4)*\exp((I/S) + \gamma - 2\lambda/rH) \quad (2)$$

where r is the radius from the line source, and γ is Euler's Constant, and H is the probe to sample conductance. Note that if H is infinite, the term $2\lambda/rH = 0$ and the volumetric heat capacity ρC is given by λ/α.

These formulas are derived from equation (3), which describes the temperatire rise in a medium at a distance r from the line source (Blackwell, 1956)

$$\Delta T = A\,[\ln t + B + (1/t)(C \ln t + D)] \quad (3)$$

With:

$A = Q/4\pi L\lambda$
$B = \ln(4\alpha/r^2) - \lambda + 2\lambda/rH$
$C = (r^2/2\alpha)[1 - \alpha mc_p/\pi r^2 L\lambda]$
$D = (r^2/2\alpha)[\ln(4\alpha/r^2) - \gamma + 1 - B\,\alpha mc_p/\pi r^2 L\lambda]$

in which L is the length of the line source (probe), and m the mass per unit length of the probe. For a futher discussion of the Blackwell equation see Goodhew and Griffiths (2004), building on previous work by Blackwell (1956), Batty *et al* (1984) and Carslaw and Jaeger (1959).

However, the application in practice is not always straightforward. Several research papers report varying levels of success in measuring λ, but little

success in obtaining values for α. While repeatability of results similar conditions (same lab, same type of samples) has been found to be excellent in many cases, application of the thermal probe technology across a broader range of materials with unknown properties remains to be demonstrated. In an attempt to improve the accuracy of the technique two different iterative routines have been developed using the Solver function within Microsoft Excel that allow the simultaneous determination of the three unknowns a, λ and H. The first routine, named Solver 2.3 is a routine that uses only the first two constants A and B from equation 3, whilst the second routine, named Solver 4.3 employs all four constants.

PROBLEM

The thermal probe equipment, shown in figure 1, together with a measurement procedure has been used in field experiments on real buildings (Pilkington *et al*, 2005; Pilkington *et al*, 2007). With this probe a large set of material samples have been studied. From these results, λ-values can mostly be identified with an accuracy of within ± 15%; this level of accuracy is well within the bounds of an ASTM standard for measuring the properties of soils and soft rock (ASTM, 2000), materials that are similar to those used in construction. However, obtaining values for α proves more challenging.

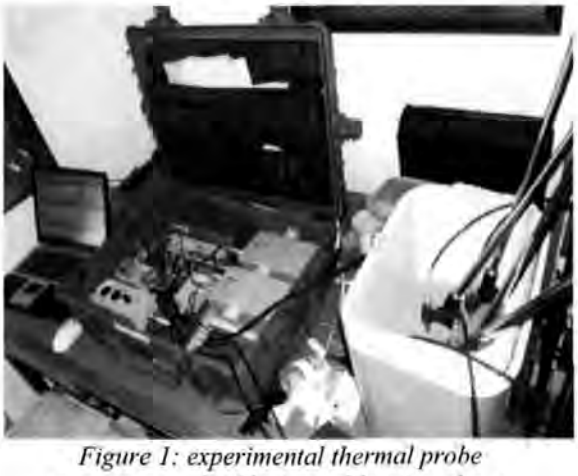

Figure 1: experimental thermal probe measurement kit (during calibration phase, measuring agar immobilised water)

Typical results obtained by using the thermal probe under laboratory conditions are demonstrated in figure 2. Values for the thermal conductivity and thermal diffusivity can be calculated from this data through using equations (1) and (2), by selecting a straight section of the dataline and then finding the slope of and intercept of this straight section. In practice this is realised by using the Solver 2.3 and 4.3 routines.

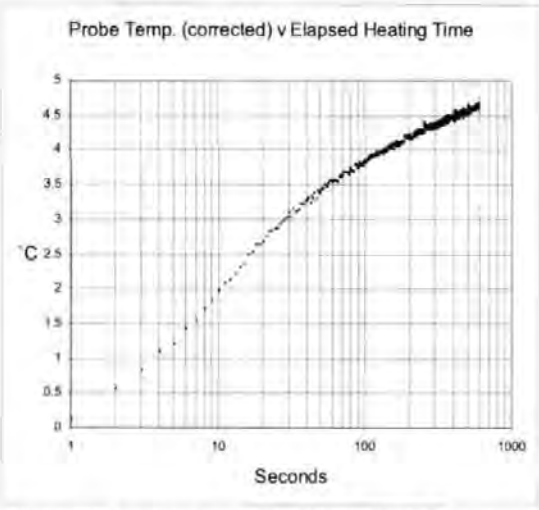

Figure 2: temperature rise ΔT against the natural logarithm of elapsed time ln(t) for a Non Hydraulic Lime sample, measured using the thermal probe under laboratory conditions

However, the measured data can be expected to be influenced by a number of physical factors like the contact resistance between the probe and the needle, heat losses at either end of the probe, heat losses from the material sample, and changeover from heating up to steady state conditions. Findings can also be influenced by the measurement procedure, for instance the amount of heating power provided to the probe or time series used. Furthermore, the data analysis techniques might need further improvement, especially regarding the identification and selection of a suitable section of the slope $\Delta T/\ln(t)$.

The assessment of the impact of each of these factors on the accuracy of measuments undertaken with a thermal probe is essential to guide the ongoing research and development of the measurement kit. Building performance simulation is a useful approach to study the relationship between single, isolated variables and results. This paper addresses the development of a model of a line source as a first step towards modelling of an actual thermal probe in full detail.

OBJECTIVE

In order to guide further development of the measurement kit and data analysis procedures, a thermal simulation model has been employed. Studies with the thermal model provide the opportunity to study the thermal probe from a theoretical point of view, allowing a rigorous testing of the assumptions, mathematics and the data analysis procedures. Results from the model can be used used to gain a better understanding of

empirical datasets and the factors influencing the measurement and analysis outcomes.

Findings will guide further development of the thermal probe technique, which might in principle follow three main different paths:

1. improvement of the data analysis techniques;
2. possible re-engineering of the actual probe itself;
3. work on improving the measurement procedure for using thermal probes in the laboratory and on actual buildings.

Results will thereby direct the future efforts needed concerning the above topics, all of which are currently believed to have an impact on experimental and analytical outcomes.

The overall objective of the use of thermal simulation is to provide numerical reference datasets that can be used to test the data analysis procedure, and to provide a series of (numerical) reference sets that can be compared with experimental results obtained with an actual thermal probe apparatus. Simulation will allow a comparison of the effects of individual factors one by one, studying their impact on results obtained, something which is hard to do in physical experiments. Furthermore the use of simulation allows the research to venture into 'extreme' situations, thereby improving the understanding of the theoretical interaction between λ, α and temperature series. This will take advantage of the fact that a model allows the study values of both the thermal conductivity and the diffusivity without being constrained by existence of actual materials with these properties.

METHODOLOGY

The general strategy followed in this research project for investigating the different factors that influence experimental results starts by modeling the ideal, theoretical situation of an infinitely thin and long line heat source in an infinite homogenous block of material. From this starting point a step-by-step process can then be followed that allows the production of a model that is progressively closer in all aspects to the real-life thermal probe. This will evolve to eventually represent a needle with finite dimensions, and a thermal contact resistance between the heater and the sample.

The work described in this paper is limited to the first stage of an infinitely thin and long line heat source in an almost infinite homogenous block of material. Numerical results thereby represent what might be labeled as data from a 'theoretically very small diameter line heat source', and do not show any effects related to presence of a (modeled) probe. For the study, use has been made of the Physibel program Voltra that allows calculation of transient heat transfer using the energy balance technique (Physibel, 2005).

Within Voltra, a model has been built of very large slice of a material sample (outer dimensions of 2400 x 2400 mm, but with a thickness of only 1 mm). The boundary conditions on both faces of this slice of material have been defined as adiabatic, rendering the material infinite in the direction perpendicular to these faces. The line source is modeled at the middle of this slice, again perpendicular to the faces (positioned at 1200 mm from the boundaries of the sample). Due to the fact that Voltra uses a rectangular grid, gridlines have been put closely together closer to the line source (1 mm apart) in order to approximate the radial distribution of heat, gradually widening the grid further away (reaching 20 mm at the outer edges), see figure 3. For this model, various combinations of thermal conductivity (λ) and thermal diffusivity (α) have been entered, with homogenous properties across the whole sample. The modeling of the thermal probe is limited to the application of power at the heart of the line source, thereby modeling an infinitesimal thin probe without any contact resistance issues.

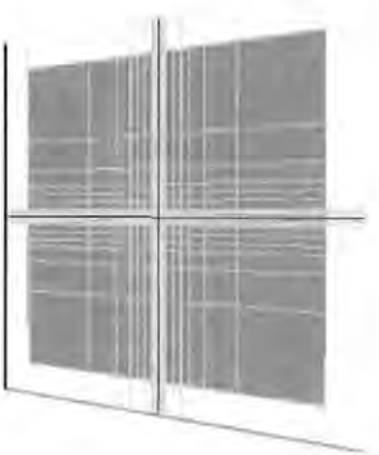

Figure 3: material sample model in Voltra. The line source is simulated at the origin, perpendicular to the (adiabatic) face of the sample

Different combinations of λ and α have been analysed, see table 2. Within the results section of this paper the heating curve, ΔT/ln(t) line and the output data for a material with middle range λ and α properties will be presented first. Then results for a broader range of typical construction materials will be presented. For comparison, material properties for λ, ρ and C have been taken from the ASHRAE Handbook of Fundamentals (2005). Finally, a range of theoretical materials has been studied, varying values of λ and ρC over a wide domain, allowing assessment over the whole range and including very extreme cases, in order to see how these impact on simulation results. The discussion of the results focusses upon the materials with low thermal conductivity, which numerically differs the most from measured data.

Each simulation experiment starts under steady state conditions, where the material sample is at 20.0°C and sits in an environment of the same temperature. After an initial 60 seconds (for acclimatisation) a step function is then used to apply a constant power of 3 W/m to the line source. The temperatures are monitored at distances of 1, 2, 5, 10 and 50 mm away from the line source. Simulation results then have been exported to Microsoft Excel, where the first 60 seconds (steady state situation at 20°C) has been discarded and the temperature rise transformed to data for $\Delta T/\ln(t)$. Regression analysis is then carried out, and the thermal conductivity (λ) and thermal diffusivity (α) calculated according to formulas (1) and (2). The values for α are then translated into volumetric heat capacity (VHC) or ρC values using the resulting λ, as VHC is a more commonly used terminology.

RESULTS

The technique has been applied to a range of materials. Initially, when the probe technique was being developed, the chosen materials were selected for their suitability for calibration purposes, materials such as agar and glycerine. When the technique had been proven within the laboratory, construction materials were then investigated and the following results are those from arguably one of the most ubiquitous.

A typical building material: brick

Typical analysis results are shown in figure 4 and 5, for the building material: brick. Input material properties for the Voltra simulation are based on values from the ASHRAE Handbook of Fundamentals (2005): λ = 0.7 W/mK, ρ = 1970 kg/m^3, and C = 800 J/kgK (giving a VHC of 1.576 MJ/m^{3}K). Figure 4 shows the heating curve resulting from the simulation at 1 mm away form the line source, figure 5 shows the $\Delta T/\ln(t)$ plot.

The data in figure 4 shows an initially steep increase in temperature when power is applied to the line source in the previously described model, then the temperature trailing of towards a steady state condition. Obviously, the actual steady state condition will only be encountered after a long time. Plotting temperature rise in the simulated brick model against $\ln(t)$ produces the almost straight line in figure 5.

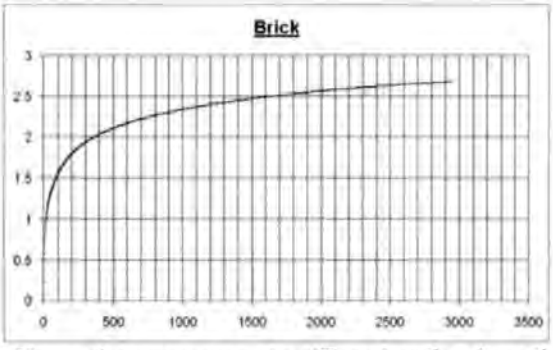

Figure 4: temperature rise ΔT against the elapsed time (t) ('heating curve') for a simulated line source in brick, obtained from Voltra simulations.

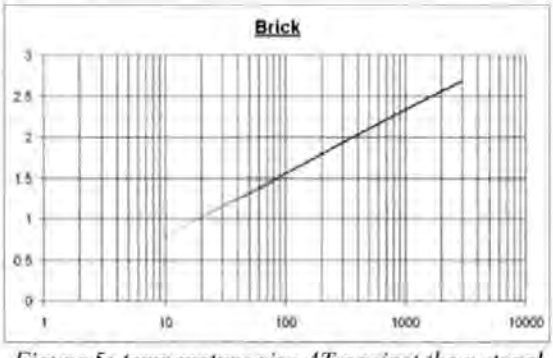

Figure 5: temperature rise ΔT against the natural logarithm of elapsed time ln (t) for a simulated line source in brick, obtained from Voltra simulations

By applying equations (1) and (2) to the data in figure 5, λ and VHC values have been calculated. Comparing the outcomes with the input parameters for the Voltra model shows that the deviaton in the resulting λ is 0%, while the deviation in the resulting ρC is within 5%.

Typical construction materials

Applying the same approach as demonstrated in section 5.1 (figures 4 and 5), further experiments across a wide range of typical construction materials have been carried out; results are presented in table 1. From the $\Delta T/\ln(t)$ plot, λ and ρC have been calculated. Table 1 presents the calculated thermal properties of the materials studied, as well as the deviation of the resulting

values related to input data. Similar results have been obtained beyond the 1 mm distance from the line source. Unsurprisingly, deviations increase with the distance to the line source, as the simulations are based on a rectangular grid with increasing distance between gridlines. These therefore are not shown in the paper.
The temperature series underlying the results in table 1 match expectations, showing that steady state temperature will be reached earlier when ρC is lower, or when λ is higher, and that these steady state temperatures will become lower with an increase in λ or distance to the line source.

Interestingly, the deviation found in calculating λ from simulation results for the materials in table 1 shows an error margin in the order of 0% to 10%, while the error in obtaining ρC from the simulation data is much larger, i.e. the order of 5% to 20%. This effect shows the same trend as experimental datasets, where obtaining values for α has been found to be less accurate than finding values for λ.

Table 1. Resulting deviations in λ and ρC values of a range of building materials after simulation and regression analysis

Material	Input λ [W/mK]	Input ρ [kg/m^3]	Input C [J/kgK]	Deviation on resulting λ [%]	Deviation on resulting ρC [%]
Brick	0.7	1970	800	0.00	4.64
Cellular glass	0.05	136	750	-0.45	6.43
Cellulose	0.057	54	1300	-1.59	12.12
Concrete/stone	0.93	2300	653	-1.27	10.21
Fireclay brick	1.0	1790	829	-1.30	10.53
Limestone	0.93	1650	909	-1.28	10.27
Marble	2.6	2600	880	-0.88	9.20
Portland cement	0.029	1920	670	5.28	-16.46
Sand	0.33	1520	800	4.48	-10.58
Wood (fir)	0.12	540	1210	7.70	-19.24
Wood (oak)	0.176	750	2390	7.41	-19.62

Theoretical materials

In order to get a better understanding of the impact of input parameters on computational outcomes, a set of theoretical materials have been studied, varying the inputs of λ and ρC. The following combinations have been reviewed, see table 2.

Table 2. The combination of the pairings of magnitude of λ and ρC

low λ low ρC	average λ low ρC	high λ low ρC
low λ average ρC	average λ average ρC	high λ average ρC
low λ high ρC	average λ high ρC	high λ high ρC

The input for the Voltra simulations as shown in table 2 has been implemented by λ values of 0.01 (low), 0.6 (average) and 2.0 (high). Values for ρC have been varied by changing C only, with ρ taken to be constant at 1000. Values used for C are 100 (low ρC), 2000 (average ρC) and 6000 (high ρC). Note that 'low', 'average' and 'high' values are related to common materials in building construction. Most of the Voltra studies showed the characteristic behaviour previously exhibited when the rise in probe temperature was plotted against the natural logarithm of the elapsed heating time. Values of the calculated thermal conductivity from the Voltra simulations generally agreed with the values inputted to the model. However, with the low thermal conductivity study, with a value of 0.01W/m^{2}K, for the three associated values of the specific heat capacity, (100, 2000 and 6000J/kgK) and with the adopted heating input of 3W/m, the rises in temperature at 1mm from the heater were large compared with the laboratory studies. The Voltra model showed typical temperature rises of 40°C to 100°C in 200s, whereas in the laboratory or field studies 6 °C to 9 °C would be expected. To analyse the low thermal conductivity data from the model studies provided an interesting vehicle for exploring the analysis routine of Goodhew and Griffiths (2004).

There are practical reasons for restricting the data analysis to 300 to 400s when analysing data from the laboratory and field. For example, when the increase

in the probe rise in temperature becomes too small for practical power inputs, there is considerable data scatter and axial heat losses mar the results. However, the Voltra studies consider the heat flow in an infinite medium with no material probe and therefore the results provide an opportunity to view the thermal probe technique from a simple theoretical stance, or to test the model, the assumptions, the mathematics or theory and the data analysis strategies. As there is no probe in the Voltra simulation the probe to sample conductance, H is infinitely large and the thermal capacity of the probe must be zero. Here is an opportunity to test the analysis routine employing equations 1 and 2 with regression analysis to determine both the thermal conductivity and the diffusivity.

When analysing probe data for each and every power level per m, probe and sample combination the question arises, "What is a long time, or when can the Blackwell (1954) two constant expression be safely applied to the collected data?". Or, in other words, what time must elapse before equations 1 and 2 describe the experimental data? Goodhew and Griffiths (2004) provided a possible solution by suggesting that the percentage error (E%) 2 or 4 constants value of 1% be used as a criterion for selecting the regression analysis time window. A Solver routine employing the Blackwell four constants expression is used to determine approximate values of sample conductivity and diffusivity, mainly as a guide, but more importantly to determine the elapsed heating time required to allow the assumption of long time; that is the time that must elapse so that the error between the Blackwell two constants and the Blackwell four constants is less than 1%.

The chosen set of data for this discussion was the Voltra study with thermal conductivity 0.01W/m^{2}K, thermal capacity 100J/kgK, and density 1000kg/m^3, giving a diffusivity of 10^{-7} m^2/s. The heater power was 3W/m, with the temperature rise in the medium measured at 1mm from the line source. A graph of the rise in temperature versus the natural logarithm of the elapsed heating time is shown in figure 6. Visual inspection of the curve in figure 6 confirms that there is the characteristic "s" shape before the asymptotic approach to the final straight line beyond natural logarithm time of 5.2, or beyond a time of about 180s. The temptation is to apply the regression analysis to this data from 30 to 1500s, or natural logarithm 3 to 7. Here, the resulting conductivity is 0.0103W/m^{2}K and diffusivity 1.12x10^{-7}m^2/s. The conductivity is 3% above the true or input value, while the diffusivity is 12% above the input value. These errors are of similar magnitude to those often found in the experimental laboratory and field work.

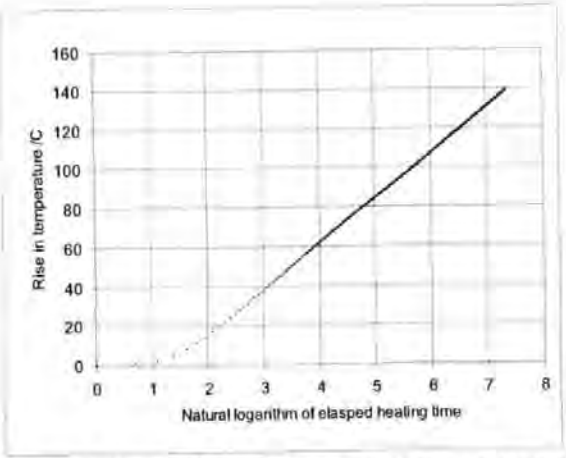

Figure6. Graph of rise in temperature versus natural logarithm of elapsed heating time for Voltra simulation. Temperature measured at 1mm from line heat source.

As described within the introduction, an analysis recipe proposed by Goodhew and Griffiths (2004) was used to simultaneously determine the three unknowns α, λ and H. A Solver 4.3 routine was applied to this data over the time interval 1300 to 1500s. Solver 4.3 is a Blackwell 4 constant expression with 2 variables, the sample thermal conductivity and diffusivity. The probe conductance was set to a large number (inferring very good thermal contact between the heat source and the medium to be measured) and the probe capacity is set to zero. Figure 7 shows the main graph from the Solver sheet. Here the Solver line describes the data only at times greater than 400 to 500s. The Solver 4.3 routine gave low values of conductivity and diffusivity, but the interesting feature here is that the time that must elapse before the error between the 2 and 4 constant expressions falls to below 1% is 750s, as can be seen in figure 8. Therefore, the conclusion to be drawn is that the equations 1 and 2 cannot be applied to this data set until the heating time exceeds 800s.

Applying the regression analysis to the Voltra data over the time interval 850 to 1500s, results in a thermal conductivity of 0.01002W/m^{2}K (+0.2%), and diffusivity 0.973x10-7m^2/s (-2.7%). These errors are calculated in terms of the known true values for conductivity and diffusivity that were initially inputted into the Voltra package. With the Solver 2.3 routine and the data set in the time window 850 to 1500s, the resulting conductivity is 0.01002W/m^{2}K, (+0.2%), diffusivity 0.975x10-7m2/s (-2.5%), again errors in terms of true values.

Finally, moving the Solver 2.3 time window to longer times, namely 1300 to 1500s, the resulting conductivity is 0.01008W/m^{2}K, (+0.8%), diffusivity 1.01x10-7m2/s (1%), again errors in terms of true value. When the regression analysis was applied to

the data set in the time window 1300 to 1500s, the resulting conductivity was found to be 0.01007W/m^{2}K, (+0.7%), and diffusivity 1.006x10-7m^2/s (0.6%). This represents close agreement between model, theory and the Voltra simulation.

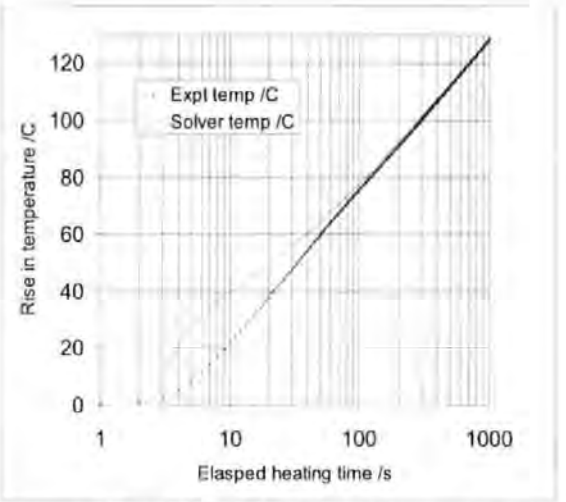

Figure 7. The Solver 4.3 predicted temperature rise plotted with the Voltra simulation results, here denoted as "Expt temp /C", both as functions of the elapsed heating time in seconds.

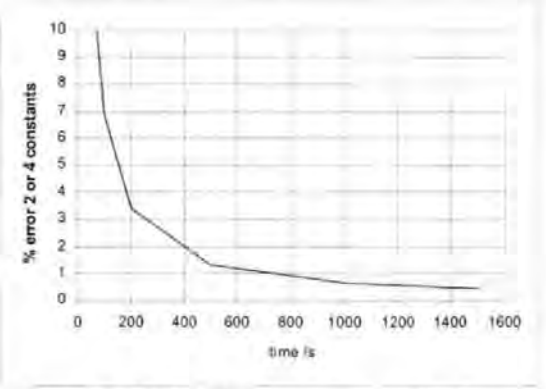

Figure 8. The E% 2 or 4 constants plotted as a function of time for the Voltra simulation. A 1% error or less is only obtainable after a heating time of 750s.

CONCLUSIONS AND REMARKS

This paper describes the use of simulation to guide the development of a thermal probe apparatus. The following conclusions have been drawn from the results:

1. Using the transient heat transfer program Voltra, a line source in an (almost) infinite material sample has been modeled. The simulation model has been used to generate datasets which have been analysed for λ and α by means of the same formula that are currently being used to analyse experimental data from an actual thermal probe apparatus.
2. The Voltra model, the assumptions and the theory provided by Blackwell (1954) appear to be satisfactorily describing the practical arrangement
3. The importance of selecting the appropriate power for the experimental work is underlined, since long times also require measurable temperature rises, i.e. temperature rises that are clearly above the experimental scatter.
4. Applying the regression analysis to data sets at inappropriate time windows, that is short times, often leads to values for the thermal constants that appear of suitable magnitude, but closer and more careful examination of the data can lead to more accurate values for these thermal constants.
5. The Solver 4.3 routine provides the answer to the question of what is a long time, by allowing the error between the Blackwell 2 and 4 constant expressions to be explored.
6. The Solver 2.3 routine applied to the correct time window leads to accurate values of both conductivity and diffusivity.
7. The Voltra study has allowed a demonstration of the probe technique and supports the analysis routine proposed, Goodhew and Griffiths (2004); albeit when applied to a simplified model.

FUTURE WORK

In general, simulation results help to gain a deeper appreciation of the behaviour of results from a theoretical line source model. This may be required to understand and address the level of error and uncertainty caused by the conditions imposed by the constraints of any practical apparatus.

Further work will be carried out to advance the understanding of the behaviour of an actual thermal probe apparatus. This will involve modeling of a probe with finite dimensions and its own material properties, moving towards both a probe and material sample with given dimensions, incorporation of the thermal resistance between probe and sample, and inclusion of boundary effects for both probe and sample.

ACKNOWLEDGEMENTS

The authors wish to thank the Carbon Trust, who funded part of the research reported in this paper.

REFERENCES

ASHRAE. 2005. *ASHRAE Handbook of Fundamentals, SI Edition.* Atlanta: American Society of Heating, Refrigerating, and Air-Conditioning Engineers.

ASTM. 2000. *Standard test method for determination of thermal conductivity of soil and soft rock by thermal needle probe procedure.* ASTM International Committee D18, designation D 5334-00

Batty ,W., S. Probert, M. Ball, P. O'Callaghan, 1984. Use of the thermal probe technique for the measurement of the apparent thermal conductivities of moist materials. *Applied Energy,* v18, 301-317

Blackwell J., 1954. A transient-flow method for determining the thermal constants of insulating materials in bulk. *Journal of Applied Physics* 25(2), 134-144.

Blackwell, J., 1956. The axial-flow error in the thermal-conductivity probe. *Canadian Journal of Physics*, 34 (4), 412-417

Carslaw H., J. Jaeger, 1959. *Conduction of heat in solids.* Oxford: Oxford University Press, 2nd edition.

Goodhew, S. and R. Griffiths 2004. Analysis of thermal-probe measurements using an iterative method to give sample conductivity and diffusivity data. *Applied Energy,* v 77, 205-223.

PHYSIBEL. 2005. *Voltra and Sectra Manual, version 5.0w.* Maldegem: Physibel Software.

Pilkington, B., P. de Wilde, P., S. Goodhew, R. Griffiths, 2006. Development of a Probe for Measuring In-situ the Thermal Properties of Building Materials. *Proceedings of PLEA'06, 23rd International Conference,* Geneva, Switzerland, September 6-8 2006, 665-670

Pilkington, B., R. Griffiths, S. Goodhew, P. de Wilde, 2007. Thermal probe technology for buildings: the transition from laboratory to field measurements. Article submitted for the ASCE Journal of Architectural Engineering

Development of a Probe for Measuring In-situ the Thermal Properties of Building Materials

Brian Pilkington, Pieter de Wilde, Steve Goodhew and Richard Griffiths

School of Engineering, University of Plymouth, Plymouth, United Kingdom

ABSTRACT: Environmentally benign materials, such as cob, rammed earth, straw and hemp are increasingly being used in construction, often in efforts to develop sustainable buildings. While this is advantageous from the point of view of embodied energy and use of local resources, it does cause concerns in the thermal engineering of buildings constructed from such materials. The thermal properties are often unknown, dependent on their in-situ production process, moisture content and local resources used. They may be of a composition that has not been entered into material properties' handbooks or (in vernacular buildings) information on their composition may have been lost over time or be anecdotal.

A variety of technical equipment is available to identify the thermal properties of materials, the more common being the guarded hot plate apparatus. Most measurements undertaken with these techniques are carried out in laboratory conditions, often requiring long times to achieve valid results. This paper reports on the development of an improved thermal probe measurement technique to enable fast assessment of the thermal properties of building materials and reports on a range of in-situ material properties measurements.

Keywords: thermal conductivity, thermal diffusivity, in-situ measurement, thermal probe

1. INTRODUCTION

The need for a fast, economical and relatively non-destructive method to establish the thermal properties of building materials, whether in-situ, site based or laboratory samples, arises as carbon emissions from fossil fuelled energy, used to heat or cool homes, escalate, and as building designers increasingly seek materials with reduced environmental impact in their manufacture. These materials often have unknown thermal properties, properties which dictate the ongoing energy requirement of buildings employing them. The same problem occurs when upgrading older housing, usually the greater consumers of fossil fuelled energy, as no records of their material thermal properties are likely to exist.

An ongoing project at the University of Plymouth, currently in collaboration with the Carbon Trust (an independent, UK Government funded company formed to promote a low carbon economy), is seeking to develop a thermal probe to measure the thermal conductivity (λ) and thermal diffusivity (α) of building materials with a view to facilitating thermal behaviour models of proposed and existing buildings. Values for λ will enable designers to show whether new materials reach required standards of insulation to exceed current regulatory requirements, under UK Building Regulations and the European Energy Performance of Buildings Directive. Values for α will equip designers to employ zero or low carbon heating or cooling strategies through quantifying and predicting the level of capture, storage and release of passive solar or internal heat gains. Likewise, in existing buildings, establishing the current levels of material thermal properties will provide a base value on which to develop designs or strategies aimed at improving thermal performance in relation to environmental impacts.

The thermal properties of construction materials are currently measured predominantly by the guarded hot plate (GHP) method [1]. Here, a substantial sample of the material is held between, and in good contact with, a heated and a cooled plate and the heat flow across the sample, once this has moved to a steady state, is measured. Some material properties can alter during the time taken to achieve steady state [2]. Earth based materials, and common concrete products, will invariably have a moisture content when in use as part of an external wall, which moisture content alters the thermal properties of the material. The steady state of heat transfer can not be reached while moisture is in the process of evaporation or migration, brought about by the action of the GHP. The thermal probe employs a transient measurement, which has a minimal effect on moisture content and so should give a more realistic representation of actual thermal properties of placed materials. The single, small hole required to take the measurement permits the method to be considered virtually non-destructive, removing the need to take large samples from existing buildings and potentially avoiding the reluctance of home owners to have tests carried out. The probe methodology is suitable for in-situ or sample measurements, where samples are

large enough to avoid heat from the probe reaching the boundary during a measurement.

Various materials, from cob walls at the Eden Project in Cornwall to unfired earth bricks in a Scottish eco-house, have been measured during the project. This paper reports on current progress and gives some provisional values for materials that have been measured in the laboratory and in-situ.

2. OBJECTIVE

The early objectives of this research project were to review the existing literature on thermal probe studies, especially in regard to practical measurement of building materials in the field and review current understanding of relevant heat transfer mechanisms. Many years of previous work on thermal probe studies has been carried out at Plymouth by Goodhew and Griffiths [3] [4] who developed laboratory apparatus and analysis routines to give λ and α values under controlled environmental conditions for many reference and construction materials, with reasonable levels of confidence and repeatability. This provided a platform from which to work. The next stage was to take the thermal probe procedure from the laboratory to practical application in the field. This required the further development of apparatus, calibration and computer analysis methods. The implications of taking measurements in 'as built' structures, at varying temperatures and with varying moisture contents, was to be investigated. New results for a range of standard and sustainable materials, including concrete block, various stones, brick, earth structures such as cob and rammed earth, straw bale and timber, all subject to varying environmental conditions, were anticipated, along with a 'handbook' methodology to make the process accessible to others.

3. THE PROJECT

The measurement of λ and α of building material samples and building materials in-situ using a thermal probe employs transient line heat source theory, which is based on the perfect model of an infinitely thin, infinitely long heating element in an infinite, homogenous sample. In the perfect model, the change in temperature created by a constant power input to the heating element charted against the natural logarithm of elapsed time would give a straight line from which λ and α could be calculated, as its gradient is dependent on the level and nature of the radial heat flow from the element into the surrounding material. In practice, the heating element, and probe needle, have limited dimensions, with thermal resistance, or conductance (H), between the probe needle components and the sample. The sample is not infinite and the level of homogeneity of most building materials is questionable, leading to a term sometimes used in this connection, 'apparent thermal conductivity' (ATC). While, in this case, it is not the true thermal conductivity of a pure material, ATC is a closer guide to the physical nature of a building material and the heat transfer mechanisms through it, including convection and radiant heat flows through voids and anisotropic conditions, that form the basis of calculations to assess real potential heat loss.

Fig. 1 shows an example of the probes used in this study with an example of a non homogenous building material, an unfired earth brick containing wood shavings, manufactured by the Errol Brick company in Scotland. Fig. 2 shows a typical heating curve, here of a cured block of lime and hemp, expressed as the change in temperature over elapsed time, plotted on logarithmic graph paper in MS Excel. The curve has a similar profile to that of change in temperature over the natural logarithm of elapsed time, $\Delta T/\ln(t)$. It can be seen that the line is not straight and, as the thermal properties are derived from the slope and intercept of the theoretical straight line, either assumptions have to be made concerning the behaviour of the heating pattern, or analysis of the temperature rise pattern influences has to be undertaken. An alternative method, which has been followed in the past, is to analyse the visible straight section of the line and compare results with those published. While this makes the probe viable for one material, the method does not necessarily transfer to other materials as those influences not yet quantified happen in varying proportions at different times for different types of material.

Figure 1: Hukseflux TP08 thermal probe and Errol unfired earth and wood shaving brick

A literature review and collaboration with mathematicians and physicists are employed in attempts to quantify the various influences acting on and around the probe during a heating cycle. These influences include the specific heat capacity and internal thermal resistances of the probe itself, the thermal resistance that always exists to varying degrees between the probe and the sample material, heat losses from the probe, apart from those radial losses to the sample which we are interested in measuring, and heat losses from the sample to other materials, including surrounding air. The first three influences have been assumed by many previous researchers to create the curve distortion at early times while the last two influences are assumed to

effect the curve at later times. What constitutes early and late times is dependent on λ and α, creating a circular problem typical of this type of study. This creates uncertainty about results from thermal probe systems that are becoming commercially available in the food and agriculture industries should they use a measurement over the same time period for all materials. Fig. 3 illustrates a typical heating curve for an insulating material having different characteristics to those of the lime and hemp block in Fig. 2.

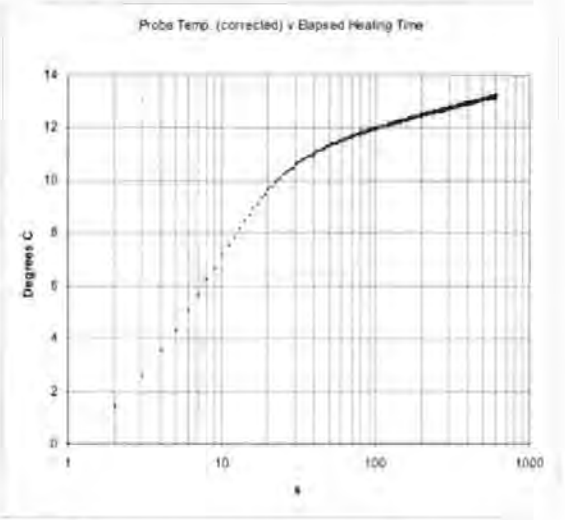

Figure 2: Heating curve at 3.24 W/m, change in temperature over elapsed time expressed logarithmically, for lime hemp block

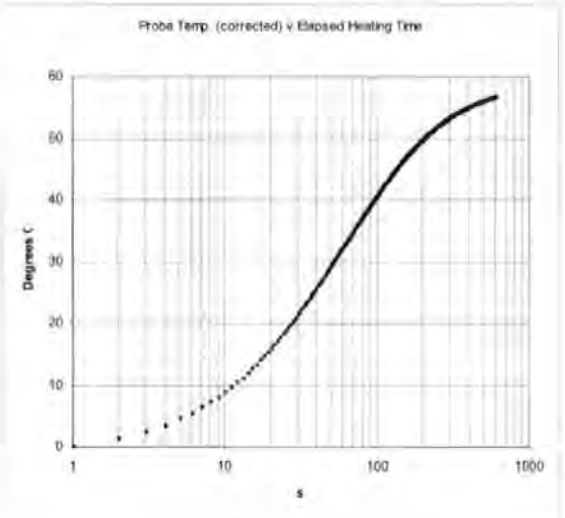

Figure 3: Heating curve at 3.24 W/m, change in temperature over elapsed time expressed logarithmically, for phenolic foam insulation

It is proposed to utilise computer modelling in order to asses these current uncertainties. Work is underway in this direction, whereby the heat transfer properties of every part of the heating process can be modelled, using known heat transfer mechanisms, in hopes that this will clarify the interaction of the various influences acting on and during the heating cycle.

Running concurrently with these explorations of theoretical physics, an experimental procedure has been developed whereby measurements are taken in the laboratory using materials of known thermal properties, the results then being compared with published results. This is complemented by measurements taken in the field, on real buildings, of similar materials, to ascertain whether results here can be given to a similar level of confidence.

This experimental procedure has led to the development, with the assistance of experienced University technicians, of a portable apparatus, rugged enough to withstand the rigours of transport and onsite activity. Early laboratory experiments and previous versions of the apparatus have informed this development.

The process of taking a measurement involves drilling a hole near to the 1.2mm diameter of the probe and just long enough, presently 72mm, to accept the length of the probe. This is currently proving impractical with hard materials such as stone or concrete and larger holes have been resorted to here. Blackwell [5] calculated the length to diameter ratio required in a thermal probe to enable confidence in the results and his calculations are generally accepted, with 20:1 being the minimum needed to achieve less than 1% inaccuracy from heat losses at the probe's ends. This imposes constraints on the probe whereby it must be strong enough to use in robust site conditions, be long enough to meet the Blackwell requirement and yet not be so long that it exceeds or comes too close to the dimensions of common building materials, often 100mm thick.

With limitations on available technology to form fine holes in many construction materials, various mediums have been trialled, with a twofold action, to compensate for larger holes, as a filler and as a contact medium, and their effect modelled experimentally. With softer mediums, such as most earth materials, a 1.5mm high speed steel drill is adequate. With light materials, such as phenolic foam insulants or spun mineral wool, the probe can simply be pushed in. Varying levels of contact filler of different types are the subject of ongoing experimental assessment.

Once the probe is inserted into the material, it is left for a time to reach thermal equilibrium and then heated at a known current, the potential difference across a series resistor is measured. The temperature rise and current are recorded at regular intervals, usually at 1 Hz. The probes are held in-situ with microphone stands when carrying out measurements onsite (see fig. 4). The data is subsequently downloaded, or it can be streamed, to a laptop computer and analysed using spreadsheets developed in MS Excel, using MS Excel macros to manipulate data, which is kept to a strictly patterned format.

Each result is stored electronically with an individual reference and kept in a directory tree. Detailed descriptions are recorded for each experimental run. Any individual result or description can be accessed from a central document containing a database of indexed hyperlinks, searchable by date, material or location. This allows any particular raw data set to be easily revisited as the analysis methodology is developed and the fixed storage pattern allows new macros to be developed as required.

Figure 4: Probes in-situ at a cob building at the Eden Project, Cornwall, here with reflective sheet under trial as a shading device

Building owners have generally been quite happy to have small holes drilled in their properties as a contribution towards sustainability related research with only some slight concerns about internal finishes in a newly decorated demonstration house. The 'field kit' can be easily transported by car (see fig. 5) and set up ready for a measurement in around half an hour

Figure 5: The 'field kit' stacked for transportation

3. PREVIOUS RESEARCH IN THE FIELD

The earliest reference found to transient line source theory, the basis of the thermal probe, is an 1888 study by Schleiermacher [6] of the thermal conductivity of gases by the hot wire method. Gases may be easier to measure as the contact resistance, H, is very much reduced and may be assumed as zero. In 1931, Stalhane and Pyk [7] developed a cased probe with a mercury thermometer. Seminal work was carried out by Hooper and Lepper [8], Blackwell [9], Vos [10] and Carslaw and Jaeger [11]. The limited resources available at those times, mercury thermometers, stopwatches and printed tables of logarithms rather than more sophisticated thermocouples, platinum resistance thermometers, dataloggers and computer analysis technology, limited their ability to compare multiple data sets. Each data analysis routine currently uses over 8,000 data points, many of them logarithmic and others individually calculated using fairly complex, data dependent equations.

The works of these, and many subsequent, researchers have led to the use of thermal probes and hot wire techniques in other industries, such as: refractory bricks [12] and plastics [13], where hot wires may be cast in samples during manufacture; the food industry, where fine probes can be inserted by simple pushing into samples, such as fruit, with reasonable thermal contact; and soil mechanics where probe length is not the limitation it is in building components. Various standards have been developed and are under constant review for these uses of the technique [14].

Other researchers have followed the path of a twin probe. While this facilitates the mathematical procedures of the analysis routine, it presents problems with construction materials as there is a difficulty in forming adequately parallel holes in construction materials and achieving sufficient thermal contact in each, and this technique may be more destructive than the single probe.

Despite the numerous researchers that have worked and are working in this field, one of the principal coordinators of the research, the Contact Transient Methods group of the European Conference on Thermophysical Properties currently states that claimed precision levels are not substantiated [15]. There is still much work to do to tie down the method and apply it reliably, in particular to construction materials with the range of types, thicknesses and locations.

4. PROGRESS AT THE UNIVERSITY OF PLYMOUTH, SCHOOL OF ENGINEERING

Building on the previous work of Goodhew and Griffiths, MS Excel analysis routines have been further developed, a 'field kit' has been created and over 600 measurement data sets have been produced, analysed and compared. Table 1 shows a sample of the results achieved so far, which should be considered merely indicative at this time. Each result is a mean average of a number of measurements taken in the same position. The

repeatability of these results, measured as the standard deviation divided by the mean value, is very good in laboratory work, as most other researchers have found, and the results from onsite measurements under various mild to extreme environmental conditions are generally within acceptable limits. While repeatability is not itself an indication of accuracy, it shows that field data may be sufficiently acceptable, once the analysis is resolved, to give reliable values for λ and α.

The present level of repeatability is sufficient to allow consideration of comparative values for similar materials with varying levels of moisture content and work has been carried out over time in this regard measuring timbers and aerated concrete products at varying moisture content with interesting results.

Material	Mean λ W/mK
Chestnut along the grain	0.192
Cob block internal	0.467
Cob block external	0.556
Agar immobilised water	0.613
Cob internal wall base	0.812
Cob external wall head	0.861
Cob internal wall head	0.935
Cob external wall base	1.139

Table 1: Indicative thermal conductivity results for a selection of studied materials

Table 1 is a small sample of results achieved. The spread of λ values for cob here, and in the rest of the data, shows that generic values for such materials are an unreliable method to employ for heat loss calculations. The same is likely to be true of α values. The use of earth or other materials, without known thermal properties, as storage mediums for captured heat gains, solar and internal, to prevent overheating or to provide passive solar heating, would be advantaged by better understanding of this property, α having a direct relationship with the volumetric heat capacity (VHC) of materials and, once the density is known, the specific heat capacity (SHC). A benefit of the methodology, if the analysis issues surrounding the calculation of α can be resolved, is that only the VHC is needed to thermally model a building design, and this is potentially available for any sample, and for existing buildings without the destructive measures of taking samples to measure by other methods, such as water immersion or calorimeter.

The 'field kit' has been developed with four commercially available Hukseflux TP08 thermal probes connected to a dt800 datalogger, with independent rechargeable battery power to the heating elements and datalogger, controlled current switching, a resistor of known resistance enabling constant current monitoring and a laptop computer (see fig. 6).

Figure 6: The 'field kit' in its robust case, here measuring agar immobilised water during calibration exercises

Work continues building up a resource of measurement data for many material types while further investigating the physical theories involved. The H problem, how to quantify the contact resistance between the probe and sample when, in practice, hole sizes and contact levels will vary, has to be overcome. Drilling small holes, 1.5mm x 72mm, in hard materials without unduly effecting moisture content has not yet been possible despite contact with many drill bit manufacturers and alternative methods are being sought. Data scatter from thermocouple and platinum resistance thermometers has been found to have little effect on the results but work is ongoing with polynomial regression analysis being carried out to smooth small irregularities in the data before linear regression analysis routines are used to calculate thermal conductivity values.

5. CONCLUSIONS AND DISCUSSION

The thermal properties of so called sustainable, and common, materials need to be known when designing for low energy building, passive solar heating or passive cooling if using the physics of the building structure for these purposes. Locally produced sustainable building materials, earth, straw, lime, glass, wool, hemp and many others vary from site to site for many reasons, such as mixture proportions and soil properties. The costs and time taken to measure their thermal properties by GHP, calorimeter or water immersion may be prohibitive, preventing their uptake on regulatory or design confidence grounds. The thermal probe has potential to overcome these restrictions.

The thermal properties of existing building structures need to be known when modelling improvements in their thermal performance. The probe here has the potential to measure these in many cases, without significant damage, an important consideration in occupied or historic properties.

There are limitations to the method, practical and, currently, theoretical. It is not probable that data can be achieved to calculate heat transfer across a layered construction, such as an insulated cavity wall. Each leaf of the wall can be assessed but the filling is unlikely to be reached. Plastered walls create a difficulty as it may not be known whether the probe is penetrating the desired component or the jointing compound or the edge of each, and care has to be taken to avoid hidden services.

The thermal properties of non homogenous materials may vary greatly from place to place within the same structure, leading to the requirement for multiple measurements.

Further work is needed on the quantification of H and its effect, especially on thermal diffusivity values, where it exerts an exponential influence. Previous assumptions regarding straight line sections of the curve $\Delta T/\ln(t)$ need to be challenged as the typical S curve achieved varies its properties as thermal values change, making reliable measurement of insulating materials currently unattainable and putting all measurements in doubt.

It is hoped that the computer modelling now embarked upon at the University of Plymouth, along with multiple measurements of a wide spectrum of materials and collaboration with other bodies will help resolve these issues.

ACKNOWLEDGEMENTS

The authors wish to thank the Carbon Trust for their support of this project, Brian Anderson of the Building Research Establishment (BRE) for his help in assessing results and Keith Stott for his technical expertise.

They would also like to thank the many building owners that have allowed measurements to be carried out at their properties.

REFERENCES

[1] BSi (1999) *Building materials and products - Procedures for determining declared and design thermal values*, BS EN ISO 10456:2000

[2] Doran S (2000) *DETR Framework Project Report: Field investigations of the thermal performance of construction elements as built*, Building Research Establishment Client Report No. 78132. BRE East Kilbride. Scotland

[3] Goodhew SM, Griffiths R (2003) *Analysis of thermal probe measurements using an iterative method to give sample conductivity and diffusivity data*, Applied Energy v77 pp205-22. Elsevier

[4] Goodhew SM, Griffiths R (2004) *Sustainable walls to meet the building regulations*, Energy and Buildings 37 451-459, Elsevier

[5] Blackwell JH (1956) *The axial-flow error in the thermal-conductivity probe*, Canadian Journal of Physics v34 n4 pp412-417

[6] Schleiermacher A (1888) *On the thermal conduction of gas*, Wiedeman Ann. Phys. V34 pp. 623-646

[7] Stalhane B and Pyk S (1931) *New method for determination of thermal coefficients*, Teknisk Tidskrift. 51. 389-96

[8] Hooper FC, Lepper FR (1950) *Transient heat flow apparatus for the determination of thermal conductivities*, Transactions American Society of Heating and Ventilation Engineers v56 pp309-324

[9] Blackwell JH (1954) *A transient-flow method for determination of thermal constants of insulating materials in bulk*. Part 1-Theory, Journal of Applied Physics v25 n2 pp137-144

[10] Vos BH (1955) *Measurements of thermal conductivity by a non-steady-state method*, Appl. Sci. Res. Section A v5 pp425-438

[11] Carslaw HS, Jaeger JC (1959) *Conduction of heat in solids*, Oxford University Press, Oxford. 2nd edtn.

[12] ASTM C1113-99 (2004) *Standard test method for thermal conductivity of refractories by hot wire (platinum resistance thermometer technique)*. American Society for Testing and Materials

[13] ASTM D 5930-01 (2005) *Standard test method for thermal conductivity of plastics by means of a transient line-source technique*, American Society for Testing and Materials

[14] ASTM D 5334-00 (2000) *Standard test method for determination of thermal conductivity of soil and soft rock by thermal needle probe procedure*, American Society for Testing and Materials

[15] National Physics Laboratory (NPL) (2006) *Standards for Contact Transient-Measurements of Thermal Properties*, accessed at: http://www.npl.co.uk/thermal/ctm/london_notes.html on 28/03/2006

OOF COPY [AE/2007/022186] 001804QAE

Thermal Probe Technology for Buildings: Transition from Laboratory to Field Measurements

Brian Pilkington[1]; Richard Griffiths[2]; Steve Goodhew[3]; and Pieter de Wilde[4]

Abstract: This paper reports the results of an investigation into the transfer of thermal probe measurement technology from laboratory use to actual buildings in order to undertake the in situ determination of thermal material properties. The imperative reasons for using in situ measurements are (1) the impact of moisture content on thermal properties; (2) the possible wide range of variation of properties across most materials used in construction; and (3) the lack of data for new and innovative materials. Thermal probe technology offers the prospect of taking building specific data, addressing these issues. Based on commercially available thermal probes a portable measurement kit and accompanying measurement procedure have been developed. Three case study buildings, each having different materials, have been studied to ascertain whether or not the technique can be transferred to relatively uncontrolled environments and remain capable of achieving a precision that is similar to an ASTM standard that can be related to thermal conductivity measurements of building materials. The results show that this is indeed the case, and that the use of thermal probe technology may yield thermal properties that vary significantly from the laboratory values currently used in building thermal engineering calculations.

DOI: XXXX

CE Database subject headings: Construction materials; Thermal factors; Energy consumption; Soil structures; Measurement; Buildings.

Rationale for In Situ Thermal Measurements

Energy use in buildings has a significant effect on the global environment with some 15% of U.K. greenhouse gas emissions attributable solely to the heating of domestic properties (DTI 2002). Reduced energy consumption in buildings, whether existing or proposed, requires reliable data on the thermal properties of building materials. The data are now invariably obtained from measurements carried out on samples under laboratory conditions and not from in situ measurements, which gives rise to the following three problems in practice:

1. The moisture content of the representative material sample used in laboratory studies can have a significant effect on its effective thermal conductivity (Salmon et al. 2002) and may be different from that of the actual material in the building on site and under actual use conditions.
2. The steady state techniques, such as guarded hot plate or two box methods, commonly used in laboratory measurements, require long times to achieve thermal equilibrium. As shown by Doran (2000), during this time, moisture present within typically hygroscopic building materials migrates and evaporates, resulting in altered thermal properties.
3. A material sample used in the laboratory may not share all qualities of the bulk material on site through varied manufacturing processes and/or differences in raw materials. As an example, a standard reference work Touloukian et al. (1970) gives 338 thermal conductivity values for the building material concrete.

Using a thermal probe offers an alternative transient method to laboratory-based thermal measurement techniques that has good prospects for measuring the thermal conductivity and, potentially, the thermal diffusivity of building materials on site. This technique has already been used successfully in other industries, such as geotechnics (ASTM International 2000), food (Xie and Cheng 2001), plastics (ASTM International 2005; Underwood and McTaggart 1960; Zhang and Fujii 2003), and refractory brick manufacture (ASTM International 2004; Davis 1984); it has been successfully applied to building materials under laboratory conditions by Goodhew and Griffiths (2004). However, when this method is to be used in situ to undertake measurements on actual buildings the technique will be subject to a relatively uncontrolled environment with fluctuations, for example, changes in air temperature, wind speed, and solar irradiation.

The prime goal of the research described in this paper is to investigate the transferability of the thermal probe technique from the laboratory to in situ measurements upon materials in real buildings. As criterion for the success of the transfer, the accuracy obtained in situ will be compared to a $\pm 15\%$ precision that can be obtained by adhering to an ASTM standard for measuring the properties for soils and soft rock (ASTM International 2000). This existing standard has been selected as it applies to materials that are in some ways similar to commonly used construction materials like brick and concrete.

[1]Researcher, School of Engineering, Univ. of Plymouth, Devon, PL4 8AA, U.K. E-mail: bpilkington@plymouth.ac.uk

[2]Research Fellow, School of Engineering, Univ. of Plymouth, Devon, PL4 8AA, U.K. E-mail: rgriffiths@plymouth.ac.uk

[3]Professor of Sustainable Technology, School of Engineering, Nottingham Trent Univ., Burton St., Nottingham, NG1 4BU, U.K. (corresponding author). E-mail: stevegoodhew@ntu.ac.uk

[4]Lecturer, School of Engineering, Univ. of Plymouth, Devon, PL4 8AA, U.K. E-mail: pdewilde@plymouth.ac.uk

Note. Discussion open until May 1, 2009. Separate discussions must be submitted for individual papers. The manuscript for this paper was submitted for review and possible publication on July 27, 2007; approved on December 20, 2007. This paper is part of the ***Journal of Architectural Engineering***. Vol. 14, No. 4, December 1, 2008. ©ASCE, ISSN 1076-0431/2008/4-1–XXXX/$25.00.

)F COPY [AE/2007/022186] 001804QAE

PROOF COPY [AE/2007/022186] 001804QAE

Apart from general applicability and accuracy, the problems with transferring thermal probe technology from existing uses in other disciplines and the laboratory to the measurement of building materials in situ also includes probe size, contact resistance between the probe and material, and performance in thermally unstable environments. In geotechnics, long probes of 600 mm or more can be used; this is not the case in buildings, where material layers are of the order of 20–50 mm, with a wall of 200 mm being considered thick. In food industries, materials are generally soft and easily penetrated allowing minute diameter probes and good thermal contact between probe and sample; in construction, many materials, especially those on the outside of the building shell, are rather hard in order to withstand environmental conditions. In plastics and refractory brick industries, uncased wires may be cast into samples during manufacture, providing excellent thermal contact; with a wide variation in construction materials, the number of wires that would need to be cast into samples to cover such eventualities would make this approach economically and practically prohibitive. This paper will describe the approach taken in developing a procedure that is suitable for the measurement of construction materials in existing buildings taking into account the construction-specific context.

Brief History of Thermal Probe Theory and Practice

The thermal probe employs transient line source theory, the application of which has been under development since the 19th Century. A chart of the probe temperature rise plotted against the natural logarithm of elapsed heating time of an infinitely thin and long line source heated at constant power within an infinitely large and homogeneous sample, referred to as the "perfect model," should have an asymptote with slope dependent on the thermal conductivity of the sample and the intercept dependent on its thermal diffusivity. Thermal diffusivity describes the relationship between thermal conductivity and volumetric heat capacity, hence the latter is theoretically obtainable from the ratio of conductivity to diffusivity.

Schleiermacher (1888) first attempted measurements of the thermal conductivity of gases using a hot wire technique in Germany in the late 19th Century. Stalhane and Pyk (1931), in Sweden in the early 20th Century, adapted the technique and encased the hot wire, with a mercury thermometer attached, forming a similar style probe to that used today, albeit with older technology. Seminal work was carried out in the 1950s, in The Netherlands, United Kingdom, and Canada, by, for example; Van der Held and Van Drunen (1949), Hooper and Lepper (1950), Carslaw and Jaeger (1959), Blackwell (1952, 1954), Vos (1955), and Woodside (1958). These developed guidelines for sample size, recommendations on probe length to radius ratios, and mathematical corrections to emulate the perfect model. An equation, sometimes known as Blackwell's equation, based on Fourier's theories of heat conduction, was developed to describe the chart of temperature rise over natural logarithm of elapsed time. Derivations of this equation are in use today in the various industries referred to earlier, where various iterative line fitting routines and regression analysis techniques are used to establish thermal properties. An accuracy of better than 3% for thermal conductivity and 5% for thermal diffusivity is often claimed for individual measurements, although recent comparative studies have shown variations greater than 10% for thermal conductivity values achieved for similar materials, and greater again for thermal diffusivity, when the technique is used across a range of materials in separate laboratories (Tye et al. 2005; Kubicar 1999; Spiess et al. 2001). Thermal probes are currently commercially available from different companies like Decagon and Hukseflux, albeit for use in nonbuilding related disciplines.

Transfer from Laboratory to In Situ Measurements on Buildings

Thermal probe measurements are normally undertaken in thermally stable conditions, such as can be created in a laboratory. This research bases itself on an apparatus and analysis methodology created by Goodhew and Griffiths (2004) to measure thermal properties of building materials in the laboratory, with development of a portable apparatus for in situ measurements.

The following research and development steps have been undertaken to transfer the existing analysis technique from the laboratory to in situ measurements on buildings:

1. Development of a portable and autonomous measurement apparatus that can be operated by one person, is rigid enough to withstand transport, and allows measurements to take place on site and within a limited time frame;
2. Development of a procedure for installing the equipment on site, carrying out the actual measurements, and storing and processing the resulting data; and
3. Field tests on three case study buildings in order to assess the use of the measurement apparatus and procedure to measure the thermal properties of materials in actual buildings, within relatively uncontrolled environmental conditions. An existing ASTM standard for measuring the properties of soils and soft rock (ASTM International 2000) has been used as the criterion for considering the technique either applicable, or not. This ASTM standard has been demonstrated to achieve a measurement precision in between ± 10 and $\pm 15\%$ in a study comparing probe results with known values of materials studied. It is applicable to a "limited range" around ambient room temperatures.

Experimental Measurement Equipment

The measurement apparatus developed for this research is built around the use of four commercially available Hukseflux TP08 thermal probes. These are connected to a power circuit running from batteries, a 16 bit datalogger, and a display unit, all mounted in a rugged transit case. If so desired the apparatus can be connected to a laptop for on-site data analysis; alternatively this data can be postprocessed away from the site.

Fig. 1 shows a TP08 thermal probe consisting of a base and needle. The base contains a platinum resistance thermometer and the two cold junctions of a K type thermocouple. The needle is a stainless steel tube, 72 mm long, 1.2 mm external diameter, containing a hairpin heater of known resistance per unit length, and the hot junction of the thermocouple, which is placed near the center of the heater Hukseflux (2001). The probe size was chosen as the needle length is suitable for many building material applications found in practice, where 100 mm is a commonly encountered thickness of walling and other materials, and thus the ratio of length to diameter of the probe needle at 60:1 exceeds Blackwell's recommendation of 20:1 (Blackwell and Misener 1951) to mimimize error from heat losses at the probe end.

The power circuit, driven by dry cell batteries in the transit case, is arranged to run at three power settings, delivering in the region of 0.1, 0.25, or 0.5 W to either one of four probes, or to a

PROOF COPY [AE/2007/022186] 001804QAE

OOF COPY [AE/2007/022186] 001804QAE

Fig. 1. A TP08 thermal probe

dummy heater. This dummy heater is installed to prevent excessive fluctuations in the power when the current is first directed to a probe; it has a resistance which is close to that of a TP08 heater, allowing a simple redirection of power. The current through a probe heater is determined by measuring the potential difference across a standard resistor placed in series with it. Knowing the current in the circuit and the resistance of the probe heater per unit length enables the power, or heat, emitted per unit length of the probe (Q') to be established.

A high resolution dt800 data logger by Datataker is used to observe and record: (1) the potential difference across the standard resistor; (2) the resistance of the platinum resistor in the probe base; and (3) the electromotive force of the K type thermocouple, all at 1 Hz. The data acquisition is observed by running the dedicated software package Delogger Pro v.4 on a connected laptop.

Experimental Measurement Procedure

For the equipment as described in the previous paragraph, a routine field measurement technique has been developed, following Batty et al. (1984) and Yang et al. (2002), but adapting the procedure to the specific conditions encountered with building materials.

Arriving on-site holes are drilled to accept the probes. The probes are placed in situ surrounded by a high thermal conductivity filler paste, originally developed to improve thermal contact between computer processor units and heat sinks. The datalogger and laptop are set to run and record and the power circuit is switched on with power directed to the dummy heater

Previous work in the laboratory has shown that hole diameters up to 2 mm do not significantly effect thermal conductivity value outcomes (B. Pilkington, unpublished interim report, Dec. 4, 2005) Here, 1.5 mm diameter HSS drill bits are used in softer materials, such as aerated concrete block, and 2 mm diameter HSS drill bits used to penetrate harder materials, such as lime mortar.

Probes are left in situ for 30 min to ensure thermal equilibrium with the material. Power is then directed to each probe in turn for 5 or 10 min with a suitable break between heating cycles. The heater current is initially set after a visual assessment of the material to estimate its thermal conductivity and can be adjusted following the first heating schedule to ensure the temperature rise meets appropriate levels, speeding up the process which alternatively would involve trial and error to obtain correct settings. The heating cycles are repeated after at least an hour, when the residual heat from the previous measurement has dissipated. Temperature stabilization can be observed via a chart in the data acquisition window of the software program. A number of measurements are recorded for each specific probe position and data stored for later analysis.

A semiautomated workbook has been built in MS Excel to carry out post measurement analysis, either on site on a laptop or away from the site in an office environment. The platinum resistance measurement is converted to temperature using the standard formula to give the probe base temperature. The electromotive force of the thermocouple is converted to a temperature difference using an appropriate formula provided by the probe manufacturer that sufficiently approximates the K type polynomial expression (Childs 2001) over the small range of temperature changes encountered, typically in the region of 7–10°C.

Data are arranged into standardized electronic files and stored for each heating cycle. Data sets are then imported into the MS Excel workbook where a macro is run to carry out the calculations required to convert resistance and voltages to probe temperature and power. The current technique charts the temperature of the probe for 200 s prior to the heating cycle to enable the user to assess potential drifts in the material sample temperature that might impact results.

A chart of probe temperature rise over the natural logarithm of time is created, which can be visually assessed for a linear asymptote. The macro calculates a series of thermal conductivity values by traditional regression analysis using Eq. (1) over 10, 50, 100, and 150 s periods starting at each second of the heating cycle, and charts the results

$$\lambda = Q'/(4\pi S) \tag{1}$$

where S=slope of the linear section of the ΔT versus $\ln(t)$ graph. From a visual inspection of the charts of $\Delta T/\ln(t)$ and of λ for the above mentioned periods, an appropriate time section can be chosen, where a linear asymptote exists through sufficient data points, for further analysis. The methodology previously developed by Goodhew and Griffiths (2004) is then employed to establish values of thermal conductivity using this time section, with 95% confidence.

In Situ Measurements on Case Study Buildings

Testing of the measurement equipment and procedure took place by means of application to three case study buildings, where properties of materials incorporated in those buildings were measured in situ. The buildings were chosen as they were easily accessible, the wall thicknesses were suitable for the probe, and previous laboratory-based studies had been carried out on similar materials, which allowed comparison of data quality and results between laboratory and field measurements.

During field studies the external conditions with regard to the weather, ambient temperature, and relative humidity were logged. Where practically feasible the equipment was sheltered from direct solar radiation. For each material, measurements were taken using four different probe positions, and using multiple heating cycles on each probe.

OF COPY [AE/2007/022186] 001804QAE

PROOF COPY [AE/2007/022186] 001804QAE

Fig. 2. Building 1, with a thermal probe inserted in the foundation blocks 120 mm below the damp-proof course, supported on a boom stand

Results of Field Testing

Three case study buildings were chosen for this study: an ecohouse in North Cornwall with walls constructed of insulating aerated concrete blocks with lime render (Building 1); a mass cob bus shelter and toilet block at the Eden Project in Cornwall (Building 2) and a summerhouse in Devon formed with cob blocks, some with a sheep's wool binder (Building 3). For those readers unfamiliar with the term cob, it is used in South West England to describe the use of a vernacular building material. Cob is a mixture of subsoil and straw and produces monolithic walls approximately 500 mm thick in layers approximately 300 mm deep without the use of formwork. Cob blocks are made from similar ingredients, but are produced from molds and can be used in more flexible circumstances.

Building 1: Aerated Concrete Block

Fig. 2 shows Building 1, a single story dwelling, constructed of 250 mm thick solid walls formed from Celcon Solar aerated concrete blocks. The interior is fully lime rendered and externally lime rendered and part timber clad on a foundation of Celcon aerated concrete foundation blocks. The building sits on a slope with foundation blocks exposed to the lower side. Internal and external measurements were taken at wall head and wall foot and also externally below damp course level.

The manufacturer's literature gives thermal conductivity values of 0.11 and 0.15 W m^{-1} K^{-1} for solar and foundation blocks, respectively. Celcon Solar samples were previously measured with the thermal probe methodology under laboratory conditions at various moisture contents, giving results for thermal conductivity from 0.193 W m^{-1} K^{-1} at 4.6% moisture content by weight to 0.113 W m^{-1} K^{-1} for a dry block (B. Pilkington, unpublished interim reports, Dec. 1, 2006).

The in situ measurements took place in June 2005, during hot, sunny weather. External measurements were taken in the morning on a west facing wall (see fig. 2) with ambient temperatures in the region of 19°C and relative humidity starting at 74%, dropping to 62% through the morning. Internal measurements were taken during the afternoon in the kitchen area on a south facing wall, exposed to an expanse of east facing glazing, with ambient temperatures in the region of 29°C and relative humidity in the region of 48%.

Fig. 3 shows measurements of a probe's needle and base temperatures before, during, and after an internal measurement. The needle temperature stabilizes with that of the sample after approximately 150 s, from insertion at 14:07, and remains reasonably stable until the heating cycle starts at 15:14. The temperature drift (y) with time (x) of the probe for 200 s prior to heating, found by calculating the slope of the data trend in MS, was given by Eq. (2). The drift was found to be insignificant in comparison with the requirements of the standard test method (ASTM 2000).

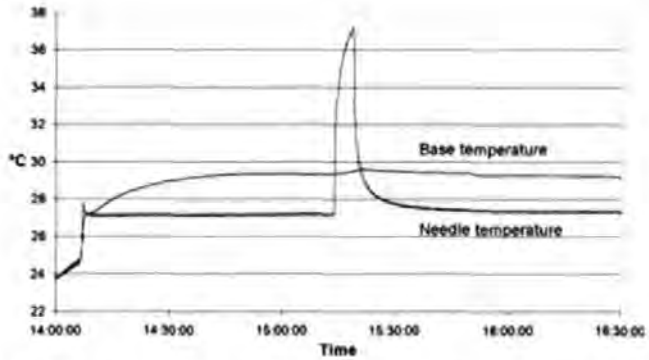

Fig. 3. Probe base and needle temperatures, before, during, and after a measurement of aerated concrete exposed to ambient temperature changes

$$y = 27.193 - 0.000006x \tag{2}$$

Fig. 4 shows the temperature rise of the heating period for the same measurement, plotted on a logarithmic scale, becoming linear after approximately 60 s. A similar pattern was found in all six locations and a section from 60 to 250 s was used for analysis in each case. The resulting thermal conductivity values are given in Table 1.

Building 2: Mass Cob

Fig. 5 shows Building 2, a single story bus shelter and toilet block known as the Body, at the Eden Project in Cornwall. Walls are of mass cob, 450 mm thick, comprising approximately 39% white china clay, 59% red Devon clay, and 2% barley straw, by weight. They are left exposed externally and are finished with 10 mm of clay plaster internally. The cob walls sit on a 450 mm high stone plinth and are protected from water ingress at their head by wide

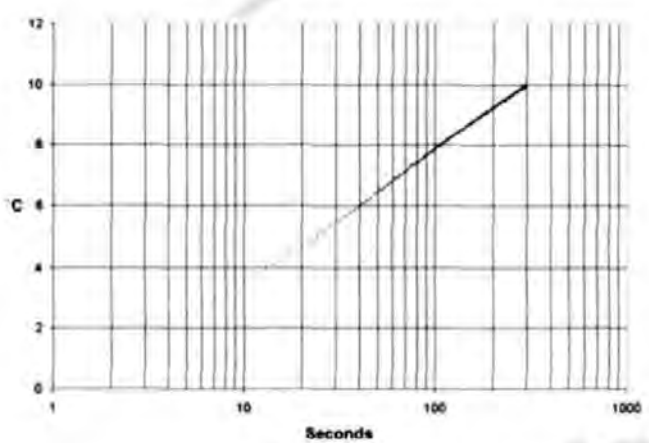

Fig. 4. Temperature rise of a probe in aerated concrete plotted against elapsed time on a logarithmic scale

PROOF COPY [AE/2007/022186] 001804QAE

Copyright statement

This copy of the thesis has been supplied on condition that anyone who consults it is understood to recognise that its copyright rests with its author and that no quotation from the thesis and no information derived from it may be published without the author's prior consent.

OOF COPY [AE/2007/022186] 001804QAE

Table 1. Thermal Conductivity Results for Aerated Concrete Measurements

Measurement location	Mean λ ($W m^{-1} K^{-1}$)	SD	SD/mean (%)
Foundation block, external			
120 mm above ground level	0.509	0.00385	0.76
Foundation block, external	0.239	0.008816	3.69
1.5 m above ground level			
120 mm below damp proof course			
Solar block, external	0.173	0.008486	4.90
200 mm above damp proof course			
Solar block, external	0.153	0.001245	0.81
1.4 m above damp proof course			
Solar block, internal	0.136	0.000155	0.11
100 mm above finished floor level			
Solar block, internal	0.132	0.00016	0.12
1.68 m above finished floor level			

projecting eaves. The building has permanent unglazed openings, allowing free ventilation. The roof is predominantly of translucent Perspex sheet with some corrugated metal sheet. Measurements were taken externally at the foot and head of the north-west-facing wall and internally at the foot and head of an internal partition wall of matching construction.

Many values for the thermal conductivity of cob or unbaked earth can be found in the literature. Goodhew et al. (2000) use 0.45 $W m^{-1} K^{-1}$ for cob made from Devon earth, and Goodhew and Griffiths (2005) note values used in practice are often approximations based on materials with similar density. Norton (1997) gives values of 0.45 or 0.65 $W m^{-1} K^{-1}$ with added stabilizer. Oughton (1986) gives a range of earth values between 0.43 $W m^{-1} K^{-1}$ for relatively dry mud to 1.7 $W m^{-1} K^{-1}$ for damp Liverpool clay. Little and Morton (2001) suggest 0.65 $W m^{-1} K^{-1}$, whereas Middleton (1987) gives a range between 1.3 and 1.4 $W m^{-1} K^{-1}$. Previous thermal probe laboratory studies by the writers have produced values similar to all the above presented values, dependent on density, soil types, mix proportions and moisture content.

The in situ measurements took place over two hot days with broken cloud in June and July 2005. Ambient temperatures ranged from 23 to 37°C and relative humidity from 22 to 62%. The layout of the building and the glazed roof areas meant that hole positions were sometimes exposed to direct solar irradiation and sometimes shaded.

Fig. 6 shows measurements of a probe's needle and base temperatures before, during, and after five measurements at the internal wall head while intermittently exposed to solar irradiation under a clear Perspex roof. The thermal lag of the cob creates a dampening of the ambient environmental conditions within the

Fig. 5. Building 2, the Body at the Eden Project, Cornwall

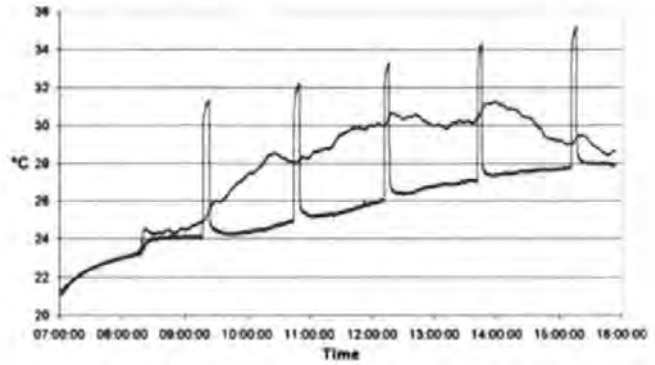

Fig. 6. Probe base and needle temperatures, before, during, and after five needle heating cycles for mass cob measurements, with apparatus and wall surface intermittently exposed to solar irradiation

material. For example, the temperature drift y with time x of the 200 s prior to the third heating cycle, given by Eq. (3), is approximately 0.01°C, or only 10% of the ASTM standard allowance (ASTM 2000)

$$y = 0.00006xx + 26.013 \quad (3)$$

Fig. 7 shows the temperature rise of the heating cycle for the same measurement, plotted on a logarithmic scale, becoming linear after approximately 50 s. A similar pattern was found in all four locations and a section from 50 to 200 s was used for analysis in each case. The resulting thermal conductivity values are given in Table 2.

Building 3: Cob Blocks

Fig. 8 shows Building 3, a single-story summerhouse located in a sheltered setting in the U.K. county of Devon. It is constructed with a mixture of exposed cob block types, with and without a lambswool binder, over a stone plinth, forming 240 mm thick walls, under a thatched roof.

Internal and external measurements were taken at the wall head and foot on an overcast day in September 2005. Ambient temperature was in the region of 18°C and relative humidity 87%.

Fig. 9 shows the measurement of a probe's needle and base temperature before, during, and after one heating cycle of a cob block measurement. The ambient temperature fluctuation is slight

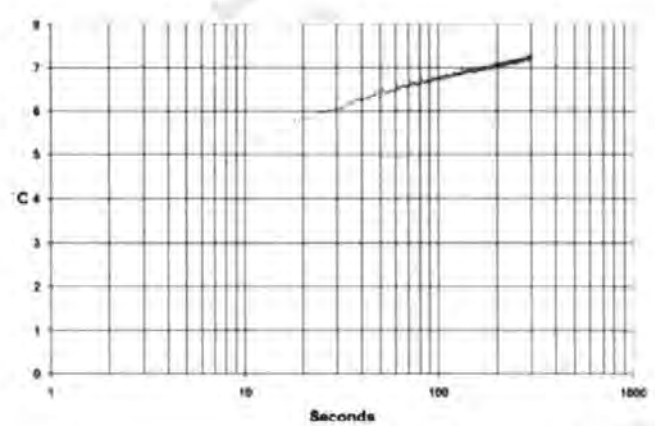

Fig. 7. Temperature rise of a probe in mass cob plotted against elapsed time on a logarithmic scale

OF COPY [AE/2007/022186] 001804QAE

PROOF COPY [AE/2007/022186] 001804QAE

Table 2. Thermal Conductivity Results for Mass Cob Measurements at the Body

Measurement location	Mean λ ($W m^{-1} K^{-1}$)	SD	SD/mean (%)
External, 180 mm above plinth 600 mm above ground level	1.165	0.098	8.44
External, 650 mm below wall head 2.67 m above ground level	0.810	0.094	11.60
Internal, 180 mm above plinth 600 mm above finished floor level	0.824	0.038	4.61
Internal, 900 mm below wall head 2.23 m above finished floor level	0.987	0.100	10.09

and not immediately reflected in the probe needle temperature. The temperature drift y with time x of the 200 s prior to this heating cycle, given by Eq. (4), is approximately 0.03°C

$$y = 0.0001x + 17.041 \quad (4)$$

Fig. 10 shows the temperature rise of the heating cycle for a cob block measurement, plotted on a logarithmic scale. The best estimation of linearity for this measurement was between 150 and 250 s. The pattern varied between measurements and various time sections were used in the analysis. The resulting thermal conductivity values are given in Tables 3–6.

Fig. 8. Building 3, Summerhouse, Bovey Tracy, Devon

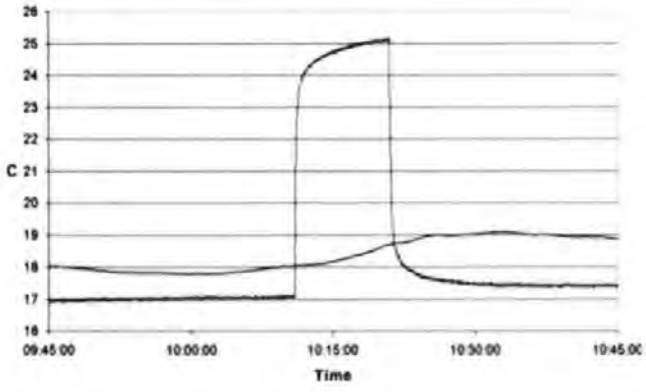

Fig. 9. Probe base and needle temperatures, before, during, and after a heating cycle for a cob block measurement

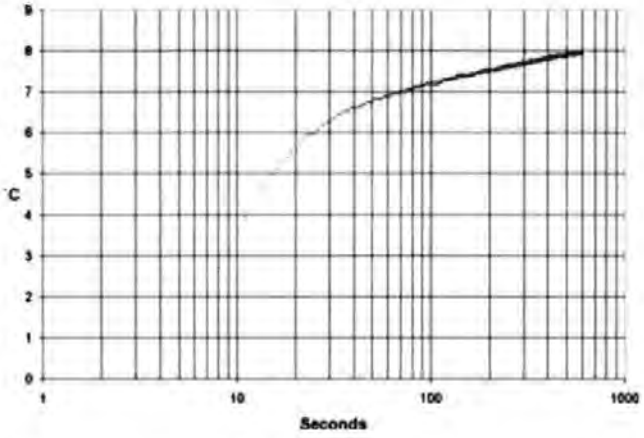

Fig. 10. Temperature rise of a probe in cob block plotted against elapsed time on a logarithmic scale

Conclusions and Recommendations

The prime goal of this paper is to investigate the transferability of the thermal probe technique from the laboratory to in situ measurements on real buildings through in situ measurements on three case study buildings.

Data analysis shows that in situations where ambient environmental fluctuations are slight, as at Buildings 1 and 3, similar accuracy to that obtained in laboratory studies can be achieved: variability values (SD/mean) as calculated are in between 0.11 and 7.03%. Where more extreme fluctuations occur, as at Building 2, variability increases to a range of 4.60–11.60%. The precision of all measurements undertaken on the three case study buildings has an accuracy that is in excess of precision of ±15%

Table 3. Cob Block with Lamb's Wool, External, Wall Head

Run	Probe	Time period for RegAnls (s)	Mean λ
A	TP08 131	50–150	0.850
E	TP08 131	60–160	0.877
L	TP08 142	60–160	0.870
P	TP08 142	60–160	0.826
S	TP08 141	50–150	0.867
		Mean	0.858
		Standard deviation	0.0205
		SD/mean	2.38%

Table 4. Cob Block, External, above Plinth

Run	Probe	Time period for RegAnls (s)	Mean λ
B	TP08 132	150–250	0.536
F	TP08 132	60–160	0.521
K	TP08 141	60–160	0.547
T	TP08 142	70–170	0.536
		Mean	0.535
		Standard deviation	0.0107
		SD/mean	2.00%

PROOF COPY [AE/2007/022186] 001804QAE

OOF COPY [AE/2007/022186] 001804QAE

Table 5. Cob Block with Lambs Wool, Internal, Wall Head

Run	Probe	Time period for RegAnls (s)	Mean λ
C	TP08 141	60–160	0.644
G	TP08 141	100–200	0.699
J	TP08 132	100–200	0.718
N	TP08 132	70–170	0.649
Q	TP08 131	90–190	0.760
		Mean	0.694
		Standard deviation	0.0487
		SD/mean	7.02%

that is indicated on the ASTM standard for soils and soft rock ASTM (2000). As far as can be concluded from the work on three cases only, it therefore is valid to apply the thermal probe technique to in situ measurements on real buildings.

The case studies also confirm the high level of variation found in similar materials. The thermal conductivities of the various cob types studied here ranged from 0.448 to 1.165 W m^{-1} K^{-1} despite similar location and apparent density. The thermal probe will measure the thermal conductivity of materials as actually present in a building, accounting for variations according to location, moisture content, mix, and manufacturing processes.

Part of the rationale for developing the thermal probe technique for field measurements on buildings on site and in use is the impact of moisture content on the thermal properties of materials. Although the initial case studies do not allow for hard conclusions on the impact of moisture content on the values obtained, it is noted that for instance the thermal conductivity of the internal walls of Building 1 were higher than those achieved in dry blocks: the calculated design U value for the walls was 0.44 W m^{-2} K^{-1} whereas, if using an average of values found above the damp proof course, the value becomes 0.51 W $m^{-2}K^{-1}$. It is highly probable that these findings relate to moisture content, either through hygroscopic moisture uptake or through moisture transfer through the solid walls. If this is indeed the case, this raises substantial doubts on the use of thermal properties that are obtained with other techniques like the guarded hot-plate method that evaporate the moisture content of a material sample during measurement. Consequently, there might be a substantial margin of error in using "established data" for energy calculations.

During this research three important issues have been identified that need further study:

1. The derivation of values for thermal diffusivity from collected field data has been attempted, which would then give values for volumetric heat capacity. The results show potential through levels of repeatability similar to that found with thermal conductivity measurements, but need further analysis.
2. Further work is needed to analyze the effects of contact resistances within the probe and between the probe and the material. This may lead to an improved temperature measurement methodology for the probe, such as the resistance of the heater wire being used to establish the probe temperature, to reduce compound scatter in the data.
3. Problems have been encountered in drilling small diameter holes in hard materials, such as stone, as making a hole of length 70 mm and diameter 2 mm is not a trivial task

Table 6. Cob Block, Internal, above Plinth

Run	Probe	Time period for RegAnls (s)	Mean λ
D	TP08 142	120–220	0.474
H	TP08 142	80–180	0.423
I	TP08 131	70–170	0.444
M	TP08 131	50–150	0.433
R	TP08 132	100–200	0.466
		Mean	0.448
		Standard deviation	0.0216
		SD/mean	4.82%

Acknowledgments

The writers wish to thank MM.ad Architecture and Design for access to Building 1 and the Eden Project for access to Building 2, and also thank Brian Anderson of the Building Research Establishment for his help and advice. This paper was prepared with support from the Carbon Trust, which accepts no liability for accuracy or completeness or for any loss arising from reliance on its content.

Notation

The following symbols are used in this paper:

Q' = power to the probe per unit length (W m^{-1});
S = slope of the linear section of the ΔT versus $\ln(t)$ graph;
t = elapsed heating time (s);
λ = thermal conductivity (W m^{-2} K^{-1}); and
ΔT = rise in probe temperature (°C).

References

ASTM. (2000). "Standard test method for determination of thermal conductivity of soil and soft rock by thermal needle probe procedure." *Designation D 5334-00*, ASTM Committee D18, Philadelphia.

ASTM. (2004). "Standard test method for thermal conductivity of refractories by hot wire (platinum resistance thermometer technique)." *C1113-99, Annual book of ASTM standards 2004, 15.01*, ASTM Committee C-8, Philadelphia, 209–224.

ASTM. (2005). "Standard test method for thermal conductivity of plastics by means of a transient line-source technique." *Designation D 5930-01*, ASTM Committee D20, Philadelphia.

Batty, W. J., Probert, S. D., Ball, M., and O'Callaghan, P. W. (1984). "Use of the thermal probe technique for the measurement of the apparent thermal conductivities of moist materials." *Appl. Energy*, 18(2), 301–317.

Blackwell, J. H. (1952). "Radial-axial heat flow in regions bounded internally by circular cylinders." *Can. J. Phys.*, 31, 472–479.

Blackwell, J. H. (1954). "A transient-flow method for determination of thermal constants of insulating materials in bulk. 1: Theory." *J. Appl. Phys.*, 25(2), 137–144.

Blackwell, J. H., and Misener, A. D. (1951). "Approximate solution of a transient heat flow problem." *Proc. Phys. Soc., London, Sect. A*, 64, 1132–1133.

Carslaw, H. S., and Jaeger, J. C. (1959). *Conduction of heat in solids*, 2nd Ed., Oxford University Press, Oxford, U.K.

Childs, P. R. N. (2001). *Practical temperature measurement*, Butterworth Heinemann, Stoneham, Mass.

)F COPY [AE/2007/022186] 001804QAE

PROOF COPY [AE/2007/022186] 001804QAE

Davis, W. R. (1984). *Compendium of thermophysical property measurement methods*, Vol. 1, K. D. Maglic, A. Cezairliyan, and V. E. Peletsky, eds., Plenum, New York, 231–254.

Doran, S. (2000). "DETR framework project report: Field investigations of the thermal performance of construction elements as built." *Building Research Establishment Client Rep. No. 78132*, BRE, East Kilbride, Scotland.

DTI. (2002). *Energy consumption in the United Kingdom*, National Statistics.

Goodhew, S., Griffiths, R., and Watson, L. (2000). "Some preliminary studies of the thermal properties of Devon cob walls." *Terra 2000, Proc., 8th Int. Conf. on the Study and Conservation of Earthen Architecture*, English Heritage, James and James, London, 139–143.

Goodhew, S. M., and Griffiths, R. (2004). "Analysis of thermal probe measurements using an iterative method to give sample conductivity and diffusivity data." *Appl. Energy*, 77(4), 205–224.

Goodhew, S. M., and Griffiths, R. (2005). "Sustainable walls to meet the building regulations." *Energy Build.*, 37, 451–459.

Hooper, F. C., and Lepper, F. R. (1950). "Transient heat flow apparatus for the determination of thermal conductivities." *Trans. Am. Soc. Heat. Ventilation Eng.*, 56, 309–324.

Hukseflux. (2001). "TP08 small size non-steady-state probe for thermal conductivity measurement." Hukseflux Thermal Sensors, Delft, The Netherlands.

Kubicar, L. (1999). "Transient methods for measuring thermophysical parameters." *Minutes of Workshop W III, 15th European Conf. on Thermophysical Properties*.

Little, B., and Morton, T. (2001). *Building with earth in Scotland: Innovative design and sustainability*, Scottish Executive Central Research Unit.

Middleton, G. F., revised by Schneider, L. M. (1987). "Bulletin 5: Earth-wall construction." CSIRO, Division of Building, Construction and Engineering, Australia.

Norton, J. (1997) *Building with earth—A handbook*, Intermediate Technology Publications, London.

Oughton, R. J. (1986). *CIBSE guide, volume A: Design data*, 5th Ed., The Chartered Institution of Building Services Engineers, London.

Salmon, D. R., Williams, R. G., and Tye, R. P. (2002). "Thermal conductivity and moisture measurements on masonry materials, insulation materials: Testing and applications." *ASTM STP 1426*, Vol. 4, A. O. Desjarlais and R. R. Zarr, eds., ASTM, West Conshohocken, Pa.

Schleiermacher, A. (1888). "On the thermal conduction of gas." *Wiedeman Ann. Phys.*, 34, 623–646.

Spiess, E. L., et al. (2001). "Thermal conductivity of food materials at elevated temperatures." *High Temp. - High Press.*, 33(15), 693–697.

Stalhane, B., and Pyk, S. (1931). "New method for determination of thermal coefficients." *Tekn. Tidskrift*, 61(28), 389–396.

Touloukian, Y. S., Powell, R. W., Ho, C. Y., and Klemens, P. G. (1970). *Thermophysical properties of matter*, Vol. 2, Thermophysical Properties Research Center, Purdue University, IFI/Plenum, New York.

Tye, R., Kubičár, L., and Lockmuller, N. (2005). "The development of a standard for contact transient methods of measurement of thermophysical properties." *Int. J. Thermophys.*, 26(6), 1917–1938.

Underwood, W. M., and McTaggart, R. B. (1960). "The thermal conductivity of several plastics, measured by an unsteady state method." *Chem. Eng. Prog., Symp. Ser.*, 56(30), 261–268.

Van der Held, E. F. M., and Van Drunen, F. G. (1949). "A method of measuring the thermal conductivity of liquids." *Physica A*, 15, 865–881.

Vos, B. H. (1955). "Measurements of thermal conductivity by a non-steady-state method." *Appl. Sci. Res., Sect. A*, 5, 425–438.

Woodside, W. (1958). "Probe for thermal conductivity measurement of dry and moist materials." *Heat./Piping/Air Cond.*, 32(9), 163–170.

Xie, H., and Cheng, S. (2001). "A fine needle probe for determining the thermal conductivity of penetrable materials." *Meas. Sci. Technol.*, 12, 58–62.

Yang, W., Sokhansanj, S., Tang, J., and Winter, P. (2002). "Determination of thermal conductivity, specific heat and thermal diffusivity of borage seeds." *Revista Biosystems Engineering*, 82(2), 169–176.

Zhang, X., and Fujii, M. (2003). "Measurements of the thermal conductivity and thermal diffusivity of polymers." *Polym. Eng. Sci.*, 43(11), 1755–1764.

PROOF COPY [AE/2007/022186] 001804QAE